NEURONAL CILIA AND APPETITE REGULATION IN *Alms1* MUTANT MICE

Déborah Heydet

May 2011

A thesis submitted for the degree of Doctor of Philosophy of

The Australian National University

The Australian National University

Medical School

Canberra, Australia.

Statement of originality

The results and analyses presented in this thesis were performed by the candidate under the supervision of Professor Geoffrey Farrell and Doctor Claire Larter within The Australian National University Medical School located at The Canberra Hospital. The research presented is my own work, except were otherwise duly acknowledged. The work in this thesis is original and has not been previously submitted for a degree or diploma in any university.

Deborah Heydet

September 2011

Acknowledgements

First I would like to thank my supervisor, Professor Geoff Farrell, for his guidance, encouragement, and his continuous support in this project. Geoff's patience, motivation, enthusiasm and immense knowledge have been really valuable throughout my PhD. These four years in the lab were full of professional and personal enrichment; I will keep these moments forever in my mind.

I also would like to express my deepest gratitude to my other main supervisor, Dr Claire Larter. Your help and guidance from the very beginning of my PhD has been extremely precious in the achievement of this project. Thank you for sharing your knowledge and scientific skills, but also thank you for providing me with always good advises and encouragement. Thank you for being there when I needed it.

I acknowledge the contribution of the other members of my PhD panel, Associate Professor Chris Nolan and Professor Caryl Hill. Their pertinent comments and valuable advice throughout this project have positively contributed to this research.

I would like to thank all the past and present people from the Liver Research Group that have assisted me in this research for both their technical and psychological support. In particular I would like to thank Ass Prof Narci Teoh, Dr to be Sharon Pok and Derrick Van Rooyen, Dr Hussam Ajamieh and Heng Jian Wong for their support, their help and of course their friendship! I am also very grateful to the animal facility staff without whom this work would not have been possible.

I also would like to acknowledge Dr Barbara Fam, Jan Elliot, Ass Prof John Bekkers and Dr Mic Cavazzini for their technical help. Without them, none of the

challenging technologies of hypothalamic dissection, Alms1 antibody production and primary neuronal culture would have been achieved.

A special thanks to Betty Rooney who has been there for me at difficult times. Thank you for your support, both administrative and personal. My PhD would have been much more different without you! Thank you for listening to my anxieties and uncertainties… I simply want to thank you for your friendship.

I cannot finish without acknowledging my friends and family, and particularly my parents. Thank you for supporting me during all those years, thank you for believing in me. Thank you for encouraging me in this life changing experience that I am living. I would never have gone so far (PhD and Australia) without you… I love you.

Last but not least, to Jean-Didier… he is the reason why I am here, Down Under. I am aware that it has not been an easy time for us, especially those past few months. But I would like you to know that you changed my life. Nothing would have been possible without your patience, support, compassion and help. Thank you for being part of my life. I love you.

I finally would like to thank all the people involved in this project, as well as everyone who supported and encouraged me during these four years and anyone that I have unintentionally omitted.

Remerciements

Je tiens tout d'abord à remercier mon directeur de thèse, le Professeur Geoffrey Farrell, sans qui ce projet n'aurait pas été réalisable. Merci de m'avoir donné une chance sans même m'avoir rencontré. Je tiens à le remercier pour sa disponibilité, ses conseils précieux et ses encouragements, ainsi que son soutien tout au long de ma thèse. Ces quatre années passées dans son laboratoire resteront inoubliables.

Je tiens également à remercier mon co-superviseur, Dr Claire Larter. Son aide et son soutien ont été extrêmement précieux durant ma thèse. Je la remercie pour ses conseils ainsi que sa disponibilité. Merci pour avoir été là quand j'en avais besoin, merci pour ton amitié.

Un grand merci aux membres de mon comité d'encadrement de thèse, l'Ass Prof Chris Nolan ainsi que le Prof Caryl Hill pour leur aide technique ainsi que leurs commentaires plus que pertinents sur mes travaux de thèse.

Je remercie tous ceux sans qui cette thèse ne serait pas ce qu'elle est : aussi bien par les discussions que j'ai eu la chance d'avoir avec eux, leurs suggestions ou contributions. Un grand merci a toute les personnes présentes et passées de l'équipe, Dr Narci Teoh, futur Dr Sharon Pok, futur Dr Derrick Van Rooyen, Dr Hussam Ajamieh et Heng Jian Wong pour leur soutien, leur aide si précieuse dans le laboratoire et bien sûr leur amitié. Merci a tous pour ces grands moments de joie et de rigolade passés ensemble à la pause déjeuner… Je tiens également a remercier tout le personnel animalier sans que ce projet n'aurait pas pu aboutir.

Je tiens à adressé un clin d'œil tout particulier à mes compagnons de galère Sharon et Derrick… je crois que l'on a tous subi les mêmes doutes et difficultés. Merci d'avoir été là pour m'écouter, merci de m'avoir supportée et encouragée toutes ces années, un grand merci pour tous vos conseils et votre amitié. Je ne vous dirai qu'une chose... courage, c'est bientôt fini !

Mes remerciements vont aussi au Dr Barbara Fam pour l'aide qu'elle m'a apporte dans la technique de dissection des hypothalami.

Je remercie aussi l'Ass Prof John Bekkers et le Dr Mic Cavazzini pour leur aide précieuse dans la mise en place de la culture neuronal. Merci pour votre disponibilité et tous vos conseils.

J'adresse également mes remerciements à Jan Elliott pour son temps passé à la culture d'hybridomes et sans qui la production des anticorps anti-Alms1 aurait été impossible. Je la remercie pour son dévouement dans la réalisation de ce projet.

Je tiens aussi à remercier Betty Rooney qui a su être là dans les moments difficiles et sans qui la vie du laboratoire serait bien différente. Merci pour avoir rendu les choses bien plus facile à vivre.

Finalement je tiens à remercier mes amis, ma famille et tout particulièrement mes parents. Merci de m'avoir laisse partir si loin… merci d'avoir toujours cru en moi et de m'avoir toujours soutenu. Je n'en serai pas arrivée là sans vous… je vous aime.

Je ne peux pas finir sans remercier celui « à cause » de qui j'ai atterri au pays des kangourous, Jean-Didier. Je sais que tout n'a pas toujours été tout beau

tout rose… surtout ces derniers mois. Merci de m'avoir encouragée et soutenue tout au long de ma thèse, merci de ta patience et de ta compréhension. Merci de partager ma vie, je t'aime.

Finalement je tiens à remercier toutes les personnes qui ont participé de près ou de loin dans l'élaboration et le développement de ce projet, toutes les personnes qui m'ont soutenues et encouragées, ainsi que toutes les personnes que j'ai pu omettre dans ces quelques lignes.

Abstract

The *foz/foz* mouse is a murine model of Alström syndrome, a monogenetic disorder characterised in humans by childhood obesity, hearing loss, blindness, hyperinsulinaemia, early-onset type 2 diabetes and liver disease. In 2006, research from the host laboratory reported that *foz/foz* mice inherit a spontaneous mutation (*foz*), an 11 base pair deletion in exon 8 of the *Alms1* gene, and develop a similar phenotype to patients suffering from Alström syndrome. Thus, *foz/foz* mice are obese and exhibit high circulating insulin and leptin levels as well as fatty liver disease and metabolic syndrome. The purpose of the studies presented in this thesis was to further characterise the pathogenesis of obesity in *foz/foz* mice, by studying the role of Alms1 and hypothalamic appetite-regulating neuropeptide expression during the development of obesity.

ALMS1 has been shown to localise at the base of primary cilia in what is termed the basal body or centrosome. Primary cilia are ubiquitously expressed hair-like organelles. Therefore, the first approach was to study primary cilia in the hypothalamus as well as hypothalamic *Alms1* gene expression and Alms1 localisation in *foz/foz* and wildtype (WT) mice from birth until the obese phenotype is evident. At birth, *foz/foz* mice showed similar number of ciliated hypothalamic neurons to WT mice. However, from weaning and onwards the number of cilia was significantly decreased in *foz/foz* mice. In addition, while cilia were present in primary neuronal cultures from *foz/foz* and WT mice, Alms1 was only detected in WT neurons, appearing as two perinuclear dots at the base of cilia.

After weaning, serum leptin levels become greatly elevated in *foz/foz* compared to WT mice. Leptin decreases appetite by acting in the hypothalamus and inducing or inhibiting the release of appetite-regulating neuropeptides. A detailed

study of key hypothalamic neuropeptides demonstrated no differences in their gene and/or protein expression or localisation between *foz/foz* and WT mice. This failure of elevated leptin levels to decrease appetite and body weight is defined as leptin resistance. Further studies were therefore performed on hypothalamic leptin receptor (Ob-R) expression and signalling pathways to characterise leptin resistance in *foz/foz* mice. These results demonstrated induction of two proteins, SOCS3 and PTP1B, which negatively regulate Ob-R signalling and have been implicated in leptin resistance.

Taken together, the data presented in this thesis strongly support the proposal that *foz/foz* mice develop leptin resistance, which correlates molecularly with over-expression of at least two negative feedback regulators of Ob-R. In addition, the post-natal reduction in ciliated hypothalamic neurons in *foz/foz* mice, in combination with the lack of Alms1 detection are consistent with the proposal that primary cilia stability/maintenance could be impaired as a consequence of the *Alms1* mutation. In conclusion, *foz/foz* mice provide new opportunities for studying the role of Alms1 and neuronal cilia in appetite regulation, particularly with respect to the onset of leptin resistance. A better understanding of Alms1, cilial stability and behavioural responses that underlie obesity could provide clues to novel therapeutic approaches to combat more common forms of obesity.

Résumé

En 2006, un nouveau modèle de souris a été caractérisé (*foz/foz* ou ‘‘fat aussie’’). Ces souris présentent une mutation spontanée (*foz*) de 11 paires de bases dans l’exon 8 du gène *Alms1*, responsable chez l’Homme du syndrome d’Alström. Ce syndrome est une maladie monogénique caractérisée par le développement précoce de l’obésité et la résistance à l’insuline ainsi que par une surdité, des problèmes visuels, un retard mental et des problèmes hépatiques. Les souris *foz/foz* sont très intéressantes car elles présentent un phénotype identique à l’Homme, dont une dérégulation du contrôle de la prise alimentaire entrainant l’obésité. Des études chez ces souris ont montrées qu’elles présentent des taux élevés d’insuline et de leptine et qu’elles développent des maladies hépatiques (stéatose hépatique) ainsi que le syndrome métabolique. Le but de ces travaux de thèse a été de caractériser les mécanismes hypothalamiques impliqués dans le développement de l’obésité chez les souris *foz/foz*. Pour cela, les études se sont focalisées sur le rôle d’Alms1 ainsi que sur le(s) changement(s) d’expression de neuropeptides impliqués dans le contrôle de la prise alimentaire chez ces souris.

Chez l’Homme, la protéine ALMS1 est localisée à la base des cils primaires (corpuscule basal/centrosome). Le cil primaire est une “antenne”, il est présent dans la plupart des types cellulaires à un seul exemplaire par cellule. La première étude de ce travail de thèse a été d’identifier les cils primaires et leur(s) relation(s) avec Alms1 chez les souris *foz/foz*. Nous avons montré que dans l’hypothalamus, à la naissance, le nombre de cils primaires chez les souris *foz/foz* ne diffère pas de celui des souris contrôles. A l’âge de 3 semaines, les souris *foz/foz* présentent une forte réduction du nombre de cils primaires comparé aux souris contrôles (‘‘normales’’).

Cette différence persiste dans le temps et elle est corrélée avec une diminution de l'expression du gène *Alms1*. En cultivant des neurones hypothalamiques (provenant de souris *foz/foz* ou contrôles) nous avons montré que les cils primaires sont présents dans les deux souches animales. Cependant, Alms1 a uniquement pu être détecté dans les cultures neuronales de souris contrôles.

Des études antérieures ont montré que les taux circulants de leptine chez les souris *foz/foz* augmentent en fonction de l'âge et du régime alimentaire. De manière générale, la leptine est connue pour son pouvoir anorexigène (diminution de la prise alimentaire) via son action sur la production et la sécrétion de peptides dans l'hypothalamus. Mais dans la majorité des cas d'obésité, de forts taux de leptine circulante sont constatés, sans pour autant induire une réponse adéquate. Cet état pathologique est appelé "résistance à la leptine". Lors de ces travaux de thèse, la caractérisation de l'expression des principaux neuropeptides (régulés par la leptine) impliqués dans la régulation de la prise alimentaire a été effectuée chez les souris *foz/foz*. Etant donné qu'aucune différence n'a été observée entre les souris *foz/foz* et les souris contrôles, nos investigations se sont poursuivies par une étude approfondie du récepteur à la leptine ainsi que de ces voies de signalisation. La découverte majeure de cette étude a été la présence en quantité anormalement élevée de deux inhibiteurs du récepteur à la leptine (SOCS3 et PTP1B), connus pour être impliqués dans le phénomène de la résistance à la leptine.

Les travaux présentés dans ce manuscrit de thèse prouvent que les souris *foz/foz* sont résistantes à la leptine à travers l'augmentation de l'expression d'au moins deux bloqueurs du récepteur à la leptine. De plus, la réduction du nombre de cils primaires chez les souris *foz/foz* suggère que leur stabilité peut être affectée. Au vu de ces résultats et de la localisation de Alms1 nous proposons que Alms1 joue

un rôle dans la stabilité et/ou le maintient des cils primaires. En conclusion, le modèle de souris *foz/foz* est très intéressant pour l'étude du rôle des cils primaires et d'Alms1 conjointement au développement de l'obésité et de la résistance à la leptine.

Table of Contents

Page

Table of Contents i

List of Figures ix

List of Tables xiv

Publications and published abstracts xv

Manuscript in preparation xv

Oral presentations to scientific meetings xvi

Poster presentations to scientific meetings xvi

Abbreviations xviii

Page

1. Introduction 1

1.1. Overview of Alström syndrome 1

1.2. Animal model of Alström syndrome 3

1.3. Role of the primary cilium in obesity 4

1.3.1. Structure of primary cilia 4

1.3.2. Primary cilia and obesity 8

1.4. Peripheral control of food intake and energy expenditure 8

1.5. Mechanisms of leptin action in the brain 10

1.5.1. Leptin receptors 10

1.5.2. Anatomy of the hypothalamus 11

1.5.3. Regulation of energy homeostasis by hypothalamic neuropeptides 14

1.5.3.1. Orexigenic neuropeptides secreted by the hypothalamus 14

Neuropeptide Y 14

Agouti-related protein 14

Page

Melanin concentrating hormone 15

1.5.3.2. Anorexigenic neuropeptides secreted by the hypothalamus 15

Pro-opiomelanocortin/α-melanocyte stimulating hormone 15

Cocaine and amphetamine-regulated transcript 16

Corticotropin-releasing hormone 16

1.6. Leptin resistance and obesity 18

1.6.1. Leptin receptor signalling 18

1.6.2. Potential mechanisms leading to leptin resistance 21

Leptin receptor overlapping transcript 21

Supressor of cytokine signalling 3 21

SH2-domain-containing protein tyrosine phosphatase 2/extracellular-signal-regulated kinase pathway 22

Phosphatidylinositol 3 kinase/phosphatase and tensin homolog/protein kinase B pathway 23

Protein tyrosine phosphatase 1B 24

SH2 B adaptor protein 1 24

1.7. Summary and aims 25

2. Materials and methods 27

2.1. Material used 27

2.2. Animal methods 29

2.2.1. Mice 29

2.2.2. Diets 29

2.2.3. Protocols and corresponding experimental groups 30

2.3. Fresh tissue collection 32

2.3.1. Dissection of the whole hypothalamus 33

2.3.2. Dissection of hypothalamic nuclei 34

Page

2.4. Preparation of perfused tissue 36

2.4.1. Cardiac perfusion for brain fixation 36

2.4.2. Vibrating blade microtome sections 36

2.5. Biochemical methods 37

2.5.1. Serum analyses 37

2.5.2. Immunohistofluorescence 37

2.5.2.1. Single labelling 37

2.5.2.2. Double labelling 38

2.5.3. Immunohistofluorescence analyses 42

2.6. Molecular methods 43

2.6.1. Gene expression 43

2.6.1.1. RNA extraction 43

2.6.1.2. RNA extraction from dissected hypothalamic nuclei 44

2.6.1.3. cDNA synthesis 45

2.6.1.4. Real time PCR 45

2.6.2. Protein analyses 47

2.6.2.1. Protein extraction 47

2.6.2.2. Western blot 47

2.7. Cell culture experiments 51

2.7.1. Hypothalamic primary neuronal culture 51

2.7.1.1. Coverslip preparation 51

2.7.1.2. Media preparation 51

2.7.1.3. Preparation of hypothalamic neurons 52

2.7.2. Immunocytofluorescence 53

2.7.2.1. Single labelling 53

2.7.2.2. Double labelling 54

2.8. Statistical analyses 54

Page

3. Loss of primary cilia in *foz/foz* mice 55

3.1. Introduction 55

3.2. Purpose of the study 57

3.3. Methods 57

3.3.1. Animals and diets 57

3.3.2. Gene expression analyses 58

3.3.3. Immunohistofluorescence 58

3.3.4. Statistical analyses 59

3.4. Results 59

3.4.1. The number of hypothalamic primary cilia is decreased after birth in *foz/foz* mice 59

3.4.2. The length of hypothalamic primary cilia is unaltered in *foz/foz* mice, despite the decrease in cilia number 65

3.4.3. Hypothalamic adenylate cyclase III gene expression is unaltered in *foz/foz* mice 67

3.4.4. Is decreased ciliogenesis responsible for the decrease in the number of ciliated neurons in *foz/foz* mice? 68

3.4.5. Hypothalamic expression of genes involved in cilial trafficking 69

3.5. Discussion 72

4. Relationships between Alms1, the primary cilium and obesity in *foz/foz* mice 77

4.1. Introduction 77

4.2. Purpose of the study 79

4.3. Methods 80

4.3.1. Animals and diets 80

4.3.2. Gene expression analyses 80

4.3.3. Protein expression analyses 81

Page

4.3.4. Neuronal primary cell culture, and immunocytofluorescence studies 81

4.3.5. Statistical analyses 82

4.4. Results 82

4.4.1. Hypothalamic *Alms1* gene expression is reduced in *foz/foz* mice 82

4.4.2. *Alms1* gene expression is reduced in white adipose tissue in *foz/foz* mice 85

4.4.3. Alms1 protein is present in the hypothalamus 86

4.4.4. Alms1 localises to the basal body of hypothalamic neurons 89

4.4.5. Alms1 localises close to the primary cilium in hypothalamic neurons cultured from WT mice, but not in *foz/foz* mice 91

4.4.6. Hypothalamic mRNA levels of peptides expressed on the cilial membrane are not changed in *foz/foz* mice 93

4.5. Discussion 95

5. Studies of appetite-regulating neuropeptides expression in *foz/foz* mice 101

5.1. Introduction 101

5.2. Purpose of the study 105

5.3. Methods 106

5.3.1. Animals and diets 106

5.3.2. Gene expression analyses 107

5.3.3. Protein expression analyses 108

5.3.4. Immunohistofluorescence 108

5.3.5. Statistical analyses 109

5.4. Results 109

5.4.1. *Foz/foz* mice are obese with increased fat mass 109

5.4.2. *Foz/foz* mice are hyperleptinaemic 112

Page

5.4.3. Studies of orexigenic neuropeptide expression in *foz/foz* and WT mice 114

5.4.3.1. Hypothalamic NPY mRNA levels and protein localisation 114

5.4.3.2. Hypothalamic AgRP mRNA levels and protein localisation 117

5.4.3.3. Hypothalamic MCH mRNA levels 120

5.4.4. Studies of anorexigenic neuropeptide expression in *foz/foz* and WT mice 121

5.4.4.1. Hypothalamic POMC mRNA and protein levels 121

5.4.4.2. Hypothalamic CART mRNA levels and protein localisation 124

5.4.4.3. Hypothalamic CRH mRNA levels 125

5.4.5. Hypothalamic MC4-R mRNA and protein levels in *foz/foz* and WT mice 126

5.5. Discussion 129

6. Hypothalamic leptin receptor expression and molecular intermediates of leptin signalling 137

6.1. Introduction 137

6.2. Purpose of the study 143

6.3. Methods 143

6.3.1. Animals and diets 143

6.3.2. Gene expression analyses 144

6.3.3. Protein expression analyses 145

6.3.4. Immunohistofluorescence 146

6.3.5. Statistical analyses 146

6.4. Results 147

6.4.1. Hypothalamic Ob-R expression at weaning, TC2 and TC12 in *foz/foz* and WT mice 147

Page

Hypothalamic Ob-R mRNA levels 147

Hypothalamic Ob-R protein levels 148

Ob-R immunohistofluorescence 151

6.4.2. Hypothalamic Leprot mRNA levels at TC2 and TC12 in *foz/foz* and WT mice 152

6.4.3. Hypothalamic Stat3 expression at weaning, TC2 and TC12 in *foz/foz* and WT mice 153

Hypothalamic Stat3 mRNA levels 153

Hypothalamic Stat3 protein levels 155

6.4.4. Hypothalamic SOCS3 expression at weaning, TC2 and TC12 in *foz/foz* and WT mice 158

Hypothalamic SOCS3 mRNA levels 158

Hypothalamic SOCS3 protein levels 159

6.4.5. Hypothalamic PTEN protein levels at weaning, TC2 and TC12 in *foz/foz* and WT mice 162

6.4.6. Hypothalamic Akt protein levels at weaning, TC2 and TC12 in *foz/foz* and WT mice 164

6.4.7. Hypothalamic FoxO1 mRNA levels at weaning, TC2 and TC12 in *foz/foz* and WT mice 167

6.4.8. Hypothalamic SHP2 expression at weaning, TC2 and TC12 in *foz/foz* and WT mice 169

Hypothalamic SHP2 mRNA levels 169

Hypothalamic SHP2 protein levels 171

6.4.9. Hypothalamic ERK protein levels at weaning, TC2 and TC12 in *foz/foz* and WT mice 173

6.4.10. Hypothalamic SH2B1 mRNA levels at weaning, TC2 and TC12 in *foz/foz* and WT mice 175

6.4.11. Hypothalamic PTP1B expression at weaning, TC2 and TC12 in *foz/foz* and WT mice 177

Hypothalamic PTP1B mRNA levels 177

Hypothalamic PTP1B protein levels 179

Page

6.5. Discussion 181

7. General discussion 191

7.1. Is Alms1 involved in the stability and maintenance of primary cilia? 192

7.2. Is obesity in *foz/foz* mice related to Alms1 function in intracellular trafficking and protein transport? 193

7.3. What else could cause leptin resistance in *foz/foz* mice? 195

7.4. Other pathways involved in obesity 196

7.5. Is energy expenditure modified in *foz/foz* mice? 198

7.6. Concluding remarks 198

Appendix 1 200

References 205

List of Figures

		Page
Figure 1.1	Cilia structure	5
Figure 1.2	Main features of anterograde and retrograde transport along the primary cilium	7
Figure 1.3	(A) Schematic representation of rodent brain. (B) Major hypothalamic regions implicated in adiposity regulation of energy homeostasis	13
Figure 1.4	Hypothalamic localisation of the main neuropeptides involved in the regulation of energy balance	17
Figure 1.5	Leptin receptor signal transduction in the hypothalamus	20
Figure 2.1	Feeding time course protocol, including 'key' to experimental group notation	30
Figure 2.2	Animal groups used for protein extraction	31
Figure 2.3	Animal groups used for RNA extraction	31
Figure 2.4	Animal groups for cardiac perfusion to fix brains prior to immunohistofluorescence	32
Figure 2.5	Whole hypothalamic dissection	33
Figure 2.6	Hypothalamic nuclei dissection	35
Figure 2.7	Hypothalamic Hsp90 protein expression at weaning and during dietary regimes in *foz/foz* and WT mice	49
Figure 3.1	Representative IHF staining for neurons and primary cilia in the hypothalamus of newborn *foz/foz* and WT mice	61
Figure 3.2	Representative IHF staining for neurons and primary cilia in the hypothalamus of weanling *foz/foz* and WT mice	62
Figure 3.3	Representative IHF staining for neurons and primary cilia in the hypothalamus of *foz/foz* and WT mice after 2-weeks on chow diet	63

		Page
Figure 3.4	Representative IHF staining for neurons and primary cilia in the hypothalamus of *foz/foz* and WT mice after 12-weeks on chow diet	64
Figure 3.5	Percentage of hypothalamic ciliated neurons of newborn, weaning, TC2, TC12 *foz/foz* and WT mice	65
Figure 3.6	Representative staining for primary cilia in the hypothalamus of TC2 *foz/foz* and WT mice	66
Figure 3.7	Primary cilia length in the hypothalamus of weaning, TC2, TC12 *foz/foz* and WT mice	67
Figure 3.8	Adenylate cyclase lll gene expression in the whole hypothalamus at TC2 and TC12 in chow and high fat-fed *foz/foz* and WT mice	68
Figure 3.9	Cep164 and ODF2 gene levels are not changed in WT or *foz/foz* mice hypothalamus	69
Figure 3.10	Hypothalamic expression of genes involved in primary cilia trafficking are unaltered in *foz/foz* mice	71
Figure 4.1	*Alms1* mRNA levels in whole hypothalamus (A) and in hypothalamic nuclei (B-D) at weaning, TC2 and TC12 are reduced by ~50% in *foz/foz* mice compared with WT mice	84
Figure 4.2	*Alms1* mRNA levels in white adipose tissue are reduced ~50% in *foz/foz* mice compared with WT after 12-weeks on diet	85
Figure 4.3	Representative western blots of Alms1 in heterozygote (*foz*/+) mice (A-C)	88
Figure 4.4	Subcellular localisation of Alms1 within hypothalamic neurons in primary culture from WT mice, and absence of Alms1 immunostaining in *foz/foz* mice	90
Figure 4.5	Subcellular colocalisation of Alms1 and the primary cilium in hypothalamic neurons from *foz/foz* and WT mice	92
Figure 4.6	SstR3 and MCH1R hypothalamic gene expression is not affected by genotype and/or diet in *foz/foz* mice	94

		Page
Figure 5.1	Hypothalamic neuropeptides involved in food intake regulation	104
Figure 5.2	Body weights of *foz/foz* and WT mice according to age and diet	111
Figure 5.3	Relative mass (% of body weight) of peri-ovarian (A) and subcutaneous (B) white adipose tissue in WT and *foz/foz* mice according to age and diet	112
Figure 5.4	Circulating leptin levels at weaning and during 2 and 12 weeks of dietary intake in *foz/foz* and WT mice	113
Figure 5.5	NPY mRNA levels in whole hypothalamus (A) and in hypothalamic nuclei (B-D) at weaning and during dietary regimes in *foz/foz* and WT mice	115
Figure 5.6	Representative hypothalamic NPY expression in chow-fed *foz/foz* (A, C) and WT mice (B, D) at TC2	116
Figure 5.7	AgRP mRNA levels in whole hypothalamus (A) and in hypothalamic nuclei (B-D) at weaning and during dietary regimes in *foz/foz* and WT mice	118
Figure 5.8	Representative hypothalamic AgRP expression in chow-fed *foz/foz* (A, C) and WT mice (B, D) at TC2	119
Figure 5.9	MCH mRNA levels in whole hypothalamus during dietary regimes in *foz/foz* and WT mice	120
Figure 5.10	POMC mRNA levels in whole hypothalamus (A) and in hypothalamic nuclei (B-C) at weaning and during dietary regimes in *foz/foz* and WT mice	122
Figure 5.11	POMC protein expression in hypothalamus at different ages during feeding experiments in *foz/foz* and WT mice	123
Figure 5.12	Representative hypothalamic CART expression at TC2 in chow-fed *foz/foz* (A, C) and WT mice (B, D)	124
Figure 5.13	CRH mRNA levels in whole hypothalamus during dietary regimes in *foz/foz* and WT mice	125

		Page
Figure 5.14	MC4-R mRNA levels in whole hypothalamus (A) and in hypothalamic nuclei (B-D) at weaning, TC2 and TC12 in chow and high fat-fed *foz/foz* and WT mice	127
Figure 5.15	Hypothalamic MC4-R protein expression at different ages during dietary regimes in *foz/foz* and WT mice	128
Figure 6.1	Activation of the leptin receptor	138
Figure 6.2	Leptin effects on PI3K and PTEN pathways	140
Figure 6.3	Hypothalamic Ob-R mRNA levels in whole hypothalamus (A) and in hypothalamic nuclei (B-D) at weaning, and during dietary regimes in *foz/foz* and WT	149
Figure 6.4	Hypothalamic Ob-R protein expression at weaning and during dietary regimes in *foz/foz* and WT mice	150
Figure 6.5	Representative example of hypothalamic Ob-R expression as shown by immunohistofluorescence in chow-fed *foz/foz* and WT mice at TC2	151
Figure 6.6	Leprot mRNA levels in whole hypothalamus at TC2 and TC12 in *foz/foz* and WT mice	152
Figure 6.7	Stat3 mRNA levels in whole hypothalamus (A) and in hypothalamic nuclei (B-D) at weaning and during	154
Figure 6.8	Hypothalamic Stat3 (A), phosphorylated Stat3 (B) and P-Stat3:Stat3 ratio (C) at different ages during dietary regimes in *foz/foz* and WT mice	157
Figure 6.9	SOCS3 mRNA levels in whole hypothalamus (A) and in hypothalamic nuclei (B-D) at weaning and during dietary regimes in *foz/foz* and WT mice	160
Figure 6.10	Hypothalamic SOCS3 protein expression at different ages during dietary regimes in *foz/foz* and WT mice	161
Figure 6.11	Hypothalamic PTEN (A), phosphorylated PTEN (B) and P-PTEN:PTEN ratio (C) at different ages during dietary regimes in *foz/foz* and WT mice	163
Figure 6.12	Hypothalamic Akt (A), phosphorylated Akt (B) and P-Akt:Akt ratio (C) at different ages during dietary regimes in *foz/foz* and WT mice	166

		Page
Figure 6.13	Hypothalamic FoxO1 mRNA levels in whole hypothalamus (A) and in hypothalamic nuclei (B-D) at weaning and during dietary regimes in *foz/foz* and WT mice	168
Figure 6.14	Hypothalamic SHP2 mRNA levels in whole hypothalamus (A) and in hypothalamic nuclei (B-D) at weaning and during dietary regimes in *foz/foz* and WT mice	170
Figure 6.15	Hypothalamic SHP2 (A), phosphorylated SHP2 (B) and P-SPH2:SHP2 ratio (C) at different ages during dietary regimes in *foz/foz* and WT mice	172
Figure 6.16	Hypothalamic ERK (A), phosphorylated ERK (B) and P-ERK:ERK ratio (C) at different ages during dietary regimes in *foz/foz* and WT mice	174
Figure 6.17	Hypothalamic SH2B1 mRNA levels in whole hypothalamus (A) and in hypothalamic nuclei (B-D) at weaning and during dietary regimes in *foz/foz* and WT mice	176
Figure 6.18	Hypothalamic PTP1B mRNA levels in whole hypothalamus (A) and in hypothalamic nuclei (B-D) at weaning and during dietary regimes in *foz/foz* and WT mice	178
Figure 6.19	Hypothalamic PTP1B protein expression at different ages during dietary regimes in *foz/foz* and WT mice	180
Figure 6.20	Diagram recapitulating the results (*foz/foz* vs. WT) from Chapter 6 on PI3K/PTEN/Akt/FoxO1 pathway, and proposed interactions between signalling peptides and transcriptional regulation	185

List of Tables

		Page
Table 2.1	Sources and conditions of primary antibodies used for immunofluorescence	40
Table 2.2	Sources and conditions of secondary antibodies used for immunofluoresce	41
Table 2.3	Primer sequences for real time PCR	46
Table 2.4	Primary antibody conditions for western blot	50
Table 5.1	Overview of the results from Chapter 5 on key appetite-regulating neuropeptides from whole hypothalamus (mRNA and/or protein levels)	130
Table 5.2	Overview of the results from Chapter 5 on key appetite-regulating neuropeptides from dissected hypothalamus (mRNA levels)	131
Table 6.1	Summary of changes in leptin, leptin receptor, signalling intermediates and leptin-regulated genes	181
Table 6.2	Summary of changes in proteins that modulate Ob-R signalling	182

Publications and published abstracts

1. CZ Larter, S Chitturi, **D Heydet**, Geoffrey C Farrell (2010) *A fresh look at NASH pathogenesis. Part 1: The metabolic movers.* Journal of Gastroenterology and Hepatology 25: 672-690 (Invited review).

2. **D Heydet**, CZ Larter, GC Farrell (2010) *Central primary cilia and leptin resistance roles in hyperphagic mice with obesity related liver disease*. Journal of Gastroenterology and Hepatology 25: A7 (Abstract of conference presentation).

3. **D Heydet**, CZ Larter, GC Farrell (2009) *Central mechanism of hyperphagia in a new model of obesity-related liver disease.* Journal of Gastroenterology and Hepatology 24: A273-A310 (Abstract of conference presentation).

Manuscript in preparation

1. **D Heydet**, LX Chen, CZ Larter, C Inglis, MA Silverman, GC Farrell, MR Leroux (2011) *A truncating mutation of Alms1 reduces the number of hypothalamic neuronal cilia in obese mice.*

2. **D Heydet**, CZ Larter, GC Farrell (2011) *Causes of central leptin resistance in Alms1 mutant mice.*

Oral presentations to scientific meetings

1. **D Heydet**, CZ Larter, GC Farrell. *Central primary cilia and leptin resistance roles in hyperphagic mice with obesity related liver disease*. Australian Gastroenterology Week, Young Investigator Award Finalist (October 2010, Gold Coast, Australia; see Reference 2, above).

2. **D Heydet**, CZ Larter, GC Farrell. *Central mechanisms of leptin resistance in hyperphagic obese mice with metabolic syndrome.* The Australian Society for Medical Research Medical Research Week, Young Investigator Forum (June 2010, Canberra, Australia).

Poster presentations to scientific meetings

1. **D Heydet**, CZ Larter, GC Farrell. *Alms1 mutation leads to decreased ciliation of hypothalamic neurons in obese* foz/foz *mice.* The Australian Society for Medical Research Medical Research, New Investigator Forum and Canberra Health Annual Research Meeting 2011 (June 2011, Canberra, Australia).

2. **D Heydet**, CZ Larter, GC Farrell. *Alms1 mutation leads to decreased ciliation of hypothalamic neurons in obese* foz/foz *mice.* Australian Neuroscience Society 31st Annual Meeting (January 2011, Auckland, New Zealand).

3. **D Heydet**, CZ Larter, GC Farrell. *Decoding the central mechanisms of leptin resistance in a new model of hyperphagic obese mice.* 7th Forum of European Neuroscience (July 2010, Amsterdam, The Netherlands).

4. **D Heydet**, CZ Larter, GC Farrell. *Central mechanisms of leptin resistance in hyperphagic obese mice with metabolic syndrome.* Australian Neuroscience Society 30th Annual meeting in conjunction with the Australian Physiological Society 50th Anniversary Meeting (January 2010, Sydney, Australia).

5. **D Heydet**, CZ Larter, GC Farrell. *Central mechanism of hyperphagia in a new model of obesity-related liver disease.* Australia & New Zealand Medical & surgical gastrointestinal week (October 2009, Sydney, Australia; see Reference 3, above).

6. **D Heydet**, CZ Larter, GC Farrell. *Hypothalamic study of a new model of obese mice.* Australian Neuroscience Society 29th Annual Meeting (January 2009, Canberra, Australia).

7. **D Heydet**, CZ Larter, GC Farrell. *Leptin and leptin receptor expression in a new model of obese mice.* The Australian Society for Medical Research Medical Research Week, Young Investigator Forum (June 2008, Canberra, Australia).

Abbreviations

ACIII	Adenylate cyclase III
AH	Anterior hypothalamic area
AgRP	Agouti-related protein
Akt	Protein kinase B (PKB)
Alms1	Murine equivalent of ALMS1 – Alström syndrome related protein
APS	Ammonium persulfate
Arc	Arcuate nucleus
B2M	Beta 2-microglobulin
BBS	Bardet-Biedl syndrome
bp	Base pair
BSA	Bovine serum albumin
CART	Cocaine and amphetamine-regulated transcript
CCK	Cholecystokinin
cDNA	Complementary deoxyribonucleic acid
Cep164	Centrosomal protein of 164 kDa
CRH	Corticotropin-releasing hormone
DEPC	Diethylpyrocarbonate
dH_2O	Distilled water
DMH	Dorsomedial hypothalamic area
dNTP	Deoxyribonucleotide triphosphate
DTT	Dithiothreitol
DYNC2H1	Cytoplasmic dynein 2 heavy chain 1
EGTA	Ethylene glycol tetraacetic acid
ELISA	Enzyme-linked immunosorbent assay
ERK	Extracellular-signal-regulated kinase
FoxO1	Forkhead box-containing protein-O1
Foz	*foz/foz*

GI	Gastrointestinal
GLP-1	Glucagon-like peptide-1
HFD	High fat diet
HRP	Horseradish peroxidase
Hsp90	Heat shock protein 90
ICF	Immunocytofluorescence
IFT	Intraflagellar transport
IHF	Immunohistofluorescence
i.p.	intraperitoneal
JAK	Janus activating kinase
kDa	kilodalton
KiF3A	Kinesin-like protein
Leprot	Leptin receptor overlapping transcript
LHA	Lateral hypothalamic area
MAPK	Mitogen-activated protein kinase
MC4-R	Melanocortin 4-receptor
MCH	Melanin concentrating hormone
MCH1R	Melanin concentrating hormone 1 receptor
$MgCl_2$	Magnesium chloride
min	Minute
mRNA	Messenger ribonucleic acid
α-MSH	α-melanocyte stimulating hormone
NaCl	Sodium chloride
NeuN	Neuronal nuclei
NPY	Neuropeptide Y
Ob-R	Leptin receptor
ODF2	Outer dense fibre 2
PBS	Phosphate buffer saline
PCR	Polymerase chain reaction

PFA	Paraformaldehyde
PI3K	Phosphatidylinositol 3 kinase
PIP2	Phosphatidylinositol-4,5-biphosphate
PIP3	Phosphatidylinositol-3,4,5-triphosphate
POMC	Pro-opiomelanocortin
PTEN	Phosphatase and tensin homolog
PVDF	Polyvinylidene fluoride
PVN	Paraventricular nucleus
PTP1B	Protein tyrosine phosphatase 1B
RPL13a	Ribosomal protein L13a
rpm	Rotation per minute
RT	Room temperature
RT PCR	Real time polymerase chain reaction
SDS	Sodium dodecyl sulfate
SDS-PAGE	Sodium dodecyl sulfate polyacrylamide gel electrophoresis
SEM	Standard error of the mean
SH2B1	SH2 B adaptor protein 1
SHP2	SH2-domain-containing protein tyrosine phosphatase 2
SOCS3	Suppressor of cytokine signalling 3
SstR3	Somatostatin receptor 3
Stat3	Signal transducer and activator of transcription 3
TBS	Tris-buffered saline
TBST	Tris-buffered saline Tween
Tyr	Tyrosine
VMH	Ventromedial hypothalamic nucleus
WAT	White adipose tissue
Wean	Weaning
wk	Week
WT	Wildtype

CHAPTER 1

Chapter 1

Introduction

Obesity is the consequence of an imbalance between food intake and energy expenditure, leading to an excessive accumulation of fat in adipose tissue, liver and other tissues involved in metabolism. About one third of obese people develop metabolic complications and their disease consequences, such as type 2 diabetes, coronary artery disease, and fatty liver disease (Ogden *et al.*, 2007). Feeding behaviour is complex, and many factors can contribute to the aetiology of obesity, both genetic determinants, particularly the desire to eat high energy foods, but also environmental factors, such as food availability, food choices and physical activity. Despite increased understanding of the pathophysiological mechanisms involved in the development of obesity, further study in this field remains of great interest, the ultimate goal being to prevent and/or treat obesity and its potentially life shortening metabolic complications.

1.1. Overview of Alström syndrome

Study of rare monogenetic causes of obesity have given great insights into the more common multifactorial condition in man. One such disorder is Alström syndrome, a rare, autosomal recessive disorder that was first described by C.H. Alström in Sweden in 1959 (Alström *et al.*, 1959). The most reproducible clinical

features of Alström syndrome are the combination of early onset congenital retinal dystrophy that leads to blindness, childhood obesity, sensorineural hearing loss, male infertility, insulin resistance, types 2 diabetes and cirrhosis (Alström *et al.*, 1959; Michaud *et al.*, 1996; Marshall *et al.*, 1997). Other features commonly observed include dilated cardiomyopathy, renal cystic disease and developmental delay (Marshall *et al.*, 2005).

Nearly a decade ago, the genetic basis of Alström syndrome was identified as mutations in the human *ALMS1* gene, which encodes a 460 kDa protein of unknown function (Collin *et al.*, 2002; Hearn *et al.*, 2002). Immunofluorescent studies, using cultured human foetal dermal fibroblasts, the human hepatocellular carcinoma cell line (HepG2 cells) and human tissues, including foetal pancreas, skeletal muscle, liver, kidney and brain, at 8-weeks post-conception but also adult pancreas and adipocytes, showed that ALMS1 has ubiquitous tissue expression, and it localises to the centrosome and the base of cilia (Hearn *et al.*, 2005). Interestingly, the phenotype of Alström syndrome is rather similar to that of Bardet-Biedl syndrome (BBS). Mutations in BBS genes lead to obesity and diabetes, retinal degeneration, hypertension, and renal anomalies, but also skeletal abnormalities such as polydactyly (Moore *et al.*, 2005; Blacque and Leroux, 2006; Tobin and Beales, 2007). In both BBS and Alström syndrome, the mutated proteins localise to the primary cilium or the centrosome/basal body (at the base of the cilium; Ansley *et al.*, 2003; Nachury *et al.*, 2007). Both syndromes are therefore now classified as ciliopathies. The general topic of ciliopathies will not be discussed in detail here; the interested readers are referred to recent excellent reviews (Cardenas-Rodriguez and Badano, 2009; Girard and Petrovsky, 2011; Hildebrandt *et al.*, 2011)

1.2. Animal model of Alström syndrome

Recent studies in the host laboratory have reported an obese mouse strain (fat aussie) with a spontaneous truncating mutation in the murine equivalent of *ALMS1*, *Alms1* gene (*foz*) (Arsov *et al.*, 2006a; Arsov *et al.*, 2006b). *foz/foz* mice bear a spontaneous 11-bp deletion in exon 8 of *Alms1* which truncates the mRNA and resulting protein. This mutation leads to a phenotype that recapitulates all features of human Alström syndrome. Thus, *foz/foz* mice exhibit disordered appetite regulation from an early age, with the resultant hyperphagia resulting in over nutrition, obesity, insulin resistance, type 2 diabetes, and fatty liver disease. *foz/foz* mice further resemble their human counterparts by developing sensorineural deafness and male infertility (Arsov *et al.*, 2006a; Arsov *et al.*, 2006b).

Characterisation of the *foz/foz* murine model of Alström syndrome could provide novel insights into the aetiopathogenesis of obesity, insulin resistance with disordered glucose metabolism, hypercholesterolemia, and fatty liver disease. The observation that the *Alms1* mutation causes hyperphagia that precedes obesity, is consistent with the proposal that appetite dysregulation may be the primary defect that leads to development of fatty liver disease, metabolic syndrome and type 2 diabetes in this novel and florid murine model of obesity and metabolic syndrome.

1.3. Role of the primary cilium in obesity

1.3.1. Structure of primary cilia

Cilia are hair-like organelles. They derived from the basal body, which in turn originates from one of the two centrioles that comprise the centrosome, and protrude from the plasma membrane of almost all human cells (Olsen, 2005; see the website http://www.bowserlab.org/primarycilia/cilialist.html for a detailed list of cells expressing cilia, and corresponding references). The common eukaryotic cilium is motile, being composed of nine separate microtubule doublets and a central pair of microtubules (9+2). In contrast, the primary cilium is non-motile, having lost the central pair of microtubules (9+0; Figure 1.1). The existence of different types of cilia tends to indicate that cilia are likely to have several functions, such as photoreception, mechanosensation, olfaction, chemosensation, thermosensation and regulation of embryonic development (Alaiwi *et al.*, 2009).

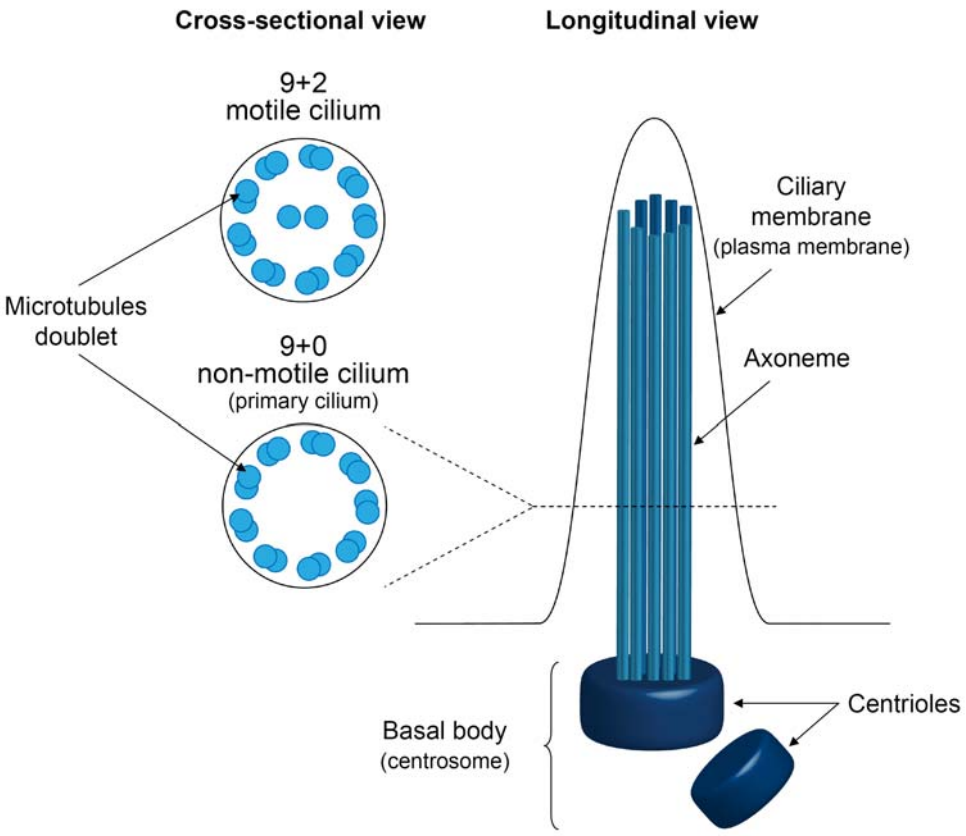

Figure 1.1. Cilia structure

A typical motile cilium consists of an axoneme of nine doublets of microtubules plus a central pair of microtubules (9+2). Non-motile cilia lack this central pair (9+0). For each type of cilium, microtubule doublets protrude from the basal body, and the axoneme is surrounded by a ciliary membrane (part of the plasma membrane).

Ciliogenesis requires the presence of “appendage” proteins, such as centrosomal protein, Cep164, and outer dense fibre 2, ODF2, which localises at the appendages of the mother centrioles (Ishikawa *et al.*, 2005; Graser *et al.*, 2007; Schweizer and Hoyer-Fender, 2009; Figure1.2). The assembly and maintenance of the cilium as well as the transport of proteins to and from it also requires an intraflagellar transport (IFT) system. IFT particles are assembled into two

complexes, complex A, and complex B. These traffic between the base and the tip of the cilium (Figure 1.2). As protein synthesis does not seem to occur in the cilium, axonemal membrane components, as well as proteins expressed on the ciliary membrane, require the IFT system for their transport to and from the cilium. Anterograde transport is mediated by a heterotrimeric kinesin-2 complex, which is composed of motor subunits KiF3A and KiF3B and a non-motor subunit (Cole *et al.*, 1993). Retrograde transport is performed by cytoplasmic dynein (DYNC2H1; Pazour *et al.*, 1998; Signor *et al.*, 1999; Figure 1.2). The transition between anterograde and retrograde transport occurs at the tip of the cilium. However, the mechanism(s) involved in this transition is/are still poorly understood. More recently, seven BBS proteins, the BBSome, have been shown to be involved in ciliogenesis and ciliary trafficking (BBS1, 2, 4, 5, 7, 8, 9; Nachury *et al.*, 2007; Nachury, 2008; Figure 1.2).

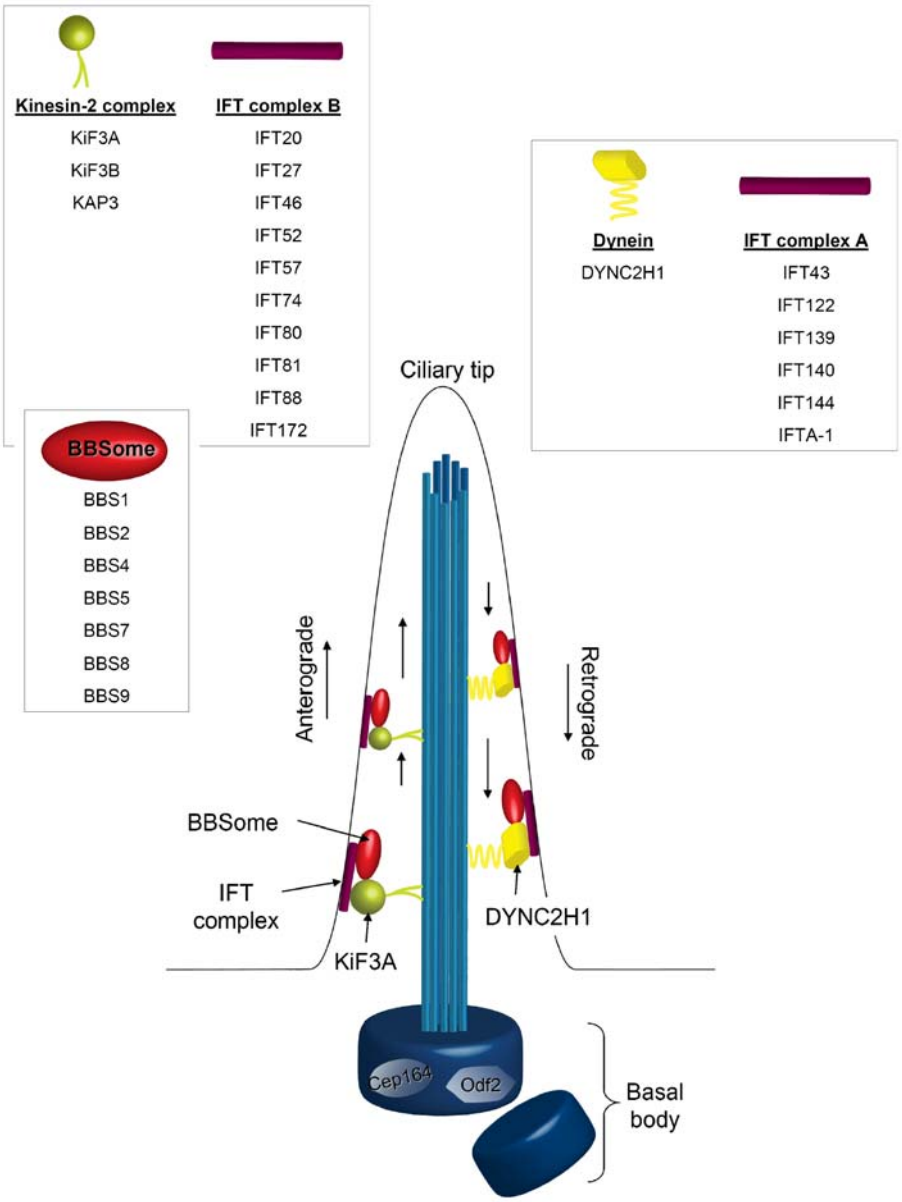

Figure 1.2. Main features of anterograde and retrograde transport along the primary cilium

Cep164 and Odf2 localise to the basal body and are involved in anchorage of the cilium. Anterograde cilial transport (from cell body to ciliary tip) is performed by the IFT complex B and the kinesin-2 complex; whereas retrograde transport (from ciliary tip to cell body) is carried out by the IFT complex A and the cytoplasmic dynein 2 heavy chain 1. The BBSome, a complex of seven proteins is also involved in bidirectional transport of proteins to and from the cilium.

Abbreviations: BBS, Bardet-Biedl syndrome; BBSome, Bardet-Biedl syndrome protein complex; Cep164, Centrosomal protein of 164 kDa; DYNC2H1, Cytoplasmic dynein 2 heavy chain 1; IFT, Intraflagellar transport; Odf2, Outer dense fibre 2.

Adapted from Gerdes *et al.,* (2009).

1.3.2. Primary cilia and obesity

The connection between defects in primary cilia and obesity was first observed in *Bbs2*$^{-/-}$ mice. The animals display heavier body weight, and they accumulate more abdominal fat by four months of age than their heterozygous and wildtype counterparts (Nishimura *et al.*, 2004). More recently, Davenport *et al.,* (2007) created adult mice that lack cilia, by disrupting KiF3A in the central nervous system; these cilia deficient mice were also obese. The authors extended their work by generating KiF3A knock-outs in a specific subpopulation of hypothalamic neurons, the pro-opiomelanocortin (POMC) neurons, which are known to be important in the regulation of food intake (Section 1.5.3.2). Such mice were obese, with increased adiposity and elevated circulating leptin levels, indicating that feeding behaviour defects are connected with ciliary deficiency in this neuronal subset.

While the exact molecular pathway(s) involved in ciliopathy-related obesity is/are still unclear, several hypotheses have been proposed; one idea is that BBS proteins could be implicated in the transport of receptors involved in the regulation of food intake and energy expenditure, such as leptin receptor (Ob-R) or melanin concentrating hormone 1 receptor (MCH1R), to the cilia membrane (Berbari *et al.*, 2008b; Seo *et al.*, 2009).

1.4. Peripheral control of food intake and energy expenditure

Numerous signals produced and secreted by the gastrointestinal (GI) tract, the pancreas and the white adipose tissue (WAT), so-called peripheral signals,

directly influence hunger and satiety. These peripheral signals can be classified as short- or long-term energy balance signals. Short-term acting signals are produced by the GI tract; they are considered as expressing the feeling of body "fullness" from postprandial satiation. Conversely, long-term signals or adiposity signals reflect the levels of energy stores. Thus, they regulate the amount of energy stored (fat) over time, and are particularly important at regulating body weight.

To date, ghrelin is the only known peripheral circulating hormone that induces hunger and increases food intake and adiposity (Tschop *et al.*, 2000; Nakazato *et al.*, 2001).

Satiety signals are generated during a meal and regulate food intake on a meal-to-meal basis by inducing a sense of fullness. The most important satiety signals are cholecystokinin (CCK), bombesin, glucagon-like peptide-1 (GLP-1), apolipoprotein A-IV, amylin, and peptide YY(3–36) (for review, see Arora and Anubhuti, 2006; Huda *et al.*, 2006; Chaudhri *et al.*, 2008). These short-term energy signals interact with long-term regulators (i.e. leptin and insulin) to maintain energy homeostasis.

Both insulin and leptin have been shown to fulfil the criteria needed to be classified as adiposity signal. They both circulate at levels proportional to fat stores (Bagdade *et al.*, 1967; Maffei *et al.*, 1995; Considine *et al.*, 1996), and they penetrate the brain in proportion to their plasma levels (Baura *et al.*, 1993; Banks *et al.*, 1996; Schwartz *et al.*, 1996b). Furthermore, Ob-R and insulin receptors are expressed in the central nervous system, including the hypothalamus, which is involved in the regulation of energy homeostasis (Marks *et al.*, 1990; Baskin *et al.*, 1999a; Baskin *et al.*, 1999c). Several studies have shown that leptin seems to be more important than insulin in the central regulation of food intake. Type 1 diabetes

mellitus is a clinical state of hyperphagia where both adiposity signals are low. Restoring insulin levels in streptozotocin-induced diabetes (in rats) lowered food intake (Sipols *et al.*, 1995). Further, treating children with new-onset type 1 diabetes with insulin leads to a progressive increase in circulating leptin levels over time (Hanaki *et al.*, 1999), confirming the role of insulin in leptin synthesis. Additional studies have shown that, by restoring leptin levels, the food consumption of diabetic rats decreases despite insulin levels remaining low (Sindelar *et al.*, 1999; Akirav *et al.*, 2004). Taken together, these results suggest that insulin deficiency itself is insufficient to cause hyperphagia, while leptin dysregulation has a more critical role in the regulation of energy homeostasis.

1.5. Mechanisms of leptin action in the brain

1.5.1. Leptin receptors

Leptin circulates in proportion to fat mass and acts in the central nervous system to regulate the balance between energy intake and expenditure. It does this by suppressing food intake and increasing energy expenditure. In rodents and humans, the lack of leptin signalling, due to mutation of leptin (*ob/ob* mice; Pelleymounter *et al.*, 1995) or leptin receptor (*db/db* mice; Halaas *et al.*, 1995), results in increase body weight due to increased food intake, conjointly with decreased energy expenditure (Montague *et al.*, 1997; Clement *et al.*, 1998; Gibson *et al.*, 2004). In the brain, leptin activates its receptor, Ob-R. The latter is produced in several alternatively spliced forms (Ob-Ra, b, c, d, e and f; Lee *et al.*, 1996; Wang

et al., 1996). These isoforms are classified into three classes: secreted (Ob-Re), short (Ob-Ra, c, d, f) and long (Ob-Rb). Ob-Rb is crucial for the biological action of leptin as it has a long cytoplasmic region that is required for signal transduction. This receptor is mainly expressed in the hypothalamus, especially in the arcuate nucleus (Arc), the ventromedial hypothalamic nucleus (VMH), paraventricular nucleus (PVN), lateral hypothalamic area (LHA) and dorsomedial hypothalamic area (DMH; Mercer *et al.*, 1996; Elmquist *et al.*, 1998b; Baskin *et al.*, 1999c).

1.5.2. Anatomy of the hypothalamus

Most early work to identify the regions of the brain involved in energy intake and energy expenditure used systematic lesioning or electrical stimulation of specific nuclei within the hypothalamus. As a result, hypothalamic nuclei were classified as “hunger” or “satiety” centres (Kennedy, 1950; Olney, 1969).

The main hypothalamic regions involved in feeding are:

- The arcuate nucleus (Arc) which is situated above the median eminence, around the base of the third ventricle (Figure 1.3). The Arc is an elongated nucleus, which occupies approximately one-half of the length of the hypothalamus. Three possible routes may be used to allow entry of circulating (peripheral) peptides and proteins, including insulin and leptin (Krisch and Leonhardt, 1978; Ciofi *et al.*, 2009). In this area, the blood brain barrier is modified to Therefore, the Arc acts as a feeding control centre, receiving inputs from the peripheral circulation through semi-permeable capillaries. Neurons from the Arc form direct and indirect connections

with others hypothalamic areas; these include the PVN, DMH, VMH and LHA (Figure 1.3).

- The paraventricular nucleus (PVN) is adjacent to the top part of the third ventricle in the anterior hypothalamus (Figure 1.3). Several neuronal pathways implicated in energy homeostasis converge on this nucleus (Figure 1.3), indicating that it is an integrative centre of nutritional signals.

- The ventromedial hypothalamic nucleus (VMH) is one of the largest hypothalamic nuclei, it is considered as a "satiety centre", as lesion in this area leads to severe hypherphagic syndromes (Satoh *et al.*, 1997). The VMH has been identified as a target for leptin, since this nucleus is rich in Ob-Rb (Mercer *et al.*, 1996). The VMH has direct and indirect connections with the PVN, LHA and DMH (Figure 1.3).

- The dorsomedial hypothalamic area (DMH) is located immediately dorsal to the VMH. It has extensive connections with other hypothalamic nuclei, including the PVN and LHA (Figure 1.3). It has a role in the integration and processing of information from the neuronal populations of these regions (Elmquist *et al.*, 1998a).

- The lateral hypothalamic area (LHA) is less precisely defined than other hypothalamic nuclei. It contains populations of neurons that express orexigenic peptides. This finding has led to categorisation of this region as the "feeding centre".

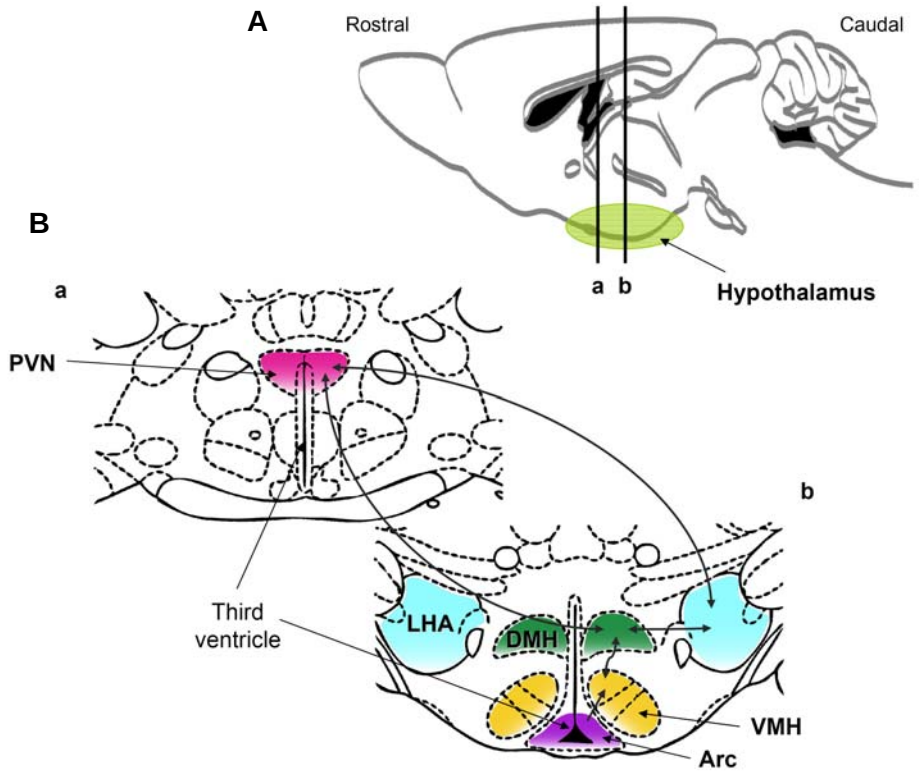

Figure 1.3. (A) Schematic representation of rodent brain. (B) Major hypothalamic regions implicated in adiposity regulation of energy homeostasis

The hypothalamus is located at the base of the rodent brain (A). The more frontal section (B-a) shows the localisation of the paraventricular nucleus surrounding the top part of the third ventricle. The second section (B-b) shows the localisation of other nuclei involved in energy homeostasis, and the main connections between these nuclei.

Abbreviations: Arc, Arcuate nucleus; DMH, Dorsomedial hypothalamic area; LHA, Lateral hypothalamic area; PVN, Paraventricular nucleus; VMH, Ventromedial hypothalamic nucleus. Adapted from Williams *et al.,* (2001).

1.5.3. Regulation of energy homeostasis by hypothalamic neuropeptides

1.5.3.1. Orexigenic neuropeptides secreted by the hypothalamus

Neuropeptide Y

Neuropeptide Y (NPY) is one of the most abundant neuropeptides in the hypothalamus. Its major site of expression is the Arc (Figure 1.4), where NPY neurons have been shown to express the long form of the leptin receptor (Ob-Rb; Baskin *et al.*, 1999a). In rodent models of energy deficiency, such as starvation and insulin-dependent diabetes mellitus, hypothalamic NPY gene expression is increased (Williams *et al.*, 1988; Williams *et al.*, 1989; Wilding *et al.*, 1993). Furthermore, leptin has been shown to have a direct effect on NPY expression. For example, leptin administration suppresses NPY expression, while leptin deficiency causes the opposite effect (Stephens *et al.*, 1995; Schwartz *et al.*, 1996a).

Agouti-related protein

Similar to NPY, Agouti-related protein (AgRP) is expressed in the Arc (Figure 1.4). A point of interest is that all AgRP-producing neurons co-express NPY (Hahn *et al.*, 1998; Haskell-Luevano *et al.*, 1999). Central administration of AgRP increases food intake, and leptin inhibits AgRP gene expression (Ebihara *et al.*, 1999). Like NPY, AgRP expression is increased in states of leptin deficiency and resistance as in *ob/ob* and *db/db* mice (Shutter *et al.*, 1997). In the hypothalamus, AgRP acts as an inverse agonist of the constitutively active melanocortin 4-receptor (MC4-R; Haskell-Luevano and Monck, 2001; Nijenhuis *et al.*, 2001; Srinivasan *et al.*, 2004).

Melanin concentrating hormone

Melanin concentrating hormone (MCH) is synthesised in neurons from the LHA (Figure1.4; Qu *et al.*, 1996). These neurons receive inputs from Arc neurons (Elias *et al.*, 1999) and are therefore considered as second order neurons. MCH plays an important role in feeding behaviour; in fact, obese mice lacking functional leptin overexpress MCH mRNA. Furthermore, central administration of MCH induces food intake (Qu *et al.*, 1996) while inhibition of the MCH pathway results in a lean phenotype (Borowsky *et al.*, 2002).

1.5.3.2. Anorexigenic neuropeptides secreted by the hypothalamus

Pro-opiomelanocortin/α-melanocyte stimulating hormone

α-melanocyte stimulating hormone (α-MSH), is a cleavage product from the pro-opiomelanocortin (POMC) gene. POMC neurons localise within the arcuate nucleus and project to many other hypothalamic areas (Figure 1.4). POMC, and ultimately α-MSH, inhibits food intake via its agonist action on MC4-R, where it competes with AgRP. Indeed, central administration of α-MSH results in decreased food intake and increased energy expenditure, and these effects can be inhibited by the administration of an MC4-R antagonist (Rossi *et al.*, 1998; Adage *et al.*, 2001). The role of POMC/α-MSH in the regulation of energy homeostasis was reinforced by the discovery on Ob-Rb on POMC neurons in the Arc (Cheung *et al.*, 1997). In conditions of low leptin levels or when leptin is non-functional, POMC mRNA levels are reduced (Mizuno *et al.*, 1998), whereas treating these animals with leptin increases hypothalamic POMC mRNA (Schwartz *et al.*, 1997).

Cocaine and amphetamine-regulated transcript

Cocaine and amphetamine-regulated transcript (CART) mRNA is found in several nuclei of the hypothalamus including Arc, PVN, DMH and LHA (Figure 1.4; Vrang *et al.*, 1999; Robson *et al.*, 2002). CART transcript is colocalised with POMC in the Arc, and with MCH in the LHA (Vrang *et al.*, 1999). CART has also been shown to interact with leptin, as its expression is upregulated following leptin administration, whereas *ob/ob* mice have decreased CART mRNA levels (Kristensen *et al.*, 1998).

Corticotropin-releasing hormone

Corticotropin-releasing hormone (CRH) is widely distributed in the brain. In the hypothalamus, CRH expressing neurons are localised in the PVN (Figure 1.4). CRH administration modulates food intake by causing anorexia which decreases spontaneous feeding and leads to loss of body weight (Levine *et al.*, 1983).

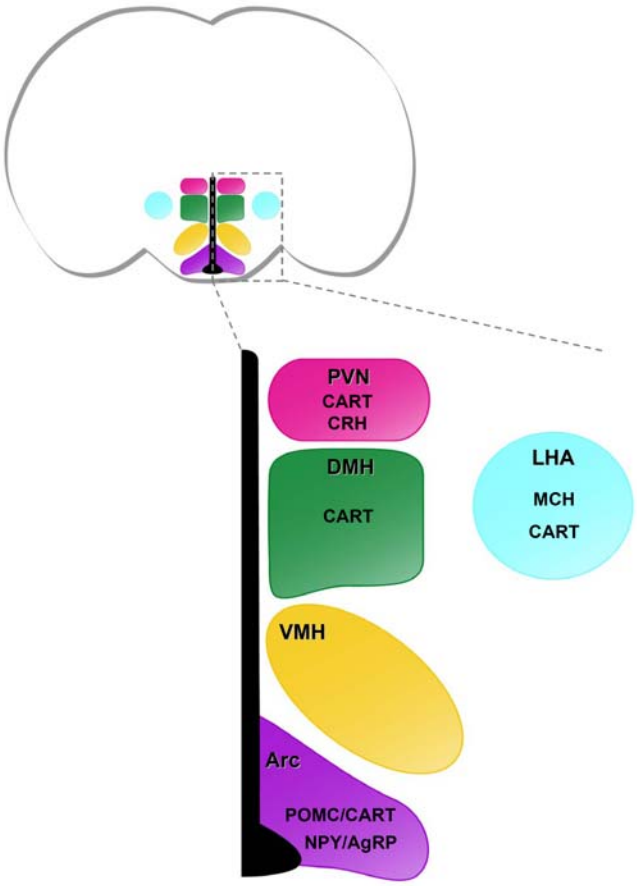

Figure 1.4. Hypothalamic localisation of the main neuropeptides involved in the regulation of energy balance

Specific hypothalamic areas have been identified to express transcripts and/or proteins of several peptides implicated in the modulation of feeding behaviour. As indicated in purple, NPY, AgRP, POMC and CART are all localised in the arcuate nucleus; whereas MCH and CRH hormone localise to the paraventricular nucleus and lateral hypothalamic area (pink and blue, respectively). Extensive neuronal circuits connect these different hypothalamic areas (as shown in Figure 1.3), allowing neuropeptides to be synthesised in one nucleus and released in another.

Abbreviations: AgRP, Agouti-related protein; Arc, Arcuate nucleus; CART, Cocaine and amphetamine-regulated transcript; CRH, Corticotropin-releasing hormone; DMH, Dorsomedial hypothalamic area; LHA, Lateral hypothalamic area; MCH, Melanin concentrating hormone; NPY, Neuropeptide Y; POMC, Pro-opiomelanocortin; PVN, Paraventricular nucleus; VMH, Ventromedial hypothalamic nucleus. Adapted from Castaneda *et al.,* (2005).

1.6. Leptin resistance and obesity

By binding and activating its hypothalamic receptor, leptin induces a decrease in food intake and an increase in energy expenditure. However, elevated plasma leptin levels have been found in obese humans suggesting that these individuals might be resistant to the anorexigenic action of leptin (Considine *et al.*, 1996). Several mechanisms have been proposed to explain such "leptin resistance". Besides genetic mutations leading to non-functional leptin (*ob/ob* mice) or the leptin receptor (*db/db* mice), the central (hypothalamic) action of leptin has been shown to be decreased by defective leptin transport across the blood brain barrier (Banks *et al.*, 1999). Leptin resistance can also be caused by reduced Ob-R signal transduction or by the failure of one or more downstream Ob-R neuropeptide(s) listed above.

1.6.1. Leptin receptor signalling

Ob-Rb is a member of the interleukin-6 receptor family of class 1 cytokine receptors. It contains an extracellular ligand-binding domain, a single transmembrane domain, and a cytoplasmic signalling domain (Tartaglia *et al.*, 1995; Baumann *et al.*, 1996; Tartaglia, 1997). The binding of leptin to the receptor results in a conformational change of the Ob-Rb homodimer (Nakashima *et al.*, 1997), enabling transphosphorylation and activation of janus activating kinase 2 (JAK2; Bjorbaek *et al.*, 1997; Ghilardi and Skoda, 1997). In turn, the activation of JAK2 promotes the tyrosine phosphorylation of several cytoplasmic residues on Ob-Rb,

which then provide docking sites for proteins with specialised phosphotyrosine binding domains. Ob-Rb contains several tyrosine phosphorylation sites including, Tyr985, Tyr1077 and Tyr1138 (Figure 1.5; Banks *et al.*, 2000; Gong *et al.*, 2007). The phosphorylation of Tyr1138 recruits the signal transducer and activator of transcription 3 (Stat3), a latent transcription factor that then becomes phosphorylated, undergoes dimerisation and translocates to the nucleus, where it regulates the transcription of several genes (Figure 1.5; Banks *et al.*, 2000). Stat3 promotes the gene transcription of POMC (Munzberg *et al.*, 2003; Xu *et al.*, 2007) and suppressor of cytokine signalling 3 (SOCS3; Bjorbaek *et al.*, 1998). Conversely, it has been shown to inhibit AgRP transcription (Figure 1.5; Kitamura *et al.*, 2006; Gong *et al.*, 2008). Tyr985 mediates the recruitment the tyrosine phosphatase, SH2-domain-containing protein tyrosine phosphatase 2 (SHP2; Carpenter *et al.*, 1998), which mediates the activation of extracellular-signal-regulated kinase (ERK) pathway (Figure 1.5; Bjorbaek *et al.*, 2001).

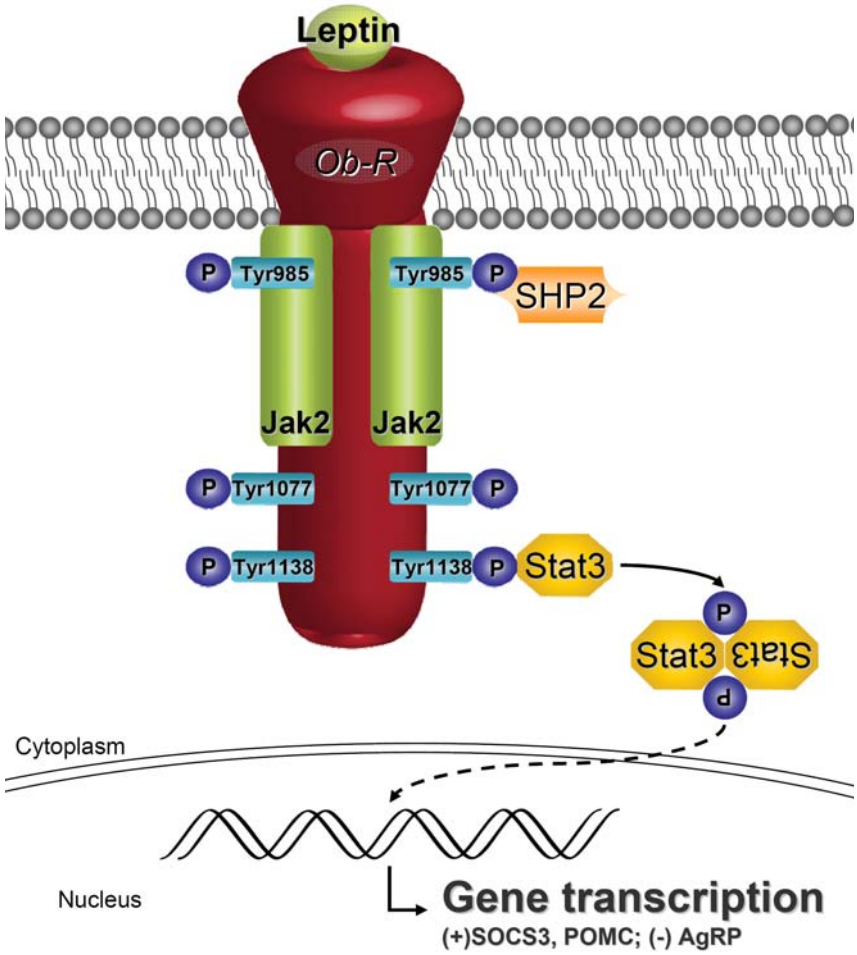

Figure 1.5. Leptin receptor signal transduction in the hypothalamus

Leptin activates JAK2, which phosphorylates tyrosine residues Tyr985, Tyr1077 and Tyr1138. These phosphorylated residues recruit specific downstream signalling molecules. SHP2 binds to Tyr985. Tyr1138 recruits Stat3, which phosphorylates, dimerises and translocates into the nucleus, where it promotes SOCS3, POMC and inhibits AgRP gene transcription.

Abbreviations: AgRP, Agouti-related protein; Ob-R, Leptin receptor; POMC, Pro-opiomelanocortin; SHP2, SH2-domain-containing protein tyrosine phosphatase 2; SOCS3, Suppressor of cytokine signalling 3; Stat3, Signal transducer and activator of transcription 3; Tyr, Tyrosine.

1.6.2. Potential mechanisms leading to leptin resistance

Leptin receptor overlapping transcript

As mention in section 1.5.1, several Ob-R mRNA splice variants have been described. Bailleul *et al.,* (1997) identified a new transcript of the Ob-R gene that encodes for another protein, so-called leptin receptor overlapping transcript (Leprot); this transcript is present in both human and mouse tissues. It has been shown to have no sequence similarity with Ob-R. By *in situ* hybridisation, Mercer *et al.,* (2000) identified Leprot expression sites and found that it colocalised with Ob-R mRNA within the hypothalamus. More recently, it was shown that, by negatively regulating Ob-R cell surface expression, Leprot is involved in Ob-R intracellular transport (Couturier *et al.*, 2007). Further, inhibiting hypothalamic Leprot expression prevented the development of diet-induced obesity in high fat-fed mice (Couturier *et al.*, 2007). According to these results, Leprot could play an important role in the regulation of leptin sensitivity.

Suppressor of cytokine signalling 3

By binding to its receptor, leptin induces hypothalamic SOCS3 expression (Bjorbaek *et al.*, 1998; Bjorbaek *et al.*, 1999). Earlier studies showed that leptin signalling is negatively regulated by SOCS3. In fact, SOCS3 provides its negative feedback by binding to JAK2 and also to the phosphorylated Tyr985 of Ob-R (Bjorbak *et al.*, 2000; Dunn *et al.*, 2005). Exogenous SOCS3 was shown to block Ob-R signalling in cultured cells, whereas Ob-R activity was enhanced by hypothalamic deletion of SOCS3 (Howard *et al.*, 2004). Furthermore, SOCS3 deficiency enhances Stat3 phosphorylation, resulting in increased hypothalamic

POMC expression and decreased feeding and body weight (Mori *et al.*, 2004). In light of these results, it has been proposed that SOCS3 over activity is involved in the development of leptin resistance (Howard *et al.*, 2004; Mori *et al.*, 2004; Dunn *et al.*, 2005).

SH2-domain-containing protein tyrosine phosphatase 2/extracellular-signal-regulated kinase pathway

As mentioned above, leptin leads to the phosphorylation of Tyr985, which in turn recruits the tyrosine phosphatase SHP2. This binding has been demonstrated to activate the extracellular-signal-regulated kinase (ERK or mitogen-activated protein kinase) signalling, an ensemble of serine/threonine kinases involved in the regulation of cellular physiology and gene transcription (Bjorbaek *et al.*, 1997; Takahashi *et al.*, 1997; Banks *et al.*, 2000; Bjorbaek *et al.*, 2001). Specific neuronal deletion of SHP2 was shown to induce leptin resistance and obesity, with increased adiposity and circulating leptin levels (Zhang *et al.*, 2004). Additionally, pharmacological inhibition of hypothalamic ERK reverses the anorexigenic effects of leptin, without decreasing leptin activation of Stat3 or PI3K (Rahmouni *et al.*, 2009). These observations suggest that SHP2/ERK pathway and SOCS3 are opposite pathways that compete for Ob-R Tyr985 (Bjorbaek *et al.*, 2001) and play a critical role in modulating leptin sensitivity.

Phosphatidylinositol 3 kinase/phosphatase and tensin homolog/protein kinase B pathway

The phosphatidylinositol 3 kinase/phosphatase and tensin homolog/protein kinase B (PI3K/PTEN/Akt) pathway also plays a role in leptin signalling and control of food intake. PI3K phosphorylates phosphatidylinositol-4,5-biphosphate (PIP2) into phosphatidylinositol-3,4,5-triphosphate (PIP3), which in turns activates Akt by phosphorylation (Paez and Sellers, 2003). Studies have demonstrated that leptin increases hypothalamic PIP3 levels (Mirshamsi *et al.*, 2004; Xu *et al.*, 2005b). Furthermore, the anorexigenic effects of leptin are abolished by inhibiting PI3K (Niswender *et al.*, 2001; Niswender and Schwartz, 2003).

The PI3K pathway can be antagonised by PTEN. Thus, PTEN has been shown to dephosphorylate PIP3 (Maehama and Dixon, 1998, 1999), therefore inhibiting the PI3K/Akt pathway. Conversely, leptin has also been shown to be able to inhibit PTEN action through effects on the PI3K/Akt pathway (Ning *et al.*, 2006; Ning *et al.*, 2009).

When Akt is activated it regulates several cellular functions, including gene transcription (e.g. forkhead transcription factor). It has been suggested that forkhead box-containing protein-O1 (FoxO1) could be an important downstream mediator of the PI3K pathway. For example, studies have demonstrated that nuclear FoxO1 stimulates the gene transcription of NPY and AgRP, while inhibiting POMC transcription (Kim *et al.*, 2006; Kitamura *et al.*, 2006). Interestingly, FoxO1 action can be inhibited by Akt. In fact, there is evidence to indicate that Akt phosphorylates FoxO1, resulting in its nuclear exclusion and proteosomal degradation (Matsuzaki *et al.*, 2003; Aoki *et al.*, 2004), thereby inhibiting its orexigenic action (see detailed diagram of PI3K/PTEN/Akt pathway in Chapter 6, Figure 6.2). Taken together, these

results suggest that the anorexigenic action of leptin is mediated by the PI3K pathway.

Protein tyrosine phosphatase 1B

Another negative regulator of leptin signalling is protein tyrosine phosphatase 1B (PTP1B). It has been shown that PTP1B regulates leptin signal transduction both *in vivo* (Cheng *et al.*, 2002; Zabolotny *et al.*, 2002) and *in vitro* (Kaszubska *et al.*, 2002). PTP1B exerts its negative feedback on leptin receptor signalling by binding to and dephosphorylating JAK2 (Cheng *et al.*, 2002; Zabolotny *et al.*, 2002). It also has been reported that mice lacking PTP1B are resistant to diet-induced obesity (Klaman *et al.*, 2000; Zabolotny *et al.*, 2002). These findings indicate that PTP1B is a potent inhibitor of leptin signalling in the hypothalamus.

SH2 B adaptor protein 1

The downregulation of SH2 B adaptor protein 1 (SH2B1) is another possible mechanism leading to leptin resistance. As explained earlier, leptin stimulates Ob-R autophosphorylation on multiple tyrosine residues. Among these, phosphorylated Tyr813 has been shown to recruit SH2B1, which binds to Tyr813 via its SH2 domain, thereby resulting in enhanced JAK2 activity (Rui and Carter-Su, 1999; Li *et al.*, 2007b). Studies on the role of SH2B1 in feeding regulation have shown that its genetic deletion results in hyperphagic obesity with leptin resistance (Ren *et al.*, 2005; Li *et al.*, 2006). Furthermore, these effects are reversed in mice overexpressing SH2B1 (Ren *et al.*, 2007). Taken together, these data indicate that SH2B1 is another potent mediator of the effect of leptin in the hypothalamus.

1.7. Summary and aims

It is evident that leptin plays a crucial role in signalling the state of bodily adiposity to the brain. Furthermore, increasing facts support the idea that leptin resistance is closely correlated with obesity. However, the exact roles of leptin in the development of obesity and leptin resistance are still not clear. Increased circulating leptin levels observed during the development of obesity have generally been treated as a consequence rather than a cause of leptin resistance and obesity. At present, the precise sequence of mechanisms involved in leptin resistance and obesity remain incompletely elucidated. However, it is clear that leptin directly targets specific hypothalamic neuronal subpopulations located in different regions (Arc, PVN, LHA, DMH, VMH); particularly implicating NPY/AgRP and POMC/CART neurons. These leptin-responsive cells directly or indirectly interconnect between hypothalamic nuclei, thus forming a complex neuronal circuitry that ultimately controls the balance between energy intake and energy expenditure.

Other genetic factors, such as ciliopathies, have also been implicated in the regulation of feeding behaviour and energy expenditure. However, the exact mechanisms underlying these defects are currently under investigation. Particularly in the case of BBS, it has been proposed that hypothalamic leptin sensitivity/leptin signalling pathways could be affected by primary cilia deficiency. Whether this could also be the case in Alström syndrome remains unclear, and is a primary focus of research within this thesis.

Leptin controls energy intake and expenditure via its action on hypothalamic Ob-R. The downstream pathways of activated Ob-R are numerous. It would be of great interest to understand whether and how positive (e.g. SH2B1) and negative

(e.g. SOCS3, PTP1B) mediators interact or are dysregulated during the development of leptin resistance and obesity.

The overall aim of the studies presented in this thesis was to characterise the role of hypothalamic primary cilia and the downstream effectors of the leptin signalling pathway in the *foz/foz* model of leptin resistance and obesity. Particular attention has been given to hypothalamic localisation and/or expression of primary cilia, the key appetite-regulating signalling pathways, and neuropeptides (NPY, AgRP, MCH, POMC, CART, CRH). An additional focus has been on leptin receptor second messengers (including Stat3, SOCS3, PTP1B, SHP2/ERK, PI3K/Akt). The general strategy was to characterise the effects of genotype and diet over time in *foz/foz* mice and their wildtype littermates. Specific hypotheses and aims are iterated in each Chapter.

CHAPTER 2

Chapter 2

Materials and methods

2.1. Materials used

Tables 2.1, 2.2, and 2.4 list the antibodies used, the dilutions, and the suppliers.

Chemicals, solvents, kits and cell culture media were obtained from the following suppliers:

Sigma-Adrich®, St Louis, MO, USA: glycogen, Tween® 20, bovine serum albumin (BSA), TRI Reagent®, ammonium persulfate (APS), isopropanol, sodium dodecyl sulfate (SDS), sodium hydroxide, agar, guanidine hydrochloride, Triton® X-100 (*Fluka*), poly-L-lysine, Insulin (bovine pancreas), chloroform, phosphatase inhibitor cocktail 1, phosphatase inhibitor cocktail 2, protease inhibitor cocktail, Dnase I, HEPES, EGTA, glycerol

Bio-Rad, Hercules, CA, USA: 30% acrylamide, Precision Plus Protein™ All Blue Standard, iQ™ SYBR® Green Supermix, Immun-Star™ WesternC™ Chemiluminescent Kit, DC™ Protein Assay Kit

ProSciTech, Kirwan, Qld, Australia: 16% paraformaldehyde, Coverslip No. 1 Ø 13 mm

Troy Laboratories, Smithfield, NSW, Australia: Ketamil (100 mg/ml), Ilium; Xylazil-20 (20 mg/ml), Ilium

Invitrogen™, Carlsbad, CA, USA: SuperScript® III Reverse Transcriptase, HiMark™ Pre-stained High Molecular Weight Protein Standard, Neurobasal® A, EBSS, HBSS, B-27® Supplement, GlutaMAX™, L-glutamine, penicillin/streptomycin, 100 mM dNTP Set, Fetal Bovine Serum

Amresco®, Solon, OH, USA: Tris, phosphate buffer saline (PBS) tablets, glycine, sodium chloride

R&D systems, Minneapolis, MN, USA: Mouse Leptin Quantikine® ELISA Kit, Recombinant Mouse EGF

Vector Laboratories, Burlingame, CA, USA: Vectashield® Mounting Medium™ Hard Set

Others: Adhesive Loctite® 406™; PlusOne™ TEMED*, Amersham Biosciences (GE Healthecare Bio-Sciences), Piscataway, NJ, USA;* SuperSignal West Pico Chemiluminescent, *Thermo Scientific, Waltham, MA, USA*; ReBlot Plus Strong Antibody Stripping Solution, *Millipore, Billerica, MA, USA*; Papain suspension, *Worthington, Lakewood, NJ, USA*; Transferrin Holo Bovine plasma, *Calbiochem®, EMD Chemicals, Gibbstown, NJ, USA*

2.2. Animal methods

2.2.1. Mice

Female NOD.B10 wildtype (WT) and *foz/foz* mice were bred and maintained in The Canberra Hospital Animal Facility. Mice were housed in groups of 3 to 5 mice per cage, under 12-hour light/dark cycle, and had *ad-libitum* access to food and water. Mice used for the experiments were either newborn (day 1-4), or aged 3 (weaning), 8 (TC2) or 18 (TC12) weeks. All experiments were performed in accordance with the Australian National Health and Medical Research Council standards of animal ethics, under Animal Ethics Protocol Numbers F.MS.07.05 and F.MS.16.08; approved by The Australian National University Animal Experimentation Ethics Committee (AEEC).

NB: only female mice were used in these studies because female *foz/foz* mice have been better characterised than males. Although the obese phenotype is the same between male and female *foz/foz* mice, the deposition of fat is greater in females. Furthermore, male *foz/foz* mice die at a younger age than females, therefore females are more appropriate for long term studies. Finally, for reasons of animal ethics (minimisation of use), it was convenient to use female mice in this work as male littermates were used for quite different studies.

2.2.2. Diets

Mice were fed two different types of diet. Standard rodent chow was obtained from Gordon's Specialty Stockfeeds (Irradiated rat/mouse pellets), and the

high fat diet (HFD) was from Glen Forrest Specialty Feeds (SF03-020, 23% Fat, Simple Carbohydrate, 0.19% cholesterol; kept at 4°C until required).

At 21 days of age (corresponding to weaning), all mice were put on chow for 3 weeks, at which time half the mice were changed to high fat diet administration while the other half remained on chow diet for either 2 (TC2) or 12 (TC12) weeks (Figure 2.1).

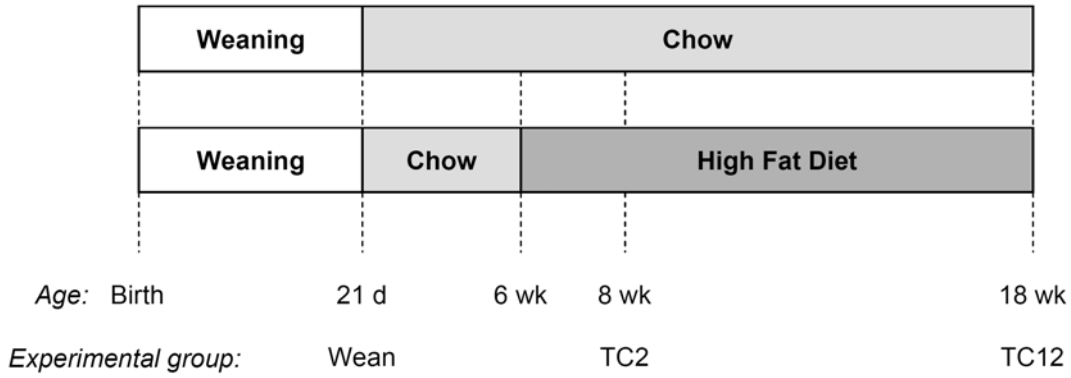

Figure 2.1. Feeding time course protocol, including 'key' to experimental group notation

2.2.3. Protocols and corresponding experimental groups

The following diagrams (Figures 2.2, 2.3, 2.4) represent the different experimental procedures performed to collect tissues. The genotype, diet, and number of animal used for each time point are given for each experiment. Blood was collected by cardiac puncture. Brains (hypothalami) were harvested for immunohistofluorescence (IHF), and to extract RNA and protein.

Figure 2.2. Animal groups used for protein extraction

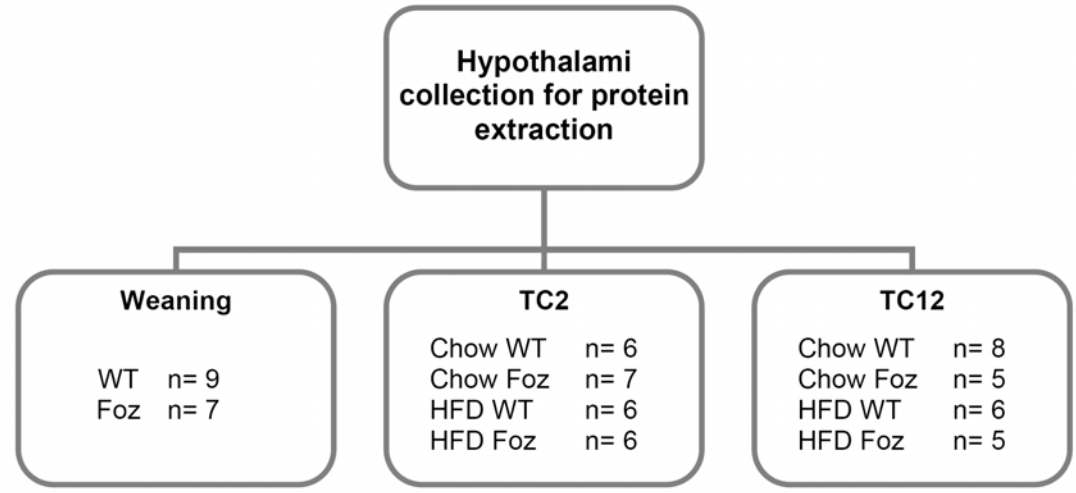

Figure 2.3. Animal groups used for RNA extraction

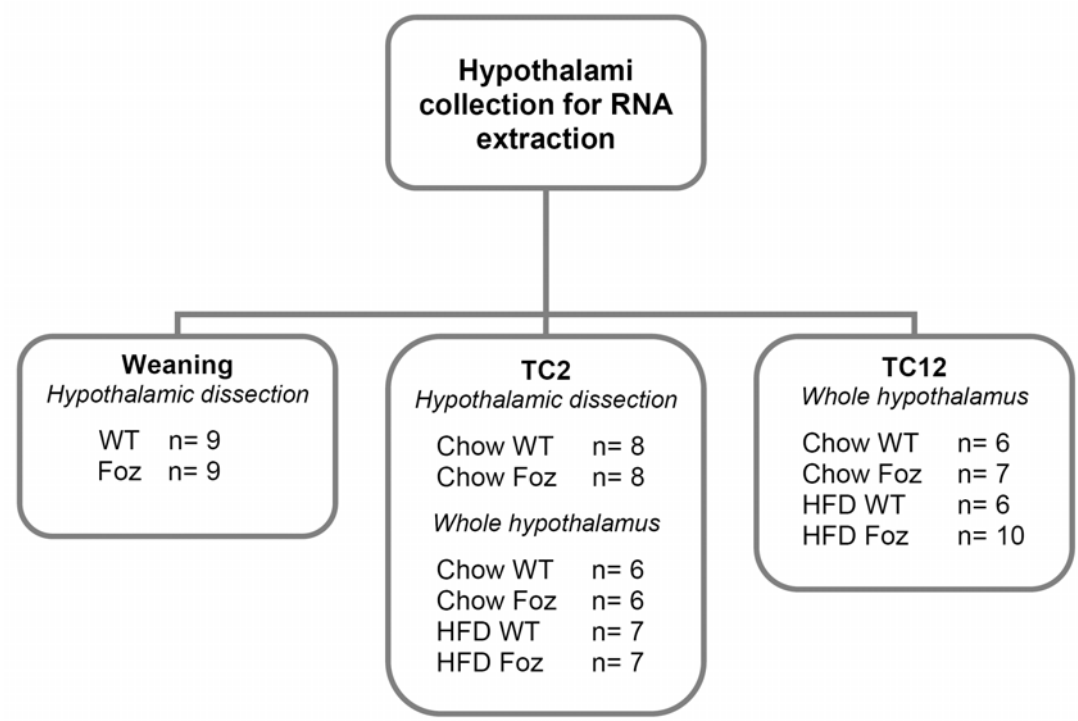

Abbreviations: Foz, *foz/foz;* HFD, high fat diet; WT, wildtype

Figure 2.4. Animal groups for cardiac perfusion to fix brains prior to immunohistofluorescence

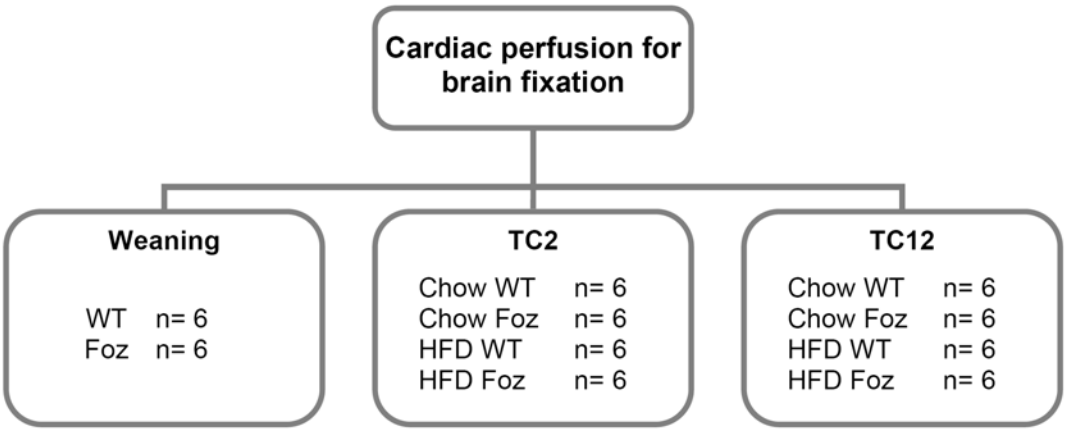

Abbreviations: Foz, *foz/foz;* HFD, high fat diet; WT, wildtype
NB: brain fixation from newborn mice (post-natal day 1-4) was performed by immersing the whole brain in 4% paraformaldehyde for 12h; WT, n = 5; Foz, n = 7.

2.3. Fresh tissue collection

Following a 4 hour fast, mice were anaesthetised by an intraperitoneal (i.p.) injection of ketamine hydrochloride (10 mg/kg body weight) and xylazine hydrochloride (2 mg/kg body weight). Blood was collected by cardiac puncture and serum was obtained after blood centrifugation (3500 rpm for 10 min at 4°C). Immediately following cardiac puncture, anaesthetised mice were decapitated. The skull was put on view and an incision made to expose the brain. Using a fine spatula, the dura (covering of the brain) was cut and the brain was removed from the skull for dissection of the whole hypothalamus or hypothalamic nuclei (Sections 2.3.1 and 2.3.2). Dissected hypothalamic were rapidly frozen in liquid

nitrogen and stored at -80°C for further experiments. Liver, gastrocnemius muscle, intestine, peri-ovarian white adipose tissue, subcutaneous white adipose tissue and brown adipose tissue were also collected and stored for later use, if required.

2.3.1. Dissection of the whole hypothalamus

After the brain had been removed from the skull and placed ventral side up, the hypothalamus was collected by dissection, using curved forceps. Briefly, the curved forceps was used to push down around the hypothalamus and gently "scoop" this region out from the rest of the brain, as described by Zapala *et al.* (2005). The method of removal, while pushing down with the forceps, is shown in Figure 2.5.

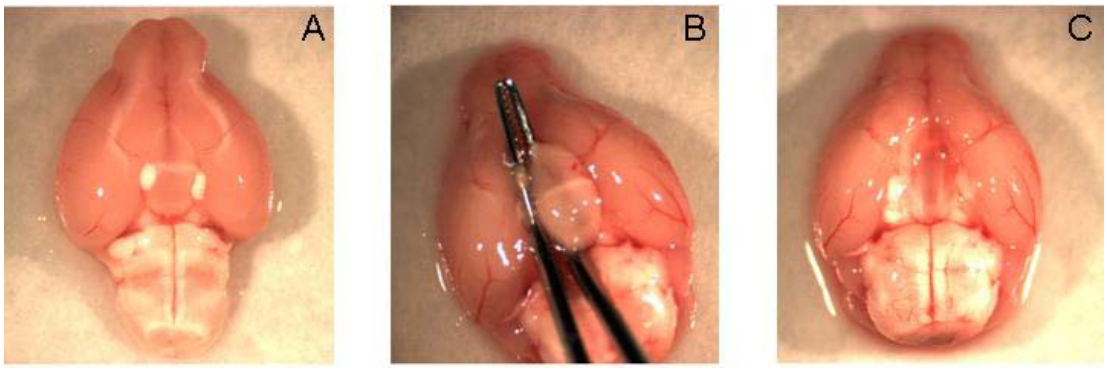

Figure 2.5. Whole hypothalamic dissection
(A) The brain was removed from the skull and placed ventral side up. (B) The hypothalamus was extracted using a pair of curved forceps. (C) After hypothalamic removal there should be a depression visible in the brain where the hypothalamus was excised. Reproduced from Zapala *et al.,* 2005.

2.3.2. Dissection of hypothalamic nuclei

Several regions of the hypothalamus were dissected using a method previously described by Hansen *et al.* (2001). Brains collected from mice were snap frozen in liquid nitrogen and placed ventral side up on a petri dish. The first section was made at the optic chiasma. The second section was made 1 mm caudal, the brain slice removed was placed rostral side down and labelled as slice 1 (Figure 2.6.A). The third section was made 1.5 mm caudal from cut 2, placed caudal side down and labelled as slice 2 (Figure 2.6.B). Hypothalamic slices were then cut at different angles, the dorsal segment containing the paraventricular nucleus (PVN) and a ventral segment containing the anterior hypothalamic area (AH; Figure 2.6.C). Figure 2.6.D illustrates the cuts made in slice 2 to yield the arcuate nucleus (Arc) from the ventral surface by dissecting out the medial triangle. Each dissected region was weighed immediately in labelled, pre-weighed 2 ml Eppendorfs and stored at -80°C for later analysis. As can be seen in Figure 2.6.E, the weight of tissue collected was consistent across groups.

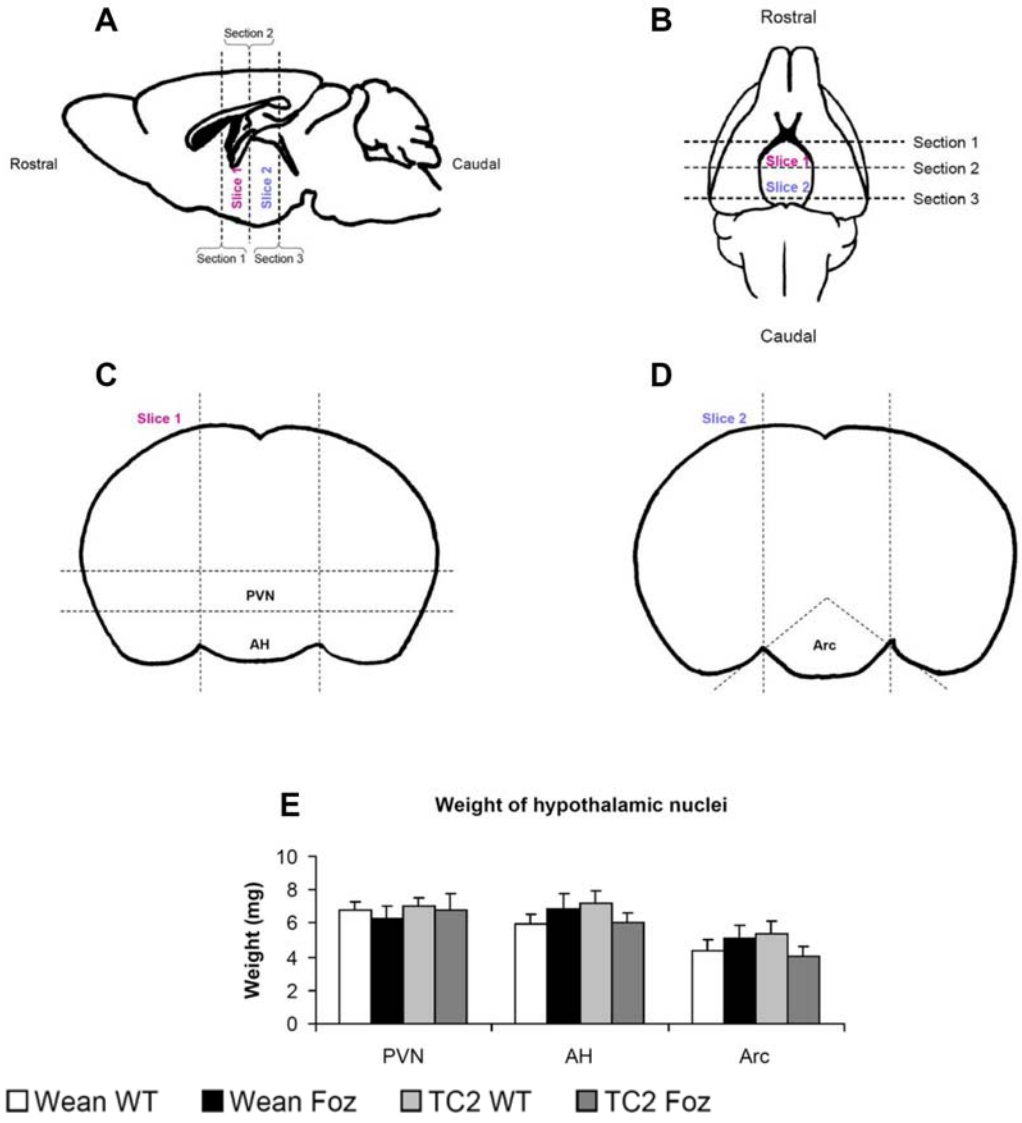

Figure 2.6. Hypothalamic nuclei dissection

A: Lateral view of the brain with dotted lines indicating cuts.

B: Ventral view of the brain, dotted lines indicating where sections are made.

C: Caudal view of slice 1 (rostral side down) with the dotted lines indicating the cuts needed to be made in order to isolate PVN and AH.

D: Rostral view of slice 2 (dorsal side down) with dotted lines indicating the cuts needed to isolated the Arc.

E: Average weight of the different isolated hypothalamic nuclei at weaning and TC2 in WT and *foz/foz* mice.

Abbreviations: AH, Anterior hypothalamic area; Arc, Arcuate nucleus; Foz, *foz/foz;* PVN, Paraventricular nucleus; WT, wildtype

2.4. Preparation of perfused tissue

2.4.1. Cardiac perfusion for brain fixation

Mice were fasted 4 hours before sacrifice. Mice were then weighed and anaesthetised (ketamine, xylazine), the heart exposed and perfusion established through the left ventricle into the aorta with cold PBS. Perfusion was continued until the exudate issuing from the atrium was clear. This was followed by perfusing with 4% paraformaldehyde (PFA) in PBS at 4°C for 15 min. Once perfused, the brain was removed from skull (described in Section 2.3), and postfixed overnight at 4°C in 4% PFA. Brain was then washed three times in PBS and stored in PBS at 4°C until sectioning.

For neonatal brain fixation, brains were collected between day 1 and 4 after birth, rinsed in PBS, and then immersed in 4% PFA for 12h. Fixed brains were then washed three times in PBS and stored in PBS at 4°C until sectioning.

2.4.2. Vibrating blade microtome sections

Fixed brains were dried and dissected caudally and rostrally from the hypothalamus. Hypothalami were then embedded in melted 4% agar (in water) and left to set for 15 min at room temperature. Moulds were mounted with Adhesive Loctite® glue on the vibrating blade microtome (VT1000 S, Leica, Germany) disc and immersed in PBS. 40 to 45 µm floating sections were cut, agar surrounding the

tissue was removed, and sections were collected in 24-well plates in PBS and stored at 4°C until staining.

2.5. Biochemical methods

2.5.1. Serum analyses

At the time of experiments, mice were anaesthetised and blood was collected by cardiac puncture to obtain serum after blood centrifugation (3500 rpm for 10 min at 4°C). Leptin concentration was measured in diluted serum (dilution range from 1:5 to 1:80) using a commercial enzyme-linked immunosorbent assay (ELISA) kit (Quantikine® Mouse leptin, R&D Systems, USA) according to the Manufacturer's instructions.

2.5.2. Immunohistofluorescence

2.5.2.1. Single labelling

Antibody dilutions and incubations time are listed in Tables 2.1 and 2.2. All incubations were performed using light agitation. Free floating sections were washed three times in PBS for 10 min at room temperature. Sections were blocked and permeabilised with a solution of 2% BSA, 0.5% Triton® X-100 in tris-buffered saline (TBS) for 1h at room temperature. The solution was aspirated and replaced

with primary antibody diluted in PBS overnight at 4°C (see Table 2.1 for primary antibody dilutions). Sections were washed three times for 10 min in PBS at room temperature. The secondary antibody was diluted in PBS (see Table 2.2 for dilutions) and applied for 1h at room temperature in the dark. The secondary antibody was removed by washing three times in PBS in the dark. Sections were mounted on slides and left to air dry in the dark. Slides were covered with coverslips with Vectashield® Mounting Medium™ Hard Set. They were then stored, protected from light, at 4°C. Immunostained tissue sections were viewed using an Olympus IX71 inverted microscope, and images were captured with a DP71 camera coupled to a U-RFL-T mecury burner (Olympus, Japan).

The specificity of the primary antibodies was tested when the corresponding control peptides were available. Negative controls for each antibody were established by pre-incubating the antibody with its control peptide (10 times in excess) in PBS for 1h at room temperature before application on hypothalamic sections. Non-specific staining due to secondary antibody was tested by omitting the primary antibody.

2.5.2.2. Double labelling

Blocking and permeabilisation protocols are the same as described in section 2.5.2.1. Free floating sections were incubated with two primary antibodies (raised in different species) diluted in PBS overnight at 4°C. Sections were washed three times in PBS for 10 min at room temperature. Secondary antibodies diluted in PBS were applied for 1h at room temperature in the dark. Sections were washed

three times in the dark and mounted on slides and left to air dry in the dark. Slides were covered with coverslips with Vectashield® Mounting Medium™ Hard Set, and stored, protected from light, at 4°C. Antibody dilutions and incubation times are listed in Table 2.1 and 2.2.

Table 2.1. Sources and conditions of primary antibodies used for immunofluorescence

Abbreviations are listed on page xviii

Protein	Host	Supplier	Primary antibody dilutions	Conditions for incubation
ACIII	Rabbit	Santa Cruz Biotechnology	1:500	3h, RT or overnight, 4°C
AgRP	Goat	R&D systems	1:20	overnight, 4°C or 1h, 37°C
Alms1	Rat	Custom made by Monash Antibody Technologies Facility	Clone 3D8 1:1000	overnight, 4°C
CART	Rabbit	Phoenix Pharmaceuticals	1:1500	overnight, 4°C
NeuN	Mouse	Millipore	1:100	overnight, 4°C
NPY	Rabbit	Abcam	1:1000	overnight, 4°C or 1h, 37°C or 2h, RT
Ob-R	Rabbit	Santa Cruz Biotechnology	1:200	overnight, 4°C

NB: Alms1 antibody was produced at the Monash Antibody Technologies Facility (MATF, Melbourne, Australia; http://www.matf.monash.org/). Briefly, rats were immunised three times with the Alms1 peptide (Li *et al.*, 2007a). Serum ELISA were then performed to measure the antibody titre. Splenocytes were isolated, and B cells were fused with myeloma to produce hybridomas. Hybridomas were screened and those producing antibodies were selected and cloned. Supernatant from several clones were provided by MATF and were tested in IHF, ICF and western blot applications. The clone 3D8 was chosen as it gave the best results in all protocols tested. Mass production of 3D8 then started at the Research School of Biology at the Australian National University (Canberra, Australia) under the supervision of Jan Eliott. The 3D8 clones were grown until 1l of supernatant was obtained. Alms1 antibody was then purified by Dr Peter Milburn at the ACRF Biomolecular Resource Facility (John Curtin School of Medical Research, Australian National University).

Table 2.2. Sources and conditions of secondary antibodies used for immunofluorescence

Secondary antibody	Supplier	Secondary antibody dilutions	Conditions for incubation
Donkey anti-rabbit Cy3	Jackson ImmunoResearch Laboratories	1:1000	1h, RT
Donkey anti-goat Cy3	Jackson ImmunoResearch Laboratories	1:1000	1h, RT
Donkey anti-mouse Cy3	Jackson ImmunoResearch Laboratories	1:1000	1h, RT
Goat anti-rat Alexa fluor® 546	Invitrogen™, Molecular Probes®	1:1000	1h, RT
Chicken anti-rabbit Alexa fluor®488	Invitrogen™, Molecular Probes®	1:1000	1h, RT
Chicken anti-goat Alexa fluor®488	Invitrogen™, Molecular Probes®	1:1000	1h, RT
Goat anti-mouse Alexa fluor®488	Invitrogen™, Molecular Probes®	1:1000	1h, RT
Chicken anti-rat Alexa fluor®488	Invitrogen™, Molecular Probes®	1:1000	1h, RT
Goat anti-rabbit IgG biotin	Santa Cruz Biotechnology	1:200	1h, RT
Streptavidin Alexa fluor®488	Invitrogen™	1:200	1h, RT

NB: Ob-R primary antibody (Santa Cruz Biotechnology, USA) was detected via biotin-streptavidin conjugated to Alexa fluor® 488 to enhance detection. Briefly, sections were washed in PBS, incubated with primary Ob-R antibody overnight at 4°C. Sections were washed again in PBS, then incubated with goat anti-rabbit biotin conjugated 1h at room temperature. After several PBS washes sections were incubated with streptavidin Alexa fluor® 488 conjugated for 1h at room temperature (RT). Sections were then mounted, following the protocol described in section 2.5.2.1.

2.5.3. Immunohistofluorescence analyses

Hypothalamic sections stained for NPY, CART, AgRP and Ob-R were analysed at the John Curtin School of Medical Research Microscopy and Cytometry Resource Facility using Image-Pro Plus (version 6.2) from MediaCybernetics (USA). Image-Pro Plus is an image-processing software working under Windows©. A custom plug-in especially designed by an applications specialist from the company was used to process the pictures. Briefly, the pictures were resized at 2040x1536 pixels and converted into 8-bit gray scale images in order to be analysed. The plug-in was then applied individually to each picture. A pseudocolour image was obtained for each brain section corresponding to a colour scale illustration of AgRP, NPY, CART and Ob-R immunoreactivity in the hypothalamus. In this system the intensity of labelling varies from blue to red; blue indicates no staining and red reflects high fluorescence. It was not possible to determine the total number of immunoreactive cells because most of the staining was found in fibres. The boundaries of nuclei were determined according to The Mouse Brain in Stereotaxic Coordinates Third Edition, Keith B.J. Fraklin & George Paxinos, Elsevier (2008).

Picture analysis for ACIII/NeuN colocalisation was performed as follows: two sections per brain were immunostained, as described in section 2.5.2.2. Three pictures per hypothalamic brain section were taken. These were processed using Pixcavator IA Student Edition (version 4.2.0.0, Intelligent Perception, USA). This software captures the contours of all objects in the image and counts them in a spreadsheet. Objects of the unwanted size or colour are removed, depending on their size, contrast and intensity. Consequently, each cilium and neuron are isolated individually to permit them to be counted. The percentage of ciliated cells per image

was calculated, the average estimated per animal, and finally per experimental group.

In order to measure the length of primary cilia, high magnification pictures from sections stained for ACIII were used. Briefly, three pictures were acquired per animal, and three measurements per picture were taken with Image-Pro Plus software. An average of primary cilium length per animal was calculated, and the mean per group was obtained.

2.6. Molecular methods

Hypothalamic expression of gene transcripts and proteins for neuropeptides, receptors and receptor signalling pathways involved in food intake regulation were assessed by real time polymerase chain reaction (RT PCR) and Western blot analysis.

2.6.1. Gene expression

2.6.1.1. RNA extraction

RNA was extracted from whole hypothalamus or from dissected hypothalamic nuclei using TRI Reagent®. Approximately 50 mg of whole hypothalamus tissue was homogenised in TRI Reagent® (1 ml for whole hypothalamus). Cell debris was removed by centrifugation, and chloroform added to

separate RNA from DNA and protein. The aqueous phase containing RNA was transferred to a sterile tube, and RNA was precipitated by mixing with isopropanol and 5 M sodium chloride (NaCl). After centrifugation, RNA was washed with 75% ethanol, then resuspended in 50 µl of diethylpyrocarbonate (DEPC)-treated water. RNA was quantitated using spectrophotometry and quality assessed by A260:280 ratio and by separation of RNA by electrophoresis on a denaturing gel.

2.6.1.2. RNA extraction from dissected hypothalamic nuclei

The RNA extraction protocol described in section 2.6.1.1 was modified to allow RNA extraction from tissues weighing ~10 mg. Tissues were homogenised in 800 µl of TRI Reagent® containing 200 µg of glycogen with an autoclavable polypropylene pestle (Sigma-Aldrich - Z359947) followed by 5 min incubation at RT. Genomic DNA was sheared by passing samples twice through a 26-gauge needle. Debris was removed by centrifugation. Chloroform was then added (160 µl) to separate RNA from DNA and proteins. After centrifugation, the aqueous phase was transferred to a new sterile tube and RNA was precipitated by adding 400 µl of ice-cold isopropanol overnight at -20°C. After centrifugation, RNA was washed with 200 µl of 70% ethanol. Pellets were air dried and resuspended in 40 µl of DEPC-treated water. RNA was quantitated using spectrophotometry (NanoDrop™ 1000, Thermo Scientific, USA), and stored at -80°C.

2.6.1.3. cDNA synthesis

In order to perform gene expression analysis, cDNA was synthesised by reverse transcription using SuperScript™ III Reverse Transcriptase (Invitrogen™, USA). Briefly, 5 µg of RNA extracted from the whole hypothalamus, or 1 µg of RNA extracted from hypothalamic nuclei, was incubated with 0.5 µg of random primers and 10 mM of dNTPs (Invitrogen™, USA) in DEPC-treated water. After incubating for 10 min at 65°C, 5X first strand synthesis buffer, 0.1 M dithiothreitol (DTT) and SuperScript™ III enzyme (200 units/µl) were added and incubated for 5 min at 25°C, 1h at 50°C and then 15 min at 72°C to inactivate the reverse transcriptase enzyme. 30 µl of PCR-grade water was added, and cDNA was stored at -20°C.

2.6.1.4. Real time PCR

Primers were designed by using Beacon Designer™ software. Primer sequences are summarised in Table 2.3. Real time PCR was performed on 1:50 diluted cDNA for the whole hypothalamus extracted samples, and 1:20 for the dissected hypothalamic nuclei, using iQ™ SYBR® Green Supermix on the iQ™5 real time thermal cycler (Bio-Rad, USA). Serial pooled cDNA dilutions were used to produce a standard curve for each primer. For each gene, a standard curve was constructed and the starting quantity (SQ) of mRNA was calculated using iQ™5 Optical System Software Version 2.0 and results were then normalised to three housekeeping genes: beta-actin, beta 2-microglobulin (B2M) and ribosomal protein L 13a (RPL13a) and are presented in figures as “relative expression”.

Table 2.3. Primer sequences for real time PCR

Abbreviations are listed on page xviii

Gene	Sense primer	Antisense primer
ACIII	AGA CCG CAA GCA CCG CAA G	GGC AGG ATG GAA AGC ATA AGG TTT
AgRP	GGG CAC AAG AGA CCA GGA CAT C	CAA CAG CAG AAC ACA ACT CAG CAA
Alms1	AGT CAC AGT GTC CAG GAA AGA AGC	GGC AAA TCA GGA GCA GCA AAG TTA
BBS2	GCG GGC AAG GTT TTC ATT CAT AAC	AGG GCT CTG GAA CAC TCT GGA
BBS4	GCT GTT CGC CTG GAT AAG TGT AAC	CGC TCT TCT TCT CAC CCT GGT TAT
Beta-actin	ACC AGT TCG CCA TGG ATG AC	ATG CCG GAG CCG TTG TC
B2M	TCC AGA AAA CCC CTC AAA TTC A	AGT ATG TTC GGC TTC CCA TTC TC
CART	TGA TGC GTC CCA CGA GAA GG	TCG GAA TGC GTT TAC TCT TGA GC
Cep164	CGT TCC CAG TGA GCA AGA AAT CC	TCT CGC CAG CCA CAT CAG TTC
CRH	ACC TAC CAA GGG AGG AGA AGA GAG	GAC AGA GCC ACC AGC AGC AT
DYNC2H1	CGG CGG ACT GTC ACA TCT TTA G	AGA CTA CCT GCT GTG CTT CAA TTC
FoxO1	ATC TAC GAG TGG ATG GTG AAG AGC	GGG ACA GAT TGT GGC GAA TTG AAT
IFT20	TGC CAC TGT CAC CCC TTC AAA G	CCC TGC CTC GCC CAA GAT G
IFT52	CGT GAC TTT ACC ACC CTC TTT GAC	TAG TTC CTC GTG AGC CTT GAT GAC
IFT172	CTC ACC TCA TCA GCG TCC GTA TC	ACC AAT GTT GTA GCC ACC AAT CAG
KiF3A	GGA CCT TCT GAA AGC CCA ACA AG	CCA CGC CGC CGA CAA TGA
Leprot	TGG GAT TGT TGT TTC TGC CTT TGG	ACG AGG AAG AAG CCT TGA ATT GTG
MCH	TGC TGA GTC CAC ACA GGA AAA GAG	ACT TGC CAA CAT GGT CGG TAG A
MCH1R	CAT CAT CAT GCC TTC AGT GTT TGG	AGA TCC ACC ACA GAG AGG TTG AT
MC4-R	CGC TGT CAT CAT CTG CCT CAT TTC	GAA GCC TCG CCA TCA GGA ACA
NPY	GCT CTG CGA CAC TAC ATC AAT CTC	GGC GTT TTC TGT GCT TTC CTT CA
Ob-R	CCA GAC CCT GAA AGC AGT TC	AGG TTA CCT GGG TGC TCT GA
ODF2	GCG GCG GAC TCG TGA TGA TG	CAT GCT GCG GTT GGT ACT CTC A
POMC	TGA ACA TCT TTG TCC CCA GAG AGC	CCT GAG CGA CTG TAG CAG AAT CT
PTP1B	AAG TCC GAG AGT CAG GCT CAC	TTG TCC ATC AGT AAG AGG CAG GT
RPL13a	CCT GCT GCT CTC AAG	GGC TGT CAC TGC CTG
SH2B1	GAG GAA GTC GCT TGG AGT TCT TTG	CAT CTC TAG GGC TGT GGC TGT G
SHP2	TGA CAG ACC TGG TGG AGC ATT AC	CAG CAG CAT TGA TAC GAG TTG TGT
SOCS3	GGA GAT TTC GCT TCG GGA CTA G	GGG AAA CTT GCT GTG GGT GAC
Sstr3	GGA CCA AAC CAG ACG CAA GC	GCC AAC CAG CCC TAA CCT TAC A
Stat3	ACA TTC TGG GCA CGA ACA CAA AAG	AGT CAC GAT CAA GGA GGC ATC AC

2.6.2. Protein analyses

2.6.2.1. Protein extraction

Proteins were extracted by homogenising whole hypothalamus (~50 mg) in nine times homogenising buffer (w/v) in presence of protease and phosphatase inhibitors (see Appendix 1 for buffer details) to make a 10% homogenate. After centrifugation, the supernatant was aliquoted and stored at -80°C.

Protein concentration was estimated using a protein estimation kit (Bio-Rad, USA). Serial BSA dilution was used to generate a standard curve and protein concentration was determined using the standard curve equation. Proteins were then diluted (2 µg/µl) in reducing buffer (Appendix 1), and stored at -20°C.

2.6.2.2. Western blot

Reduced proteins were heated for 5 to 10 min at 90°C in order to optimise the denaturation. Protein (20 µg) was then loaded onto a SDS-PAGE gel. Precision Plus Protein Standard All Blue marker (Bio-Rad, USA) was used to indicate protein migration through the gel. For high molecular weight proteins, HiMark™ Pre-stained High Molecular Weight Protein Standard (Invitrogen™, USA) was used. After separation, proteins were transferred onto Immobilon-P PVDF membrane (Millipore, USA) using a wet transfer technique. Following transfer, membranes were washed in TBST (TBS Tween), blocked, then probed for the protein of interest. Membranes were washed several times in TBST before incubation with secondary antibody

conjugated to horse radish peroxidase (HRP). Bands were detected by enhanced chemiluminescence using Supersignal West Pico Chemiluminescent (Thermo Scientific, USA). Bands were visualised with a luminescent image analyser, LAS-4000 mini (Fujifilm, Japan) and analysed with Multi Gauge 3.0 software (Fujifilm, Japan). Results were normalised to Hsp90 indicated in figures as “relative expression” (see Figure 2.7, example of western blot raw data for Hsp90). Differences were then assessed at each time point for each group. No western blot assays were carried out between different time points due to limited availability of protein material, therefore no comparison between experimental time points were performed. Blocking solution, antibody dilutions and incubation time are collated in Table 2.4.

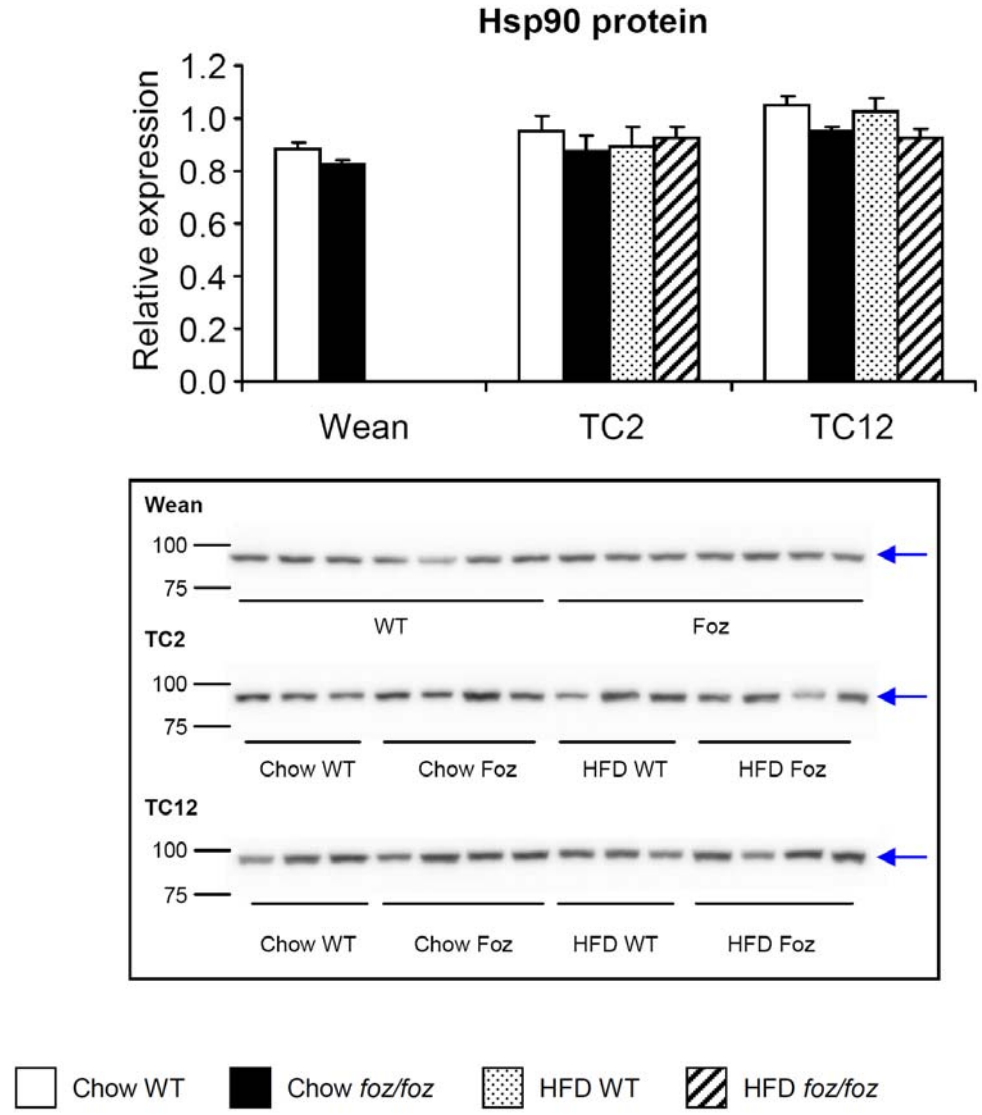

Figure 2.7. Hypothalamic Hsp90 protein expression at weaning and during dietary regimes in *foz/foz* and WT mice

Hsp90 was used as a loading control for western blot analyses. ANOVA confirmed that no significant differences were found between genotype and diet. On the above representative western blot, Hsp90 migrates at 90 kDa (arrows), and is consistent between groups.

Table 2.4. Primary antibody conditions for western blot

All primary antibodies were incubated overnight at 4°C. Secondary antibodies were incubated at room temperature for 1h. All secondary antibodies were obtained from Santa Cruz Biotechnology (Santa Cruz Biotechnology, USA).

Protein	Supplier	Protein size (kDa)	Blocking solution	Primary antibody conditions	Secondary antibody	Secondary antibody conditions
Akt	Cell Signaling	60	3% BSA	1:1000 in 3% BSA	Rabbit	1:10000 in 3% BSA
P-Akt	Cell Signaling	60	3% BSA	1:1000 in 3% BSA	Rabbit	1:10000 in 3% BSA
Alms1	Custom made by Monash University	360	Numerous blocking and antibody conditions were tested with limited success. Western blot protocol for Alms1 requires further optimisation			
ERK	Cell Signaling	42	5% Skim	1:1000 in 5% BSA	Rabbit	1:10000 in 1% Skim
P-ERK	Cell Signaling	42	5% Skim	1:1000 in 5% BSA	Rabbit	1:10000 in 1% Skim
Hsp90	R & D	90	5% Skim	1:1000 in 2% Skim	Goat	1:10000 in 2% Skim
MC4-R	Cayman	37	5% Skim	1:500 in 5% Skim	Rabbit	1:10000 in 5% Skim
Ob-R	ABR	100	5% Skim	1:2000 in 5% Skim	Rabbit	1:10000 in 5% Skim
POMC	Novus	26-28	2% Skim	1:500 in 2% Skim	Goat	1:10000 in 2% skim
PTEN	Cell Signaling	54	5% Skim	1:1000 in 5% BSA	Rabbit	1:10000 in 5% Skim
P-PTEN	Cell Signaling	54	5% Skim	1:500 in 5% BSA	Rabbit	1:7500 in 1% Skim
PTP1B	R & D	50	5% Skim	1:500 in 5% Skim	Goat	1:10000 in 5% Skim
SOCS3	R & D	25	5% Skim	1:5000 in 5% Skim	Mouse	1:10000 in 5% Skim
SHP2	Cell Signaling	72	5% Skim	1:1000 in 5% BSA	Rabbit	1:10000 in 1% Skim
P-SHP2	Cell Signaling	72	5% Skim	1:1000 in 5% BSA	Rabbit	1:10000 in 1% Skim
Stat3	Abcam	80	5% Skim	1:100 in 5% Skim	Mouse	1:10000 in 5% Skim
P-Stat3	Abcam	80	5% Skim	1:250 in 5% Skim	Rabbit	1:10000 in 5% Skim

2.7. Cell culture experiments

2.7.1. Hypothalamic primary neuronal culture

2.7.1.1. Coverslip preparation

Coverslips (Ø 13 mm) were sterilised by soaking in 70% ethanol for 1h, followed by rinsing with distilled water. They were then air dried, flamed, and stored in sterile 24-well plates. Poly-L-lysine solution (Sigma-Aldrich®, USA) was made to a final concentration of 0.1 mg/ml in distilled water. Solution was then sterilised by passage through a 0.22 µm filter. Coverslips were immersed with the poly-L-lysine solution for 3 to 12 h at room temperature, then rinsed three times with sterile water, and finally air dried. To complete the sterilisation process coverslips were placed under UV light for 20 min under sterile conditions.

2.7.1.2. Media preparation

All media and reagents needed for the cell culture experiment were made the day before the experiment, except for the enzyme solution which was made freshly on the day. All media preparations are described in Appendix 1. All media were incubated in a 37°C water bath prior to experiments, enzyme solutions were activated at 37°C in a water bath prior to sterilisation.

2.7.1.3. Preparation of hypothalamic neurons

Hypothalami from new born mice (defined as between post-natal day 1 and 4), were collected in dissection medium. Briefly, after decapitation, the skull was gently removed, the brain extracted and the hypothalamus scooped out (as described in section 2.3.1) and quickly transferred into pre-warmed dissection medium. Under sterile conditions, hypothalamus was then transferred into activated and pre-warmed enzyme solution, with the minimum volume of dissection medium possible. After 20 min incubation in a 37°C water bath, the hypothalamus was washed three times in culture medium, followed by a mechanical dissociation using flame-polished Pasteur pipettes. Supernatant was collected in a new tube, and the trituration step was repeated 6-7 times until tissue was completely dissociated. Cells were then centrifuged at 200 g for 10 min at room temperature. Supernatant was discarded and cells were resuspended in 200 µl of pre-warmed culture medium. Cell density was measured by counting phase-bright cells using a hemocytometer. Cell death was assessed by using trypan blue. Cells were diluted at 7-9 x 10^4 cells/ml in culture medium and 500 µl was added in each well. Once per week 150 µl of medium was removed from each well and replaced with fresh pre-warmed culture medium.

2.7.2. Immunocytofluorescence

2.7.2.1. Single labelling

Antibody dilutions and incubation time are listed in Tables 2.1 and 2.2. All incubations were performed using light agitation. Cells were fixed in 3% PFA for 15 min at room temperature, followed by three washes in PBS. Cells were blocked and permeabilised with a solution of 2% BSA, 0.5% Triton® X-100 in TBS for 10 min at room temperature. The solution was withdrawn and replaced with primary antibody diluted in PBS overnight at 4°C (see Table 2.1 for primary antibodies dilutions). Cells were washed three times in PBS at room temperature. The secondary antibody was diluted in PBS (see Table 2.2 for dilutions) and applied for 1h at room temperature in the dark. The secondary antibody was removed by washing three times in PBS in the dark. Cell-coated coverslips were mounted on slides with Vectashield® Mounting Medium™ Hard Set. Slides were stored, protected from light, at 4°C. Immunostained cells were viewed using an Olympus IX71 inverted microscope, and images were captured with a DP71 camera coupled to a U-RFL-T mecury burner (Olympus, Japan).

As for immunohistofluorescent experiments, the specificity of the primary antibodies was tested when the corresponding control peptides were available. Negative controls for each antibody were established by pre-incubating the antibody with its control peptide (10 times in excess) in PBS for 1h at room temperature before application on cells. Non-specific staining due to secondary antibody was tested by omitting the primary antibody.

2.7.2.2. Double labelling

Blocking and permeabilisation protocols are the same as described in Section 2.7.2.1. Cells were incubated with the first primary antibody diluted in PBS, 3h at room temperature. Cells were washed three times in PBS for 10 min at room temperature; secondary antibody diluted in PBS was applied for 1h at room temperature in the dark. Cells were washed three times in the dark and incubated with second primary antibody diluted in PBS, overnight at 4°C, in the dark. Cells were then washed three times in PBS, followed by incubation with second secondary antibody, diluted in PBS, for 1h at room temperature, in the dark. Cells were mounted on slides with Vectashield® Mounting Medium™ Hard Set, and stored, protected from light, at 4°C. Antibody dilutions and incubation times are listed in Table 2.1 and 2.2.

2.8. Statistical analyses

Statistical analyses were performed using SPSS software (version 19.0, IBM). The effects of genotype and diet were determined via 2-way analysis of variance (ANOVA), followed by Tukey post-hoc testing. The effect of genotype at weaning between *foz/foz* and WT mice was determined by using the Student's T-test. In all cases, $P < 0.05$ was considered significant. Data are presented as mean ± SEM.

CHAPTER 3

Chapter 3

Loss of primary cilia in *foz/foz* mice

3.1. Introduction

Cilia are organelles common to many cell types, including neurons (Dahl, 1963). Primary cilia are solitary and non-motile, comprised of specialised plasma membrane surrounding an organised “core” of microtubules. The assembly of primary cilia is closely related to the cell cycle. It occurs from the distal end of the mother centriole as cells enter growth arrest. It has been suggested that, in the brain, the primary cilium is involved in the transduction of a multitude of stimuli, including concentrations of growth factors, hormones, osmolarity, pH and fluid flow (Singla and Reiter, 2006).

It has been shown that the centrosomal protein of 164 kDa (Cep164) and the outer dense fiber protein 2 (ODF2) are involved in early stages of ciliogenesis (Ishikawa *et al.*, 2005; Graser *et al.*, 2007). Indeed, they are both involved in the docking of the basal body at the plasma membrane (Figure 1.2). The assembly and maintenance of the primary cilium also requires a system of intraflagellar transport proteins (IFT; Rosenbaum and Witman, 2002). This system is involved in the transport of proteins from the cytoplasm to the primary cilium and vice versa (Figure 1.2). Two motor proteins, kinesin-like protein (KiF3A) and cytoplasmic dynein 2 heavy chain 1 (DYNC2H1) drive and transport in the anterograde and retrograde directions, respectively (Figure 1.2). When one of the transport proteins

(IFTs) or one of the transport motors (KiF3A or DYNC2H1) is missing, the cilium cannot be assembled. Davenport *et al*., (2007) also showed that mice with genetic ciliary defects are hyperphagic. Mice with mutations in another group of proteins involved in ciliogenesis and ciliary trafficking, the Bardet-Biedl syndrome (BBS) proteins, develop Bardet-Biedl syndrome (Nachury *et al.*, 2007; Nachury, 2008), a complex of disorders, in which obesity is uniformly part of the phenotype.

Recently, Nordman *et al.,* (2008) showed that adenylate cyclase III (ACIII) gene polymorphisms are associated with obesity in a group of Swedish men. ACIII is a specific neuronal marker for primary cilia (Bishop *et al.*, 2007). It has also been shown in mouse models that ACIII deficiency is involved in obesity. Thus, mice lacking ACIII are obese, and this seems to be due to low locomotor activity, hyperphagia and leptin insensitivity (Wang *et al.*, 2009).

The *foz/foz* mice phenotype was shown to be caused by a mutation in *Alms1* gene leading to a prematurely terminated Alms1 protein (Arsov *et al.*, 2006b). Similarly to BBS, mutations in *Alms1* gene lead to a multisystemic disease with severe metabolic disorders including liver disease, type 2 diabetes, hyperphagia and obesity. Alms1 protein was shown to localise to the primary cilium (Hearn *et al.*, 2005). Furthermore, Collin *et al.,* (2005) developed a mouse model resembling *foz/foz* mice given that they both express a truncated form of Alms1 leading to the same phenotype observed in *foz/foz* mice. All these studies tend to suggest that primary cilia play an important role in obesity-related hyperphagia. These considerations about *Alms1* mutations and likely initial defects, and the role primary cilia in appetite regulation, motivated the present studies into the role of neuronal primary cilia in *foz/foz* mice.

3.2. Purpose of the study

Hypothesis to be tested:

That neuronal primary cilia are involved in appetite dysregulation in *foz/foz* mice.

Aims of this study:

1) Determine whether defects in hypothalamic cilial number and/or length occurs in *Alms1* mutant (*foz/foz*) mice.

2) Determine whether variations in mRNA levels from hypothalamic proteins involved in ciliogenesis and/or cilia trafficking occur in *foz/foz* mice.

3.3. Methods

3.3.1. Animals and diets

Female WT and *foz/foz* mice were bred and maintained in The Canberra Hospital Animal Facility as outlined in Chapter 2 (section 2.2.1). Following brain dissection (see Chapter 2, section 2.3), hypothalami were collected from chow and high fat-fed *foz/foz* and WT mice at birth, weaning, TC2 (8 weeks of age), and TC12 (18 weeks of age) for real time PCR and immunohistofluorescence (IHF) studies.

3.3.2. Gene expression analyses

As detailed in Chapter 2 (section 2.6.1), hypothalamic gene expression was determined by real time PCR. Briefly, hypothalami were snap frozen immediately after collection. RNA was extracted via TRI Reagent® protocol (Sigma-Aldrich, USA). cDNA was synthesised using SuperScript™ III Reverse Transcriptase (Invitrogen™, USA). Real time PCR was then performed using iQ™ SYBR® Green Supermix on the iQ™5 real time thermal cycler (Bio-Rad, USA). Experiments were repeated in duplicate and data normalised to the following housekeeping genes: beta-actin, B2M and RPL13a (specific primers are detailed in Chapter 2, Table 2.3).

3.3.3. Immunohistofluorescence

The localisation, number and length of neuronal primary cilia were assessed by IHF, using the specific cilial marker, ACIII. Briefly, brains from WT and *foz/foz* mice fed chow or high fat diet were collected at birth, weaning, TC2 and TC12 after transcardiac perfusion with 4% paraformaldehyde (see Chapter 2, section 2.4). Brains were then sectioned and IHF performed. ACIII IHF was analysed by counting the number of primary cilia per section in relation to the number of neurons. The latter were detected by neuronal nuclei immunofluorescence (NeuN). The software used to analyse the immunohistofluorescent pictures was Pixcavator (Intelligent Perception, USA). Primary cilium length was assessed by using ImagePro Plus (MediaCybernetics, USA).

3.3.4. Statistical analyses

The effects of genotype, diet and time were compared using 2-way analysis of variance (ANOVA), with Tukey post-hoc testing. Differences between genotypes at birth and weaning were determined by using the Student's T-test. For all comparisons $P < 0.05$ was considered significant. Data are presented as mean ± SEM. The number of individuals (n) per experimental group is given in the text relative to each experiment as well as in Chapter 2, section 2.2.3.

3.4. Results

3.4.1. The number of hypothalamic primary cilia is decreased after birth in *foz/foz* mice

In the first 4 post-natal days, brain fixation could not be achieved by cardiac perfusion because of tiny organs and vessel size. However, brains were collected following decapitation, washed in PBS and immediately soaked in ice-cold 4% paraformaldehyde for 12h. Brains were then washed several times in PBS and sectioned by using a vibrating blade microtome (see section 2.4.2). After several attempts, satisfactory slides of hypothalamic tissue were obtained. The morphology of neuronal nuclei and cilia appeared normal on those sections (Figure 3.1A-D). However, cilia/neuronal colocalisation appeared less compelling than for sections prepared by the usual approach at weaning or later (Figures 3.2 - 3.4). Nonetheless, using the best sections obtained, the number of ciliated nuclei was consistently

~60% in the immediate post-natal period in both *foz/foz* and WT mice (Figures 3.1E, F; 3.5). However, at weaning, the number of ciliated cells was less in *foz/foz* mice compared to their WT littermates (Figure 3.2A-F, Figure 3.5). Thus, in weanling *foz/foz* mice, 19 ± 3.8% of hypothalamic neurons were ciliated, compared to 60 ± 4.0% for weanling WT mice ($P < 0.05$). The percentage of neurons bearing cilia eventually declined in WT mice, in a range of ~34 – 41% (in chow and high fat diet) at TC2 and ~43 – 54% (in chow and high fat diet) at TC12. However, the same pattern of substantially reduced percentage of ciliated cells in *foz/foz* mice versus WT mice was observed at TC2 and TC12, irrespective of whether animals were fed chow or high fat diet. For example, at TC2, *foz/foz* mice fed chow expressed 13 ± 3.8% (Figure 3.3C, E and Figure 3.5) of hypothalamic ciliated cells compared to 34 ± 2.5% for their WT diet-matched littermates ($P < 0.05$; Figure 3.3D, F, Figure 3.5). When fed high fat diet for 2 weeks, 14 ± 4.0% of *foz/foz* mice hypothalamic cells were ciliated compared to 41 ± 5.9% in WT mice ($P < 0.05$; Figure 3.5). When fed chow for 12 weeks, the number of hypothalamic ciliated cells was significantly reduced in *foz/foz* mice (9.0 ± 2.1%) compared to their WT littermates (43 ± 2.8%; $P < 0.05$; Figure 3.4A-F and Figure 3.5). At TC12, high fat-fed *foz/foz* mice expressed 16 ± 2.1% of ciliated cells compared to 54 ± 3.3% for their WT diet-matched littermates ($P < 0.05$; Figure 3.5).

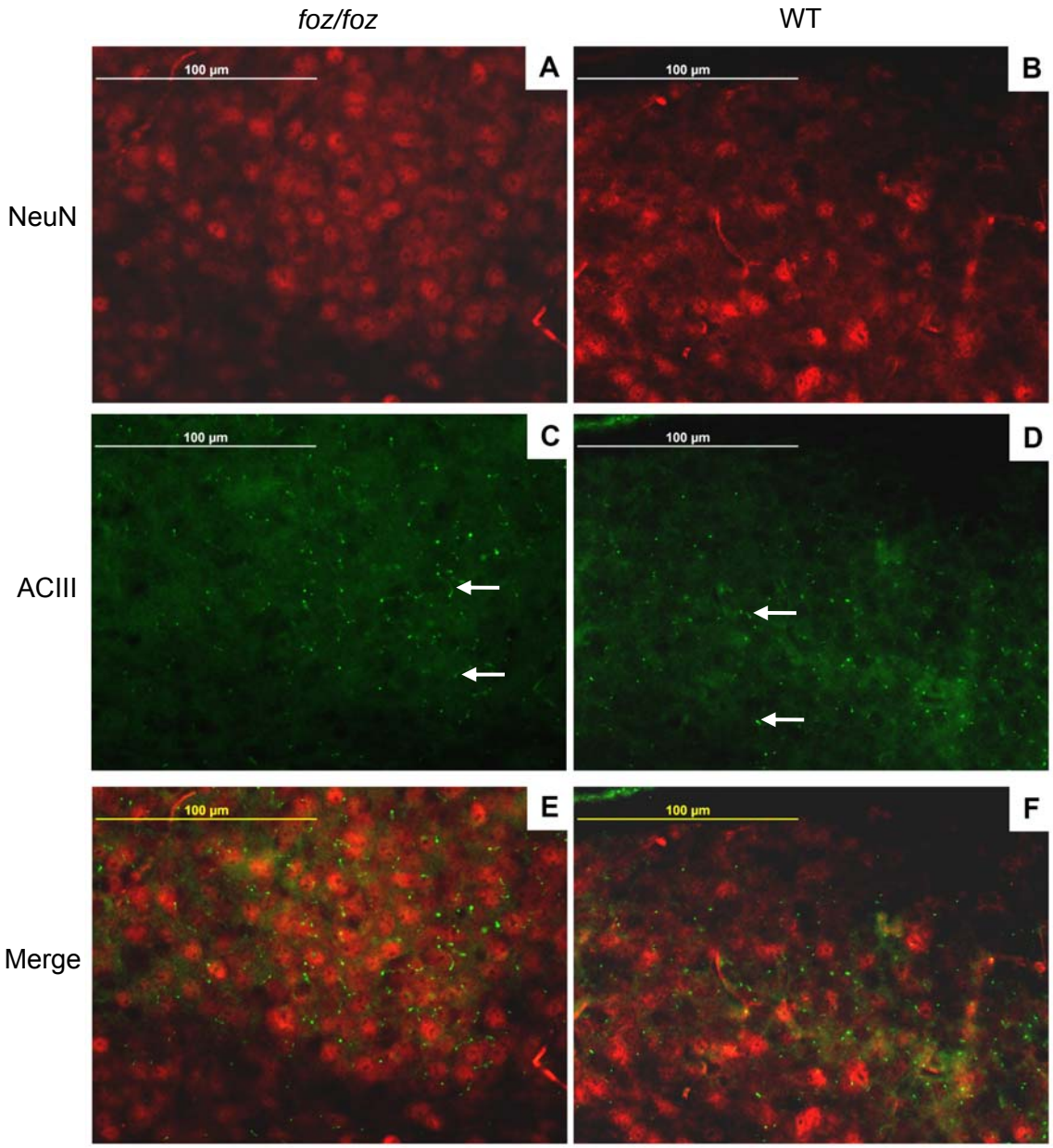

Figure 3.1. Representative IHF staining for neurons and primary cilia in the hypothalamus of newborn *foz/foz* and WT mice

Brain sections were stained with NeuN (to identify neuronal nuclei) and ACIII (to identify cilia) antibodies. A-D: There appeared to be similar numbers of neurons and primary cilia (arrows) in hypothalamic sections from *foz/foz* (A, C) and WT (B, D) mice. E, F: Possibly due to suboptimal fixation, cilia and neuronal colocalisation is not as compelling on the composite images as in older mice (see Figures 3.2 – 3.4), shown for *foz/foz* mice (E) vs. WT (F). Scale: 100 µm, n ≥ 5 mice per group, staining was performed in duplicate.

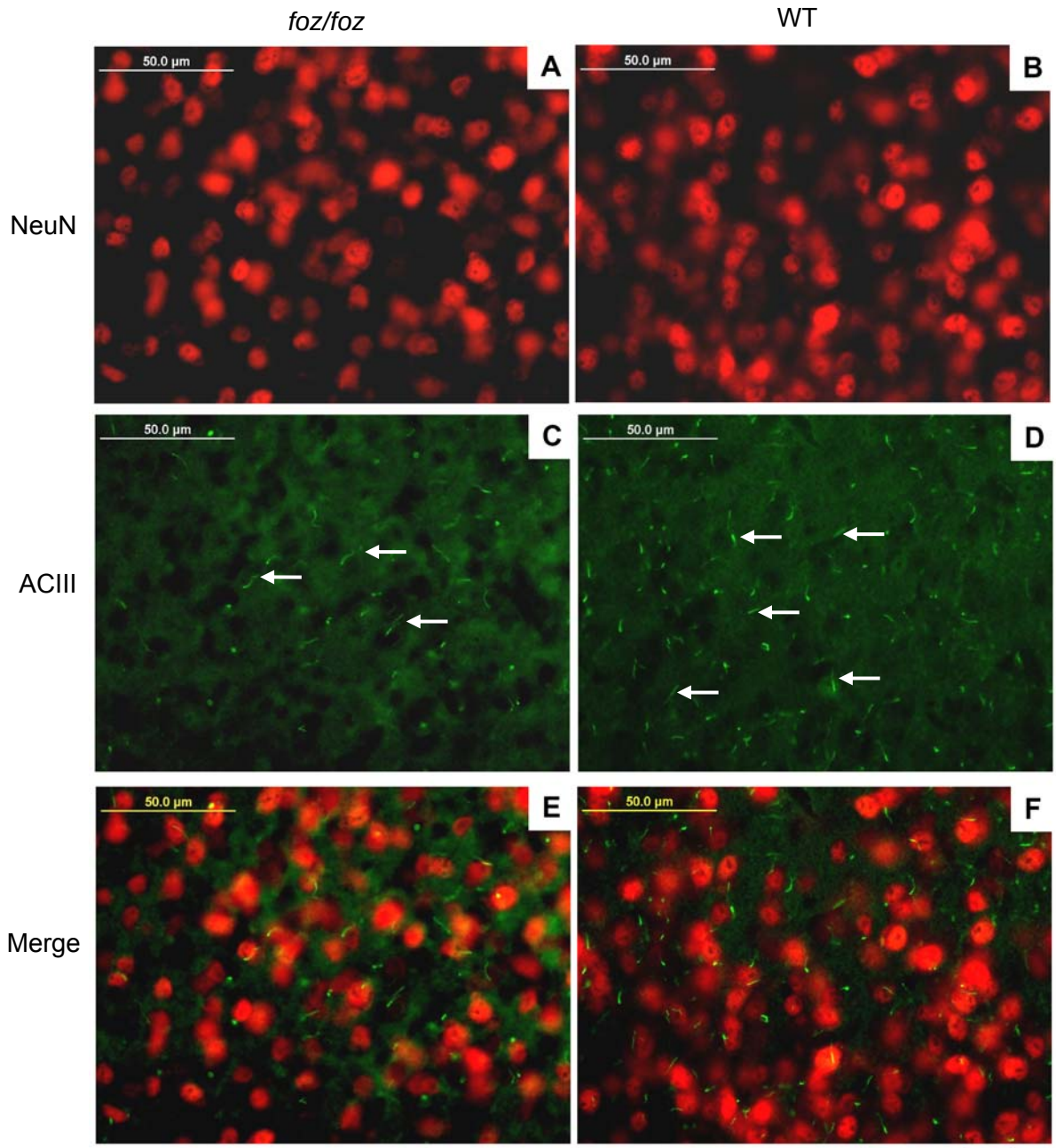

Figure 3.2. Representative IHF staining for neurons and primary cilia in the hypothalamus of weanling *foz/foz* and WT mice

Brain sections were stained with NeuN (to identify neuronal nuclei) and ACIII (to identify cilia) antibodies. A-D: There appeared to be similar numbers of neurons in hypothalamic sections from *foz/foz* (A) and WT (B) mice. However, there were fewer cilia (arrows) in *foz/foz* (C) than WT (D) mice. E, F: This becomes more evident for the composite images, shown for *foz/foz* mice (E) vs. WT (F). It is evident that all cilia are attached to neurons. Scale: 50 µm, n = 6 mice per group, staining was performed in duplicate.

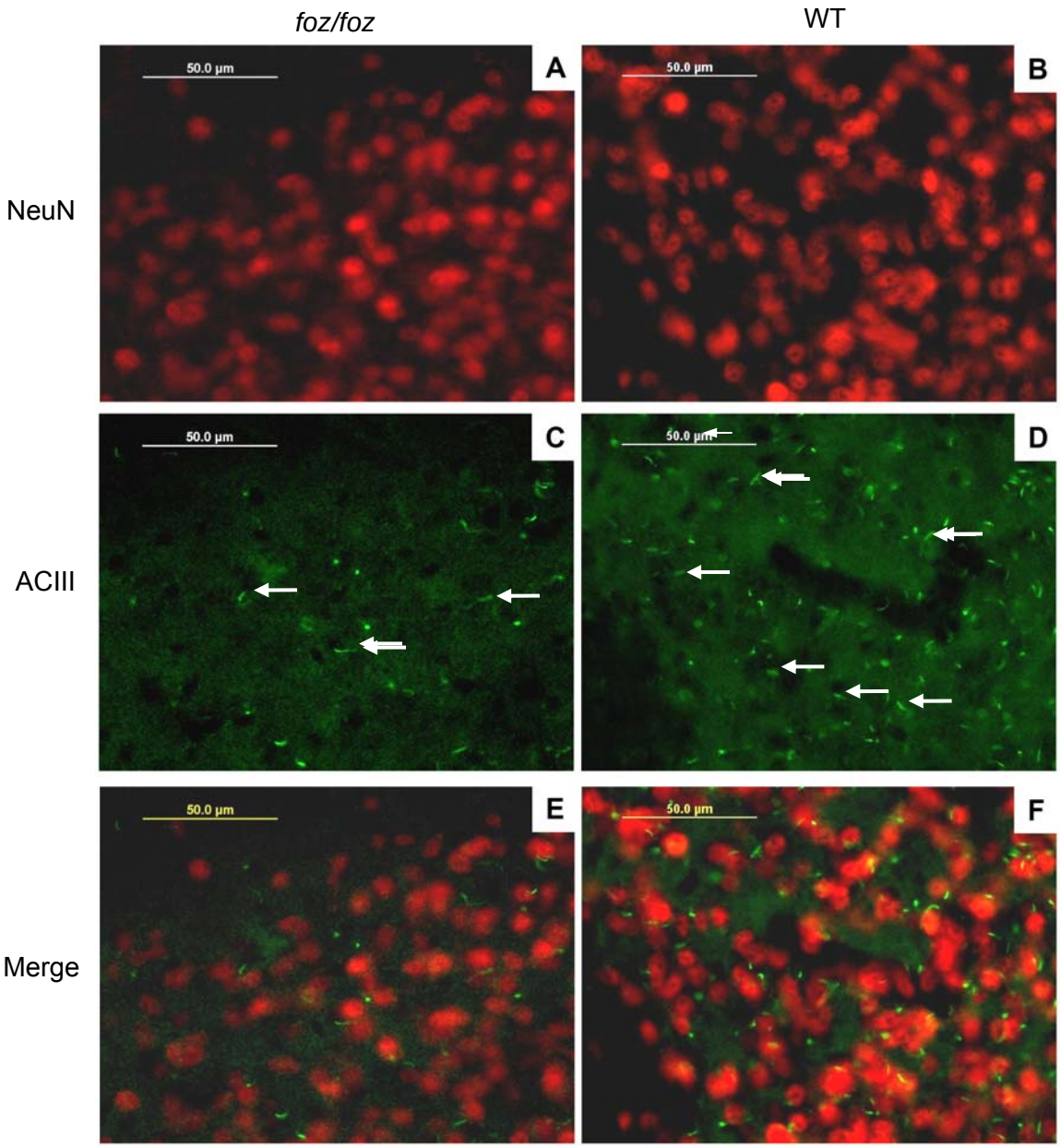

Figure 3.3. Representative IHF staining for neurons and primary cilia in the hypothalamus of *foz/foz* and WT mice after 2-weeks on chow diet

Brain sections were stained with NeuN and ACIII antibodies, as in Figure 3.2. Numbers of neurons in hypothalamic sections appeared to be similar between chow-fed *foz/foz* (A) and WT (B) mice. There were significantly less cilia (arrows) in *foz/foz* (C) than WT (D). This becomes more evident for the composite images shown for chow-fed *foz/foz* mice (E) vs. WT (F). Scale: 50 µm, n = 6 mice per group, staining was performed in duplicate.

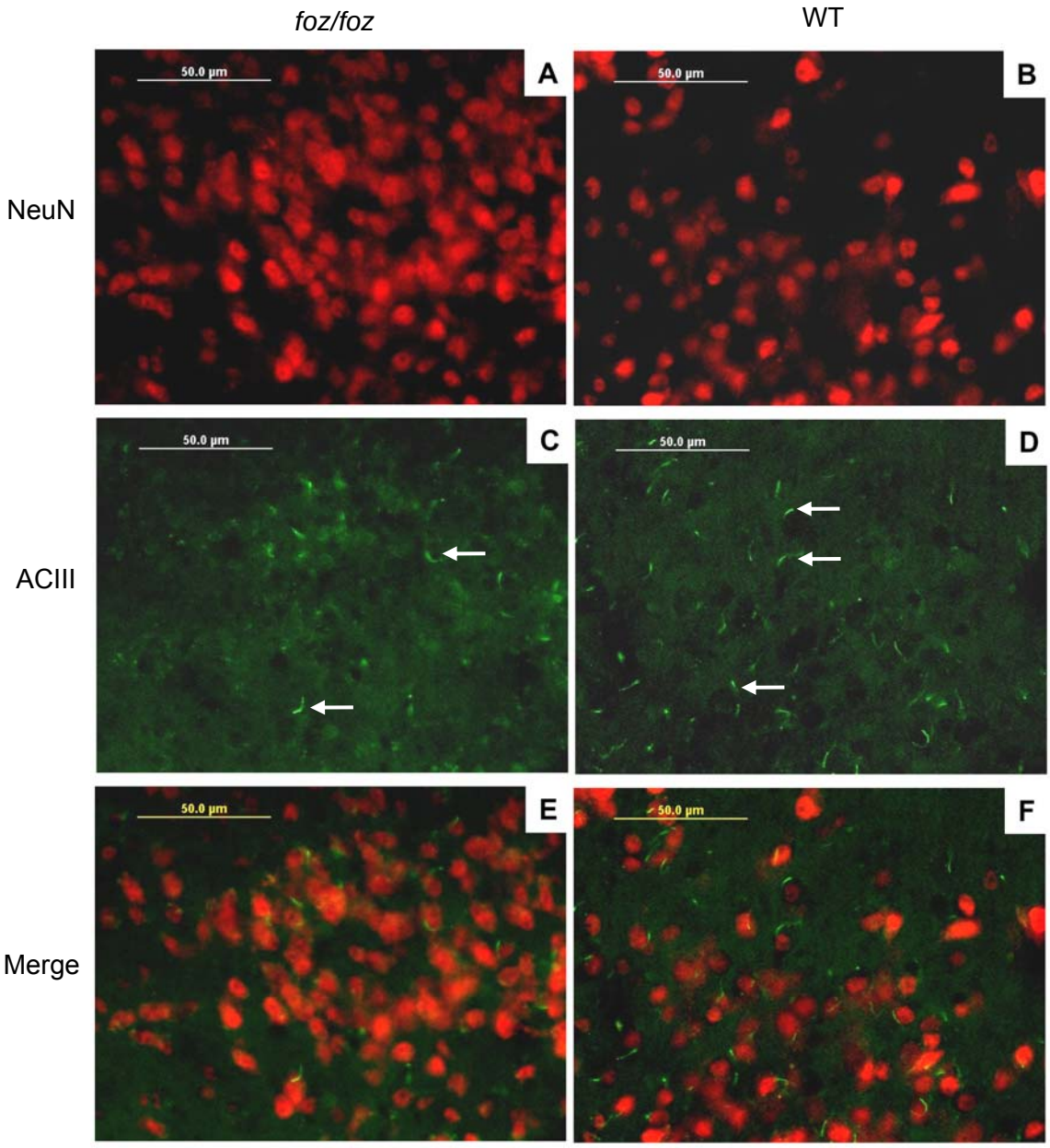

Figure 3.4. Representative IHF staining for neurons and primary cilia in the hypothalamus of *foz/foz* and WT mice after 12-weeks on chow diet

Brain sections were stained against NeuN and ACIII. There appeared to be similar numbers of neurons in hypothalamic sections from chow-fed *foz/foz* (A) and WT (B) mice. However, there were less cilia (arrows) in *foz/foz* (C) than WT (D). This becomes more evident for the composite images shown for chow-fed *foz/foz* mice (E) vs. WT (F). Scale: 50 µm, n = 6 mice per group, staining was performed in duplicate.

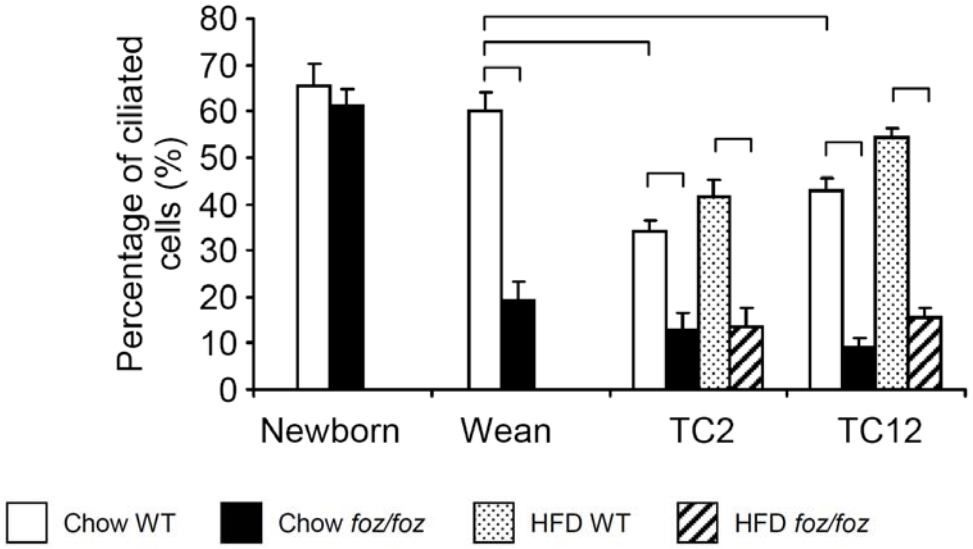

Figure 3.5. Percentage of hypothalamic ciliated neurons of newborn, weaning, TC2, TC12 *foz/foz* and WT mice

The proportion of hypothalamic neurons that were ciliated appeared similar at birth, but was significantly decreased in the *foz/foz* mice at all later time points, regardless of the diet. This graphic represents the quantification of data in Figures 3.1 - 3.4. Statistical bars show significance of post-hoc testing between indicated groups, $P < 0.05$. $n \geq 5$ mice per group.

3.4.2. The length of hypothalamic primary cilia is unaltered in *foz/foz* mice, despite the decrease in cilia number

For the purpose of measuring cilial length at weaning, TC2 and TC12 in *foz/foz* and WT mice fed chow and high fat diet, a separate study was performed (Figures 3.6, 3.7). No significant differences were observed between *foz/foz* and WT mice at any time points, regardless of the diet (Figure 3.7).

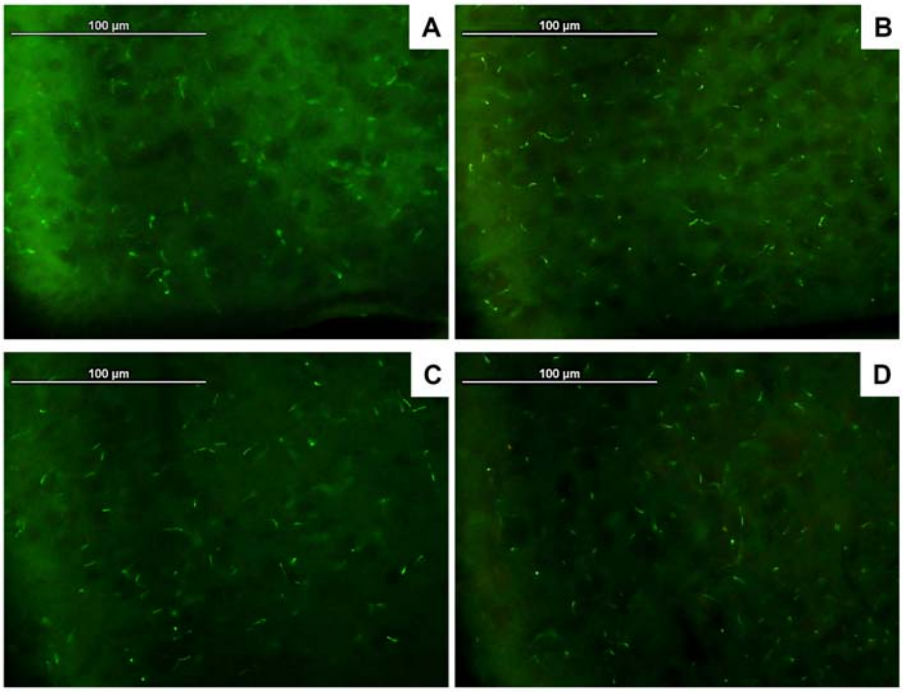

Figure 3.6. Representative staining for primary cilia in the hypothalamus of TC2 *foz/foz* and WT mice

Primary cilia length at TC2 (A-D) was not different between *foz/foz* mice (A, C) and WT (B, D) mice. Primary cilium size was not affected by high fat-feeding (C, D) compared to chow diet (A, B).

Brain sections were stained with ACIII antibody, scale: 100 µm, n = 6 mice per group, staining was performed in duplicate.

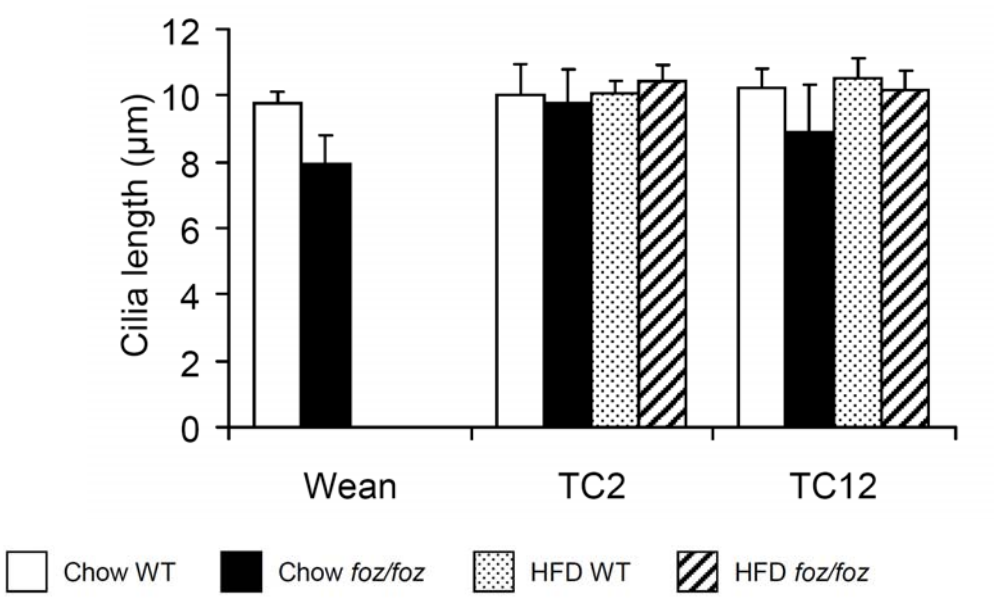

Figure 3.7. Primary cilia length in the hypothalamus of weaning, TC2, TC12 *foz/foz* and WT mice

There was no significant effect of genotype, diet or time on primary cilia length. n = 6 mice per group, staining was performed in duplicate.

3.4.3. Hypothalamic adenylate cyclase III gene expression is unaltered in *foz/foz* mice

To examine whether the decrease in the number of primary cilia on hypothalamic neurons in *foz/foz* could be attributed to changes in ACIII expression, we measured ACIII mRNA levels in whole hypothalamus samples from mice on diet for 2- (TC2) and 12-weeks (TC12), using real time PCR. After 2-weeks on diet, hypothalamic ACIII mRNA levels were not different between groups (Figure 3.8). After 12-weeks on diet, there were still no significant changes in hypothalamic ACIII gene expression between *foz/foz* and WT mice (Figure 3.8). In light of the global

decrease in number of ciliated cells throughout the hypothalamus, ACIII mRNA levels were not measured in the PVN, AH or Arc.

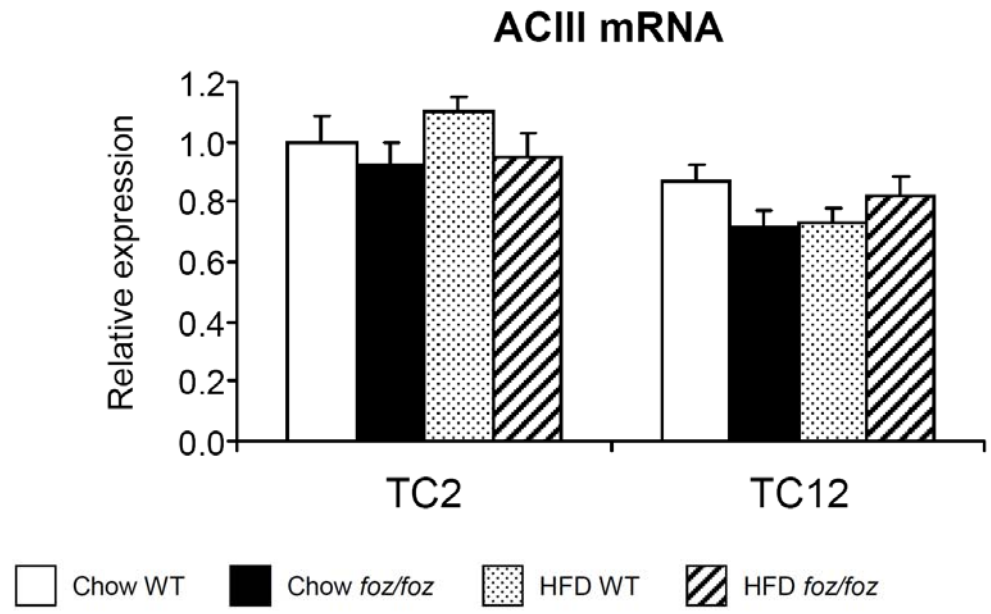

Figure 3.8. Adenylate cyclase III gene expression in the whole hypothalamus at TC2 and TC12 in chow and high fat-fed *foz/foz* and WT mice

ACIII mRNA levels were measured in whole hypothalamic samples at TC2 and TC12 in both *foz/foz* and WT mice fed either chow or high fat diet. No effects of genotype or diet were detected. n ≥ 6 mice per group, samples were measured in duplicate.

3.4.4. Is decreased ciliogenesis responsible for the decrease in the number of ciliated neurons in *foz/foz* mice?

Cep164 and ODF2 are both involved in cilia appendage to the plasma membrane of neurons (and other cells). Absence or decreased expression of one of these proteins could explain the decrease in the number of ciliated cells observed in

foz/foz mice. Therefore, whole hypothalamic mRNA levels of Cep164 and ODF2 were measured in both *foz/foz* and WT mice fed chow or high fat diet in TC2 and TC12 cohorts. After 2-weeks on diet, both Cep164 and ODF2 hypothalamic mRNA levels were not different between groups (Figure 3.9A, B). Likewise, after 12-weeks on diet, there were no significant variations in hypothalamic Cep164 and ODF2 gene expression between groups (Figure 3.9A, B).

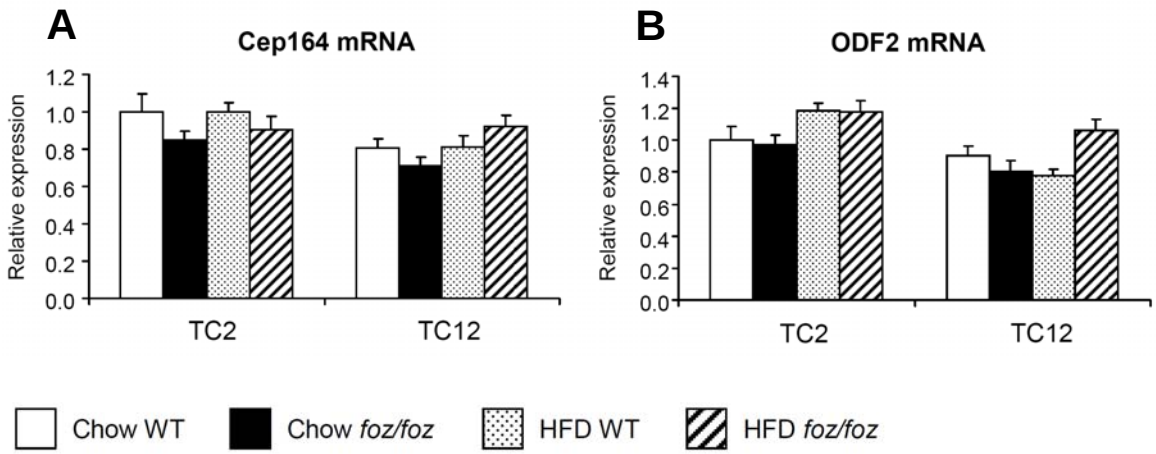

Figure 3.9. Cep164 and ODF2 gene levels are not changed in WT or *foz/foz* mice hypothalamus

There was no effect of genotype on Cep164 (A) and ODF2 (B) gene expression in *foz/foz* or WT mice fed either chow or high fat diet at TC2 and TC12. High fat-feeding did not change Cep164 and ODF2 hypothalamic gene expression at either time point. n ≥ 6 mice per group, real time PCR were repeated in duplicate.

3.4.5. Hypothalamic expression of genes involved in cilial trafficking

KiF3A is a component of the anterograde transport apparatus of the primary cilium, whereas DYNC2H1 plays an opposite role, being part of the retrograde

transport. Hypothalamic KiF3A and DYNC2H1 mRNA expression at TC2 and TC12 were similar between *foz/foz* and WT mice fed either chow or high fat diet (Figure 3.10A, B).

Intraflagellar transport (IFT) proteins are proteins involved in bidirectional movement of particles along the cilium. The same consistent pattern was observed in mRNA levels of the three genes studied (IFT20, IFT52, IFT172). No significant changes were noticed between *foz/foz* and WT mice on chow or high fat diet at TC2 or TC12 (Figure 3.10C-E).

Bardet-Biedl syndrome proteins (BBS) are also involved in cilia trafficking. More particularly, they are required for the localisation of G protein-coupled receptors to primary cilia (Berbari *et al.*, 2008b). BBS2 and BBS4 showed a similar pattern in their hypothalamic mRNA levels as the previously described genes. Specifically, there were no changes in mRNA levels in *foz/foz* compared to WT mice, either at TC2 or TC12, and regardless of the diet (Figure 3.10F, G).

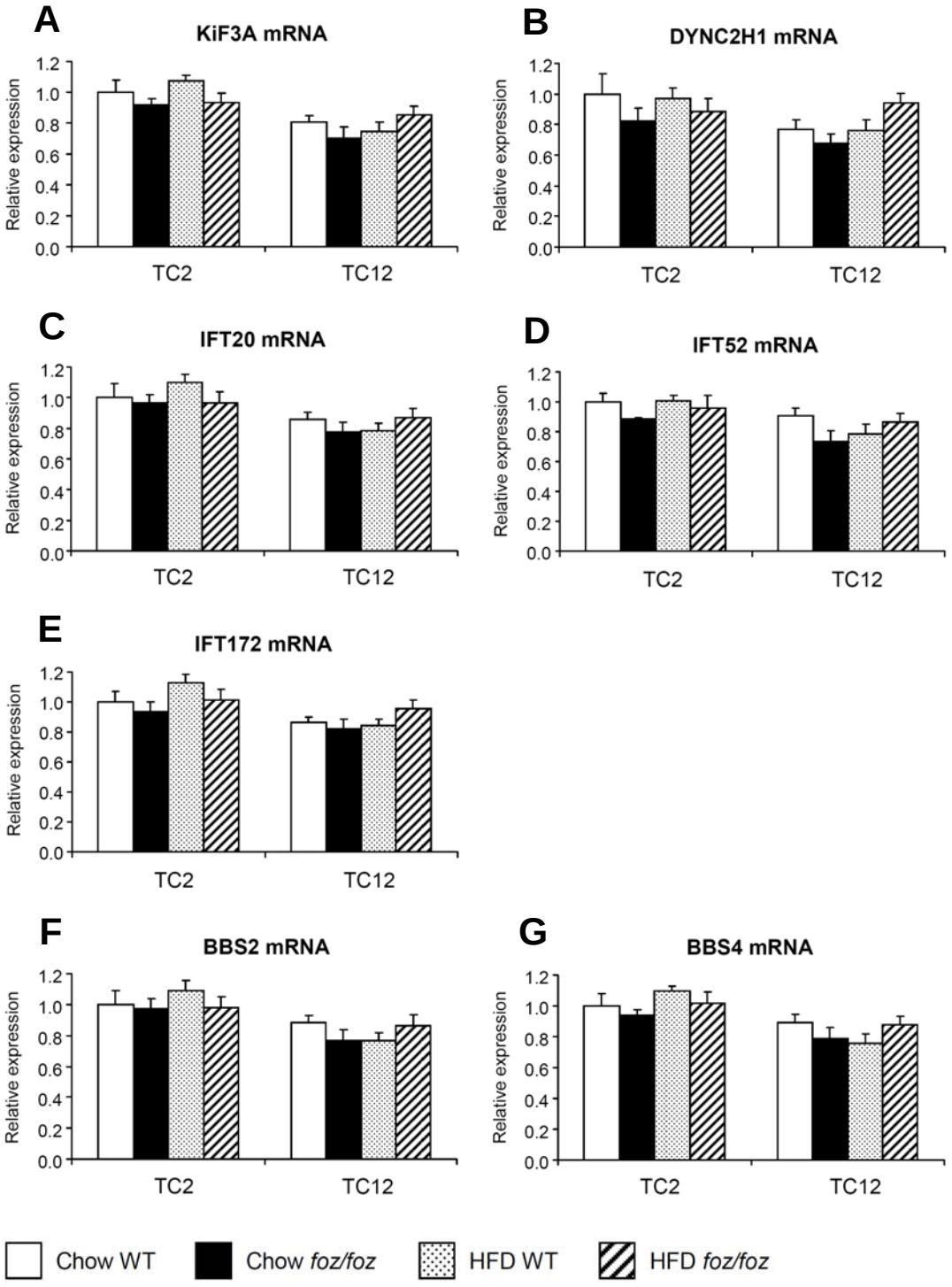

Figure 3.10. Hypothalamic expression of genes involved in primary cilia trafficking are unaltered in *foz/foz* mice

Hypothalamic gene expression of KiF3A (A), DYNC2H1 (B), IFT20 (C), IFT52 (D), IFT172 (E), BBS2 (F), BBS4 (G) was not affected by genotype, diet or time. n ≥ 6 mice per group, experiments were performed in duplicate.

3.5. Discussion

Patients suffering Alström syndrome as well as *foz/foz* (*Alms1* mutant) mice exhibit evidence of cilial disorders with male infertility, sensory deafness, retinal defects, and renal cystic disorder (Goldstein and Fialkow, 1973; Edwards *et al.*, 1976; Arsov *et al.*, 2006b). These pathological changes seem likely to be caused by cilial defects related directly to *Alms1* mutation. This is because Alms1 is a basal body protein, closely related to the primary cilium. To date, the function of Alms1 is still unknown, but this work tested the hypothesis that it influences cilial structure and/or function.

Alms1 mutant mice exhibit hyperphagia and obesity similar to the human phenotype of Alström syndrome. *Foz/foz* mice have also been found to have severe metabolic disorders and liver disease, including type 2 diabetes, hypercholesterolaemia, and non-alcoholic steatohepatitis (Arsov *et al.*, 2006a; Larter *et al.*, 2009). Mice with ACIII deficiency (a specific neuronal marker of primary cilia) are similarly obese (Wang *et al.*, 2009). In 2007, Davenport *et al.* (2007) investigated the effect of a gene knock-out strategy for deleting primary cilia in adult mice. They found that such animals were hyperphagic, leading to obesity. Bardet-Biedl syndrome (BBS) is another cause of ciliopathy-related obesity. Thus, BBS proteins are involved in cilial transport, and mice lacking BBS2 protein are obese, as well as developing retinal degeneration and male infertility (Nishimura *et al.*, 2004). Since primary cilial defects clearly lead to hyperphagia, it seemed an attractive hypothesis to investigate in *foz/foz* mice the role of neuronal primary cilia in the development of metabolic phenotype of these animals.

The role of primary cilia is still unknown. It was earlier speculated that they could be vestigial organelles with no physiological function (Sorokin, 1962). Noting the structural relationship of the basal body to the centriole, another hypothesis has been that the primary cilium is involved in cell cycle control (Tucker *et al.*, 1979). More recent insights indicate that the primary cilium can play a role as a sensory organelle (Wheatley *et al.*, 1996; Pazour and Witman, 2003). In the present study, we show that a post-natal decrease in the number of neuronal primary cilia has a close relationship with *Alms1* mutation, and we propose that this may be related to the development of obesity in *foz/foz* mice. Genetic studies on *foz/foz* mice showed that they exhibit a mutation in the *Alms1* gene, leading to a truncated protein. In the present study, we showed that *Alms1* mutation does not affect primary cilia length in *foz/foz* mice, indicating that Alms1 is not involved in cilial length. Further we found normal expression of a suite of genes that influence ciliogenesis and cilial trafficking, further supporting that *Alms1* mutation does not affect any of these pathways.

We focused our studies on hypothalamic expression of primary cilia in *foz/foz* and WT mice, as the hypothalamus is the main centre involved in regulation food intake and energy expenditure. An outstanding question is: “Are the number and length of primary cilia affected by *Alms1* mutation in other brain regions, or is it hypothalamic specific?”. While this question was not assessed in the present studies, our colleagues, Lesley Chen and Prof. Michel Leroux (Master of Science, 2010, Simon Fraser University, Canada) showed, in contemporaneous studies (not known to us at the time) that *foz/foz* mice have reduced numbers but not length of primary cilia in the hippocampus (unpublished data). For this reason, we conclude

that the decrease in the number of ciliated cells in *foz/foz* mice brain is not confined to the hypothalamus.

Perhaps one of the most interesting observations in the present work was that the number of ciliated hypothalamic neurons at birth was similar between *foz/foz* and WT mice. Brains from newborn mice were fixed by immersion in paraformaldehyde as cardiac perfusion was not possible due to small organ size. As a consequence, the brain fixation was not as optimal compared to perfused tissue. 50 to 55 µm sections were cut even though the tissue was extremely fragile. Sections were then incubated individually to avoid any further damage by friction with other sections. A first double labelling for ACIII and NeuN was performed and staining was analysed using Pixcavator (see Chapter 2, section 2.5.3). This experiment was repeated in duplicate, and as similar results were obtained each time, data were considered reliable. This IHF result suggests that primary cilia are lost early in post-natal life as there was no difference between *foz/foz* and WT mice in newborn pups. To confirm this hypothesis a more detailed time course experiment (between birth and weaning) should be performed in order to determine when the decrease in ciliated cells appears. However, the logistics and technicality (no transcardic fixation possible because of small animal size leading to suboptimal IHF) of such an experiment are daunting.

The primary cilium is a non-motile, solitary organelle that emerges from the cell surface of most mammalian cells. Primary cilia are subject to physical forces as they were shown to act as mechanosensors in the kidney (Nauli *et al.*, 2003). In addition, Doetsch *et al.,* (1999) showed that primary cilia are subject to the same role in the brain. Indeed, astrocytes in the subventricular zone process primary cilia into the ventricle. Primary cilia are also abundantly found in the hypothalamus

(Bishop *et al.*, 2007), which surround the third ventricle. Taken together these data suggest a role for primary cilia to sense the cerebrospinal fluid. The loss of primary cilia between birth and weaning in *foz/foz* mice could be due to primary cilia fragility or weak stability/maintenance to the plasma membrane. To test this, one could attempt neuronal culture from *foz/foz* and WT mice, and establish a physical stress, such as vibration that may be insufficient to fracture normal cell cilia but which could shear cilia from *Alms1* mutant cells. Likewise, *Alms1* knockdown has been achieved by others (Mutant Mouse Regional Resource Center, MMRRC# 008633, see Collin *et al.*, 2005; Knorz *et al.*, 2010; and Jagger *et al.*, 2011). This strategy could be used to decrease Alms1 expression in cultured ciliated neurons (Chapter 7), followed by the mechanical shear stress approach mentioned earlier.

One of the implications of the loss of primary cilia is a direct effect on receptor expression on the cilial surface. Indeed, the decrease in the number of cilia should lead to a decrease in receptor expression. It has been shown that melanin concentrating hormone 1 receptor (MCH1R) and somatostatin receptor 3 (SstR3), are specifically expressed to the cilia membrane (Handel *et al.*, 1999; Berbari *et al.*, 2008a). MCH1R as well as SstR3 ligands have been shown to act on energy homeostasis through the leptin pathway. Furthermore, MCH stimulates leptin mRNA expression and leptin secretion (Bradley *et al.*, 2000), while somatostatin (Sst), has been shown to reduce leptin action in the brain by diminishing hypothalamic signal transducer and activator of transcription 3 (Stat3) phosphorylation, as well as Stat3 nuclear translocation, which leads a reduction in leptin receptor (Ob-R) activity (Stepanyan *et al.*, 2003; Stepanyan *et al.*, 2007). The role of leptin and Ob-R in *foz/foz* mice will be examined in Chapter 5 and 6.

Furthermore one should not overrule a possible implication of primary cilia in central nervous system development. The exact role of primary cilia in cell migration is not clear yet, but one can hypothesise that the loss of primary cilia in *foz/foz* mice can lead to impaired cell migration, axonal projection or axonal guidance (Louvi and Grove, 2011). Another possibility is that impaired formation of the "normal" hypothalamic network in *foz/foz* mice could be at the genesis of the ciliopathy-related obesity.

In summary, the present data details that primary cilia deficiency occurs in *foz/foz* mice. In contrast, cilia that are present in *foz/foz* hypothalami, albeit in reduced numbers, show normal length. In addition, expression of genes involved in ciliogenesis is normal in *foz/foz* mice and is unaltered by diet, which exacerbates the *foz/foz* phenotype. These studies indicate that primary cilia deficiency is closely related to *Alms1* mutation; this assumption will be tested in the following chapter.

CHAPTER 4

Chapter 4

Relationships between Alms1, the primary cilium and obesity in *foz/foz* mice

4.1. Introduction

As discussed previously, mutations in the *Alms1* gene cause Alström syndrome, a rare progressive condition characterised by childhood obesity, insulin resistance, retinal degeneration, sensorineural hearing loss and other features, such as liver and kidney disorders. *ALMS1* encodes a 461 kDa protein in humans, and *Alms1*, the mouse homolog, encodes a 360 kDa protein (for more information see UniProtKB/Swiss-Prot website, http://www.uniprot.org/, references Q8TCU4 and Q8K4E0, respectively). Alms1 protein is known to localise to the centrosome and to the basal body (Andersen *et al.*, 2003; Hearn *et al.*, 2005; Knorz *et al.*, 2010), an organising centre for microtubules specifically associated with cilia. In cells, microtubules can be visualised by immunohistochemical detection of α-tubulin. Several studies have shown that Alms1 is closely associated with α-tubulin, and it is also required for the proper formation and/or maintenance of primary cilia (Graser *et al.*, 2007; Li *et al.*, 2007a). Thus, even though the precise function of Alms1 is unknown, the available observations can be interpreted as indicating that Alms1 is related to the primary cilium, a proposal that is consistent with the fact that some or all the features of Alström syndrome can be explained by ciliary dysfunction.

Primary cilia may play a role in cellular signalling functions pertinent to development and sensory detection. Thus, in the eye, photoreceptors, which are modified primary cilia, sense and respond to light. In the nose, specialised olfactory cilia detect odours and initiate signalling pathways that activate olfactory neurons. Disruption of the intracellular signalling pathways in these cilia can alter development and/or cause disease (Pan *et al.*, 2005). In general, however, the function of the primary cilium remains largely unknown. Probably contributing to this gap in knowledge is the fact that proteins localising to primary cilia are still mostly unknown.

In the past ten years, studies have shown that somatostatin receptor 3 (SstR3) and melanin concentrating hormone 1 receptor (MCH1R) localise specifically to neuronal cilia (Handel *et al.*, 1999; Berbari *et al.*, 2008a). Interestingly, these two receptors are involved in the regulation of food intake (Borowsky *et al.*, 2002; Tavares *et al.*, 2006; Sasmal *et al.*, 2010). Further, SstR3 is expressed on hypothalamic neurons targeted by leptin (Stepanyan *et al.*, 2003). Functional interactions between somatostatin and the leptin receptor (Ob-R) are also indicated by the inhibitory effects of somatostatin on Ob-R signalling pathway, leading to increased food consumption (Stepanyan *et al.*, 2007).

In Chapter 3, studies of hypothalamic neuronal cilia showed a striking decline in the number of ciliated neurons between the immediate post-natal period (when numbers were the same in *foz/foz* as WT mice) and weaning (when numbers of ciliated neurons decreased by ~60%). This structural loss of primary cilia provided a clear indication of a functional link between the Alms1 mutation and the appetite regulation circuitry. In the present chapter, experiments were designed to clarify the relationship between Alms1 and the primary cilium, with particular

attention to provide an explanation for the loss of primary cilia and the mechanism for obesity in *foz/foz* mice.

4.2. Purpose of the study

Hypotheses to be tested:

1) That Alms1 interacts with the structure of primary cilia on hypothalamic neurons.

2) That SstR3 and MCH1R hypothalamic expression is affected by the decrease in hypothalamic primary cilia number in *foz/foz* mice.

Aims of this study:

1) To measure *Alms1* mRNA levels in hypothalamus, and for comparison of a non-neuronal tissue, in white adipose tissue (WAT).

2) Establish the subcellular localisation of Alms1 in relation to neuronal cilia in *foz/foz* and WT mice.

3) Determine whether the reduction in number of hypothalamic cilia alters hypothalamic expression of MCH1R and SstR3 mRNA in *foz/foz* mice.

4.3. Methods

4.3.1. Animals and diets

Female WT and *foz/foz* mice were bred and maintained in The Canberra Hospital Animal Facility, as detailed in Chapter 2 (section 2.2.1). Peri-ovarian and subcutaneous WAT were collected from chow and high fat-fed mice at TC2 and TC12. Following brain dissection, hypothalami were collected from the same group of mice at weaning, TC2 and TC12 for real time PCR and immunofluorescent experiments. For primary cell culture experiments, hypothalami were collected between post-natal day 1 and 4.

4.3.2. Gene expression analyses

Gene expression in hypothalami and WAT was determined by real time PCR, as presented in Chapter 2 (see section 2.6.1). Experiments were repeated in duplicate and normalised to three house keeping genes: beta-actin, B2M and RPL13a (sense and antisense primers sequences are detailed in Chapter 2, Table 2.3).

4.3.3. Protein expression analyses

After homogenising the whole hypothalamus in homogenising buffer (see Chapter 2, section 2.6.2, and Appendix 1), hypothalamic proteins were extracted. The amount of protein was estimated using a protein estimation kit (Bio-Rad, USA). Proteins were then diluted to 4 µg/µl, and 10 µl of each sample was loaded onto a 5% SDS-PAGE gel (see Appendix 1). After transfer, membranes were incubated with Alms1 primary antibody overnight, followed by 1h incubation with HRP-conjugated secondary antibody. Bands were detected with enhanced chemiluminescence and visualised with a luminescent analyser (see Chapter 2, section 2.6.2.2).

4.3.4. Neuronal primary cell culture, and immunocytofluorescence studies

Between post-natal days 1 to 4, brains were collected from WT and *foz/foz* mice. Hypothalami were dissected and incubated in enzyme solution for 20 min. Hypothalamic tissue was then dissociated in culture medium using a flame-polished Pasteur pipette. Cells were centrifuged and counted using a hemocytometer. Cell suspensions were then diluted, plated onto 24-well plates and cultured for at least 4 days (for more details see Chapter 2, section 2.7.1.3). Primary cilium and Alms1 subcellular localisation were assessed by immunocytofluorescence. For this purpose, cells were fixed in 3% paraformaldehyde for 15 min followed by several washes in PBS. They were then blocked and permeabilised in 2% BSA containing 0.5% Triton® X-100 for 10 min, followed by incubation with primary and secondary

antibodies under conditions outlined in Chapter 2 (Tables 2.1 and 2.2). Detailed immunocytofluorescence (ICF) protocols are outlined in Chapter 2, section 2.7.2.

4.3.5. Statistical analyses

The effects of genotype and diet were compared using 2-way analysis of variance (ANOVA), with Tukey post-hoc testing. For all comparisons $P < 0.05$ was considered significant. Data are presented as mean ± SEM, with the number of individuals per group (n) given in the text and in Chapter 2, section 2.2.3.

4.4. Results

4.4.1. Hypothalamic *Alms1* gene expression is reduced in *foz/foz* mice

In order to study the role of *Alms1* mutation in appetite regulation, we first measured its hypothalamic gene expression in whole hypothalami as well as in dissected hypothalamic nuclei. In hypothalamus of *foz/foz* mice fed chow for 2-weeks, *Alms1* mRNA expression was substantially less (0.50 ± 0.09 arbitrary units) than in WT mice (1.00 ± 0.17; $P < 0.01$; Figure 4.1A). Likewise, values were ~50% those of WT in high fat-fed *foz/foz* mice ($P < 0.01$; Figure 4.1A). After 12-weeks on diet, *foz/foz* mice fed chow or high fat diet showed the same substantial decrease in hypothalamic *Alms1* mRNA levels compared to their WT diet-matched littermates ($^{\#}P < 0.05$; Figure 4.1A). *Alms1* mRNA levels in *foz/foz*

mice paraventricular nucleus were also significantly decreased at both weaning and TC2 compared to their WT littermates ($P < 0.01$; Figure 4.1B). The same pattern of 50% less *Alms1* mRNA was observed in the AH and Arc nuclei ($P < 0.01$; Figure 4.1C, D). These findings are interpreted as indicating that *Alms1* transcript levels, as detected by the primers used in this study (designed to encompass the mutated/deleted region), are constitutively reduced by ~50% in *foz/foz* mice, with no effect of age (at least over the interval studied) or diet.

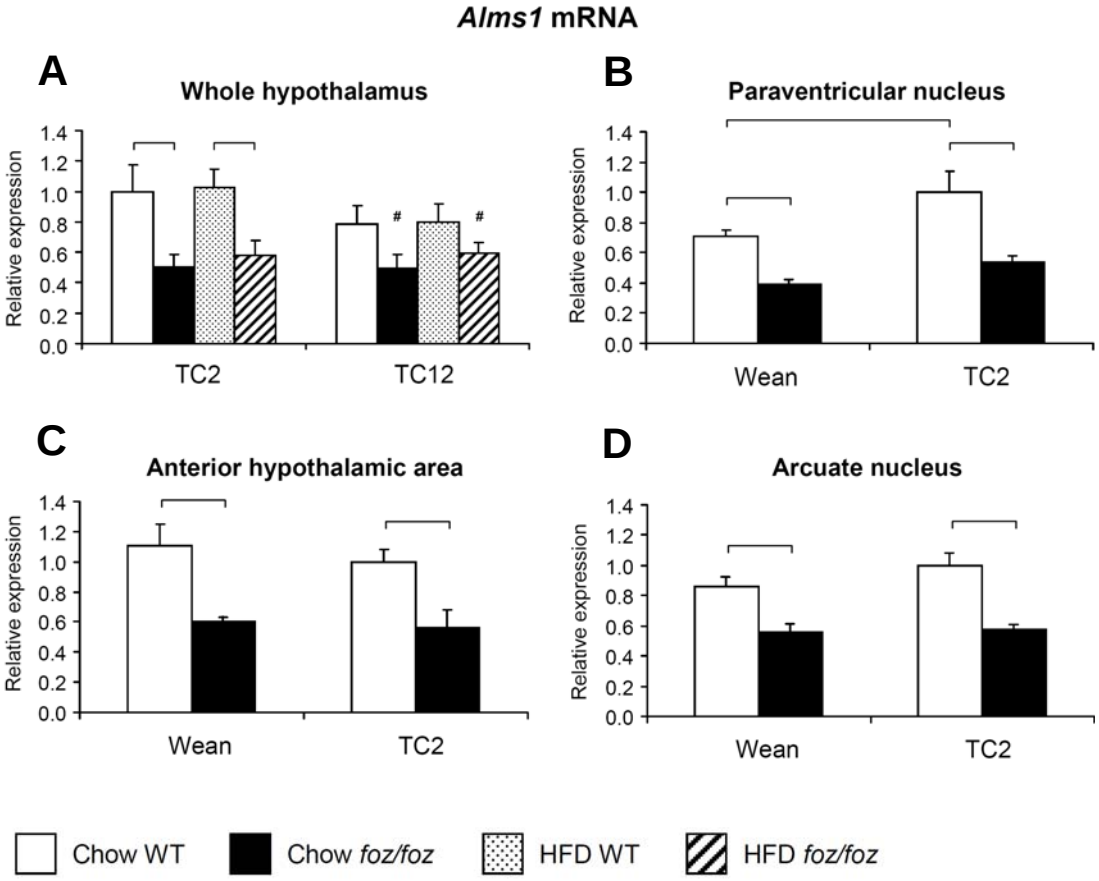

Figure 4.1. *Alms1* mRNA levels in whole hypothalamus (A) and in hypothalamic nuclei (B-D) at weaning, TC2 and TC12 are reduced by ~50% in *foz/foz* mice compared with WT mice

At weaning (Wean), 2 (TC2) or 12 weeks (TC12) on a chow or high fat diet (see section 2.2.2), animals were sacrificed, hypothalamus removed, and used whole, as indicated, or dissected for major nuclei (see section 2.3.2). Total RNA was extracted and *Alms1* determined by real time PCR (see section 2.6).

A: *Alms1* hypothalamic mRNA levels were significantly lower (by ~50%) in *foz/foz* mice at both TC2 and TC12, regardless of the diet.

B: In the paraventricular nucleus, *Alms1* gene expression was reduced in *foz/foz* mice at weaning and TC2.

C: In the anterior hypothalamic area, *Alms1* gene expression was significantly reduced in *foz/foz* mice at weaning and TC2.

D: In the arcuate nucleus, *Alms1* mRNA levels were lower in *foz/foz* mice compared to their WT littermates at both weaning and TC2.

$^{\#}P < 0.05$, ANOVA results for effect of genotype.

Statistical bars show significance of post-hoc testing between indicated groups, $P < 0.01$. n ≥ 6 mice per group, experiments were repeated in duplicate.

4.4.2. *Alms1* gene expression is reduced in white adipose tissue in *foz/foz* mice

To confirm that what was observed in the hypothalamus was not tissue specific, we performed real time PCR of *Alms1* in adipose tissue. A single experimental time point was selected because hypothalamic changes were not dependent on development. After 12-weeks on diet, *Alms1* mRNA levels in WAT were similar to those observed in the hypothalamus. A significant and similar effect of genotype is evident. Thus, *foz/foz* mice either fed chow or high fat diet exhibit ~50% lower expression of *Alms1* mRNA levels compared to corresponding dietary groups of WT mice ($^{\#}P < 0.05$, effect of genotype; Figure 4.2). There is no evident effect of diet.

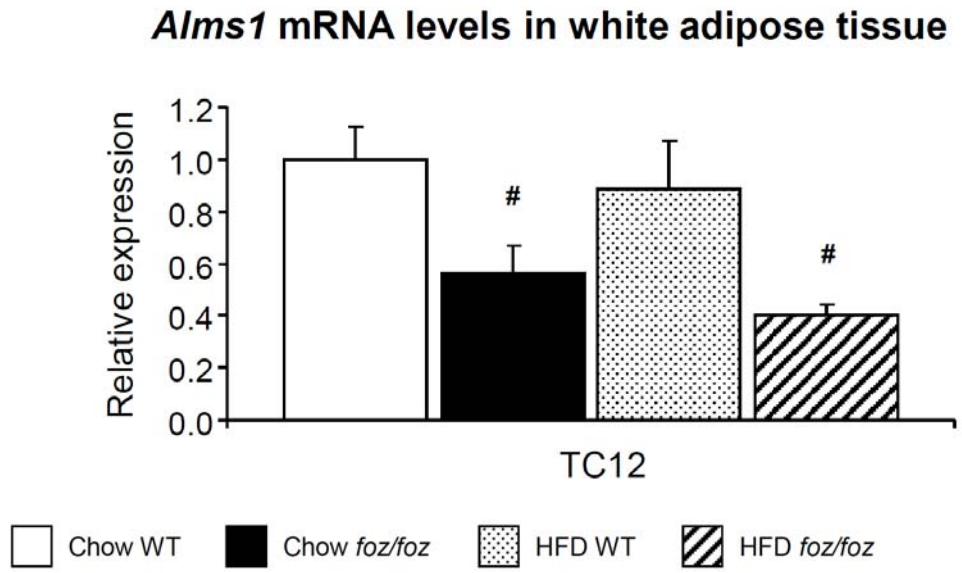

Figure 4.2. *Alms1* mRNA levels in white adipose tissue are reduced ~50% in *foz/foz* mice compared with WT after 12-weeks on diet

Alms1 mRNA levels in WAT were lower (~ 50%) in *foz/foz* mice compared to their WT littermates, regardless of the diet.

$^{\#}P < 0.05$, ANOVA results for effect of genotype, n = 5 mice per group, real time PCR was performed in duplicate.

4.4.3. Alms1 protein is present in the hypothalamus

To further study Alms1 protein expression in *foz/foz* and WT mice, western blot analysis was attempted. Several different procedures were tested in order to optimise Alms1 antibodies using hybridoma supernatant and purified antibody from the clone 3D8 (see Chapter 2, Table 2.1 NB for Alms1 antibody production). In order to detect both the native and truncated form of Alms1, brains collected from *foz*/+, heterozygous, mice were used for these experiments. As Alms1 antibody was produced from Alms1-expressing hybridoma, membranes were first incubated with non-diluted supernatant. Briefly, 40 µg of non-reduced proteins were loaded onto a 5% SDS-PAGE gel. Proteins were transferred overnight in the cold room, using a high molecular weight transfer buffer (see Appendix 1). Membranes were then blocked for 1h in 1% BSA and incubated overnight in non-diluted hybridoma supernatant. Membranes were then incubated with secondary antibody conjugated to horseradish peroxidase. Figure 4.3A corresponds to the images obtained after detection with chemiluminescence using Supersignal West Pico Chemiluminescent (Thermo Scientific, USA).

After analysis with Multi Gauge 3.0 software (Fujifilm, Japan), the approximate molecular weight of the bands observed could be determined. The top bands were located at ~400 kDa, whereas the bottom bands migrated at ~165 kDa. Alms1 is known to be a 360 kDa protein in mice; it was therefore concluded that the top bands could be the native form of Alms1. In *foz/foz* mice, Alms1 is truncated due to an 11-base pair (bp) deletion in the exon 8 of the *Alms1* gene, creating a stop codon at bp 3918 (Arsov *et al.*, 2006b). By dividing the number of base pairs by 3 one can calculate the approximate number of amino acids in the truncated Alms1 protein (~1306). Dividing this number by 110 (which corresponds to the average molecular weight of an amino acid in Daltons), an estimate of ~143 kDa was

obtained for the molecular weight of the truncated Alms1. Consequently, the bottom bands observed in Figure 4.3A could correspond to the truncated form of Alms1. This proposal was supported by the abolition of this band achieved by pre-incubating Alms1 antibody with its blocking peptide (Figure 4.3B).

These experiments were then repeated with the purified Alms1 antibody. Unfortunately, it was not possible to reproduce the same results (Figure 4.3C). While the low molecular weight protein was still present, the high molecular weight protein was not. Instead of detecting a protein at 360 kDa, there was a faint band at 500 kDa. Unfortunately the stock of original hybridoma anti-Alms1 supernatant was completely exhausted by extensive attempts to optimise conditions for western blot analysis. The blot illustrated in Figure 4.3 is from *foz*/+ hypothalamus. It was not possible to perform western blot analysis on *foz/foz* or homozygous WT animals due to this logistic restraint (it had been expected the purified antibody would be more useful for this purpose). Despite its utility for ICF (see Chapter 4, section 4.4.4), it has not been possible yet to optimise the use of this antibody in western blot analysis.

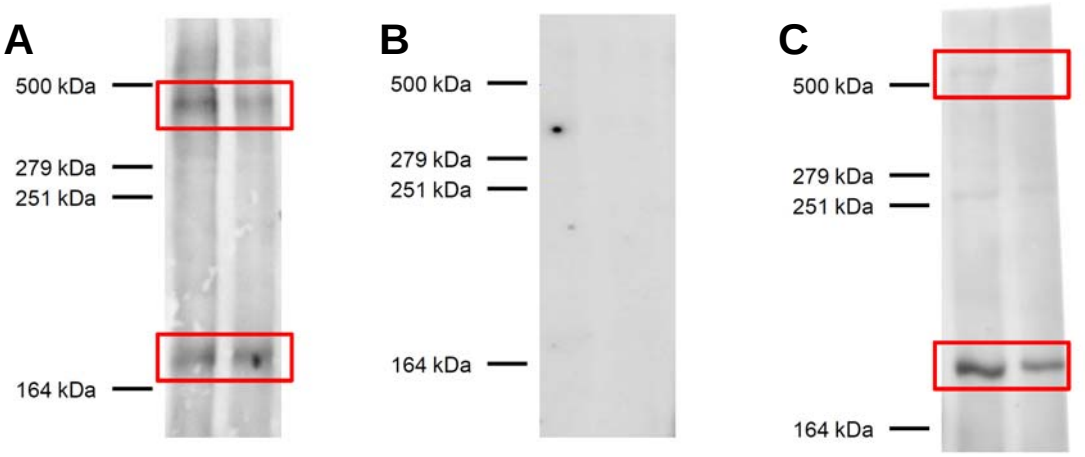

Figure 4.3. Representative western blots of Alms1 in heterozygote (*foz*/+) mice (A-C)

A: Two bands, thought likely to represent the native (~400 kDa) and truncated (~165 kDa) forms of Alms1, were detected when the membranes were incubated with the hybridoma crude supernatant.

B: These bands are proposed to be the native and truncated forms of Alms1 proteins, respectively. Both were blocked by pre-incubation of Alms1 antibody with its control peptide.

C: Only the low molecular weight band was detected when membranes were incubated with the purified Alms1 antibody.

4.4.4. Alms1 localises to the basal body of hypothalamic neurons

Immunocytofluorescence was used to determine the subcellular localisation of Alms1 in hypothalamic neurons grown in primary culture. In hypothalamic neurons cultured from WT mice (Figure 4.4A, B), Alms1 was expressed in the basal body, close to the nucleus. Expression localised as a spherical doublet, as observed in the magnified picture (Figure 4.4B). In striking contrast, no such immunocytofluorescence was observed in hypothalamic neurons cultured from *foz/foz* mice (Figure 4.4C, D). Further, such immunocytofluorescent staining observed in cells from WT mice was completely blocked by pre-incubating Alms1 antibody with its control peptide (Figure 4.4E, F).

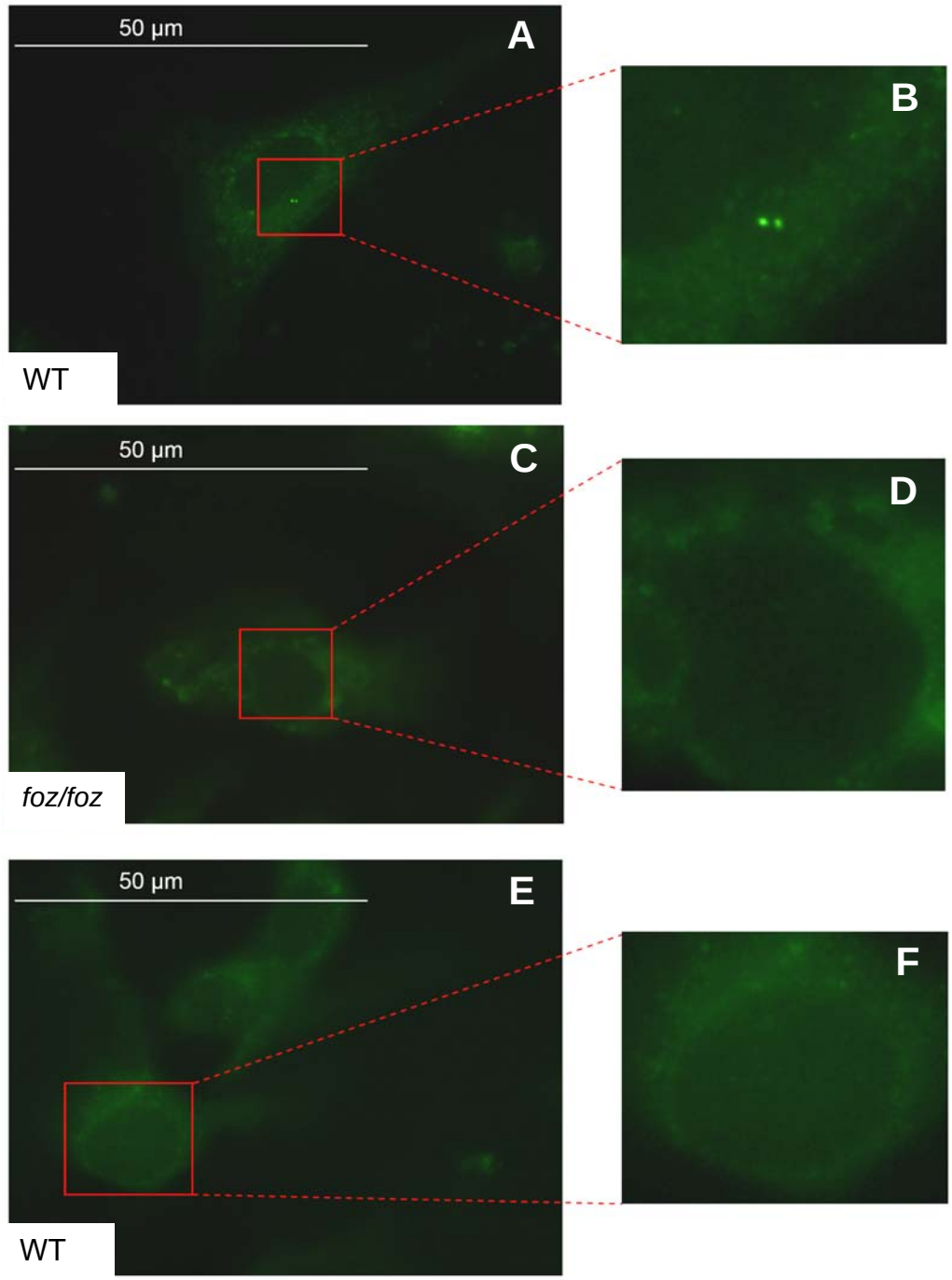

Figure 4.4. Subcellular localisation of Alms1 within hypothalamic neurons in primary culture from WT mice, and absence of Alms1 immunostaining in *foz/foz* mice

Alms1 was present in fixed hypothalamic cells cultured from WT mice (A, B), but not in those from *foz/foz* mice (C, D). The morphology of Alms1 as spherical doublets in WT hypothalamic cells is evident with higher magnification (B). Alms1 staining was blocked by pre-incubating Alms1 antibody with its peptide control (E, F). n ≥ 6 mice per group, staining was repeated in triplicate. Scale: 50 µm.

4.4.5. Alms1 localises close to the primary cilium in hypothalamic neurons cultured from WT mice, but not in *foz/foz* mice

Using ACIII antibody (in red) to stain the primary cilia and Alms1 purified antibody (in green) to demonstrate localisation of Alms1, further studies were performed on neuronal primary cultures to test whether Alms1 expression was structurally related to primary cilia. In Figure 4.5A and B, it can be seen that Alms1 is localised at the base of the primary cilium. Such localisation was not the case in hypothalamic primary cell culture from *foz/foz* mice. It can be seen that primary cilia are still present, despite the lack of Alms1 immunostaining (Figure 4.5C, D). This result was a consistent finding among at least five cultures (obtained from 5 mice), with at least 10 samples immunostained for each experiment. Thus, while Alms1, when present, localises to the base of primary cilia, it is not essential for cilial expression on hypothalamic neurons at birth. This finding is consistent with the data in Figure 3.5, which show a normal number of ciliated cells just after birth.

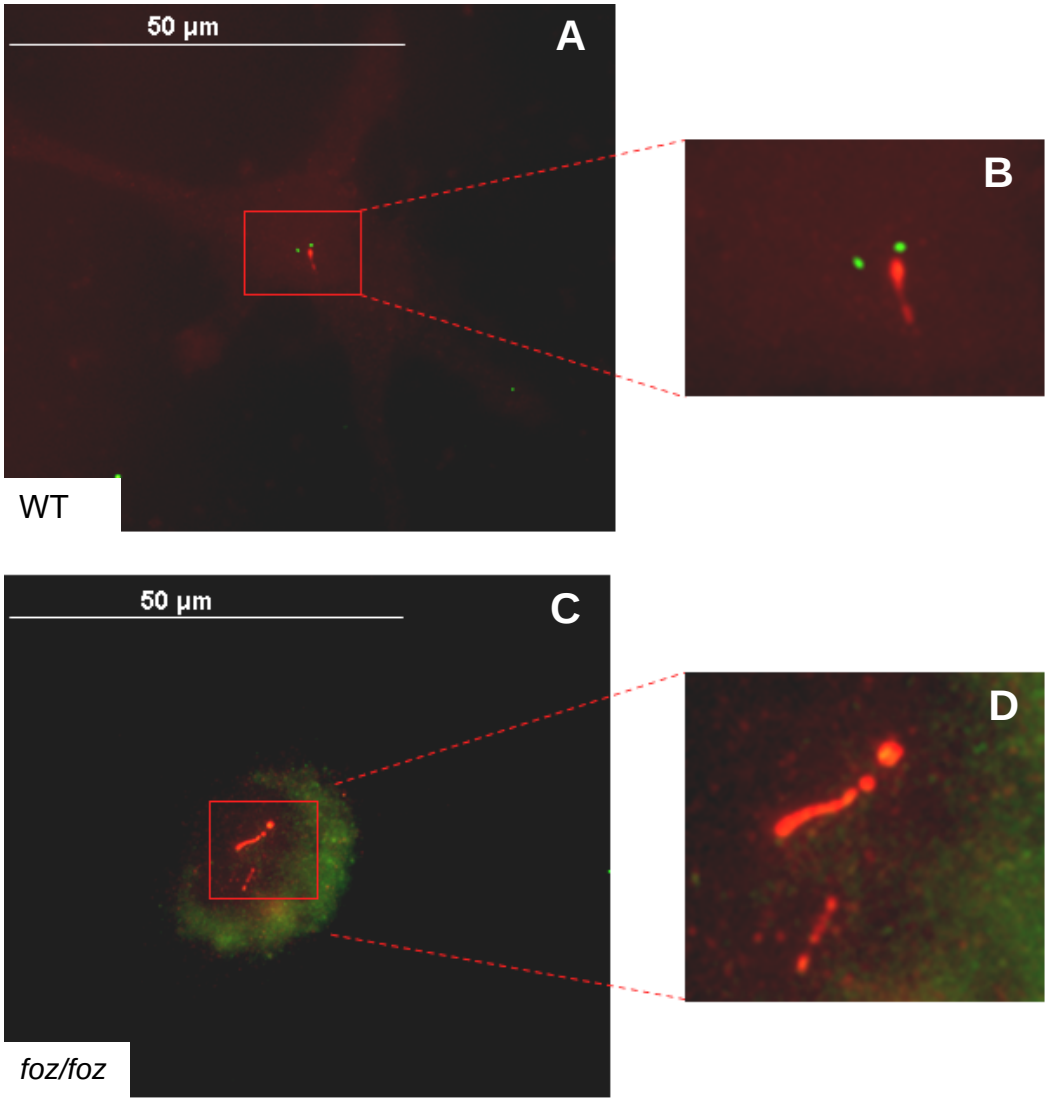

Figure 4.5. Subcellular colocalisation of Alms1 and the primary cilium in hypothalamic neurons from *foz/foz* and WT mice

Alms1 localises at the base of primary cilia in hypothalamic primary culture from WT mice (A, B). This is more evident in the higher magnification picture (B). Although primary cilium staining was present on hypothalamic neurons cultured from *foz/foz* mice, there was no Alms1 fluorescence observed (C, D). n ≥ 5 mice per group. Scale: 50 µm.

4.4.6. Hypothalamic mRNA levels of peptides expressed on the cilial membrane are not changed in *foz/foz* mice

As for all the cilial genes reported in section 3.4.5, there was no difference between hypothalamic transcript levels of SstR3 in *foz/foz* and WT mice, at TC2 or TC12 (Figure 4.6A). When WT mice were fed high fat diet for 2-weeks, hypothalamic MCH1R gene expression appeared to increase compared to chow-fed WT mice ($P < 0.05$, Figure 4.6B). However, no significant changes were observed at TC2 and TC12 in *foz/foz* mice either fed chow or high fat diet compared to their WT matched littermates (Figure 4.6B).

It would have been ideal to perform protein studies of these receptors, but we were already aware of data from our Canadian collaborators with respect to MCH1R and SstR3 immunohistofluorescence, as will be mentioned in the Discussion.

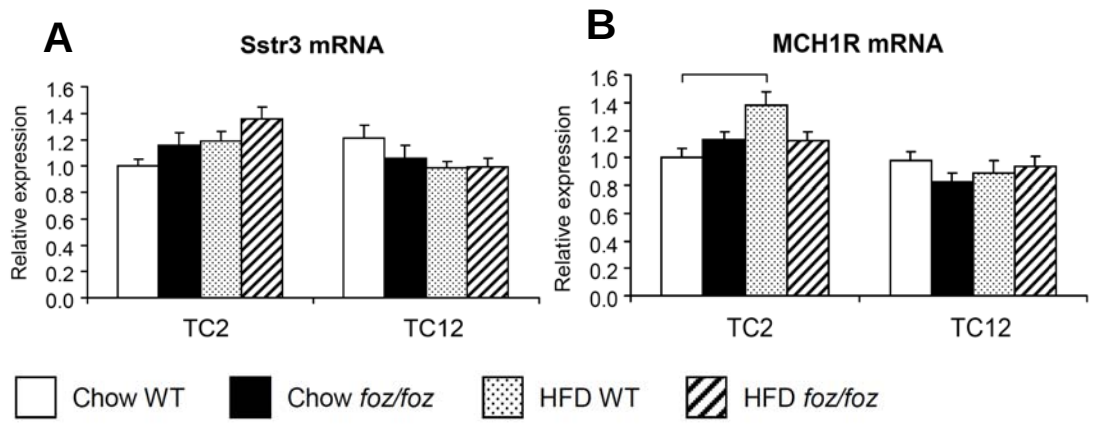

Figure 4.6. SstR3 and MCH1R hypothalamic gene expression is not affected by genotype and/or diet in *foz/foz* mice

A: There was no effect of genotype, diet or time on hypothalamic SstR3 mRNA levels.

B: After 2-weeks on diet, high fat-fed WT mice exhibited a small but significantly higher level of MCH1R mRNA in the hypothalamus compared to chow-fed WT mice. No changes were observed in *foz/foz* mice (on either diet) at the same time point. At TC12, MCH1R mRNA levels were clearly not affected by genotype or diet.

Statistical bar shows significance of post-hoc testing between indicated groups, $P < 0.05$. n ≥ 6 mice per group, real time PCR were repeated in duplicate.

4.5. Discussion

The Alms1 protein has been shown to be ubiquitously expressed in both human and mouse tissues (Collin *et al.*, 2002; Hearn *et al.*, 2002). However, its cellular role is still unknown, and this constitutes a limitation in the understanding of Alström syndrome, and particularly its role in appetite regulation.

In the previous Chapter we showed that *Alms1* mutant, *foz/foz* mice, exhibit a decrease in the number of cilia in the hypothalamus. In the present studies we showed that these mice also exhibit significantly lower *Alms1* mRNA levels, not only in the hypothalamus, but also in white adipose tissue. The first important result in the present Chapter is the demonstration that Alms1 is expressed at the base of the primary cilium in hypothalamic neurons from WT NOD.B10 mice; this is consistent with reported observations in other tissues from humans, other animal models and other cell types (Hearn *et al.*, 2005; Li *et al.*, 2007a; Knorz *et al.*, 2010). However, Alms1 could clearly not be detected in primary hypothalamic neuronal cultures from *foz/foz* mice. Bearing in mind the post-natal loss of neuronal primary cilia in *foz/foz* mice described in the previous Chapter, taken together, these results are consistent with a role for Alms1 either in maintenance/stability of the primary cilium, and/or protein transport to the ciliary membrane.

In order to study the cellular function of Alms1, immunocytofluorescent studies of relevant peptides should be conducted. For example, the possible involvement of Alms1 in cilial trafficking and/or maintenance of cilial integrity has been investigated by performing double staining experiments against Alms1 and the centrosomal marker, γ-tubulin (Hearn *et al.*, 2005; Jagger *et al.*, 2011). Both studies showed that Alms1 colocalises with γ-tubulin, indicating that Alms1 has a

centrosomal function. However, one cannot exclude a role for Alms1 in protein transport. To progress this idea, one could perform double-labelling immunocytofluorescent studies, using antibodies against Alms1 and BBS or IFT proteins.

In 2006, Arsov *et al.* showed that *foz/foz* mice bear an 11 base pair deletion in exon 8 of the mouse *Alms1* gene. This deletion induces a frame-shift mutation, leading to two neo-codons that encode two amino acids not present in the normal sequence, followed by a stop codon (Arsov *et al.*, 2006b). In the present study, we showed that *Alms1* mRNA levels in the hypothalamus and white adipose tissue are significantly lower in *foz/foz* mice than in WT mice. As the primers were designed to detect *Alms1* mRNA before its mutation, the ~50% decrease in *Alms1* mRNA levels was unexpected. Some general explanations/mechanisms for such a drop in the mutated gene mRNA levels would include increased transcript instability (faster destruction), a lower transcription rate or a dysregulation in Alms1 transcription factors (Sp1 and regulatory factor X proteins; Purvis *et al.*, 2010). To confirm these hypotheses, one would need to measure mRNA transcription and degradation rates, but these specialised molecular studies were beyond the scope of the present research.

As described in Chapter 2, the Alms1 antibody was custom made in a way designed to detect both native and truncated forms of Alms1 protein. Briefly, Alms1 antibody was produced from hybridoma cells, and then purified. Both hybridoma supernatant and purified Alms1 antibodies were tested in immunocytofluorescence and immunoblotting assays. The purified Alms1 antibody appeared to demonstrate Alms1 successfully by ICF on WT neuronal primary culture, consistently detecting two tiny dots per cell that correspond to basal body (juxtanuclear) or centrosomal

localisation. However, neither the purified antibody nor hybridoma supernatant demonstrated any Alms1 staining by ICF on *foz/foz* hypothalamic neurons in primary culture. This can be explained by the *Alms1* gene mutation in *foz/foz* mice, which leads to synthesis of a shortened protein. This truncated protein could under go conformational changes so as to be misfolded compared to the native form, so that the antigen is no longer available for antibody binding. Another possibility is that the truncated Alms1 protein is degraded, or there could be reduced translation because of reduced transcription; the latter consistent with the decreased *Alms1* mRNA levels observed in *foz/foz* mice.

When used for immunoblotting on hypothalamic samples from heterozygous mice, which should express both the native and truncated forms of Alms1, the antibody contained in hybridoma supernatant was able to detect two bands. Their molecular mass approximately corresponded to those predicted for native Alms1 and truncated Alms1. Moreover, pre-incubating the supernatant with the corresponding Alms1 peptide (used for rat immunisation and antibody production) resulted in loss of both bands. Therefore, we hypothesised that protein purification of the supernatant should concentrate Alms1 antibodies and improve the signal detected by immunoblotting. Unfortunately, that was clearly not the case. Instead, the purified antibody was not able to detect Alms1 in its native form, although the apparently mutated form was still detected. Owing to the importance of developing these materials, the candidate tried more than twenty different protocols to optimise the antibody without success. A final option would be to regrow the hybridoma cells and use the supernatant, as it seems to give the best results.

In summary, we do not have any concrete explanation on the reason why the purified antibody does not detect Alms1, whereas the supernatant does.

However, we are aware that in order to positively conclude on the absence (or reduction) of Alms1 in *foz/foz* mice, immunoblotting on both *foz/foz* and WT hypothalamic samples is required.

Over the past ten years, several studies have shown that G protein-coupled receptors localise to neuronal primary cilia in rodents. Such receptors include SstR3 (Handel *et al.*, 1999) and MCH1R (Berbari *et al.*, 2008a), both of which are expressed in regions of the brain involved in food intake regulation, including the hypothalamus (Handel *et al.*, 1999; Saito *et al.*, 2001). In the present study, hypothalamic mRNA levels of SstR3 and MCH1R were assessed. Notwithstanding the observation that *foz/foz* mice exhibit a strong decrease in the number of hypothalamic cilia, there were no changes in SstR3 or MCH1R hypothalamic gene expression. It is therefore clear that gene expression is not affected by the decrease in primary cilia number. However, it does remain possible that the respective protein levels or their subcellular localisation might be altered. This has been reported in Bardet-Biedl syndrome (BBS) knock-down mutants, which mislocalise MCH1R and SstR3 to the cytoplasm and the plasma membrane, respectively (Berbari *et al.*, 2008b). While this question was not assessed in the present studies, our colleagues, Prof. Michel Leroux and Lesley Chen (Simon Fraser University, Canada) have shown, in contemporaneous studies, not known to us at the time, that SstR3 and MCH1R are expressed on *foz/foz* mice hypothalamic primary cilia and did not mislocalise in *Alms1* mutant (*foz/foz*) mice (unpublished data from Lesley Chen, Master of Science Thesis, SFU). Alternatively, to test whether the decrease in the number of ciliated cells leads to lower SstR3 and MCH1R protein expression in *foz/foz* mice, the expression of these receptors could be studied by western blot analyses.

Interestingly, another important receptor involved in feeding regulation, Ob-R, has been shown to be expressed on the ciliary membranes of olfactory sensory neurons (Baly *et al.*, 2007). Ob-R has not yet been reported to be localised on hypothalamic primary cilia. However, Seo *et al.,* showed in 2009 that BBS proteins involved in ciliary protein trafficking physically interact with Ob-R and mediate Ob-R trafficking. In regards of those findings, one could hypothesise that Ob-R is expressed on the primary cilial membrane. To assess this hypothesis, one could perform a double labelling against primary cilia and Ob-R on hypothalamic primary neurons from WT and *foz/foz* mice. Several attempts to detect Ob-R on *foz/foz* and WT mice hypothalamic neurons in primary culture have been made by the candidate. To date, three different antibodies against Ob-R have been tried, and for each antibody several dilutions were employed. Unfortunately, all attempts to detect Ob-R on neuronal plasma membrane have been unsuccessful. Further studies will employ immunoprecipitation experiments to determine whether Ob-R interacts with cilial proteins in the hypothalamus. One idea is to investigate the role of Alms1 as well as BBS or IFT proteins in Ob-R expression and cilial transport in *foz/foz* mice.

Davenport *et al.,* (2007) created a mouse model with a hypothalamic ciliary defect in one neuronal subpopulation, the pro-opiomelanocortin (POMC) neurons, which are well known to mediate anorexigenic effects of leptin. They showed that these mice are hyperphagic, leading to obesity, and have high circulating leptin levels. The authors concluded that primary cilia and/or the basal body are involved in regulating feeding behaviour. Other ciliary-deficient mouse models with mutation in BBS proteins also develop obesity associated with increased food intake (Rahmouni *et al.*, 2008). These mice exhibit high serum leptin levels as well as

lower hypothalamic POMC gene expression. The combined results of these earlier studies indicate that defects in hypothalamic primary cilia are closely correlated with feeding behaviour; they lead to obesity, with hyperleptinaemia and variations in hypothalamic neuropeptide expression. In the present work, we have shown that *foz/foz* mice also exhibit a structural defect in hypothalamic primary cilia. This defect is not present at birth, despite failure to express Alms1 at this time, and it is not related to altered expression of two key appetite regulator molecules, SstR3 and MCH1R. Rather, the importance of Alms1 mutation appears related to either late (post-natal) phase development of cilia, or (we believe more likely) to stability of neuronal cilia expression in *foz/foz* mice. In light of the findings discussed above, the next Chapter will focus on circulating leptin levels and their relationship to hypothalamic expression of appetite-regulating neuropeptides in *foz/foz* mice.

CHAPTER 5

Chapter 5

Studies of appetite-regulating neuropeptides expression in *foz/foz* mice

5.1. Introduction

In the previous two Chapters, studies of Alms1 expression demonstrated its localisation to the basal body of hypothalamic neurons at what appeared to be attachment sites for the primary cilium. In *foz/foz* mice, which have a truncating mutation in exon 8 of *Alms1*, there was no evidence of Alms1 protein expression. Further, although the majority (~60%) of *foz/foz* hypothalamic neurons expressed a primary cilium just after birth, by weaning (and thereafter) the number of primary cilia was reduced substantially compared to WT mice. The studies in Chapter 4 showed normal levels of SstR3 and MCH1R mRNA in *foz/foz* mice, but fuller exploration of how decreased cilial number could lead to obesity and its metabolic complications (diabetes, dyslipidaemia, fatty liver disease) is indicated. The present chapter will describe efforts to characterise in more detail the relationships between onset of obesity in *foz/foz* mice and the changes in circulating leptin levels, and hypothalamic expression of appetite-regulating neuropeptides.

According to the World Health Organization “overweight and obesity” are defined as: “abnormal or excessive fat accumulation that may impair health”. White adipose tissue (WAT) not only stores triglycerides, it also secretes a large range of

signalling peptides, among which is leptin. Production of leptin correlates positively with WAT mass (Maffei *et al.*, 1995; Considine *et al.*, 1996). The brain, more specifically the hypothalamus, receives leptin inputs. Central leptin action was first discovered using two *in vivo* models, *ob/ob* mice (which exhibit a mutation in the leptin gene, *ob*) and *db/db* mice (which harbour a mutation in leptin receptor, Ob-R); both genotypes exhibit obesity and type 2 diabetes (Ingalls *et al.*, 1950; Coleman and Hummel, 1969; Coleman, 1973, 1978). In the hypothalamus, leptin binds to its receptor (Ob-R) on specific neurons, located in different hypothalamic nuclei. The leptin receptor has been shown to be expressed principally in the arcuate nucleus (Arc), but lower levels of expression can also be detected in other hypothalamic regions (Mercer *et al.*, 1996). After binding to its receptor in the hypothalamus, leptin inhibits the release of several orexigenic peptides, while it actives anorexigenic cascades (Figure 5.1).

The orexigenic neuropeptides affected by leptin are neuropeptide Y (NPY), agouti-related peptide (AgRP) and melanin concentrating hormone (MCH). AgRP and NPY are coexpressed in the same subpopulation of hypothalamic neurons in the arcuate nucleus (Arc) (Schwartz *et al.*, 1996c; Hahn *et al.*, 1998). Low leptin levels, and conditions of negative energy balance enhance NPY mRNA expression in the Arc, whereas central administration of NPY enhances food intake (for review see Williams *et al.*, 2004). Similar to NPY, AgRP release in the Arc is inhibited by leptin infusion, while its expression is upregulated in *ob/ob* leptin-deficient mice (Shutter *et al.*, 1997). AgRP influences food intake mainly through the competitive antagonism of melanocortin 4-receptor (MC4-R; Ollmann *et al.*, 1997; Rossi *et al.*, 1998; Haskell-Luevano and Monck, 2001). MCH is an orexigenic peptide mostly expressed in the lateral hypothalamic area. Studies have shown that administration

of MCH increases food intake (Qu *et al.*, 1996; Ludwig *et al.*, 1998), whereas knocking down the MCH gene leads to a reduction in body weight (Shimada *et al.*, 1998).

The anorexigenic peptides upregulated by leptin are pro-opiomelanocortin (POMC) which is cleaved into α-melanocyte stimulating hormone (α-MSH), cocaine and amphetamine-regulated transcript (CART), and corticotropin-releasing hormone (CRH). Leptin stimulates POMC expression in the hypothalamus (Schwartz *et al.*, 1997; Mizuno *et al.*, 1998). There, it is proteolytically cleaved to generate α-MSH which inhibits food intake via the MC4-R. The balance between AgRP and α-MSH determines MC4-R activity (Rossi *et al.*, 1998). CART colocalises within POMC and MCH neurons, and as for α-MSH, its expression is positively regulated by leptin (Kristensen *et al.*, 1998). CRH is mainly expressed in the paraventricular nucleus (PVN) of the hypothalamus. Administration of this peptide to the PVN leads to a marked suppression of food intake in normal rats (Arase *et al.*, 1988), as well as in genetically obese rats (Arase *et al.*, 1989).

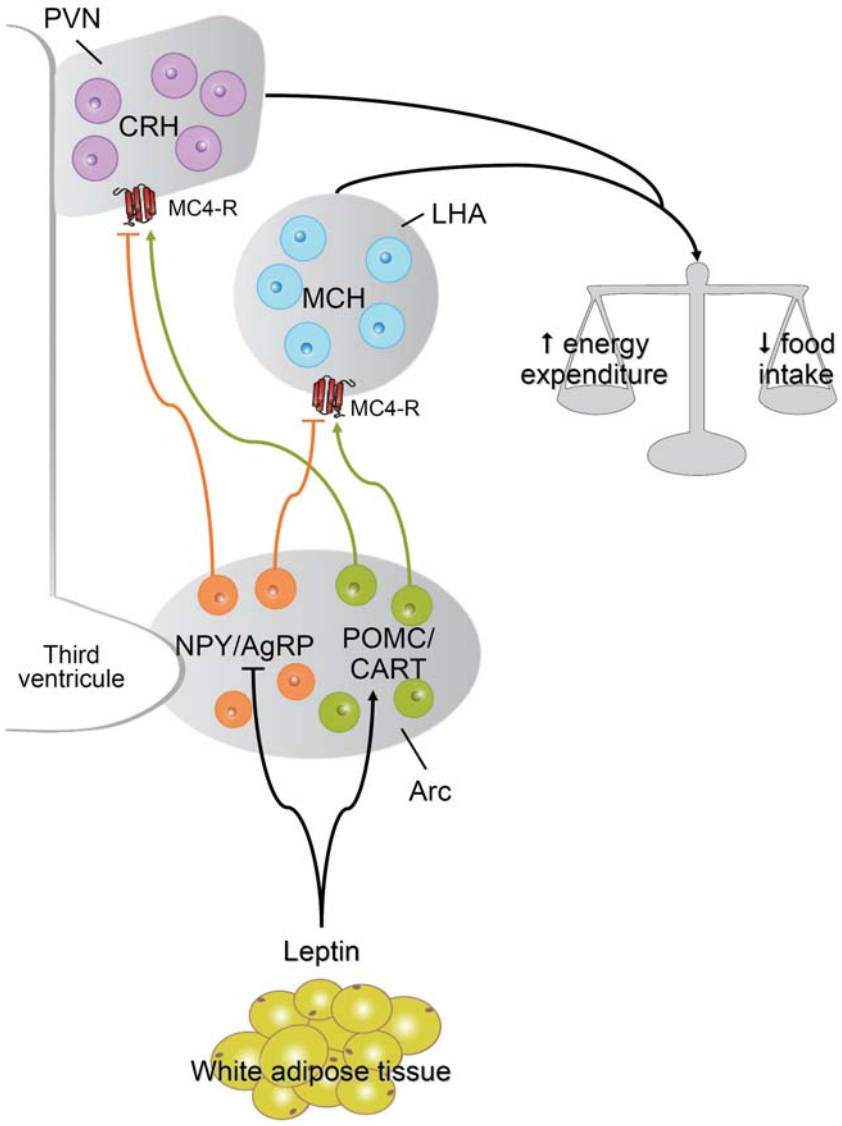

Figure 5.1. Hypothalamic neuropeptides involved in food intake regulation

Leptin is released from adipose tissue and stimulates hypothalamic anorexigenic signalling pathways (POMC/CART, CRH), while inhibiting orexigenic pathways (NPY/AgRP, MCH). Therefore, leptin triggers a decrease in food intake. It also increases energy expenditure (not discussed further).

Abbreviations: AgRP, Agouti-related protein; Arc, Arcuate nucleus; CART, Cocaine and amphetamine-regulated transcript; CRH, Corticotropin-releasing hormone; LHA, Lateral hypothalamic area; MC4-R, Melanocortin 4-receptor; MCH, Melanin concentrating hormone; NPY, Neuropeptide Y; POMC, Pro-opiomelanocortin; PVN; Paraventricular nucleus.

Recent discoveries indicate a close relationship between primary cilia and hypothalamic neuropeptides. As discussed in Chapter 4, one set of cilial proteins, Bardet-Biedl syndrome (BBS) proteins, are involved in the membrane localisation of MCH1R and SstR3 on primary cilia (Berbari *et al.*, 2008b). Furthermore, Davenport *et al.,* (2007) showed that genetic deletion of primary cilia, specifically those on POMC neurons, resulted in mice with increased body weight and adiposity, and elevated circulating leptin levels.

These findings show that hypothalamic primary cilia and neuropeptides both play an important role in feeding behaviour. In the present Chapter, we explore the hypothesis that hyperphagia-related obesity in *foz/foz* mice could be due to cilial defects that dysregulate expression of key appetite-regulating hypothalamic neuropeptide(s). It is noted here that earlier studies in the host laboratory showed that *foz/foz* mice have greatly elevated circulating leptin levels at 18 wks of age. In the present Chapter, studies on the role of leptin on hypothalamic neuropeptides expression in *foz/foz* mice were performed. For this purpose, hypothalamic gene and protein expression/localisation of key appetite-regulating neuropeptides were studied at selected time points.

5.2. Purpose of the study

From studies completed shortly after the onset of this project (Larter *et al.*, 2009), it had been noted that circulating leptin levels appeared to increase disproportionally in high fat-fed *foz/foz* mice compared to their WT counterparts. It should also be noted that *foz/foz* mice consume more food than their WT

littermates, indicating that hyperphagia is at least partly responsible for excessive weight gain (preliminary studies also show that *foz/foz* mice are underactive). It was therefore hypothesised that early onset hyperleptinaemia leads to a state of central (hypothalamic) leptin resistance with corresponding changes in the anorexigenic and/or orexigenic peptides subject to leptin regulation.

Thus, the specific aims of this study were to:

1) Compare the changes in serum leptin after weaning between *foz/foz* and WT mice fed chow or high fat diet.

2) Determine hypothalamic expression of key appetite-regulating peptides in *foz/foz* mice.

5.3. Methods

5.3.1. Animals and diets

Female WT and *foz/foz* mice were bred at The Canberra Hospital Animal Facilities. Mice were housed under a 12 hour light-dark cycle and given free access to food and water. At 6 weeks after birth (2-3 weeks post-weaning,) mice were fed either chow or high fat diet (see Chapter 2, section 2.2.2). Mice were sacrificed at weaning or after 2 or 12 weeks on diet (see Chapter 2, section 2.2.2). Briefly, they were fasted for at least 4h before tissue collection. Mice were then anaesthetised, blood collected by cardiac puncture (between 11:00 am and 1:00 pm), hypothalamus, liver, muscle, white adipose tissue (WAT), and brown adipose tissue rapidly excised and frozen in liquid nitrogen for later analysis, as described in

Chapter 2, section 2.3. Peri-ovarian WAT was collected and weighed from the right side only, while subcutaneous WAT was collected from the right lower quadrant.
A second cohort of mice was bred in order to perform 4% paraformaldehyde cardiac perfusion of the brain for IHF experiments, as described in Chapter 2, section 2.4.

5.3.2. Gene expression analyses

Hypothalamic mRNA levels for NPY, AgRP, MCH, POMC, CRH, MC4-R were measured by real time PCR. Briefly, whole hypothalami were collected from chow and high fat-fed *foz/foz* and WT mice at TC2 and TC12. Dissected hypothalami were collected from chow-fed *foz/foz* and WT mice at weaning and TC2 (see Chapter 2, section 2.3). Hypothalami were snap frozen immediately after collection. After thawing, RNA was extracted following the TRI Reagent® protocol (Sigma-Aldrich, USA). cDNA was synthesised using SuperSript® III Reverse Transcriptase (Invitrogen™, USA). Real time PCR was then performed using iQ™ SYBR® Green Supermix on the iQ™5 real time thermal cycler (Bio-Rad, USA). Experiments were repeated in duplicate and normalised to three housekeeping genes: beta-actin, B2M, RPL13a (see primers in Chapter 2, Table 2.3). The details of this strategy are outlined in Chapter 2, section 2.6.1.

5.3.3. Protein expression analyses

An initial trial to extract both RNA and protein following the TRI Reagent® protocol was attempted, but unfortunately the protein yield was low and variable between individuals, leading to abandonment of this approach. Therefore, to conduct hypothalamic protein expression analyses, another animal cohort was raised. In this work, hypothalamic proteins were extracted after homogenising the whole hypothalamus in homogenising buffer (see Chapter 2, section 2.6.2, and Appendix 1). The amount of protein was estimated using a protein estimation kit (Bio-Rad, USA). Protein extracts were then diluted to 2 µg/µl, and 10 µl of each sample was loaded onto a SDS-PAGE gel (Appendix 1), followed by separation, transfer and quantification.

5.3.4. Immunohistofluorescence

The localisation of hypothalamic neuropeptides was assessed by immunofluorescence, using specific antibodies against AgRP, NPY and CART. Briefly, brains from WT and *foz/foz* mice fed chow or high fat diet were collected at weaning, TC2 and TC12 after transcardiac perfusion with 4% paraformaldehyde (see Chapter 2, section 2.4.1). Brains were then sectioned and immunohistofluorescence performed. Immunostained brain sections were viewed using an Olympus (Japan) IX71 inverted microscope, and images were captured with a DP71 camera coupled to a U-RFL-T mecury burner (Olympus, Japan). Pictures were then transformed to pseudocolour images corresponding to the

relative immunoreactivity for each neuropeptide. The logic of this method is described in Chapter 2, section 2.5.3.

5.3.5. Statistical analyses

The effect of genotype and diet were compared using 2-way analysis of variance (ANOVA), with Tukey post-hoc testing. Differences between genotypes at weaning were determined by using the Student's T-test. For all comparisons, $P < 0.05$ was considered significant. Data are presented as mean ± SEM. The number of individuals per experimental group (n) is given in the text and also in Chapter 2, section 2.2.3.

5.4. Results

5.4.1. *Foz/foz* mice are obese with increased fat mass

At weaning there were no obvious differences in body weight between *foz/foz* and WT mice. However, at TC2 (corresponding to 8 weeks of age), high fat-fed *foz/foz* mice showed significantly increased body weight compared to their diet-matched WT littermates and to chow-fed *foz/foz* mice ($^{*,\ \#}P <$ 0.001; Figure 5.2). When fed for 12-weeks on chow, *foz/foz* mice body weight was significantly higher (41 ± 1.5 g) compared to their WT counterparts (25 ± 0.4 g; $^{\dagger}P < 0.001$; Figure 5.2). This was exacerbated by high fat-feeding. Indeed, such

high fat-fed *foz/foz* mice weighed 55 ± 1.4 g, compared to 31 ± 1.8 g for their diet-matched WT littermates (*$P < 0.001$; Figure 5.2). At TC12, high fat-fed *foz/foz* mice also showed increased body weight compared to their chow-fed genotype-matched littermates ($^{\#}P < 0.001$; Figure 5.2).

At weaning, the amount of white adipose tissue (WAT) was too small to be harvested reliably. Thus, data are confined to TC2 and TC12 measurements of peri-ovarian and subcutaneous fat pads (see Chapter 2, section 2.3). In Figure 5.3, the results are shown as a percentage of body weight. Changes in the peri-ovarian WAT mass over time displayed the same pattern as body weight (Figure 5.3A). After 2-weeks on diet, both chow and high fat-fed *foz/foz* mice showed a significant increase in peri-ovarian WAT mass compared to their WT littermates and also between high fat- and chow-fed *foz/foz* mice ($^{\dagger, \#, *}P < 0.05$; Figure 5.3A). After 12-weeks on diet, *foz/foz* mice either fed chow or high fat diet, exhibited a robust increase in the peri-ovarian WAT mass compared to their corresponding WT littermates ($^{\dagger, *}P < 0.05$; Figure 5.3A).

Subcutaneous fat mass was also affected by genotype and diet. As such, after 2-weeks of high fat-feeding, *foz/foz* mice showed significant increase in subcutaneous WAT mass compared to their genotype and diet-matched littermates ($^{\#, *}P < 0.05$; Figure 5.3B). After 12-weeks on diet, both chow and high fat-fed *foz/foz* mice exhibited a major increase in subcutaneous WAT mass compared to their diet-matched WT littermates ($^{\dagger, *}P < 0.05$; Figure 5.3B).

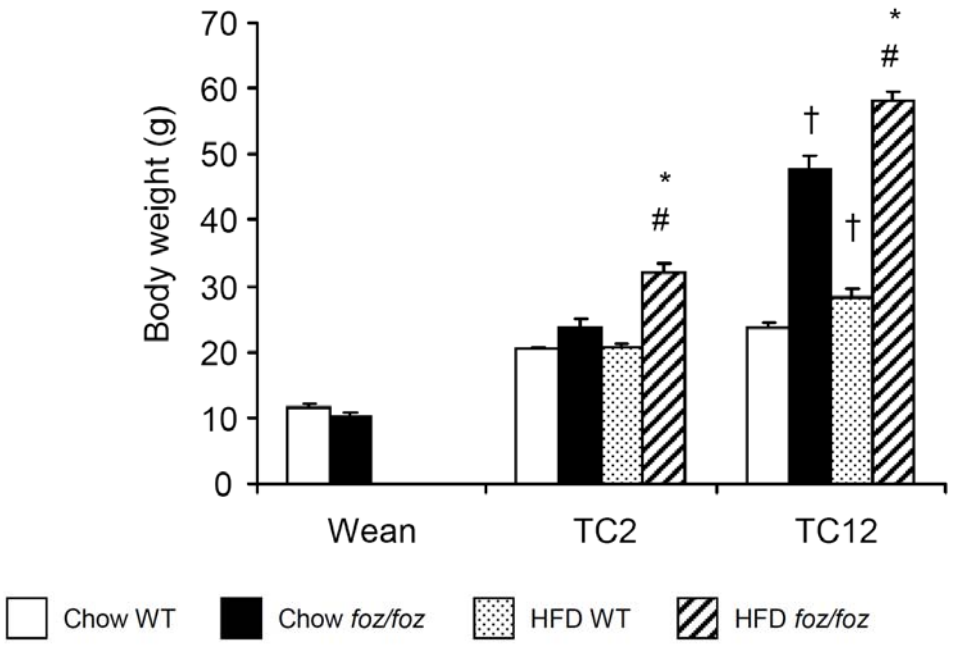

Figure 5.2. Body weights of *foz/foz* and WT mice according to age and diet

At weaning and TC2 (8 weeks of age), there were no changes in body weight between chow-fed *foz/foz* and WT mice. High fat feeding did not increase body weight of WT mice until TC12, but an increase in body weight was observed earlier (TC2) in *foz/foz* mice. At TC12, body weight was affected by both genotype and diet in *foz/foz* mice. n ≥ 6 mice per group.

*$P < 0.001$, compared to WT HFD at TC2 or TC12.

#$P < 0.001$, compared to *foz/foz* chow at TC2 or TC12.

†$P < 0.001$, compared to WT chow at TC12.

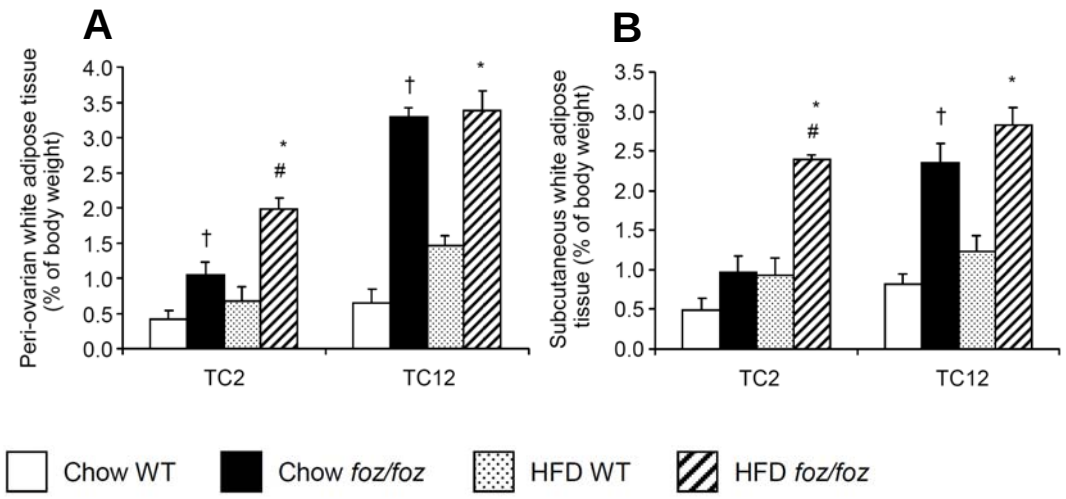

Figure 5.3. Relative mass (% of body weight) of peri-ovarian (A) and subcutaneous (B) white adipose tissue in WT and *foz/foz* mice according to age and diet

A: At TC2 and TC12, *foz/foz* mice showed robust increase in peri-ovarian WAT mass compared to their WT littermates. n ≥ 6 mice per group.

B: At TC2, high fat-fed *foz/foz* mice exhibited a significant increase in subcutaneous WAT mass at TC2. After 12-weeks on diet, both chow and high fat-fed *foz/foz* mice showed major increases in subcutaneous WAT mass compared to their WT littermates. n ≥ 6 mice per group.

$^{*}P < 0.05$, compared to WT HFD at TC2 or TC12.

$^{\#}P < 0.05$, compared to *foz/foz* chow at TC2.

$^{\dagger}P < 0.05$, compared to WT chow at TC2 or TC12.

5.4.2. *Foz/foz* mice are hyperleptinaemic

At weaning, mean plasma leptin levels were 0.7 ± 0.1 and 1.3 ± .0.2 ng/ml for *foz/foz* and WT mice, respectively (Figure 5.4); this apparent difference is not significant. After 2-weeks on diet (TC2), high fat-fed *foz/foz* mice showed a

significant increase in circulating leptin levels compared to high fat-fed WT and chow-fed *foz/foz* mice ($^{\#,*}P < 0.05$; Figure 5.4). After 12-weeks on diet, all *foz/foz* mice presented a robust increase in circulating leptin levels. Thus, in chow-fed *foz/foz* mice (73 ± 14 ng/ml), serum leptin level was ~35-fold higher than in chow-fed WT mice (2.0 ± 0.4 ng/ml; $^{\dagger}P < 0.05$; Figure 5.4). High fat-feeding caused further elevation of serum leptin; thus, high fat-fed *foz/foz* mice showed mean values of 119 ± 10.6 ng/ml, compared to 22 ± 4.3 ng/ml in high fat-fed WT controls ($^{*}P < 0.05$; Figure 5.4).

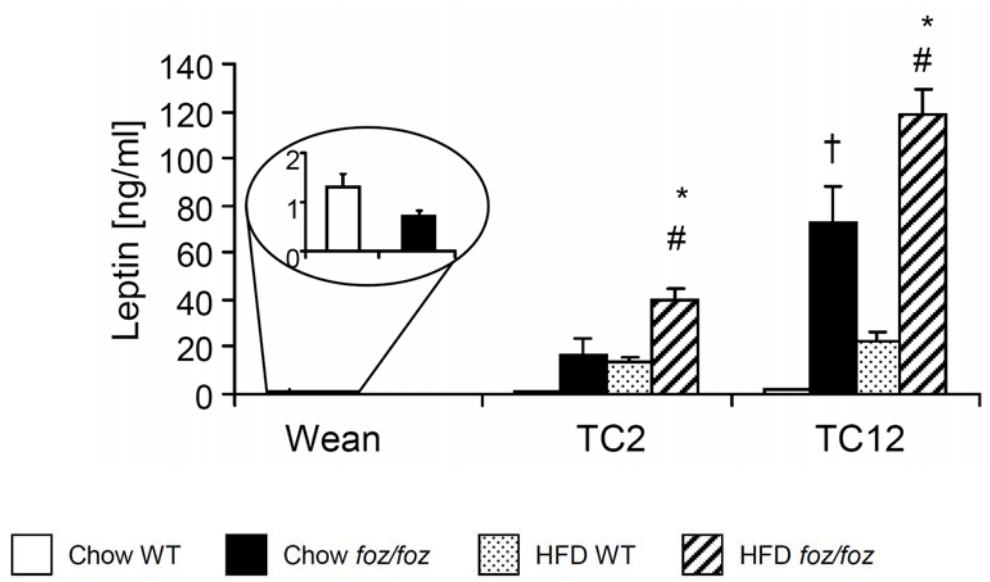

Figure 5.4. Circulating leptin levels at weaning and during 2 and 12 weeks of dietary intake in *foz/foz* and WT mice

No differences in plasma leptin levels were observed at weaning between *foz/foz* and WT mice, as shown more clearly in the inserted scale magnification. Leptin levels were increased in all *foz/foz* mice, as well as in high fat-fed WT mice at TC2, but values were highest in high fat-fed *foz/foz* mice. After 12-weeks on diet, *foz/foz* mice showed an even greater increase in circulating leptin levels compared to diet-matched littermates. n ≥ 6 mice per group.

$^{*}P < 0.05$, compared to WT HFD at TC2 or TC12.

$^{\#}P < 0.05$, compared to *foz/foz* chow at TC2 or TC12.

$^{\dagger}P < 0.05$, compared to WT chow at TC12.

5.4.3. Studies of orexigenic neuropeptide expression in *foz/foz* and WT mice

5.4.3.1. Hypothalamic NPY mRNA levels and protein localisation

After 2-weeks on diet, high fat-fed WT mice showed a significant increase in hypothalamic NPY mRNA levels compared to chow-fed WT and high fat-fed *foz/foz* mice, and values were not increased in high fat-fed versus chow-fed *foz/foz* mice ($P < 0.05$, Figure 5.5A). At TC12, the apparent increase in NPY mRNA levels in high fat-fed WT compared with chow was no longer significant, although values remained significantly higher than in high fat-fed *foz/foz* mice ($P < 0.05$, Figure 5.5A). In localisation studies, NPY mRNA was shown to be expressed mainly in the PVN and Arc (Figure 5.5B, D). There was a significant effect of time in paraventricular and arcuate nuclei NPY mRNA levels, but no effect of genotype. Thus, NPY gene expression was significantly lower at TC2 than at weaning in both *foz/foz* and WT mice ($^{\S}P < 0.05$; Figure 5.5B). This decrease was even stronger in the arcuate nucleus ($P < 0.05$; Figure 5.5D). In addition to the generally low expression levels, there were no differences in NPY mRNA levels observed in the anterior hypothalamic area (Figure 5.5C).

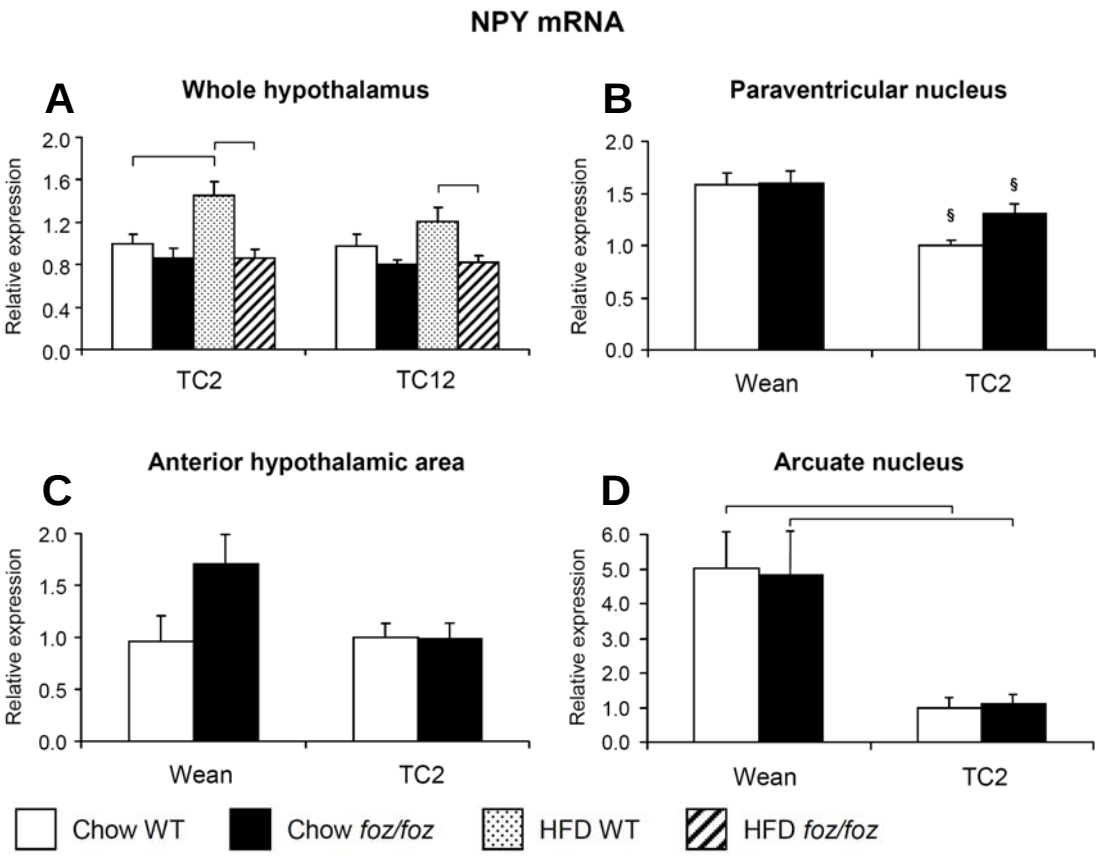

Figure 5.5. NPY mRNA levels in whole hypothalamus (A) and in hypothalamic nuclei (B-D) at weaning and during dietary regimes in *foz/foz* and WT mice

At weaning (Wean), 2 (TC2) or 12 weeks (TC12) on chow or high fat diet (see Chapter 2, section, 2.2.2), animals were sacrificed, hypothalamus removed, and used whole as indicated or dissected for major nuclei (see Chapter 2, section 2.3.2). Total mRNA was extracted (n ≥ 6 mice per group) and NPY mRNA levels determined by semi-quantitative real time PCR (see Chapter 2, section 2.6).

A: Compared to chow-fed controls, NPY mRNA levels were significantly higher in high fat-fed WT mice (but not in *foz/foz* mice) at both TC2 and TC12.

B: In the paraventricular nucleus, NPY gene expression decreased significantly with time in both genotypes.

C: In the anterior hypothalamic area, there were no variations in NPY mRNA levels between *foz/foz* and WT mice with genotype or time.

D: In the arcuate nucleus, NPY gene expression was significantly reduced in both *foz/foz* and WT mice at TC2 compared to weaning.

Statistical bars show significance of post-hoc testing between indicated groups, $P < 0.05$. $^{\S}P < 0.05$, ANOVA results for effect of time.

NPY immunofluorescence in brain sections was analysed by applying a pseudocolour plug-in to the initial picture. This device allowed NPY localisation in the hypothalamus to be shown more precisely. The results showed no obvious changes in NPY hypothalamic localisation at TC2 between *foz/foz* and WT mice (Figure 5.6). Here we show representative pictures of NPY hypothalamic expression at TC2 in *foz/foz* and WT mice fed chow. The same results were observed at weaning and TC12, and in high fat-fed mice at both TC2 and TC12 (data not shown).

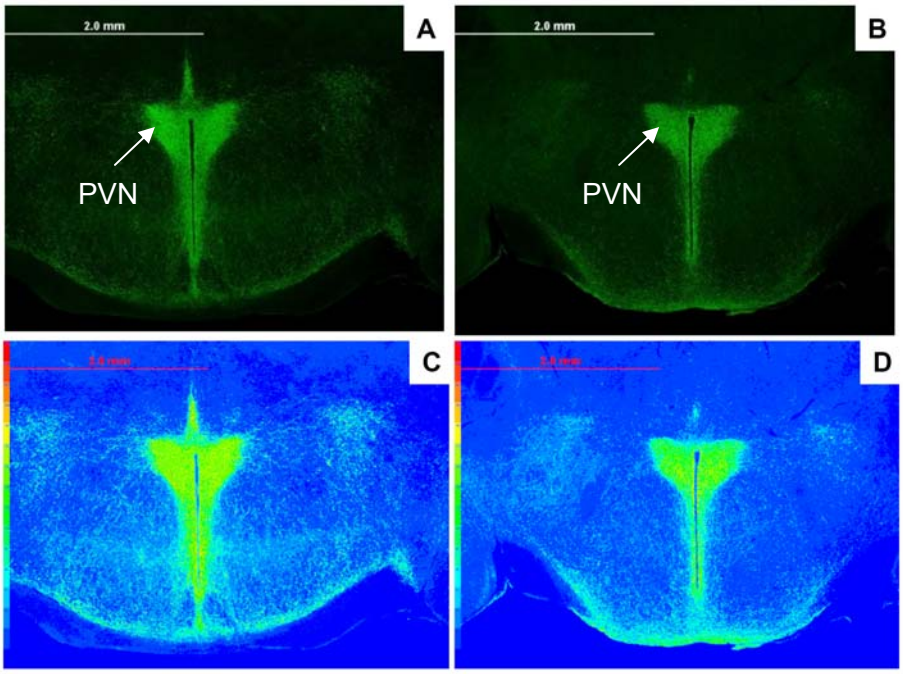

Figure 5.6. Representative hypothalamic NPY expression in chow-fed *foz/foz* (A, C) and WT mice (B, D) at TC2

Immunohistofluorescence pictures (A, B) were transformed in pseudocolour images (C, D) corresponding to a colour scale illustration of NPY. No obvious differences in NPY hypothalamic localisation were observed between *foz/foz* (A, C) and WT (B, D) mice. A similar pattern of immunohistofluorescent staining and corresponding pseudocolour images was obtained both at weaning and at TC12 as well as in high fat-fed mice at both TC2 and TC12 (n = 6 mice per group).

5.4.3.2. Hypothalamic AgRP mRNA levels and protein localisation

There were no variations in hypothalamic AgRP mRNA levels at TC2 between *foz/foz* and WT mice (Figure 5.7A). However, after 12-weeks on high fat diet, both *foz/foz* and WT mice showed higher hypothalamic AgRP gene expression (**P* < 0.05; Figure 5.7A). Like NPY, AgRP mRNA levels in the Arc were substantially decreased at TC2 compared to weaning in both *foz/foz* and WT mice fed chow (*P* < 0.05; Figure 5.7D). There were no significant variations in AgRP mRNA levels in both PVN and AH, regardless of genotype and time (Figure 5.7B and C, respectively).

Hypothalamic expression of AgRP by IHF was not affected by genotype or diet at TC2 (see representative AgRP staining, Figure 5.8). In contrast to data for transcript expression, we did not observe variations in AgRP hypothalamic localisation between *foz/foz* and WT mice at weaning or after 12-weeks on diet, regardless of the diet (data not shown).

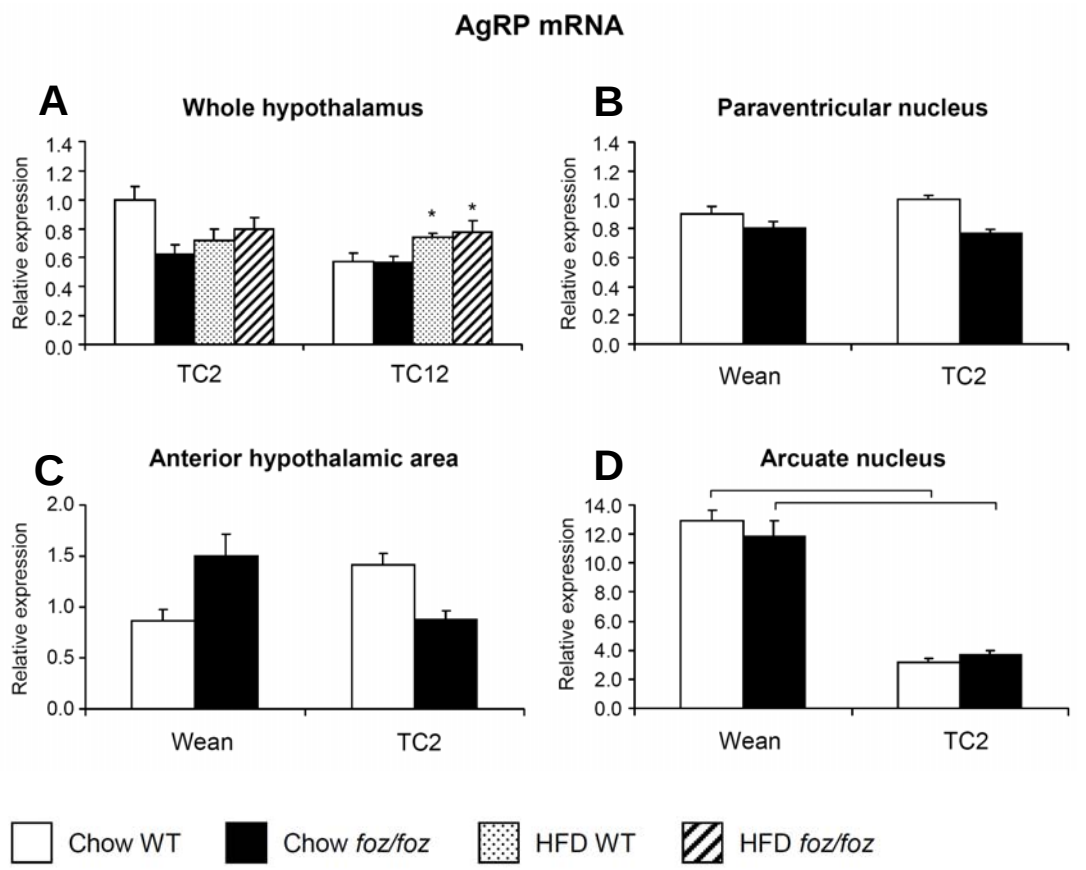

Figure 5.7. AgRP mRNA levels in whole hypothalamus (A) and in hypothalamic nuclei (B-D) at weaning and during dietary regimes in *foz/foz* and WT mice

Dietary experiments and collection of samples are described in Figure 5.5. Total mRNA was extracted (n ≥ 6 mice per group) and AgRP mRNA levels determined by semi-quantitative real time PCR (see Chapter 2, section 2.6).

A: AgRP mRNA levels were increased by high fat feeding at TC12 in both *foz/foz* and WT mice, but no earlier changes are apparent.

B: In the paraventricular nucleus, AgRP gene expression was not affected by genotype or time in chow-fed mice.

C: In the anterior hypothalamic area, there were no variations in AgRP mRNA levels between chow-fed *foz/foz* and WT mice with time.

D: In the arcuate nucleus, AgRP gene expression was reduced in chow-fed *foz/foz* and WT mice at TC2 compared to weaning.

Statistical bars show significance of post-hoc testing between indicated groups, $P < 0.05$.

*$P < 0.05$, ANOVA results for effect of diet.

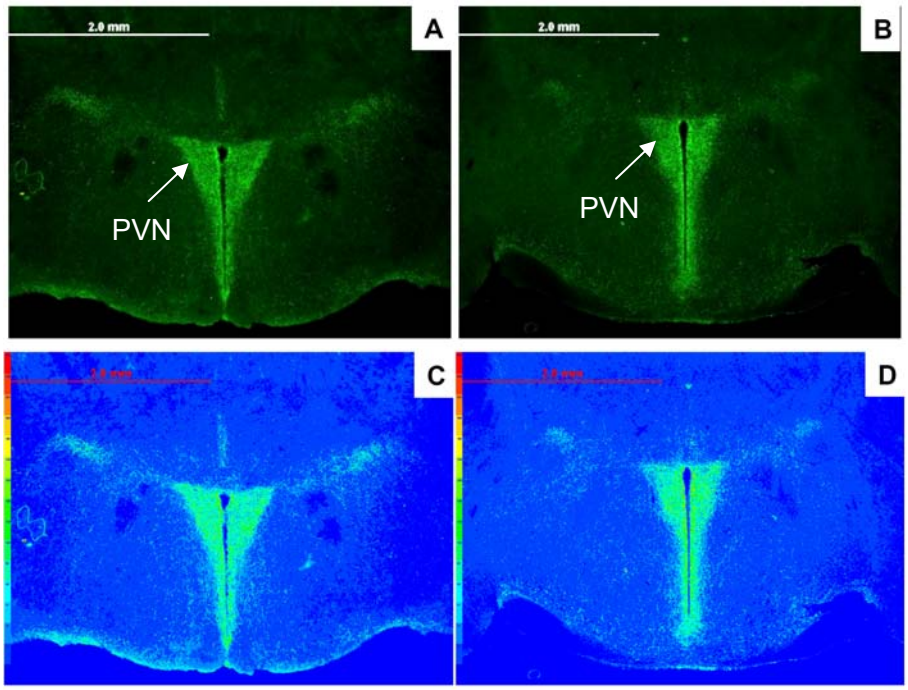

Figure 5.8. Representative hypothalamic AgRP expression in chow-fed *foz/foz* (A, C) and WT mice (B, D) at TC2

Immunohistofluorescence pictures (A, B) were transformed in pseudocolour images (C, D) corresponding to a colour scale illustration of AgRP. No obvious differences in AgRP hypothalamic localisation are evident between *foz/foz* (A, C) and WT (B, D) mice. The same immunohistofluorescent staining and corresponding pseudocolour images were obtained at weaning and TC12 and in high fat-fed mice (n = 6 mice per group).

5.4.3.3. Hypothalamic MCH mRNA levels

Expression of MCH mRNA in the whole hypothalamus was not affected by genotype or diet at TC2 (Figure 5.9). After 12-weeks on diet, a significant decrease in MCH hypothalamic expression was found in high fat-fed *foz/foz* and WT mice compared to respective chow-fed animals (*$P < 0.01$; Figure 5.9). For reasons of insufficient material from dissected hypothalamic nuclei, no attempt was made to measure MCH expression in those hypothalamic regions.

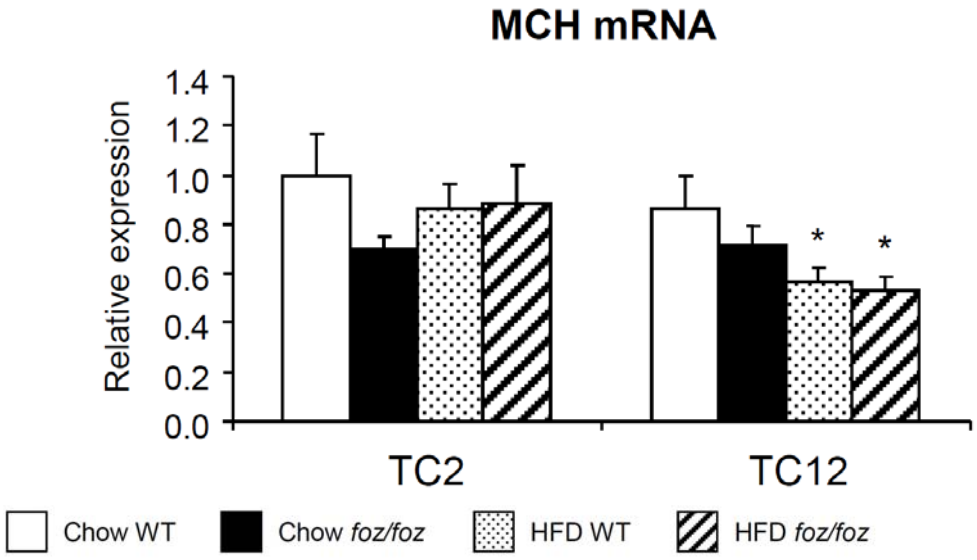

Figure 5.9. MCH mRNA levels in whole hypothalamus during dietary regimes in *foz/foz* and WT mice

At 2 (TC2) or 12 weeks (TC12) on a chow or high fat diet (see Chapter 2, section 2.2.2), animals were euthanised and hypothalamus removed (see Chapter 2, section 2.3.1). Total mRNA was extracted and MCH mRNA levels determined by semi-quantitative real time PCR (see Chapter 2, section 2.6; n ≥ 6 mice per group). There was a modest decrease in MCH mRNA levels in mice fed a high fat diet for 12 weeks.

*$P < 0.01$, ANOVA results for effect of diet.

5.4.4. Studies of anorexigenic neuropeptide expression in *foz/foz* and WT mice

5.4.4.1. Hypothalamic POMC mRNA and protein levels

In the whole hypothalamus, POMC gene expression did not vary with genotype or diet at TC2 or TC12 (Figure 5.10A). However, in the AH POMC mRNA levels varied greatly between individuals. Despite this, a significant increase in POMC mRNA expression was observed at TC2 in WT mice compared to weaning ($P < 0.05$; Figure 5.10B). A similar pattern was observed in *foz/foz* mice, but the apparent difference was not significant. Likewise, POMC mRNA data in Arc were variable; there was no significant differences, irrespective of genotype and time (Figure 5.10C). POMC gene expression in the PVN was below the levels of detection; therefore, no PVN POMC mRNA data are included in Figure 5.10.

POMC hypothalamic protein expression was not affected by genotype at weaning (Figure 5.11). After 2- and 12-weeks on diet, hypothalamic POMC protein expression appeared similar between genotypes and by diet (Figure 5.11).

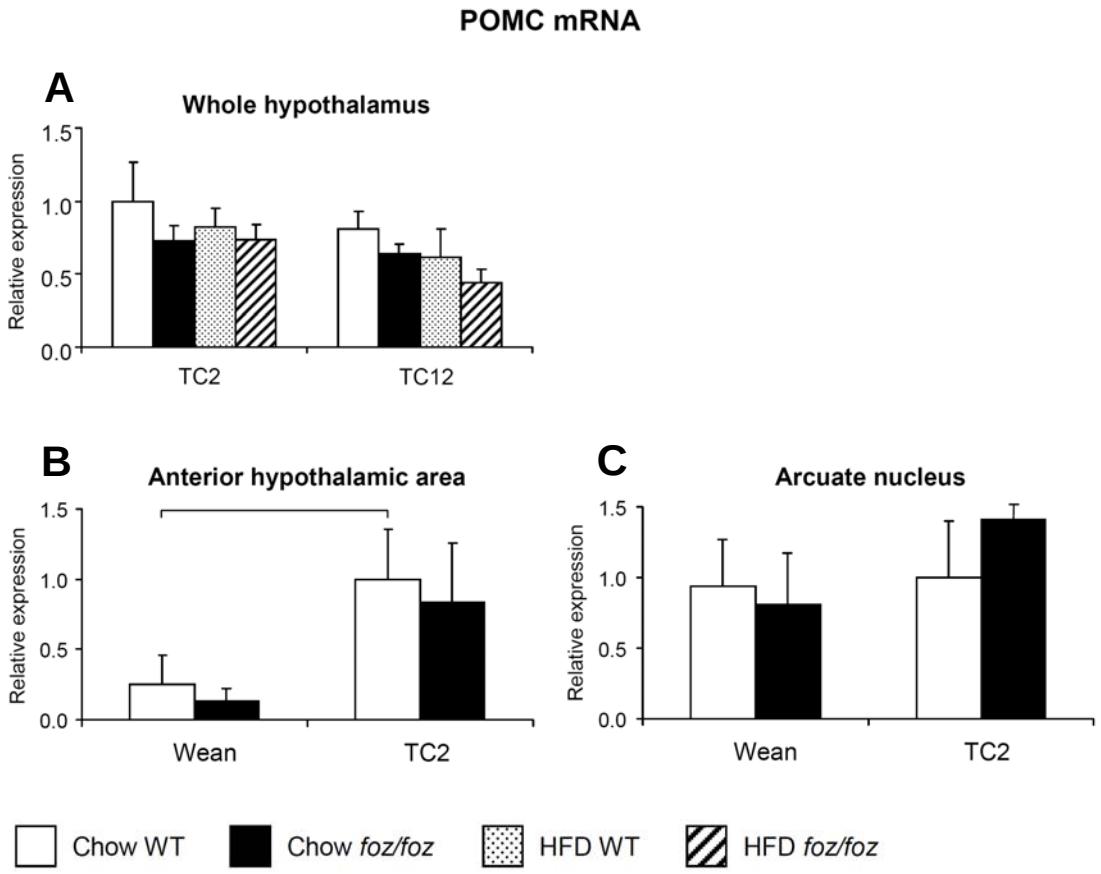

Figure 5.10. POMC mRNA levels in whole hypothalamus (A) and in hypothalamic nuclei (B-C) at weaning and during dietary regimes in *foz/foz* and WT mice

Dietary experiments and collection of samples are described in Figure 5.5. Total mRNA was extracted (n ≥ 6 mice per group) and POMC mRNA levels were determined by semi-quantitative real time PCR (see Chapter 2, section 2.6).

A: POMC mRNA levels were not affected by genotype or diet in the whole hypothalamus at either TC2 or TC12.

B: In the anterior hypothalamic area, POMC gene expression was increased in WT mice at TC2 compared to weaning. There was no difference between *foz/foz* and WT mice.

C: There were no variations in POMC mRNA levels between *foz/foz* and WT mice in the arcuate nucleus at either time of the study.

Statistical bar shows significance of post-hoc testing between indicated groups, $P < 0.05$.

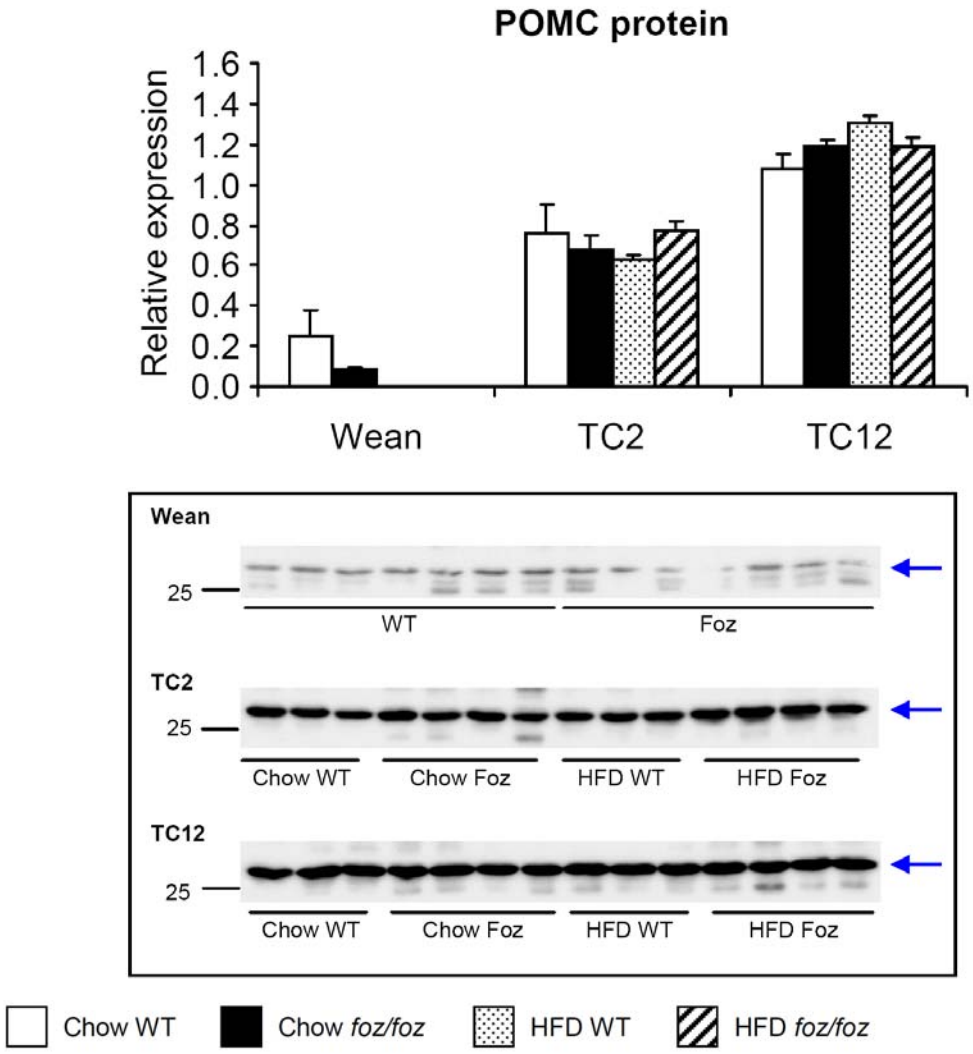

Figure 5.11. POMC protein expression in hypothalamus at different ages during feeding experiments in *foz/foz* and WT mice

At weaning, TC2 and TC12, hypothalamic POMC protein expression was unaffected by genotype or diet ($n \geq 5$ mice in each group). In the immunoblots shown above POMC protein migrates at around 26-28 kDa (arrows).

Representative loading controls are presented in Chapter 2, Figure 2.7.

5.4.4.2. Hypothalamic CART mRNA levels and protein localisation

Several primers were tested in order to measure hypothalamic CART mRNA levels. Unfortunately, none of these produced reliable results.

There were no changes in CART hypothalamic localisation between *foz/foz* (Figure 5.12A, C) and WT (B, D) mice at TC2, regardless of the diet. The same result was observed at weaning and TC12 in both *foz/foz* and WT mice, regardless of the diet (data not shown).

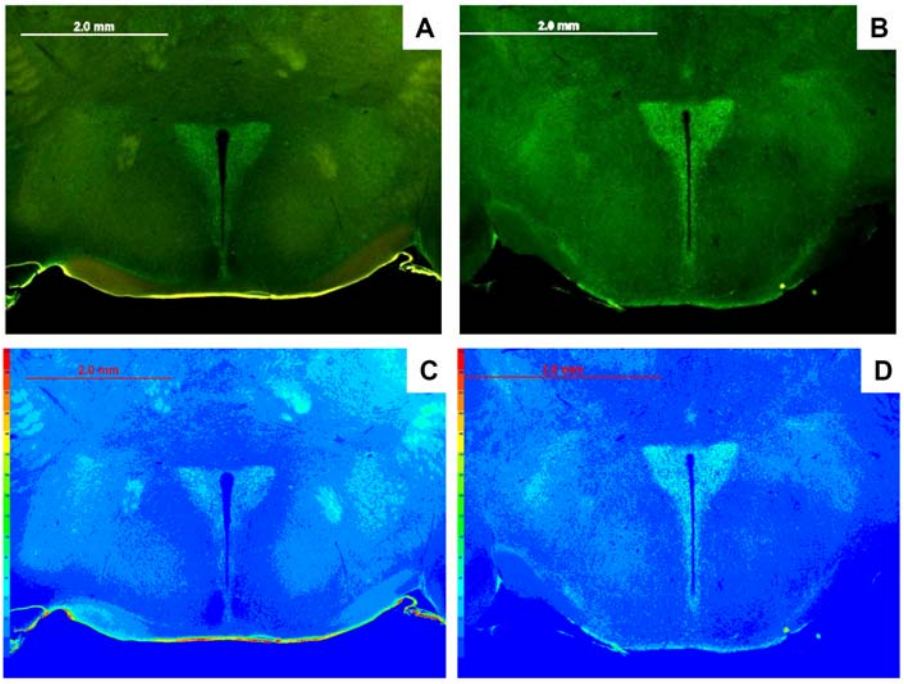

Figure 5.12. Representative hypothalamic CART expression at TC2 in chow-fed *foz/foz* (A, C) and WT mice (B, D)

Immunohistofluorescence pictures were transformed in pseudocolour images corresponding to a colour scale illustration of CART. No obvious differences in CART hypothalamic localisation were observed between *foz/foz* (A, C) and WT (B, D) mice. The same pattern of immunohistofluorescent staining and corresponding pseudocolour images were obtained at weaning and TC12 in chow and high fat-fed mice (n = 6 mice per group).

5.4.4.3. Hypothalamic CRH mRNA levels

After 2-weeks on high fat diet, WT mice showed significantly higher CRH mRNA levels compared to chow-fed WT mice or high fat-fed *foz/foz* mice (Figure 5.13). However, this increase was not sustained at TC12, when values for CRH mRNA did not vary between genotype and diet (Figure 5.13). For reasons of insufficient material for dissected hypothalamic nuclei, no attempt was made to measure CRH expression in those hypothalamic regions.

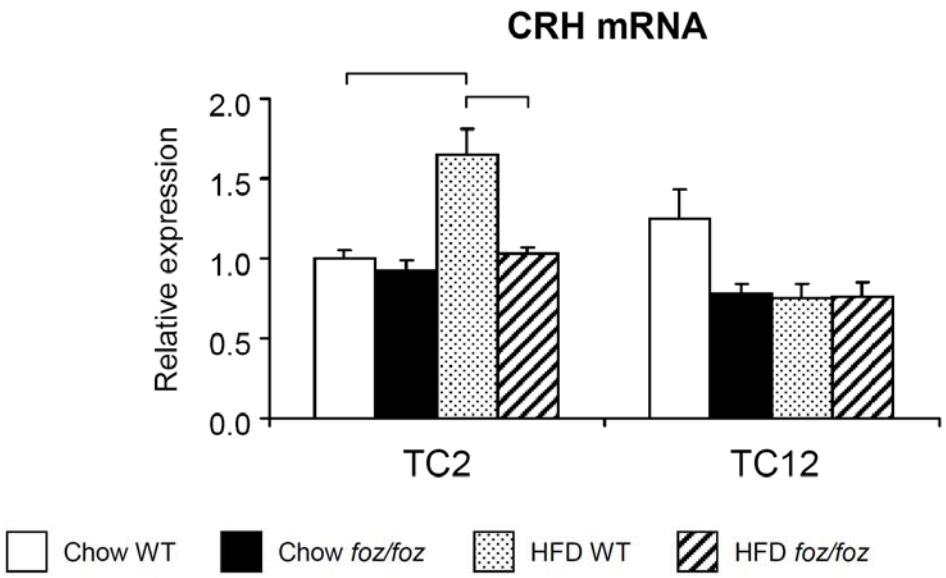

Figure 5.13. CRH mRNA levels in whole hypothalamus during dietary regimes in *foz/foz* and WT mice

Dietary experiments and collection of samples are described in Figure 5.9. Total mRNA was extracted and CRH mRNA levels were determined by semi-quantitative real time PCR (see Chapter 2, section 2.6; n ≥ 6 mice per group).

Statistical bars show significance of post-hoc testing between indicated groups, $P < 0.05$.

5.4.5. Hypothalamic MC4-R mRNA and protein levels in *foz/foz* and WT mice

Hypothalamic MC4-R mRNA levels did not change with genotype or diet at either TC2 or TC12 (Figure 5.14A). Despite an apparent (NS) increase in *foz/foz* mice at 2 weeks, MC4-R gene expression in the PVN was not significantly affected by genotype or time (Figure 5.14B). However, AH and Arc MC4-R mRNA levels decreased with time in both *foz/foz* and WT mice ($^{\S}P < 0.05$; Figure 5.14C, D).

Hypothalamic MC4-R protein expression was similar between genotypes, at weaning (Figure 5.15). After 2-weeks on diet, MC4-R expression remained similar between *foz/foz* and WT mice, regardless of the diet (Figure 5.15). After 12-weeks on diet, hypothalamic MC4-R protein levels were lower in high fat-fed WT mice and in *foz/foz* mice fed both diets compared to chow-fed WT mice ($P < 0.05$; Figure 5.15).

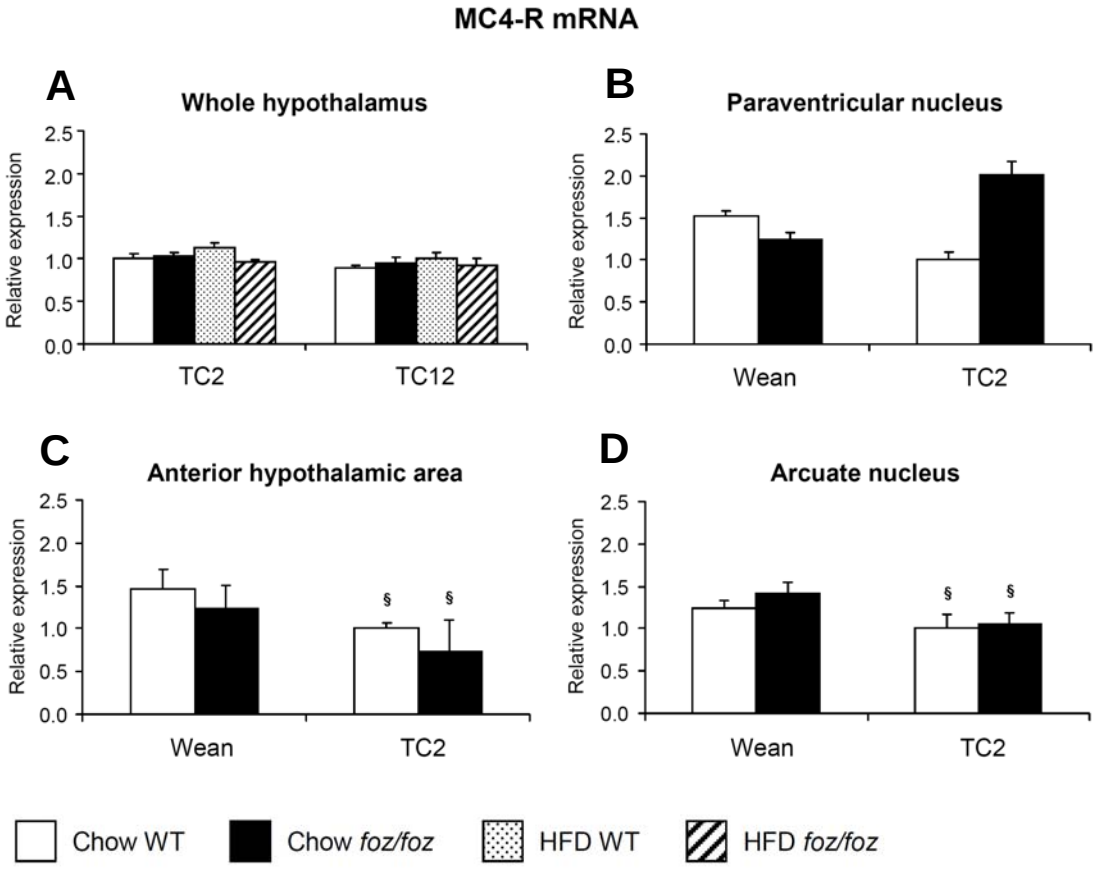

Figure 5.14. MC4-R mRNA levels in whole hypothalamus (A) and in hypothalamic nuclei (B-D) at weaning, TC2 and TC12 in chow and high fat-fed *foz/foz* and WT mice

Dietary experiments and collection of samples are described in Figure 5.5. Total mRNA was extracted (n ≥ 6 mice per group) and MC4-R mRNA levels determined by semi-quantitative real time PCR (see Chapter 2, section 2.6).

A: In the whole hypothalamus, MC4-R mRNA levels were not affected by genotype or by diet.

B: There were no significant variations in MC4-R gene expression in the paraventricular nucleus.

C: In the anterior hypothalamic area, MC4-R mRNA levels were reduced at TC2 versus weaning in both *foz/foz* and WT mice.

D: Similarly, MC4-R gene expression in the arcuate nucleus was decreased between weaning and TC2 in both *foz/foz* and WT mice.

$^{\S}P < 0.05$, ANOVA results for effect of time.

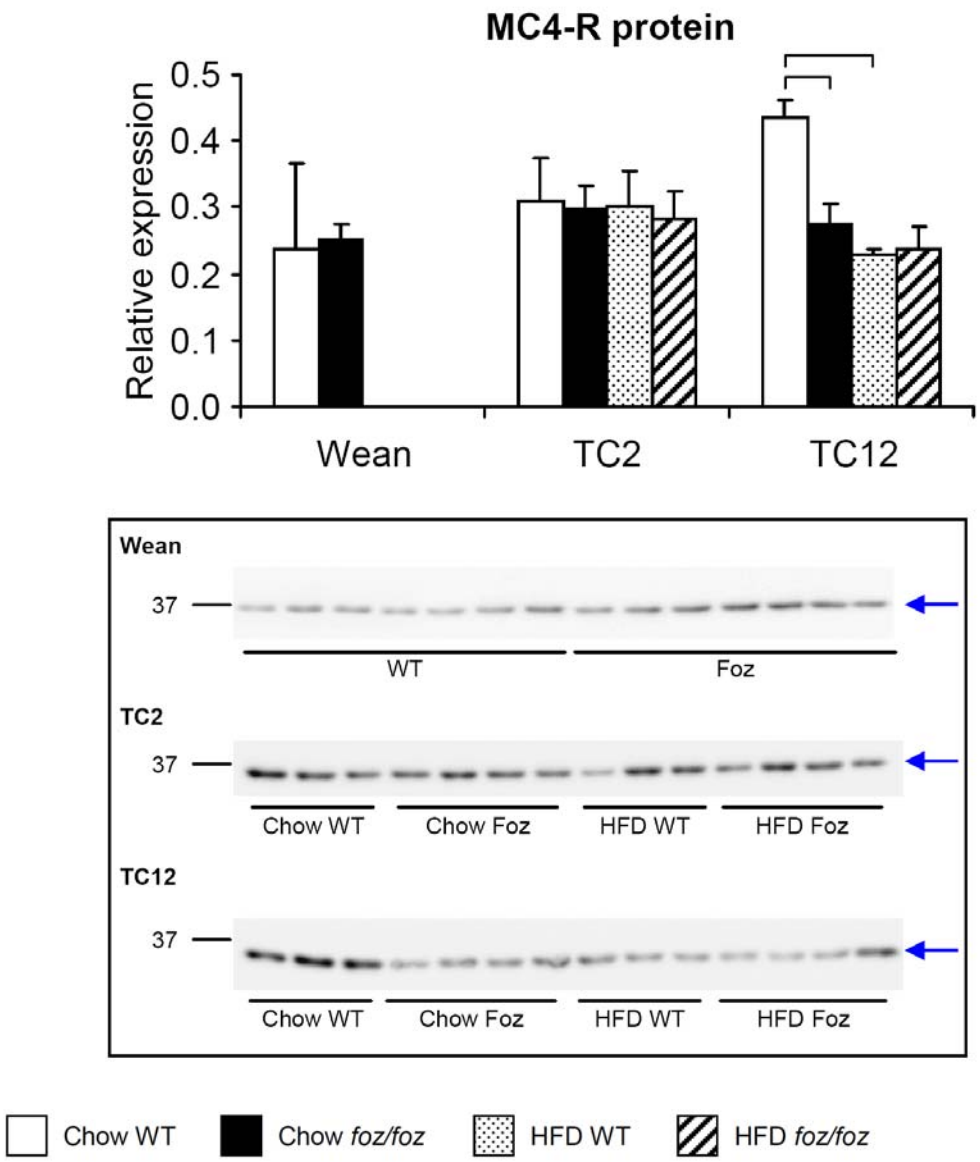

Figure 5.15. Hypothalamic MC4-R protein expression at different ages during dietary regimes in *foz/foz* and WT mice

Hypothalamic MC4-R protein expression was reduced in chow-fed *foz/foz* and high fat-fed *foz/foz* and WT mice compared to chow-fed WT mice at TC12. In the immunoblots (above), MC4-R protein migrates with an apparent molecular mass of 37 kDa (arrows).

A representative loading control western blot is presented in Chapter 2, Figure 2.7.

Statistical bars show significance of post-hoc testing between indicated groups, $P < 0.05$. n ≥ 6 mice per group.

5.5. Discussion

The previous Chapters demonstrated the localisation of Alms1 to the basal body of hypothalamic neuronal cilia, and described a striking late post-natal loss of hypothalamic cilia in *foz/foz* (*Alms1* mutant) mice. This raised the issue as to how such cilial disruption could alter appetite regulation in a way that leads to obesity. In the past five years, several studies have addressed the role of hypothalamic primary cilia in obesity. For example, Rahmouni *et al.,* (2008) showed that gene deletion for three different BBS proteins in mice also produces an obese phenotype with high serum leptin levels, reduced hypothalamic POMC mRNA levels but unchanged NPY and AgRP mRNA expression. Davenport *et al.,* (2007) also showed that deleting primary cilia on POMC neurons in the hypothalamus causes a phenotype of obesity with high circulating leptin levels, a similar phenotype observed in the *foz/foz* mice. Since *foz/foz* mice are similarly obese and hyperleptinaemic, in the present Chapter attention was focused on the link between increased body weight, adiposity, circulating leptin levels, and variations in hypothalamic expression of appetite-regulating molecules.

The first observation was that at the age of 18 weeks (12 weeks on diet) *foz/foz* mice are obese, regardless of the diet. At weaning, *foz/foz* mice actually tend to be smaller (in body mass) compared to their WT littermates. However, from 2-weeks on diet (TC2, 8 weeks of age) *foz/foz* mice are heavier than their WT littermates, and feeding a high fat diet further exacerbates weight gain. By 18 weeks of age, *foz/foz* mice had gained more weight than WT mice.

Measures of peri-ovarian and subcutaneous white adipose tissue (WAT) mass in *foz/foz* mice at TC2 correlated with the observed increase in body weight. However, when fed chow or high fat diet for 12-weeks, WAT mass of *foz/foz* mice

seemed to reach a plateau. This corresponds to the time point when *foz/foz* mice start storing lipids in their liver with steatosis and the onset of diabetes and metabolic syndrome (Larter *et al.*, 2009). This increase in WAT mass correlated closely with the increase in circulating leptin levels, consistent with other data indicating that leptin circulates at levels that reflect the WAT mass (Considine *et al.*, 1996). Thus both high fat-fed and chow-fed *foz/foz* mice are hyperleptinaemic.

In the present Chapter, attention was focused on the study of hypothalamic appetite-regulating neuropeptides by real time PCR and, when possible western blot analysis. Immunohistofluorescence was conducted to provide additional semi-quantitative information, but more particularly information about protein localisation. The main positive and negative findings are summarised in Table 5.1 and 5.2.

Table 5.1. Overview of the results from Chapter 5 on key appetite-regulating neuropeptides from whole hypothalamus (mRNA and/or protein levels)

Whole hypothalamic gene/protein expression		**Effect of genotype** (*foz/foz* vs. WT)	**Effect of diet** (HFD vs. Chow)	
			WT	*foz/foz*
NPY		↓ at TC2 and TC12 (HFD)	↑ at TC2	None
AgRP		None	↑ at TC12	↑ at TC12
MCH		None	↓ at TC12	↓ at TC12
POMC	mRNA and protein	None	None	None
CRH		↓ at TC2 (HFD)	↑ at TC2	None
MC4-R	mRNA	None	None	None
	Protein	↓ at TC12 (Chow)	↓ at TC12	None

Table 5.2. Overview of the results from Chapter 5 on key appetite-regulating neuropeptides from dissected hypothalamus (mRNA levels)

Dissected hypothalamic gene expression		Effect of genotype (*foz/foz* vs. WT)	Effect of time (TC2 vs. Wean)	
			WT	*foz/foz*
NPY	PVN	None	↓ at TC2	↓ at TC2
	AH	None	None	None
	Arc	None	↓ at TC2	↓ at TC2
AgRP	PVN	None	None	None
	AH	None	None	None
	Arc	None	↓ at TC2	↓ at TC2
POMC	PVN*	-	-	-
	AH	None	↑ at TC2	None
	Arc	None	None	None
MC4-R	PVN	None	None	None
	AH	None	↓ at TC2	↓ at TC2
	Arc	None	↓ at TC2	↓ at TC2

*Levels of transcripts below limit of detection

Our finding that high fat-fed WT mice exhibit higher hypothalamic NPY mRNA levels compared to their chow-fed littermates at both experimental times (TC2 and TC12) is consistent with an effect of high fat-diet on hypothalamic expression (Table 5.1). Indeed, other studies have demonstrated that hypothalamic NPY mRNA levels are increased in several rodent models of diet-induced obesity (Huang *et al.*, 2003b; Wang *et al.*, 2007). However, the lack of change of NPY mRNA levels in hyperleptinaemic *foz/foz* mice (Table 5.1) was unexpected, as several studies have shown that central administration (intracerebroventricularly) of leptin strongly suppresses NPY mRNA levels in rat hypothalamus (Schwartz *et al.*, 1996c). We propose that the mutation in *Alms1*, resulting in decreased number of hypothalamic primary cilia, plays a role in the observed results. However, there are

limited data on the effects of high leptin on hypothalamic neuropeptide expression in Alström syndrome. One explanation could reside in the study performed in BBS mutant mice, which develop obesity with increased adiposity and hyperleptinaemia, without significant alteration in hypothalamic NPY mRNA levels (Rahmouni *et al.*, 2008). The proposed explanation in those studies was refractoriness to the hypothalamic actions of leptin consequent to ciliary dysfunction. Taken together, with earlier data (Rahmouni *et al.*, 2008), the present results indicate that the obese phenotype observed in hyperleptinaemic *foz/foz* mice is not related to hypothalamic NPY dysregulation. In addition, as in BBS mutant mice, NPY neurons are refractory to the NPY suppressive effect of leptin.

In the present study, hypothalamic AgRP mRNA levels were also not affected by genotype. However, 12-weeks of high fat-feeding increased the hypothalamic expression of this orexigenic neuropeptide in both *foz/foz* and WT mice (Table 5.1). This is consistent with earlier work by Harrold *et al.,* (1999) and Stofvoka *et al.,* (2009), who showed that hypothalamic AgRP mRNA expression increases during intake of a high fat diet. In the present experiments, IHF showed no difference in hypothalamic AgRP localisation between *foz/foz* and WT mice. Taken together, these results indicate that AgRP mRNA expression is enhanced by high fat-feeding, but the high leptin levels observed in *foz/foz* mice do not have an effect on AgRP hypothalamic transcript levels. This leads us to conclude that AgRP-expressing neurons in *foz/foz* mice are resistant to the leptin-mediated suppression of AgRP.

Studies of hypothalamic MCH mRNA expression in *foz/foz* and WT mice showed a small decrease in its expression at TC12 in high fat-fed mice, irrespective of genotype (Table 5.1). This is in accord with earlier experiments showing that

leptin directly suppresses hypothalamic MCH mRNA expression (Sahu, 1998). It is therefore concluded that MCH neurons remain at least partially responsive to leptin in this model, and that changes in MCH gene expression are not responsible for the obese phenotype observed in *foz/foz* mice.

Our study on POMC hypothalamic expression showed no differences in transcript or protein expression between *foz/foz* and WT mice at the different experimental time (Table 5.1). There was a trend for POMC mRNA levels to decrease at TC12 in high fat-fed *foz/foz* and WT mice compared to their chow-fed counterparts. This tendency seem consistent with earlier studies, which have demonstrated that only long-term high fat feeding (19 vs. 8 wks) is able to suppress hypothalamic POMC mRNA expression (Lin *et al.*, 2000; Huang *et al.*, 2003a). Longer feeding experiments are needed to test whether the observed trend is a real one, leading eventually to a significant fall in hypothalamic POMC mRNA expression. In the meantime, the possibility remains that the POMC pathway could be downregulated in *foz/foz* mice.

In the present studies, several attempts were made to determine CART mRNA levels by real time PCR or CART protein expression by western blot, but unfortunately these attempts were technically unsuccessful. By IHF, there were no obvious changes in the hypothalamic localisation of CART. In the future, attempts could be made to discern CART hypothalamic expression by immunohistochemistry, a technique which is somewhat more amenable to semi-quantitation than IHF, due to better resolution of background staining. However, the results of the present IHF experiments lead us to tentatively conclude that CART localisation is not affected by the *Alms1* mutation.

In the present work, the elevated leptin levels observed in *foz/foz* mice at TC2 and TC12 did not affect hypothalamic CRH mRNA expression. Feeding WT mice a high fat diet for 2 weeks increased hypothalamic CRH mRNA levels in WT mice, compared to their chow-fed littermates, but had no such effect in *foz/foz* mice (Table 5.1). These results in WT mice are in accord with previous studies in rats, where it has been shown, that leptin as well as short-term high fat feeding increases hypothalamic CRH mRNA levels (Schwartz *et al.*, 1996c). Due to the lack of literature on long-term high fat-feeding and changes in CRH hypothalamic mRNA levels, it is hard to conclude on the effect of high fat-feeding observed at TC2 but not at TC12 in WT mice. However, we can conclude from this study that in *foz/foz* mice CRH neurons are not responsive to high circulating leptin levels.

Our studies also showed that at TC12, MC4-R protein expression was lower in chow-fed *foz/foz* mice and high fat-fed mice (both genotypes), compared to chow-fed WT mice (Table 5.1). These results indicate that hypothalamic MC4-R protein expression is altered (downregulated) by genotype as well as by high fat feeding. This could be due to either a decrease in translation and/or a decrease in protein stability (e.g. increased degradation) in both *foz/foz* mice and high fat-fed WT mice. Due to the limited information available on hypothalamic MC4-R protein regulation, it is difficult to interpret the results observed in the present study.

In the present Chapter, we focused our attention on the effect of the *Alms1* mutation on hypothalamic orexigenic and anorexigenic gene expression. In particular, we studied the gene expression of key appetite-regulating neuropeptides in the hypothalamus and in dissected hypothalamic nuclei (PVN, AH and Arc). In chow-fed mice studies were confined to weaning and TC2, as these experimental

times corresponded to similar circulating leptin levels between *foz/foz* and WT mice. Interestingly, none of the studied genes (NPY, AgRP, POMC, MC4-R) were affected by genotype (Table 5.2). However, NPY, AgRP and MC4-R mRNA levels fell with time in specific nuclei (corresponding to nuclei where these peptides are the most abundantly expressed), whereas POMC appeared to increase with time (Table 5.2). These results correlate with the increase in circulating leptin levels observed at this time. As described above, we observed changes in mRNA transcript levels in dissected nuclei that were not reflected in whole hypothalamus. These changes are attributable to the dilution of transcripts across the hypothalamus, as it has been shown that neuropeptides are more abundantly express in some hypothalamic area than others (Chapter 1, section 1.5.3). As there is very little literature on mRNA levels in dissected hypothalamic nuclei over time, it is difficult to comment on these results in the context of previous studies. Indeed, the only studies the candidate could source were all performed at early post-natal time points (from post-natal day 5 to 22; Ahima and Hileman, 2000), but not later. Notwithstanding developmental changes in hypothalamic neuropeptide expression, it is clear from the present results on dissected hypothalamic nuclei gene expression that hypothalamic neuropeptides mRNA levels are not affected by the *Alms1* mutation.

In summary, the present Chapter reports detailed study of hypothalamic gene expression of multiple key appetite-regulating molecules in *foz/foz* mice. Despite increased circulating leptin levels in *foz/foz* mice, that correlated with obesity and increased WAT mass, there were no striking variations in hypothalamic neuropeptide expression that could explain the obese phenotype. In regards of the present studies, we can conclude that the hypothalamic action of leptin in

suppressing appetite is impaired in *foz/foz* mice. This could result in the development of, or contribute to the pathogenesis of, leptin resistance in these mice. To date, several theories exist on the possible causes for central leptin resistance, including reduced permeability of the blood brain barrier, disruption in neuronal pathways participating in leptin action (studied in the present Chapter), and alterations in leptin receptor (Ob-R) or Ob-R signalling pathways. To assess the molecular mechanisms involved in leptin resistance in *foz/foz* mice, we designed experiments to study the Ob-R signalling pathways in *foz/foz* mice. The conduct of the experiments and the results obtained are in the following Chapter.

CHAPTER 6

Chapter 6

Hypothalamic leptin receptor expression and molecular intermediates of leptin signalling

6.1. Introduction

In obese humans, serum leptin levels are increased compared to lean individuals, yet leptin infusion fails to suppress appetite. This observation has led to the concept of central leptin resistance (see Chapter 1, section 1.6). From a broad pathophysiological viewpoint, leptin resistance has been associated with one or more of the following changes (Tups, 2009):

- reduced leptin uptake by the brain (blood brain barrier deficit)
- mutation or deletion of the long form of the leptin receptor (Ob-R)
- induction of suppressor of cytokine signalling 3 (SOCS3) and other molecular pathways that modulate leptin receptor signalling
- alterations in hypothalamic neuropeptides that convey the "effector" pathways of leptin signalling on appetite regulation (as studied in Chapter 5)

As detailed in Chapter 5, no changes were found in hypothalamic gene or protein expression of the main appetite-regulating neuropetides in *foz/foz* mice, whether fed chow or high fat diet, despite markedly increased serum leptin levels. Since leptin has multiple effects on these pathways, the conclusion was drawn that

refractoriness to leptin signalling was either due to diminished Ob-R expression on neurons, or to one or more molecular impediments to Ob-R signalling and downstream gene regulation (as reviewed in Chapter 1, section 1.6).

Leptin signalling is mediated by phosphorylation cascades initiated by leptin binding to its receptor. Many downstream signalling pathways are activated, some of which are involved in feedback loops which dampen Ob-R signalling; these are summarised in Figure 6.1 and will now be discussed.

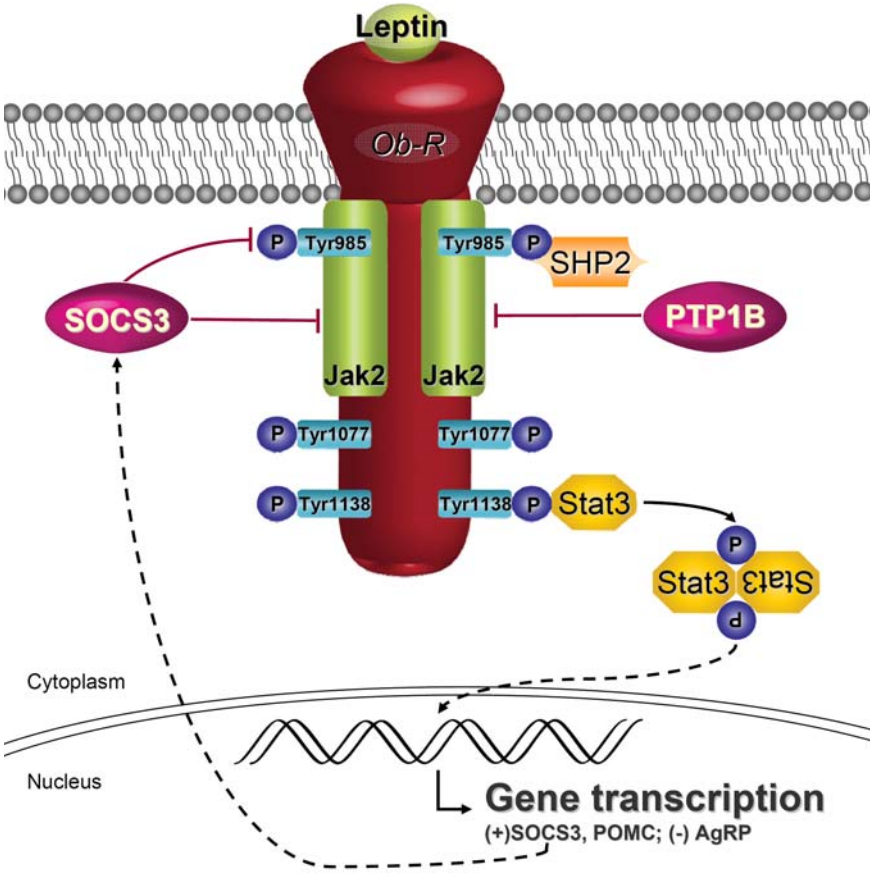

Figure 6.1. Activation of the leptin receptor

Ob-R activation by leptin leads to Stat3 phosphorylation, dimerisation and translocation to the nucleus, where it acts as a transcription factor. SOCS3 and PTP1B can inhibit the phosphorylation of Ob-R and thereby inhibit leptin signalling.

Abbreviations: AgRP, Agouti-related protein; Jak, Janus activating kinase; Ob-R, Leptin receptor; POMC, Pro-opiomelanocortin; PTP1B, Protein tyrosine phosphatase 1 B; SHP2, SH2-domain-containing protein tyrosine phosphatase 2; SOCS3, Suppressor of cytokine signalling 3; Stat3, Signal transducer and activator of transcription 3; Tyr, Tyrosine.

Multiple Ob-R isoforms are formed via alternative mRNA splicing of the Ob-R gene transcript (Mercer *et al.*, 1996; Elmquist *et al.*, 1998b). All isoforms have an extracellular leptin-binding site. The murine Ob-R receptor contains three conserved intracellular tyrosine residues, located at amino acid positions 985, 1077, and 1138 (Villanueva and Myers, 2008). Tyrosine phosphorylation sites are the binding region for signalling proteins such as signal transducer and activator of transcription (Stat). When leptin binds to its receptor, it activates the Janus activating kinase (JAK) enzymes, while in turn JAK mediates leptin-dependent tyrosine phosphorylation of Ob-R itself (Bjorbaek et al., 1997). Phosphorylated Tyr1138 recruits Stat3, facilitating its phosphorylation by JAK. This leads to dimerisation of Stat3, which then translocates to the nucleus where it regulates the transcription of target genes (see Figure 6.1).

Stat3 has been shown to induce the hypothalamic expression of SOCS3. By binding to Tyr985 and inhibiting JAK2 kinase activity, SOCS3 is a potent inhibitor of leptin signalling (Bjorbaek *et al.*, 1998), thereby acting as a negative feedback loop for the biological actions of leptin (Bjorbaek *et al.*, 1999; Bjorbak *et al.*, 2000).

Another regulator of leptin receptor signalling is protein tyrosine phosphatase 1B (PTP1B). PTP1B binds to and dephosphorylates JAK2 (Myers *et al.*, 2001; Kaszubska *et al.*, 2002; Zabolotny *et al.*, 2002), thereby negatively regulating leptin signalling (Figure 6.1). Mice with neuronal PTP1B deficiency have reduced body weight and adiposity (Zabolotny *et al.*, 2002; Lund *et al.*, 2005; Bence *et al.*, 2006), findings which are consistent with enhanced responsiveness ("sensitivity") to leptin.

Interestingly, leptin also activates the phosphatidylinositol 3 kinase (PI3K) intracellular pathway (Niswender *et al.*, 2001; Niswender *et al.*, 2004; Xu *et al.*,

2005b). PI3K catalytic subunit (p110) phosphorylates phosphatidylinositol-4,5-biphosphate (PIP2) to form phosphatidylinositol-3,4,5-triphosphate (PIP3). PIP3 binds to and activates such downstream molecules as protein kinase B (PKB), also known as Akt. In this way, the PI3K/Akt pathway in hypothalamic neurons is implicated in the regulation of food intake and energy homeostasis. For example, inhibition of this pathway attenuates the anorexigenic effect of leptin.

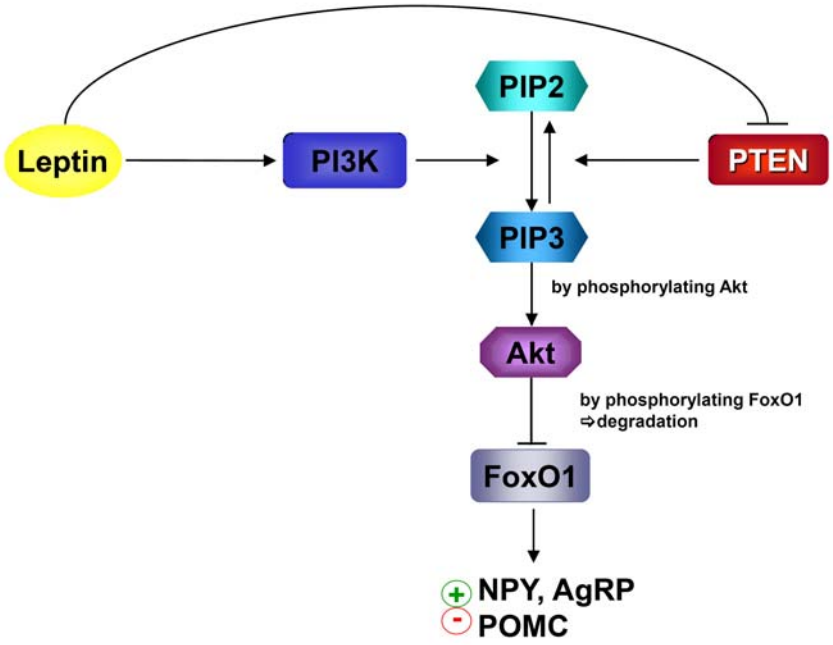

Figure 6.2. Leptin effects on PI3K and PTEN pathways

Leptin activates the PI3K pathways, which in turns phosphorylates PIP2 to PIP3, leading to Akt activation and FoxO1 degradation, thereby preventing FoxO1-mediated induction of NPY and AgRP, and suppression of POMC gene transcription.

Abbreviations: Akt, Protein kinase B (or PKB); FoxO1, Forkhead box-containing protein-O1; PI3K, Phosphatidylinositol 3 kinase; PIP2, Phosphatidylinositol-4,5-biphosphate; PIP3, Phosphatidylinositol-3,4,5-triphosphate; PTEN, Phosphatase and tensin homolog.

Among the targets of activated Akt is the forkhead box-containing protein-O1 (FoxO1). Nuclear FoxO1 expression stimulates the transcription of the orexigenic peptides, NPY and AgRP, and suppresses the transcription of anorexigenic POMC by antagonising the activity of Stat3 (Kim *et al.*, 2006; Kitamura *et al.*, 2006). Direct phosphorylation of FoxO1 by Akt prevents its nuclear translocation, leaving it vulnerable to proteosomal degradation (Matsuzaki *et al.*, 2003; Aoki *et al.*, 2004), and thereby inhibiting its orexigenic function in the hypothalamus.

The PI3K pathway can be antagonised by the tumour suppressor protein, phosphatase and tensin homolog (PTEN), which has been shown to dephosphorylate PIP3 (Ning *et al.*, 2006). Recent work has shown that leptin can inhibit PTEN by stimulating its phosphorylation. As a result, this enhances the PI3K signalling pathway (Ning *et al.*, 2006). For review see Paez and Sellers (2003). The relationship between leptin, PI3K, PIP2, PIP3, Akt, FoxO1 and PTEN are depicted in Figure 6.2.

Leptin also stimulates the mitogen-activated protein kinase (MAPK), also known as extracellular-signal-regulated kinase (ERK) pathway. Leptin has been shown to activate ERK via SH2-domain-containing protein tyrosine phosphatase 2 (SHP2) in cultured cells and in whole hypothalamus (Bjorbaek *et al.*, 2001; Zhang *et al.*, 2004; Rahmouni *et al.*, 2009). SHP2 binds via its SH2 domain to phosphorylated Tyr985 on the leptin receptor (Figure 6.1) to activate the ERK pathway (Carpenter *et al.*, 1998; Li and Friedman, 1999; Bjorbaek *et al.*, 2001). Neuron-specific deletion of SHP2 results in leptin resistance and obesity (Zhang *et al.*, 2004). Thus, SHP2 appears to play an important role in leptin signal transduction in neurons.

SH2 B adaptor protein 1 (SH2B1) is ubiquitously expressed in cytoplasm. *In vitro*, SH2B1 binds to JAK2 via its SH2 domain resulting in potentiation of JAK2 activation (Rui and Carter-Su, 1999). Genetic deletion of the *SH2B1* gene results in severe leptin resistance, hyperphagia, and obesity (Ren *et al.*, 2005); whereas neuron-specific restoration of SH2B1 restores leptin sensitivity and reverses the obese phenotype in SH2B1-null mice (Ren *et al.*, 2007). Additionally, neuron-specific overexpression of SH2B1 protects against diet-induced leptin resistance and obesity (Ren *et al.*, 2007). These data indicate that, in the brain, SH2B1 is a key regulator of leptin sensitivity, energy balance, and body weight regulation.

As explained earlier, Ob-R generates multiple transcripts. These encode at least five Ob-R isoforms. Leptin receptor overlapping transcript (Leprot) is a protein generated from the same locus as Ob-R, but does not share any sequence similarities with it. Ob-R and Leprot were shown to be coexpressed in the mouse brain (Mercer *et al.*, 2000). In 2007, it was shown that Leprot overexpression in mouse hypothalamus decreases Ob-R cell surface expression (Couturier *et al.*, 2007). Leprot is therefore another protein that could play an important role in mediating leptin resistance, hyperphagia and obesity.

The profound hyperletinaemia present in obese *foz/foz* mice indicates that the appetite-regulating centres of the brain have reduced sensitivity to leptin. Thus, the phenomenon of leptin resistance, which is common in human obesity, also appears to be present in this hyperphagic mouse strain. In order to establish the molecular basis for such leptin resistance in the hypothalamus, we investigated the role of leptin receptor expression and the above signalling pathways in development and maintenance of obesity in *foz/foz* mice.

6.2. Purpose of the study

The experiments described in this Chapter were performed to test the following hypotheses:

1) That defective leptin receptor expression is responsible for obesity and hypothalamic leptin resistance.

2) That the molecular basis of hypothalamic leptin resistance is caused by changes in molecules that modulate Ob-R signal transduction.

The broad aim of this study was to determine the cause(s) of leptin resistance in *foz/foz* mice by:

1) Studying the changes of hypothalamic Ob-R mRNA and protein levels between genotypes, the effects of dietary manipulations which influence the degree of obesity, and at different experimental times during the development of obesity.

2) Characterising hypothalamic changes in peptides involved in Ob-R signalling pathway.

6.3. Methods

6.3.1. Animals and diets

Female *foz/foz* and WT mice were bred at The Canberra Hospital Animal Facilities. Mice were housed under a 12 hour light-dark cycle and given free access to food and water. Mice were weaned onto chow, and at 6 weeks of age (3 weeks

post-weaning) mice were either continued on chow or fed high fat diet (see Chapter 2, section 2.2.2). Mice were sacrificed at weaning or after 2 (TC2) or 12 weeks (TC12) on diet (see Chapter 2, section 2.2.2). Briefly, mice were fasted for at least 4h before tissue collection. Mice were then anaesthetised, blood collected by cardiac puncture (between 11:00 am and 1:00 pm), and then hypothalamus, liver, muscle, white adipose tissue, and brown adipose tissue were rapidly excised and frozen in liquid nitrogen for later analysis, as described in Chapter 2, section 2.3. A second cohort of mice was used for brain fixation by cardiac perfusion of 4% paraformaldehyde, as described in Chapter 2, section 2.4.

6.3.2. Gene expression analyses

Because neuropeptides and receptors are expressed to differing extents in different regions of the hypothalamus, RNA studies were performed on three nuclei; PVN, AH, and Arc (prepared as described in Chapter 2, section 2.3.2). These studies were performed at two different time points, but dissected hypothalami were only collected from chow-fed mice because we considered that any variations attributable to genotype or time should be evident, regardless of the diet. RNA was also extracted from whole hypothalamus of *foz/foz* and WT mice at TC2 and TC12 in mice either fed chow or high fat diet.

Hypothalamic, and individual dissected nuclear, mRNA levels were measured by real time PCR as described in Chapter 2 (section 2.6.1). Briefly, tissues were snap frozen immediately after collection. RNA was extracted via TRI Reagent® protocol (Sigma-Aldrich, USA). cDNA was synthesised using

SuperSript® III Reverse Transcriptase (Invitrogen™, USA). Real time PCR was then performed using iQ™ SYBR® Green Supermix on the iQ™5 real time thermal cycler (Bio-Rad, USA). Experiments were repeated in duplicate and normalised to three house keeping genes: beta-actin, B2M, RPL13a (see Chapter 2, Table 2.3). The logic of this technique is detailed in Chapter 2, section 2.6.1.

6.3.3. Protein expression analyses

An initial trial to extract both RNA and protein following the TRI Reagent® protocol was attempted, but unfortunately the protein yield was low and variable between individuals, leading to abandonment of this approach. In order to conduct satisfactory hypothalamic protein expression analyses, it was necessary to raise another cohort. In this work, hypothalamic proteins were extracted after homogenising the whole hypothalamus in homogenising buffer in the presence of protease and phosphatase inhibitor (see Chapter 2, section 2.6.2, and Appendix 1). The amount of total protein was estimated by colorimetric assay using a protein estimation kit (Bio-Rad, USA). Proteins were then diluted to 2 µg/µl in reducing buffer, and 10 µl of each sample was loaded onto a SDS-PAGE gel (Appendix 1), followed by separation, transfer and quantification.

6.3.4. Immunohistofluorescence

The localisation of hypothalamic leptin receptor was assessed by immunohistofluorescence. Briefly, brains from *foz/foz* and WT mice fed chow or high fat diet were collected at weaning, TC2 and TC12 after transcardiac perfusion with 4% paraformaldehyde (see Chapter 2, section 2.4.1). Brains were then sectioned and immunohistofluorescence performed, as described in section 2.5.2. Images of the immunostained brain sections were captured and then transformed to pseudocolour images corresponding to the relative immunoreactivity of Ob-R. The logic of this method is described in Chapter 2, section 2.5.3.

6.3.5. Statistical analyses

The effects of genotype and diet were compared using 2-way analysis of variance (ANOVA), with post-hoc Tukey testing. Differences between genotypes at weaning were determined by using the Student's T-test. For all comparisons $P < 0.05$ was considered as significant. Data are presented as mean ± SEM. The number of individuals (n) per experimental group is given in the text relative to each experiment, as well as in Chapter 2, section 2.2.3.

6.4. Results

6.4.1. Hypothalamic Ob-R expression at weaning, TC2 and TC12 in *foz/foz* and WT mice

As described in the introduction (see section 6.1), the leptin receptor (Ob-R) has several isoforms. However, the most important one in the brain/hypothalamus is the long form (Ob-Rb). Therefore, the present results will focus only on the long form of the Ob-R.

Hypothalamic Ob-R mRNA levels

Ob-R mRNA levels were similar between *foz/foz* and WT mice at all times studied and with no further effect of diet (Figure 6.3A). In the paraventricular nucleus, Ob-R mRNA levels were similar between *foz/foz* and WT mice at weaning. However, compared to WT, *foz/foz* mice showed a significant decrease in paraventricular nucleus Ob-R gene expression after 2-weeks on diet ($P < 0.05$; Figure 6.3B). Similarly, there was a trend for Ob-R transcript levels to be reduced in the AH of *foz/foz* mice at TC2 compared to WT mice, albeit the change was not significant (Figure 6.3C). In contrast, there were no genotype or time-dependent differences in Ob-R mRNA levels in the Arc of *foz/foz* or WT mice (Figure 6.3D).

Hypothalamic Ob-R protein levels

In accordance with the mRNA data, there was no effect of genotype on hypothalamic Ob-R protein expression at weaning (Figure 6.4). Likewise, after 2- or 12-weeks on diet, no significant variations in hypothalamic Ob-R protein expression were identified between *foz/foz* and WT mice, irrespective of the diet (Figure 6.4). At TC12, there was an apparent decrease in Ob-R protein levels in high fat-fed *foz/foz* and WT mice, compared to chow-fed mice, but this was not significant by 2-way ANOVA.

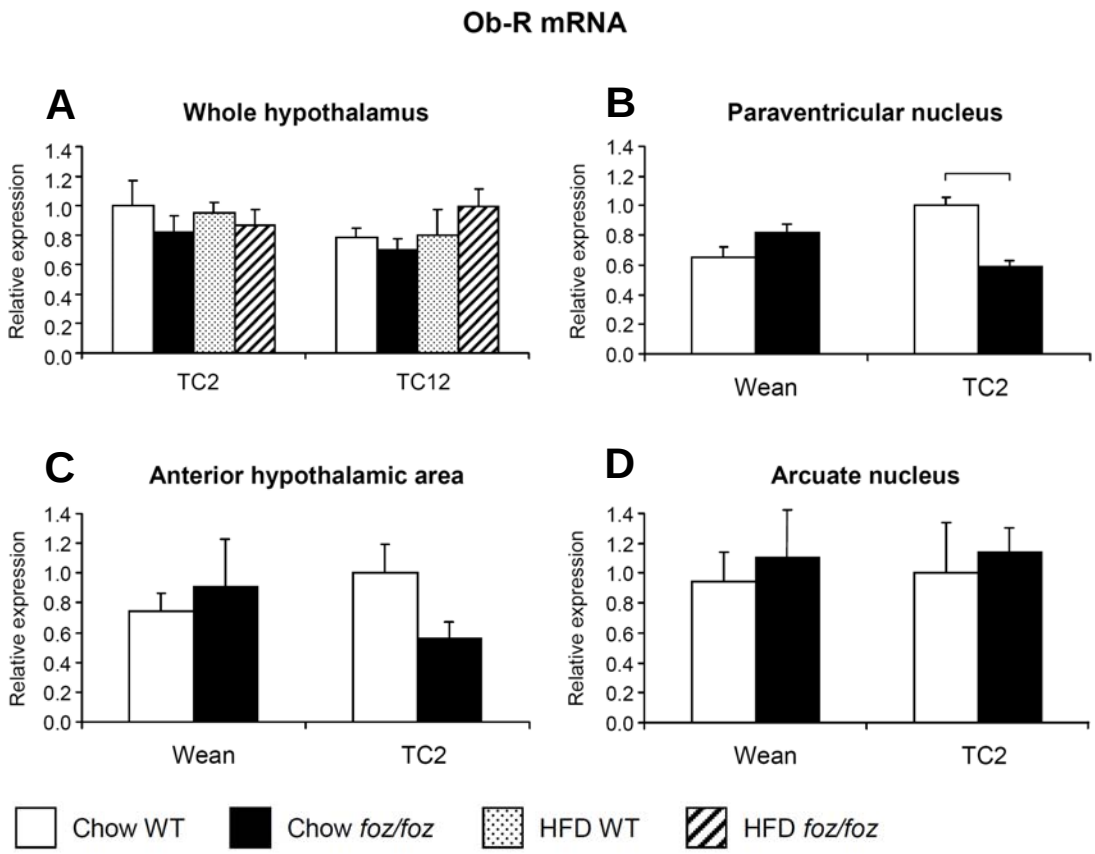

Figure 6.3. Hypothalamic Ob-R mRNA levels in whole hypothalamus (A) and in hypothalamic nuclei (B-D) at weaning, and during dietary regimes in *foz/foz* and WT mice

At weaning (Wean), TC2 or TC12 on a chow or high fat diet (see Chapter 2, section 2.2.2), animals were euthanatized, and hypothalamus was removed, and used whole as indicated or dissected for major nuclei (see Chapter 2, section 2.3.2). Total mRNA was extracted (n ≥ mice 6 per group) and Ob-R mRNA levels determined by semi-quantitative real time PCR (see Chapter 2, section 2.6).

A: In whole hypothalamus, Ob-R mRNA levels did not vary at TC2 or TC12 between *foz/foz* or WT mice, or diet (HFD vs. chow).

B: In the paraventricular nucleus, chow-fed *foz/foz* mice Ob-R mRNA levels were unchanged at weaning but reduced after 2-weeks on chow, compared to WT mice.

C: In the anterior hypothalamic area, Ob-R mRNA levels were not significantly different with genotype or diet.

D: In the arcuate nucleus, Ob-R mRNA levels were similar between *foz/foz* and WT mice.

Experiments were repeated in duplicate. Statistical bar shows significance of post-hoc testing between indicated groups, $P < 0.05$.

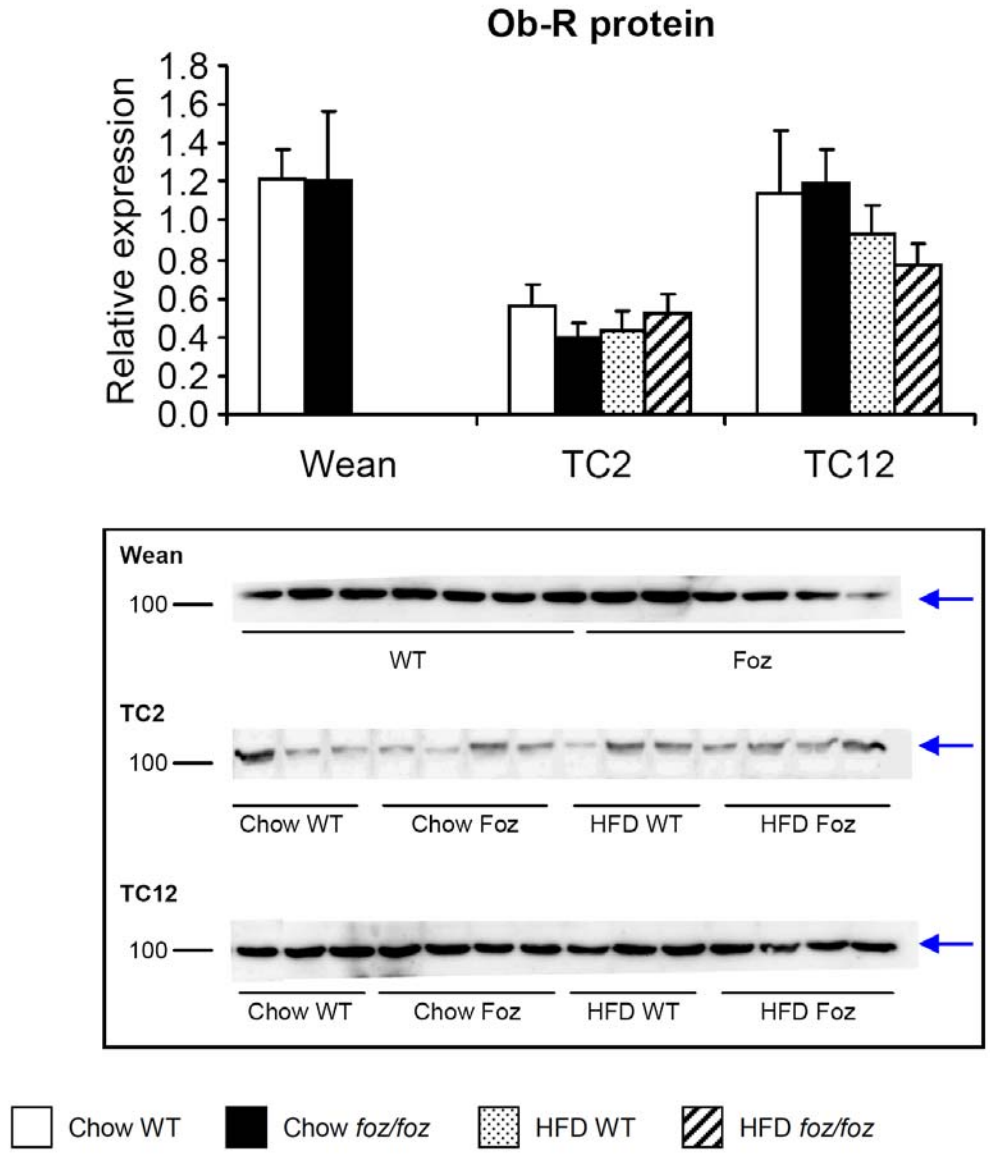

Figure 6.4. Hypothalamic Ob-R protein expression at weaning and during dietary regimes in *foz/foz* and WT mice

There were no significant differences in hypothalamic Ob-R expression between *foz/foz* and WT mice at the time points studied. The apparent lower levels of Ob-R expression in *foz/foz* and WT high fat-fed versus chow-fed mice at TC12 are not significant (n ≥ 5 mice per group).

On the above representative western blot, Ob-R migrates at around 100 kDa (arrows). Representative loading gels, Hsp90, are presented in Chapter 2, Figure 2.7. Experiments were repeated in triplicate.

Ob-R immunohistofluorescence

Ob-R immunofluorescence on brain sections was analysed by applying a pseudocolour plugin on the initial picture. Results obtained showed more precise Ob-R localisation within regions of the hypothalamus. There were no obvious changes in Ob-R hypothalamic location between *foz/foz* and WT mice after 2-weeks on diet (Figure 6.5). Shown in Figure 6.5 are representative pictures of Ob-R expression in the paraventricular nucleus in chow-fed *foz/foz* and WT at TC2. As critically identical results were observed at weaning and TC12, regardless of the diet, these results are not shown.

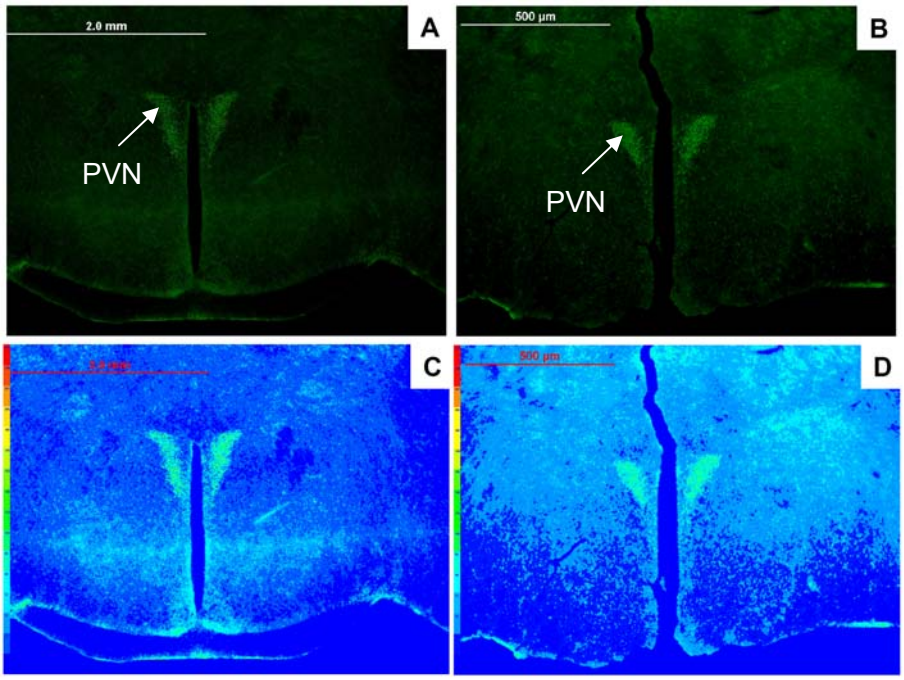

Figure 6.5. Representative example of hypothalamic Ob-R expression as shown by immunohistofluorescence in chow-fed *foz/foz* and WT mice at TC2
Immunohistofluorescence pictures (A, B) were transformed in pseudocolour images (C, D) corresponding to a colour scale illustration of Ob-R. No obvious differences in Ob-R hypothalamic localisation are evident between *foz/foz* (A, C) and WT (B, D) mice. The same immunohistofluorescent staining and corresponding pseudocolour images were obtained at weaning and TC12 and in high fat-fed mice (n = 6 mice per group).

6.4.2. Hypothalamic Leprot mRNA levels at TC2 and TC12 in *foz/foz* and WT mice

In the present studies, there were no significant differences in whole hypothalamic Leprot mRNA expression between *foz/foz* and WT mice at TC2 or TC12, irrespective of diet (Figure 6.6).

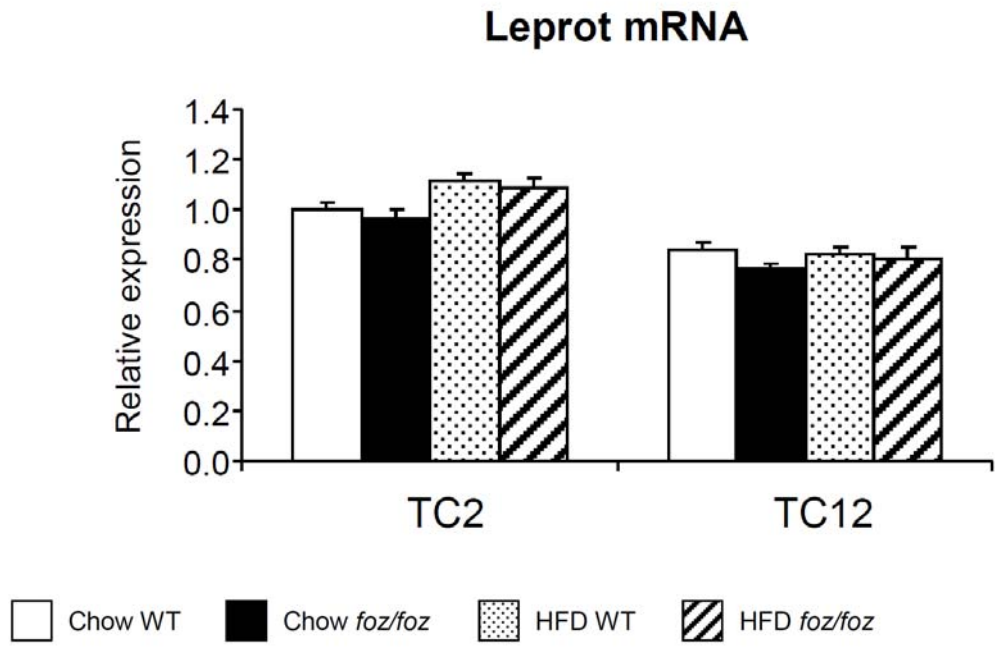

Figure 6.6. Leprot mRNA levels in whole hypothalamus at TC2 and TC12 in *foz/foz* and WT mice

Foz/foz and WT mice were fed chow or high fat diet for 2- or 12-weeks (see Chapter 2, section 2.2.2), following which animals were sacrificed, hypothalamus removed and total RNA extracted. Leprot mRNA levels were determined by semi-quantitative real time PCR (see Chapter 2, section 2.6).

In whole hypothalamus, Leprot mRNA levels were similar between *foz/foz* and WT mice at TC2 and TC12, regardless of diet (n ≥ 6 mice per group). Experiments were repeated in duplicate.

6.4.3. Hypothalamic Stat3 expression at weaning, TC2 and TC12 in *foz/foz* and WT mice

Hypothalamic Stat3 mRNA levels

Hypothalamic Stat3 mRNA levels were not significantly different between *foz/foz* and WT mice after 2 or 12-weeks on diet, regardless of dietary composition (Figure 6.7A). In the PVN, Stat3 mRNA levels were higher in *foz/foz* compared to WT mice at weaning ($P < 0.05$; Figure 6.7B). Stat3 mRNA levels in the PVN subsequently fell to be lower in *foz/foz* mice at TC2 compared to their genotype-matched controls at weaning ($P < 0.05$; Figure 6.7B). In the anterior hypothalamic area, Stat3 mRNA levels were comparable between *foz/foz* and WT mice at weaning. A similar time-dependent decrease in Stat3 gene expression was observed in the AH for both *foz/foz* and WT mice, however this difference was only significant in *foz/foz* genotype ($P < 0.05$; Figure 6.7C). There were no variations in Stat3 gene expression in the Arc nucleus between *foz/foz* and WT mice, regardless of time (Figure 6.7D).

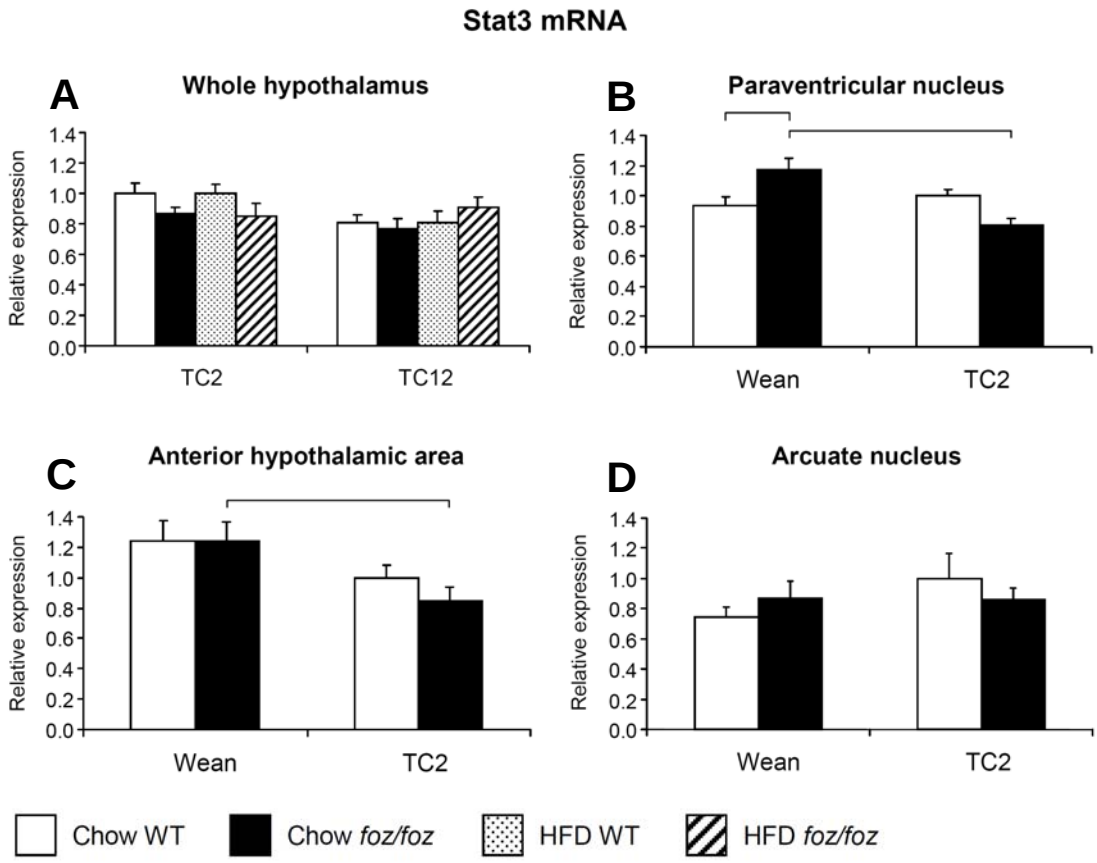

Figure 6.7. Stat3 mRNA levels in whole hypothalamus (A) and in hypothalamic nuclei (B-D) at weaning and during dietary regimes in *foz/foz* and WT mice

Dietary experiments and collection of samples are described in Figure 6.3. Total mRNA was extracted (n ≥ mice 6 per group) and Stat3 mRNA levels determined by semi-quantitative real time PCR (see Chapter 2, section 2.6).

A: No significant differences were observed in whole hypothalamic Stat3 mRNA levels between *foz/foz* and WT mice, or between high fat- and chow-fed animals.

B: In the paraventricular nucleus, Stat3 mRNA levels were higher in *foz/foz* mice than WT littermates at weaning. Values fell significantly in *foz/foz* mice after 2-weeks on chow, compared to weaning controls, but at this time there was no difference between *foz/foz* and WT.

C: In the anterior hypothalamic area, Stat3 mRNA levels were reduced in *foz/foz* mice at TC2 compared to weanling mice.

D: No variations in Stat3 mRNA levels were observed in the arcuate nucleus.

Statistical bars show significance for post-hoc testing between indicated groups, $P < 0.05$. Experiments were repeated in duplicate.

Hypothalamic Stat3 protein levels

The hypothalamic expression of Stat3 protein generally followed that of transcript levels at weaning and TC2. Thus, values were similar between *foz/foz* and WT mice at weaning (Figure 6.8A), and Stat3 hypothalamic protein expression was not affected by genotype or diet at TC2 (Figure 6.8A). However, after 12-weeks on diet, hypothalamic Stat3 protein levels were higher in *foz/foz* mice ($^{\#}P < 0.05$), and were also enhanced by high fat-feeding in both *foz/foz* and WT mice ($^{*}P < 0.05$; Figure 6.8A). Indeed, compared to WT controls, chow-fed *foz/foz* mice showed a strong increase in Stat3 expression. Furthermore, when fed a high fat diet for 12-weeks, both *foz/foz* and WT mice exhibited higher hypothalamic Stat3 expression, compared to their chow-fed genotype matched littermates ($^{*}P < 0.05$; Figure 6.8A). This increase was greater in high fat-fed *foz/foz* mice compared to high fat-fed WT mice (Figure 6.8A).

Hypothalamic protein levels of phosphorylated Stat3 (P-Stat3, the activated form) were similar between genotypes at weaning. Likewise, when fed a chow diet for 2-weeks, no differences between *foz/foz* and WT mice hypothalamic P-Stat3 expression were observed (Figure 6.8B). In contrast, 2-weeks of high fat-feeding increased P-Stat3 protein levels in both genotypes, and values were significantly greater in high fat-fed *foz/foz* mice compared to high fat-fed WT and chow-fed *foz/foz* mice ($P < 0.05$; Figure 6.8B). After 12-weeks on diet, no variations in P-Stat3 hypothalamic expression were observed, irrespective of genotype or diet (Figure 6.8B), and despite difference in total Stat3 protein levels.

The most relevant way to indicate Stat3 activation at the whole tissue level is to express data as the ratio of P-Stat3 to Stat3. There were no variations in this ratio between *foz/foz* and WT mice at weaning (Figure 6.8C). The apparent reduction in P-Stat3 to Stat3 ratio between chow-fed *foz/foz* and WT mice at TC2 was not significant by 2-way ANOVA. However, P-Stat3 to Stat3 ratio was higher in high fat-fed *foz/foz* mice compared to their chow-fed littermates after 2-weeks on diet ($P < 0.05$; Figure 6.8C). No such changes/differences were observed in WT mice at the same time point. When put on chow diet for 12-weeks *foz/foz* mice showed lower P-Stat3 to Stat3 ratio compared to their WT counterparts ($P < 0.05$; Figure 6.8C). After 12-weeks of high fat-feeding P-Stat3 to Stat3 ratio also decreased in WT mice compared to chow-fed WT mice ($P < 0.05$; Figure 6.8C). This ratio remained similarly low in high fat-fed *foz/foz* mice. This apparent decrease in P-Stat3 to Stat3 ratio in high fat-fed WT mice as well as in *foz/foz* mice (fed both diets) is related to increases in total Stat3 protein levels, while P-Stat3 remains similar.

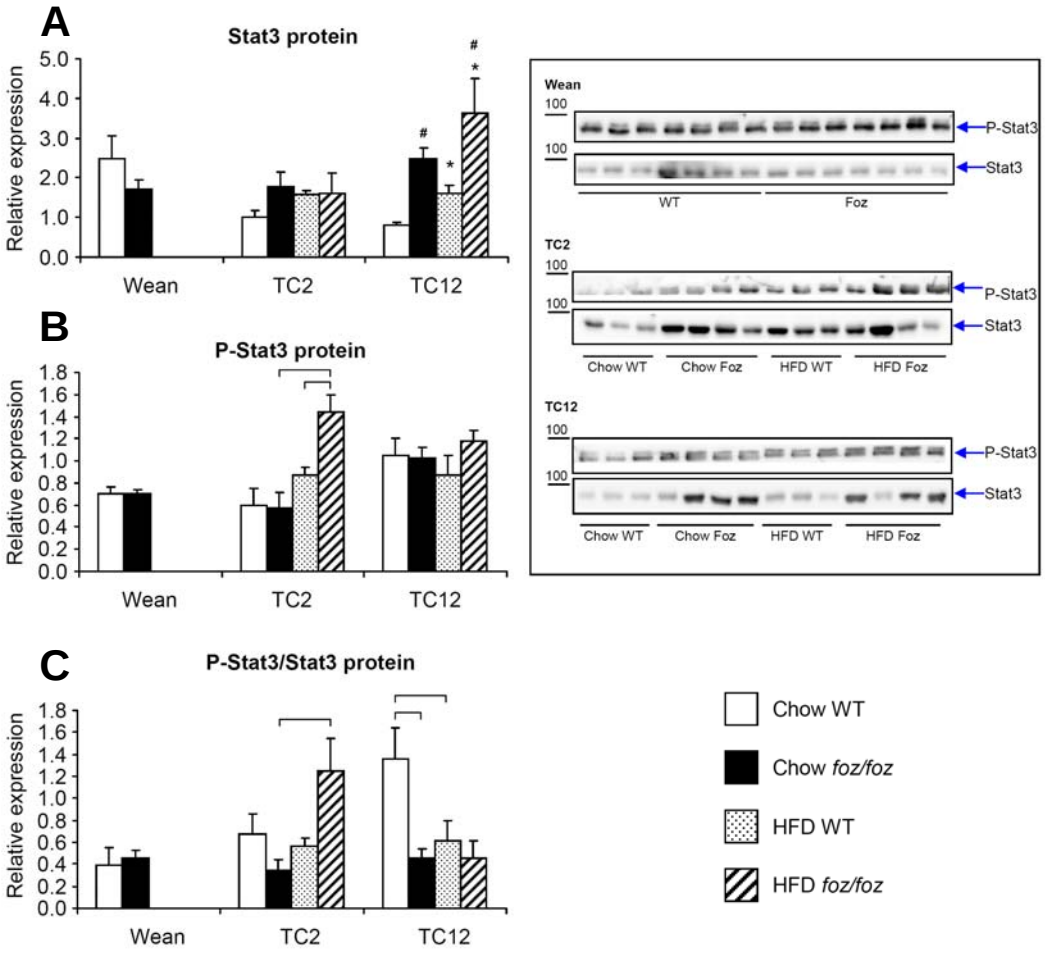

Figure 6.8. Hypothalamic Stat3 (A), phosphorylated Stat3 (B) and P-Stat3:Stat3 ratio (C) at different ages during dietary regimes in *foz/foz* and WT mice

A: A significant increase in Stat3 protein expression was observed at TC12 in high fat-fed *foz/foz* and WT mice as well as in chow-fed *foz/foz* mice, compared to chow-fed controls (n ≥ 5 mice per group).

B: P-Stat3 was significantly higher in high fat-fed *foz/foz* mice at TC2 compared with chow-fed *foz/foz* and high fat-fed WT mice (n ≥ 5 mice per group).

C: The ratio of P-Stat3 to Stat3 was higher in high fat-fed *foz/foz* mice at TC2 compared to their chow-fed counterparts. After 12-weeks on diet, the ratio was reduced in *foz/foz* mice and high fat-fed WT mice compared to chow-fed WT mice.

On the above representative western blots, Stat3 and P-Stat3 migrate as bands at around 80 kDa (arrows). Representative loading gels were performed for each experiment; examples are presented in Chapter 2, Figure 2.7.

Statistical bars show significance for post-hoc testing between indicated groups, $P < 0.05$. Symbols show results of ANOVA:*$P < 0.05$, effect of diet, $^{\#}P < 0.05$, effect of genotype. Experiments were repeated in triplicate.

6.4.4. Hypothalamic SOCS3 expression at weaning, TC2 and TC12 in *foz/foz* and WT mice

Hypothalamic SOCS3 mRNA levels

Whole hypothalamic SOCS3 mRNA levels were not measured at weaning but at TC2 SOCS3 expression was higher in *foz/foz* than WT mice at TC2, and this was maintained at TC12. Thus, as after only 2-weeks on diet (chow- or high fat-fed), *foz/foz* mice expressed higher levels of hypothalamic SOCS3 compared to WT littermates ($^{\#}P < 0.05$; Figure 6.9A). Hypothalamic SOCS3 mRNA levels were similarly elevated by high fat-feeding in both genotypes, compared to chow-fed controls ($^{*}P < 0.05$; Figure 6.9A). However, high fat-fed *foz/foz* mice showed the highest SOCS3 mRNA levels. After 12-weeks on diet, a significant effect of genotype was observed in hypothalamic SOCS3 gene expression. As such, both high fat- and chow-fed *foz/foz* mice exhibited higher hypothalamic SOCS3 transcript levels compared to their WT diet-matched counterparts ($^{\#}P < 0.05$; Figure 6.9A). No effect of high fat-feeding on hypothalamic SOCS3 mRNA levels was observed in WT mice at this time.

SOCS3 mRNA levels in the paraventricular nucleus were not influenced by genotype or time (Figure 6.9B). Similarly, there were no variations in SOCS3 anterior hypothalamic area (AH) gene expression between *foz/foz* and WT mice at weaning and TC2. However, SOCS3 mRNA levels in the AH were higher at TC2 than at weaning in both *foz/foz* and WT mice ($^{\S}P < 0.05$; Figure 6.9C). As in the

PVN, SOCS3 transcript levels in the arcuate nucleus were not different between *foz/foz* and WT mice, nor were they affected by time (Figure 6.9D).

Hypothalamic SOCS3 protein levels

There were no differences in hypothalamic SOCS3 protein expression in *foz/foz* and WT at weaning (Figure 6.10). Hypothalamic SOCS3 protein levels broadly reflected the pattern that was observed for SOCS3 mRNA at TC2. Specifically, hypothalamic SOCS3 expression was higher in *foz/foz* compared to WT mice, irrespective of diet ($^{\#}P < 0.01$; Figure 6.10). At TC2, high fat-feeding enhanced SOCS3 protein levels, as both high fat-fed *foz/foz* and WT mice exhibited higher hypothalamic SOCS3 expression than chow-fed mice ($^{*}P < 0.01$; Figure 6.10). This effect was more robust in high fat-fed *foz/foz* mice than high fat-fed WT mice. After 12-weeks on diet, neither *foz/foz* nor WT mice showed differences in hypothalamic SOCS3 expression, irrespective of diet (Figure 6.10).

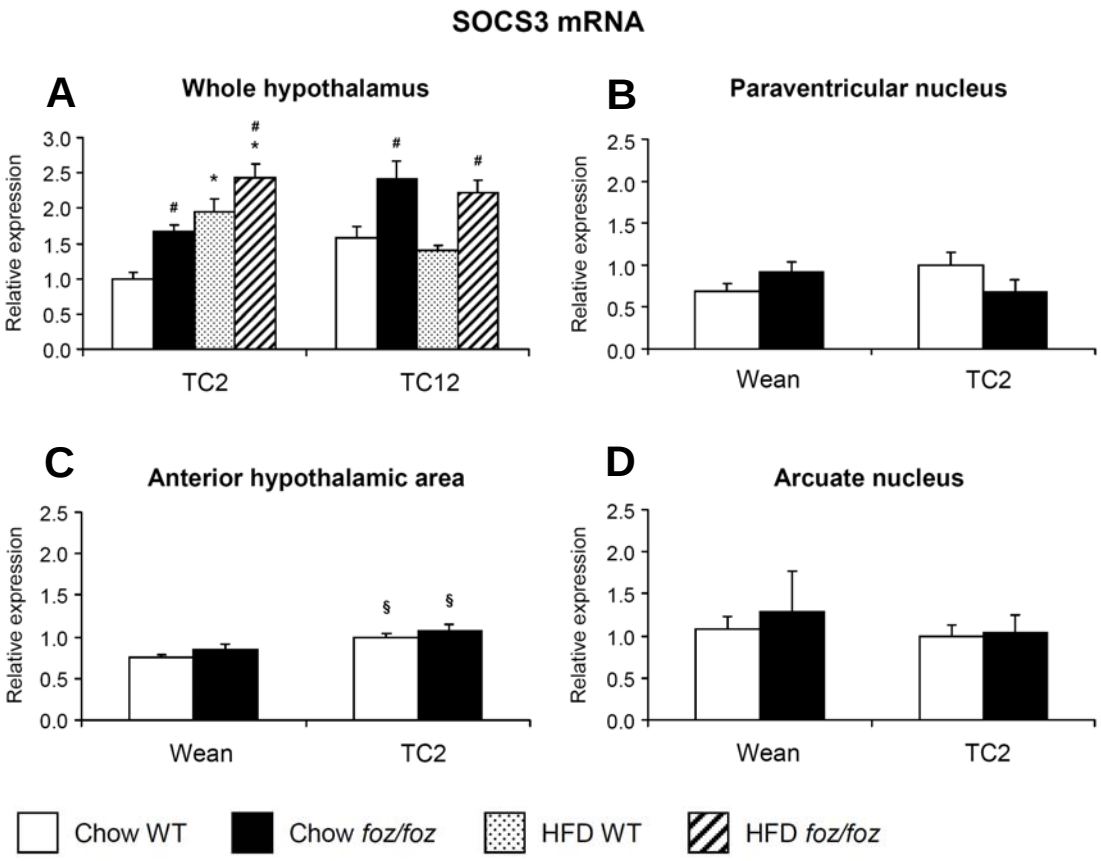

Figure 6.9. SOCS3 mRNA levels in whole hypothalamus (A) and in hypothalamic nuclei (B-D) at weaning and during dietary regimes in *foz/foz* and WT mice

Dietary experiments and collection of samples are described in Figure 6.3. Total mRNA was extracted (n ≥ 6 mice per group) and SOCS3 mRNA levels determined by semi-quantitative real time PCR (see Chapter 2, section 2.6).

A: Hypothalamic SOCS3 mRNA levels were higher in *foz/foz* mice compared to WT mice at TC2 and TC12. Two weeks of high fat feeding also increased SOCS3 mRNA levels in both *foz/foz* and WT mice compared to chow-fed mice.

B: SOCS3 gene expression did not vary in the paraventricular nucleus, regardless of genotype or time.

C: In the anterior hypothalamic area, SOCS3 mRNA levels were higher at TC2 in both *foz/foz* and WT mice, compared to weanling mice.

D: There were no genotype or time differences in SOCS3 mRNA expression in the arcuate nucleus.

Symbols show results of ANOVA: $^{\#}P < 0.05$, effect of genotype, $^{*}P < 0.05$, effect of diet, $^{\S}P < 0.05$, effect of time. Experiments were repeated in duplicate.

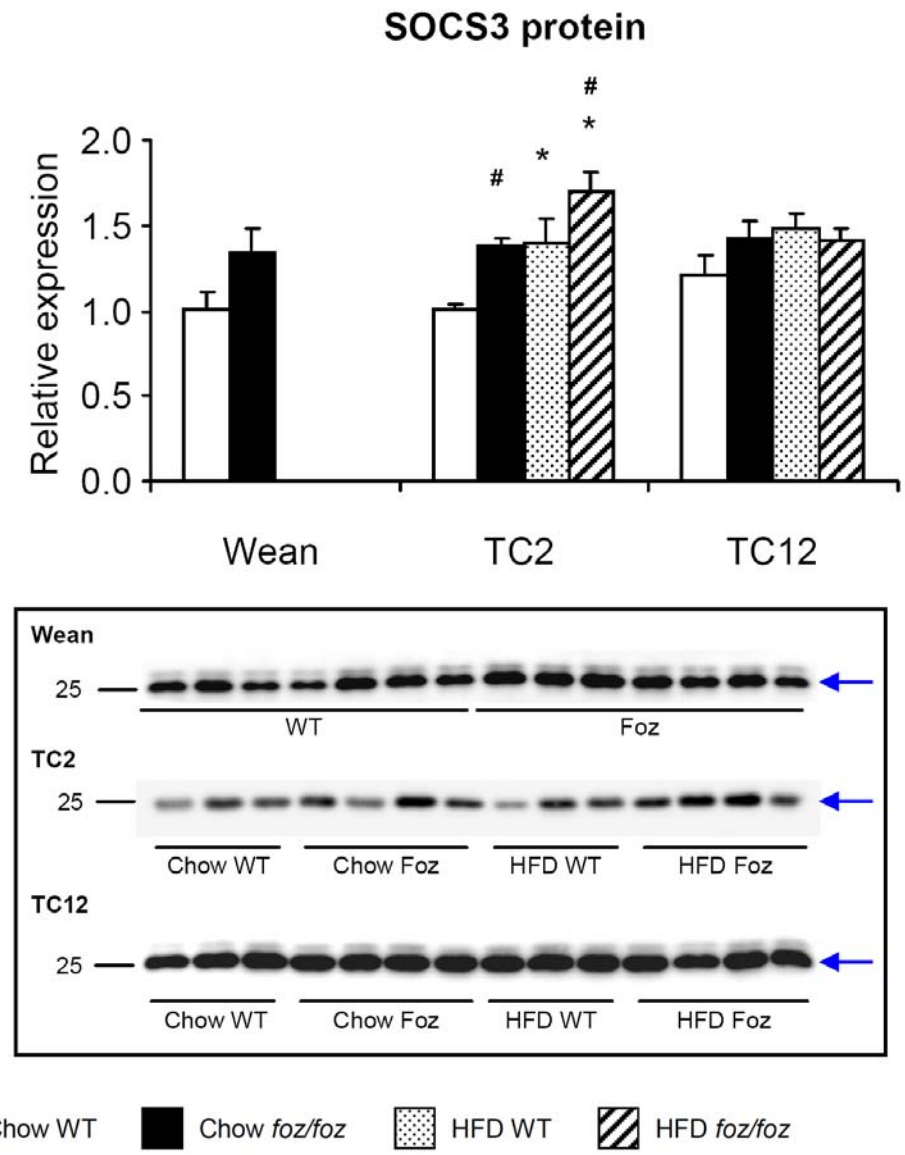

Figure 6.10. Hypothalamic SOCS3 protein expression at different ages during dietary regimes in *foz/foz* and WT mice

Hypothalamic SOCS3 expression was increased in *foz/foz* compared to WT mice at TC2, irrespective of diet. High fat-feeding increased hypothalamic SOCS3 expression in both genotypes after 2-weeks (n ≥ 5 mice per group).

On the above representative western blots, SOCS3 migrates at around 25 kDa (arrows). Representative loading controls were performed for each experiment, but are not presented here, for clarity reasons. Examples are presented in Chapter 2, Figure 2.7. Experiments were repeated in triplicate.

Symbols show results of ANOVA: $^{\#}P < 0.01$, effect of genotype,$^{*}P < 0.01$, effect of diet.

6.4.5. Hypothalamic PTEN protein levels at weaning, TC2 and TC12 in *foz/foz* and WT mice

In weanling mice, hypothalamic PTEN expression was not influenced by genotype (Figure 6.11A). After 2-weeks on diet, *foz/foz* mice exhibited a significant increase in hypothalamic PTEN expression compared to WT mice, regardless of diet ($^{\#}P < 0.05$; Figure 6.11A). This pattern was preserved after 12-weeks on diet ($^{\#}P < 0.05$; Figure 6.11A).

At weaning, TC2 and TC12, hypothalamic levels of phosphorylated PTEN (P-PTEN) was not affected by genotype or diet (Figure 6.11B).

At weaning, the ratio of P-PTEN to PTEN was similar between *foz/foz* and WT mice (Figure 6.11C). After 2-weeks on diet, there was an apparent decrease in P-PTEN to PTEN ratio between *foz/foz* and WT mice (fed both diets), but due to large variance in WT mice this was not significant by ANOVA. After 12-weeks on diet, *foz/foz* mice did not exhibit any changes in the ratio P-PTEN to PTEN, compared to WT mice, regardless of the diet (Figure 6.11C). The apparent increase in P-PTEN to PTEN ratio in high fat-fed WT mice compared to chow-fed controls or high fat-fed *foz/foz* mice was not significant.

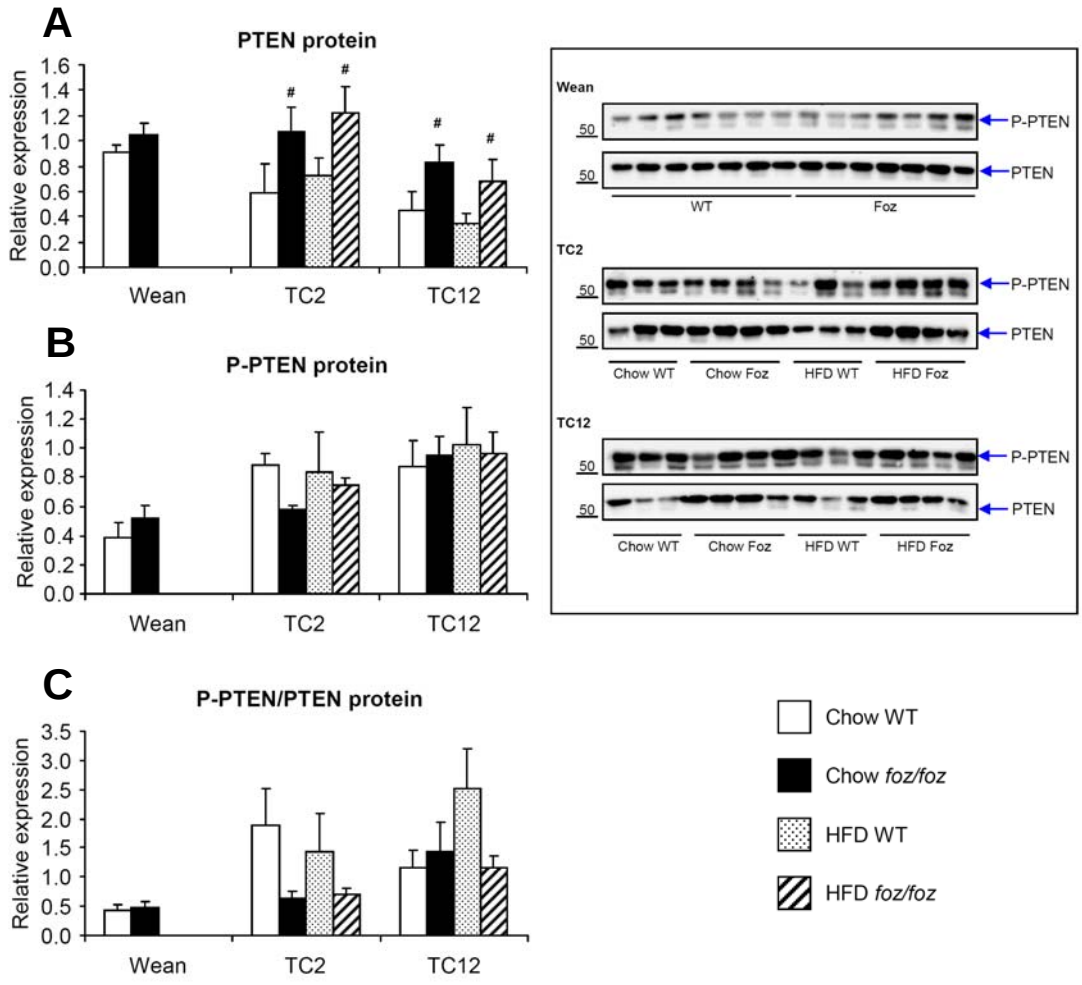

Figure 6.11. Hypothalamic PTEN (A), phosphorylated PTEN (B) and P-PTEN:PTEN ratio (C) at different ages during dietary regimes in *foz/foz* and WT mice

A: Hypothalamic PTEN expression was higher in *foz/foz* compared to WT mice at both TC2 and TC12, and in both dietary regimes (n ≥ 5 mice per group).

B: Hypothalamic phosphorylated PTEN expression was similar between *foz/foz* and WT mice, regardless of age or diet (n ≥ 5 mice per group).

C: The ratio P-PTEN to PTEN was not influenced by genotype, age or diet.

On the above representative western blots, PTEN and phosphorylated PTEN migrate as bands at around 54 kDa (arrows). Representative loading gels, were done for each experiment and examples are presented in Chapter 2, Figure 2.7. Experiments were repeated in duplicate.

$^{\#}P < 0.05$, ANOVA result for effect of genotype.

6.4.6. Hypothalamic Akt protein levels at weaning, TC2 and TC12 in *foz/foz* and WT mice

Hypothalamic Akt protein expression was higher in weanling *foz/foz* than WT mice ($P < 0.05$; Figure 6.12A) and this difference appeared to be maintained at TC2 and TC12 (but it was not significant by 2-way ANOVA). Hypothalamic Akt protein levels also appeared to be increased by high fat-feeding in both genotypes, at TC2 and TC12. Thus, *foz/foz* and WT mice fed a high fat diet for 2- and 12-weeks expressed higher levels of hypothalamic Akt than their chow-fed controls ($P < 0.05$; Figure 6.12A). However, the apparent increase in hypothalamic Akt protein expression in high fat-fed *foz/foz* mice at both TC2 and TC12 was not significant by 2-way ANOVA.

The hypothalamic abundance of phosphorylated Akt (P-Akt) followed that of Akt at weaning. Thus, P-Akt levels were higher in *foz/foz* mice compared to WT mice at weaning ($P < 0.05$; Figure 6.12B). In contrast, hypothalamic P-Akt protein levels were similar between chow-fed *foz/foz* and WT mice at TC2 and TC12. Meanwhile 2- or 12-weeks of high fat-feeding decreased P-Akt levels in both genotypes. Thus, after 2-weeks on high fat diet, values were lower in *foz/foz* and WT mice compared to their chow-fed littermates ($P < 0.05$; Figure 6.12B). However, the apparent decrease in high fat-fed *foz/foz* mice was not significant by ANOVA. In contrast, after 12-weeks on high fat diet both genotypes exhibited significantly lower hypothalamic P-Akt protein levels, compared to their chow-fed controls ($P < 0.05$; Figure 6.12B).

The difference in hypothalamic P-Akt to Akt ratio between *foz/foz* and WT mice at weaning was not significant by the Student's T-test (Figure 6.12C). P-Akt to Akt ratio was similar between chow-fed *foz/foz* and WT mice at TC2. However, 2- or 12-weeks of high fat-feeding decreased P-Akt to Akt ratio in *foz/foz* and WT mice (Figure 6.12C). Thus, at TC2 and TC12, P-Akt to Akt ratio values were significantly lower in high fat-fed WT mice compared to their chow-fed controls ($P < 0.05$; Figure 6.12C). After 12-weeks on diet, hypothalamic P-Akt to Akt ratio was also significantly lower in chow-fed *foz/foz* mice compared to their WT controls ($P < 0.05$; Figure 6.12C).

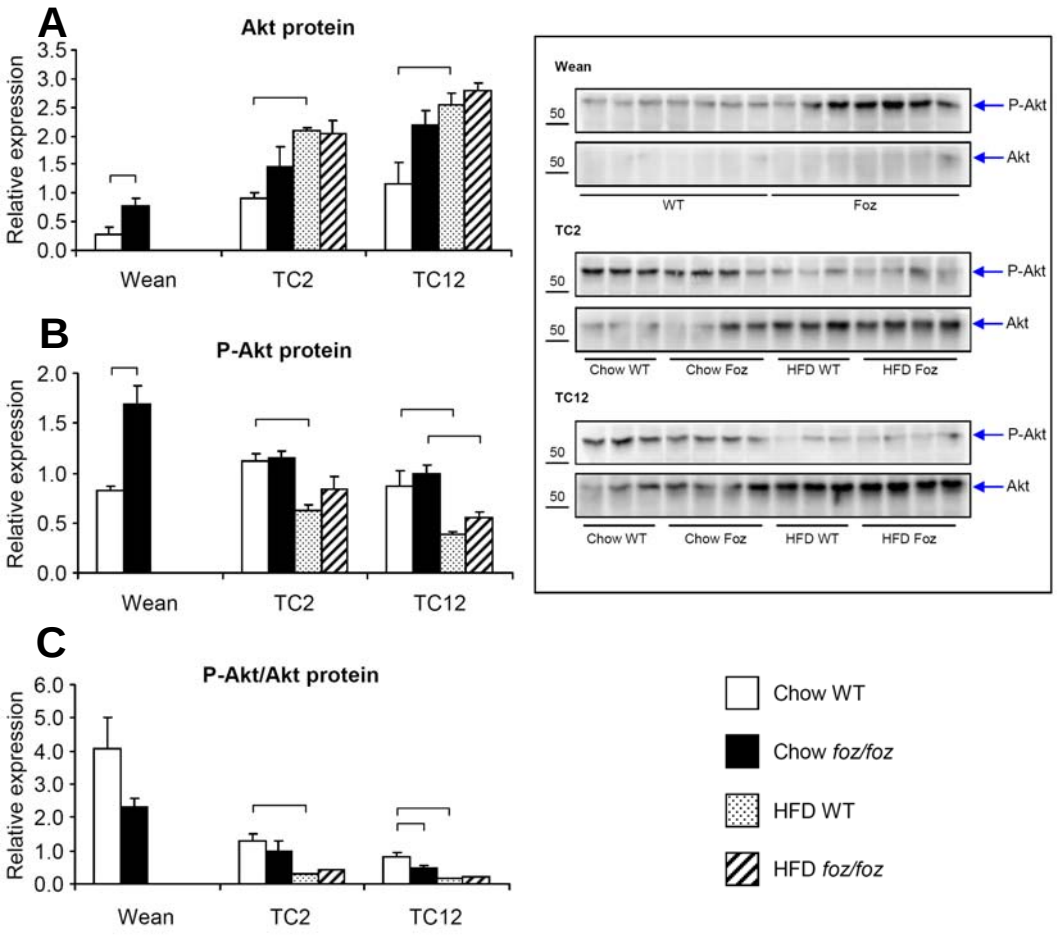

Figure 6.12. Hypothalamic Akt (A), phosphorylated Akt (B) and P-Akt:Akt ratio (C) at different ages during dietary regimes in *foz/foz* and WT mice

A: At weaning, hypothalamic Akt expression was increased in *foz/foz* compared to WT mice. Akt levels were also higher in high fat-fed WT mice compared to their chow-fed littermates at both TC2 and TC12 (n ≥ 5 mice per group).

B: Phosphorylated Akt levels were higher in *foz/foz* compared to WT mice at weaning. A significant decrease in P-Akt levels were observed in high fat-fed WT mice at TC2 and TC12 as well as in high fat-fed *foz/foz* mice at TC12, compared to their respective chow-fed littermates (n ≥ 5 mice per group).

C: Hypothalamic P-Akt to Akt ratio was lower in high fat-fed WT mice at TC2 compared to their chow-fed littermates, and in chow-fed *foz/foz* and high fat-fed WT mice at TC12 compared to chow-fed WT mice.

On the above representative western blots, Akt and phosphorylated Akt migrate at ~60 kDa (arrows). Loading controls were performed for each experiment; representative examples are presented in Chapter 2, Figure 2.7. Statistical bars show significance of post-hoc testing between indicated groups, $P < 0.05$. Experiments were repeated in duplicate.

6.4.7. Hypothalamic FoxO1 mRNA levels at weaning, TC2 and TC12 in *foz/foz* and WT mice

Hypothalamic FoxO1 mRNA levels were similar between chow-fed *foz/foz* and WT mice at TC2. After 2-weeks of high fat-feeding, hypothalamic FoxO1 gene expression was significantly lower in *foz/foz* mice compared to their WT littermates ($P < 0.05$; Figure 6.13A). However, FoxO1 mRNA levels remained unchanged in high fat-fed *foz/foz* mice compared to their chow-fed littermates. Whole hypothalamic FoxO1 gene expression was similar between *foz/foz* and WT mice at TC12, irrespective of diet (Figure 6.13A).

In the paraventricular nucleus, FoxO1 mRNA levels were higher in *foz/foz* compared to WT mice at both weaning and TC2 ($^{\#}P < 0.05$; Figure 6.13B). In contrast, in the anterior hypothalamic area, FoxO1 gene expression was reduced in both genotypes at TC2 compared to their genotype-matched weaning controls ($P < 0.05$; Figure 6.13C). In the arcuate nucleus, FoxO1 transcript levels were higher in *foz/foz* mice compared to WT mice at weaning ($P < 0.05$; Figure 6.13D), while similar levels between *foz/foz* and WT mice were observed at TC2.

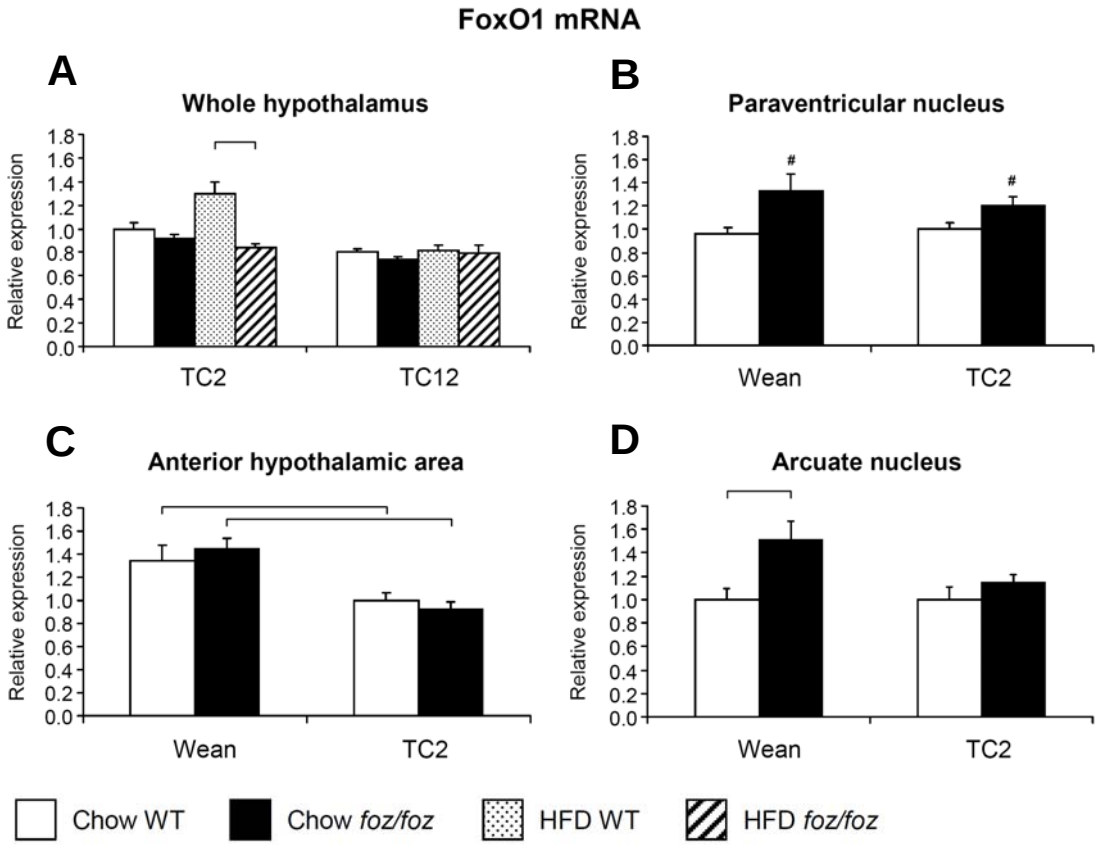

Figure 6.13. Hypothalamic FoxO1 mRNA levels in whole hypothalamus (A) and in hypothalamic nuclei (B-D) at weaning and during dietary regimes in *foz/foz* and WT mice

Dietary experiments and collection of samples are described in Figure 6.3. Total mRNA was extracted (n ≥ 6 mice per group) and FoxO1 mRNA levels determined by semi-quantitative real time PCR (see Chapter 2, section 2.6).

A: Whole hypothalamic FoxO1 mRNA levels were lower in high fat-fed *foz/foz* mice compared to their WT diet-matched littermates at TC2.

B: In the paraventricular nucleus, FoxO1 gene expression was higher in *foz/foz* mice at weaning and TC2 compared to WT mice.

C: In the anterior hypothalamic area, FoxO1 mRNA expression was decreased in both *foz/foz* and WT mice at TC2, compared to their weaning littermates.

D: In the arcuate nucleus, FoxO1 gene expression was higher in *foz/foz* mice compared to WT mice, at weaning.

Statistical bars show significance of post-hoc testing between indicated groups, $P < 0.05$.; $^{\#}P < 0.05$, ANOVA result for effect of genotype. Experiments were repeated in duplicate.

6.4.8. Hypothalamic SHP2 expression at weaning, TC2 and TC12 in *foz/foz* and WT mice

Hypothalamic SHP2 mRNA levels

Whole hypothalamic SHP2 mRNA levels were similar between chow-fed *foz/foz* and WT mice at TC2. However, when fed a high fat diet for 2-weeks, hypothalamic SHP2 mRNA levels were higher in both genotypes compared to chow-fed controls (*$P < 0.05$; Figure 6.14A). After 12-weeks on diet, whole hypothalamic SHP2 gene expression was similar between *foz/foz* and WT mice, irrespective of diet. The apparent decrease in SHP2 mRNA levels in chow-fed *foz/foz* mice and high fat-fed WT mice, compared to chow-fed controls, was not significant by ANOVA.

In the paraventricular nucleus, SHP2 mRNA levels were higher in *foz/foz* than WT mice at weaning ($P < 0.05$; Figure 6.14B), whereas similar levels were observed between *foz/foz* and WT mice at TC2. In the anterior hypothalamic area, a significant decrease in SHP2 mRNA levels was observed at TC2 in both genotypes compared to weaning controls ($^{\S}P < 0.05$; Figure 6.14C). There were no differences in SHP2 transcript levels in the arcuate nucleus between *foz/foz* and WT mice irrespective of time (Figure 6.14D).

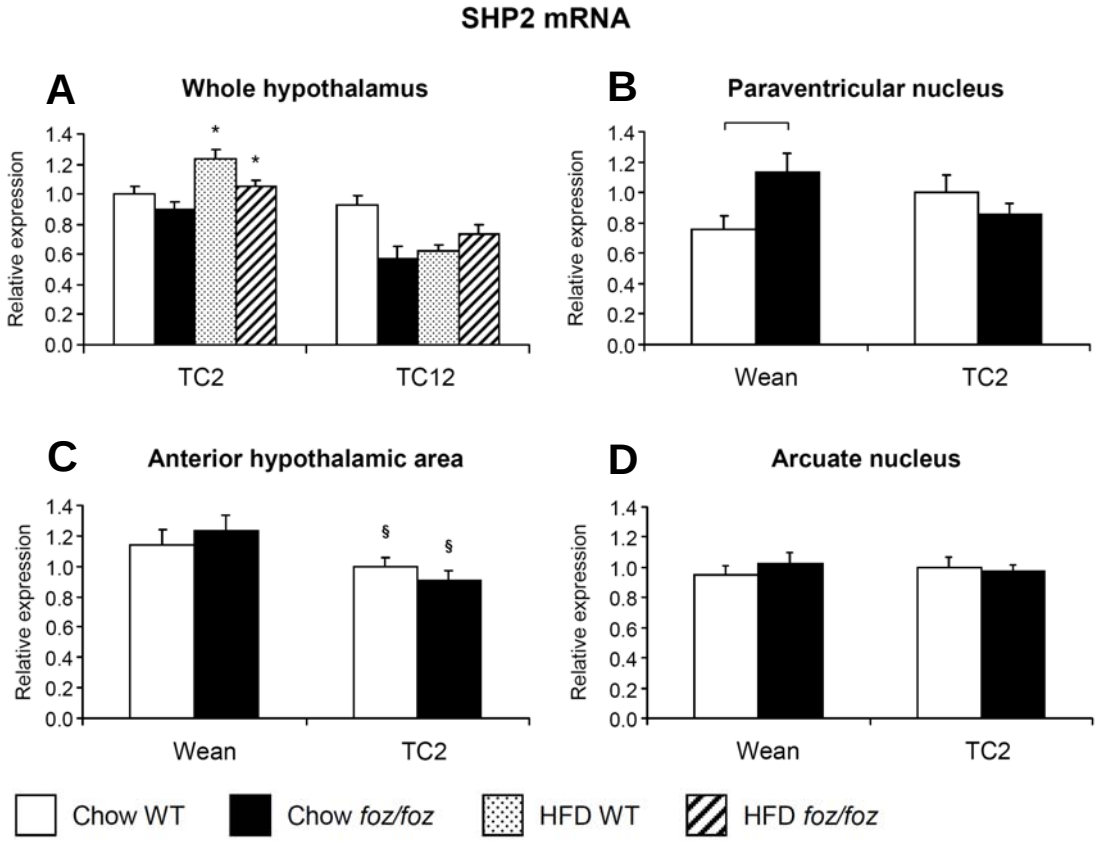

Figure 6.14. Hypothalamic SHP2 mRNA levels in whole hypothalamus (A) and in hypothalamic nuclei (B-D) at weaning and during dietary regimes in *foz/foz* and WT mice

Dietary experiments and collection of samples are described in Figure 6.3. Total mRNA was extracted (n ≥ 6 mice per group) and SHP2 mRNA levels determined by semi-quantitative real time PCR (see Chapter 2, section 2.6).

A: In whole hypothalamus, SHP2 mRNA levels were increased by high fat-feeding at TC2 in both genotypes compared to chow-fed controls.

B: In the paraventricular nucleus, SHP2 gene expression was higher in *foz/foz* compared to WT mice at weaning.

C: In the anterior hypothalamic area, SHP2 mRNA expression was lower in both *foz/foz* and WT mice at TC2 compared to weaning controls.

D: In the arcuate nucleus, SHP2 mRNA levels were not affected by genotype or time.

Statistical bar shows significance of post-hoc testing between indicated groups, $P < 0.05$. Symbols show results of ANOVA: $^{*}P < 0.05$, effect of diet, $^{\S}P < 0.05$, effect of time. Experiments were repeated in duplicate.

Hypothalamic SHP2 protein levels

Hypothalamic SHP2 protein expression was similar between chow-fed *foz/foz* and WT mice at weaning, TC2 and TC12 (Figure 6.15A). After 2-weeks on a high fat diet, *foz/foz* mice showed higher levels in hypothalamic SHP2 protein levels, compared with WT mice ($P < 0.05$; Figure 6.15A). In contrast, 12-weeks of high fat-feeding significantly reduced hypothalamic SHP2 protein levels in both *foz/foz* and WT mice, compared to their corresponding chow-fed controls ($^{*}P < 0.05$; Figure 6.15A).

At weaning, phosphorylated SHP2 (P-SHP2) was significantly higher in *foz/foz* mice compared to WT mice ($P < 0.05$; Figure 6.15B). However, after 2- or 12-weeks on chow, P-SHP2 protein levels were similar between *foz/foz* and WT mice. Furthermore, no genotypes differences were observed after 2- or 12-weeks on high fat diet in P-SHP2 expression (Figure 6.15B).

The ratio P-SHP2 to SHP2 was higher at weaning in *foz/foz* compared to WT mice ($P < 0.05$; Figure 6.15C). After 2-weeks on diet, both chow- and high fat-fed *foz/foz* mice both exhibited a lower P-SHP2 to SHP2 ratio compared to corresponding WT controls ($^{\#}P < 0.05$; Figure 6.15C). After 12-weeks on a chow diet, *foz/foz* and WT mice exhibited the same P-SHP2 to SHP2 ratio. When fed a high fat diet for 12-weeks, both genotypes showed comparable increase in P-SHP2 to SHP2 ratio compared to chow-fed mice ($^{*}P < 0.05$; Figure 6.15C).

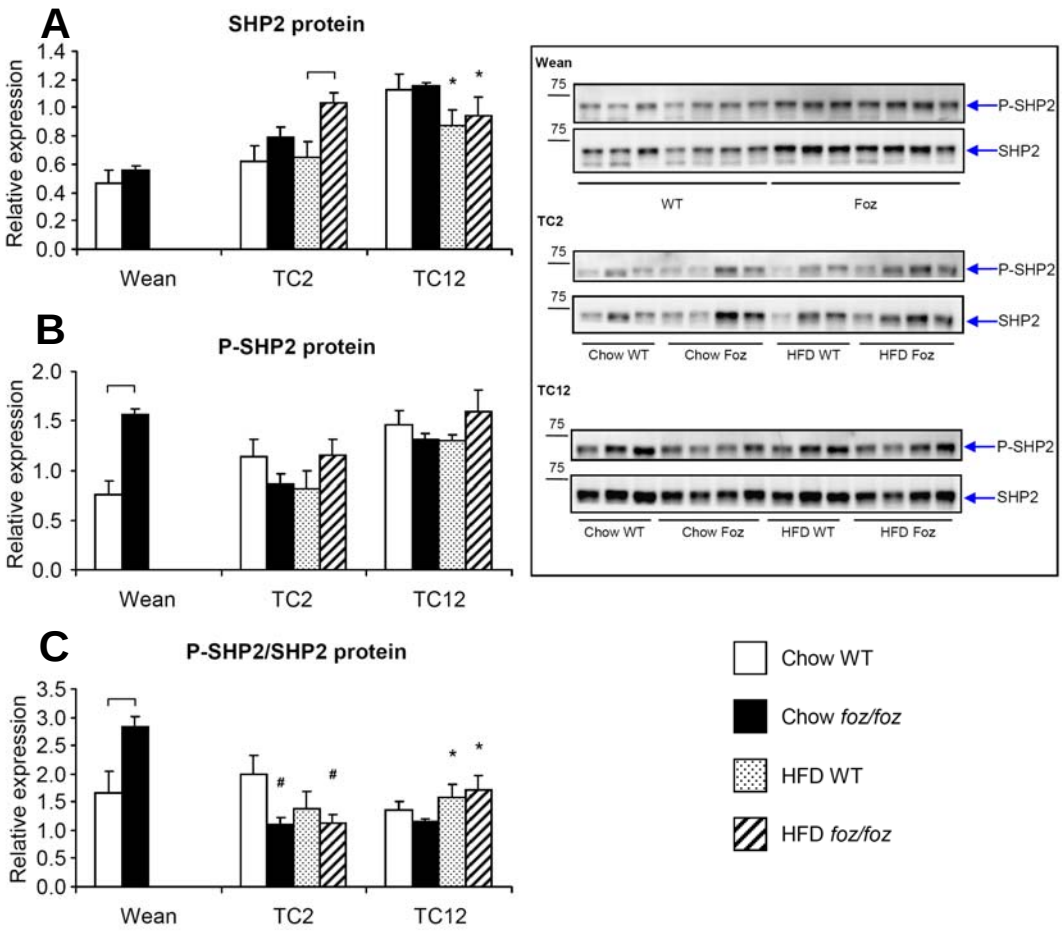

Figure 6.15. Hypothalamic SHP2 (A), phosphorylated SHP2 (B) and P-SPH2:SHP2 ratio (C) at different ages during dietary regimes in *foz/foz* and WT mice

A: At TC2, hypothalamic SHP2 expression was higher in high fat-fed *foz/foz* compared to WT mice. After 12-weeks of high fat-feeding both *foz/foz* and WT mice showed less SHP2 expression than corresponding WT mice.

B: At weaning, P-SHP2 expression was higher in *foz/foz* compared to WT mice.

C: At weaning P-SHP2 to SHP2 ratio was higher in *foz/foz* compared to WT mice. At TC2 chow- and high fat-fed *foz/foz* mice showed lower P-SHP2 to SHP2 ratio than their WT controls. After 12-weeks of high fat-feeding, both *foz/foz* and WT mice showed higher P-SHP2 to SHP2 ratio than their chow-fed genotype-matched littermates.

On the above representative western blots, SHP2 and P-SHP2 migrate at ~70 kDa (arrows). Representative loading gels are presented in Chapter 2, Figure 2.7.

Statistical bars show significance of post-hoc testing between indicated groups, $P < 0.05$; $^{*}P < 0.05$, ANOVA results for effect of diet; $^{\#}P < 0.05$, ANOVA results for effect of genotype. n ≥ 5 mice per group; experiments were repeated in triplicate.

6.4.9. Hypothalamic ERK protein levels at weaning, TC2 and TC12 in *foz/foz* and WT mice

Weanling *foz/foz* mice showed higher hypothalamic levels of total ERK than WT mice ($P < 0.05$; Figure 6.16A). After 2-weeks on diet, hypothalamic ERK levels were not significantly different between *foz/foz* and WT mice, irrespective of diet. By TC12, however, hypothalamic ERK expression was significantly increased in *foz/foz* mice fed either diet than in corresponding WT mice ($^{\#}P < 0.05$; Figure 6.16A).

The hypothalamic abundance of phosphorylated ERK (P-ERK) generally followed that of total ERK at weaning, TC2 and TC12. Thus, P-ERK was higher in *foz/foz* than WT mice at weaning ($P < 0.05$; Figure 6.16B). At TC2, there was no obvious effect of genotype or diet in hypothalamic P-ERK levels; but at TC12, P-ERK expression was consistently higher in *foz/foz* mice than WT mice, irrespective of diet ($^{\#}P < 0.05$; Figure 6.16B).

At weaning and TC2, P-ERK to ERK ratios were similar between *foz/foz* and WT mice, regardless of diet. While, at TC12, P-ERK to ERK ratio was actually lower in *foz/foz* mice fed both diets, compared to WT mice ($^{\#}P < 0.05$; Figure 6.16C).

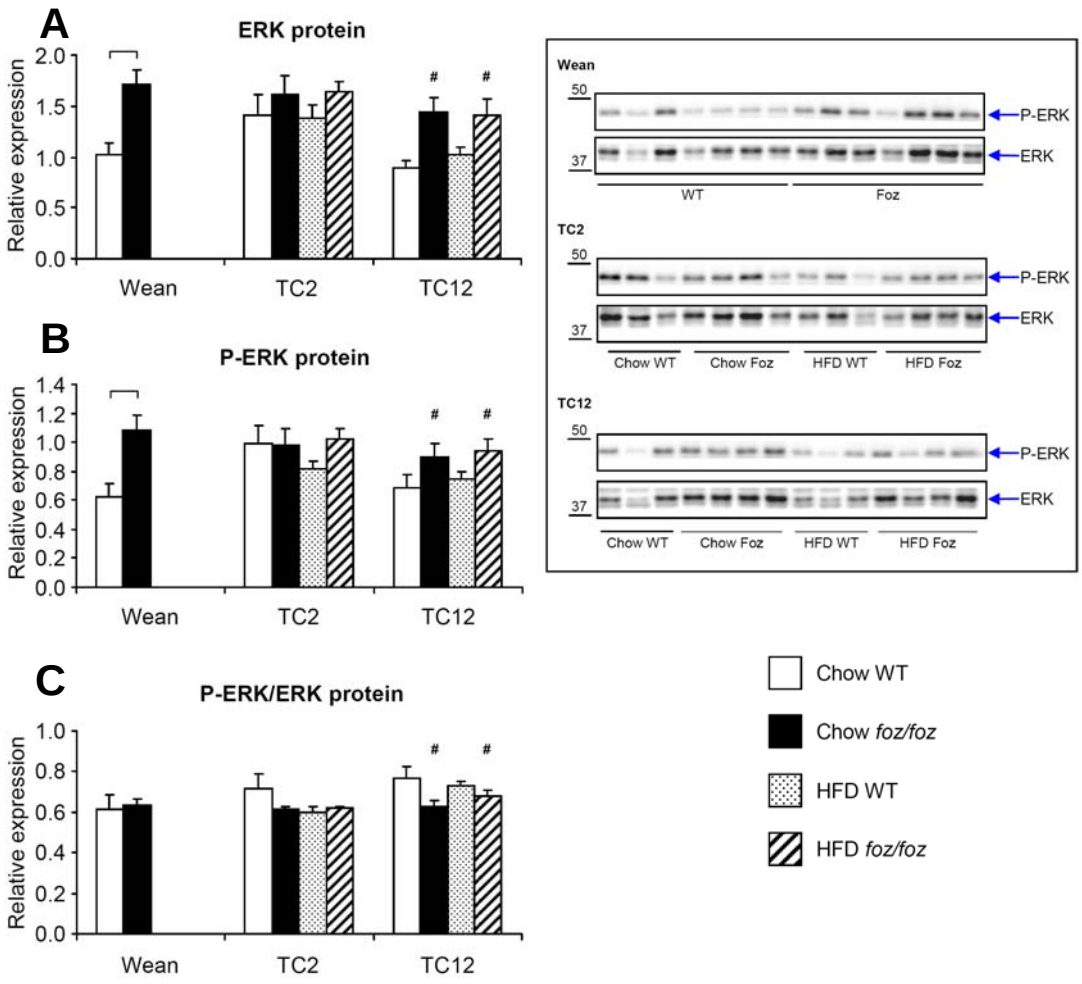

Figure 6.16. Hypothalamic ERK (A), phosphorylated ERK (B) and P-ERK:ERK ratio (C) at different ages during dietary regimes in *foz/foz* and WT mice

A: Hypothalamic ERK expression was higher at weaning in *foz/foz* than WT mice. At TC12 chow- and high fat-fed *foz/foz* mice showed higher ERK levels than corresponding WT mice (n ≥ 5 mice per group).

B: At weaning, phosphorylated ERK expression was higher in *foz/foz* than WT mice. After 12-weeks on chow and high fat diet *foz/foz* mice exhibited higher levels of phosphorylated ERK compared to WT mice (n ≥ 5 mice per group).

C: P-ERK to ERK ratio was lower in chow- and high fat-fed *foz/foz* mice, compared to diet-matched WT mice at TC12.

On the above representative western blots, ERK and P-ERK migrate at ~42 and ~44 kDa, respectively (arrows). Representative loading controls are presented in Chapter 2, Figure 2.7. Statistical bars show significance of post-hoc testing between indicated groups, $P < 0.05$. $^{\#}P < 0.05$, ANOVA results for effect of genotype. Experiments were repeated in triplicate.

6.4.10. Hypothalamic SH2B1 mRNA levels at weaning, TC2 and TC12 in *foz/foz* and WT mice

Hypothalamic SH2B1 mRNA levels were similar between chow-fed *foz/foz* and WT mice at TC2. However, 2-weeks of high fat-feeding induced an increase in SH2B1 mRNA levels in WT mice but not in chow-fed WT controls ($P < 0.05$; Figure 6.17A). In contrast, no differences were observed in SH2B1 mRNA levels in *foz/foz* mice, regardless of the diet. The diet-induced difference in SH2B1 mRNA in WT mice was no longer evident at TC12, when SH2B1 mRNA levels were also similar between *foz/foz* and WT mice, irrespective of dietary regime (Figure 6.17A).

In the paraventricular nucleus, SH2B1 gene expression was higher in *foz/foz* than WT mice at weaning ($P < 0.05$; Figure 6.17B). After 2-weeks on diet, SH2B1 mRNA levels were lower in *foz/foz* mice compared to weanling *foz/foz* mice ($P < 0.05$; Figure 6.17B). The apparent differences in SH2B1 transcript levels between *foz/foz* and WT mice at TC2 and between WT at weaning and TC2 were not significantly different. In the anterior hypothalamic area, SH2B1 mRNA levels were lower in both *foz/foz* and WT mice at TC2 compared to their wealning controls ($^{\S}P < 0.05$; Figure 6.17C), but there were no differences between genotypes. In the arcuate nucleus, there were no variations in SH2B1 mRNA levels between genotypes or time (Figure 6.17D).

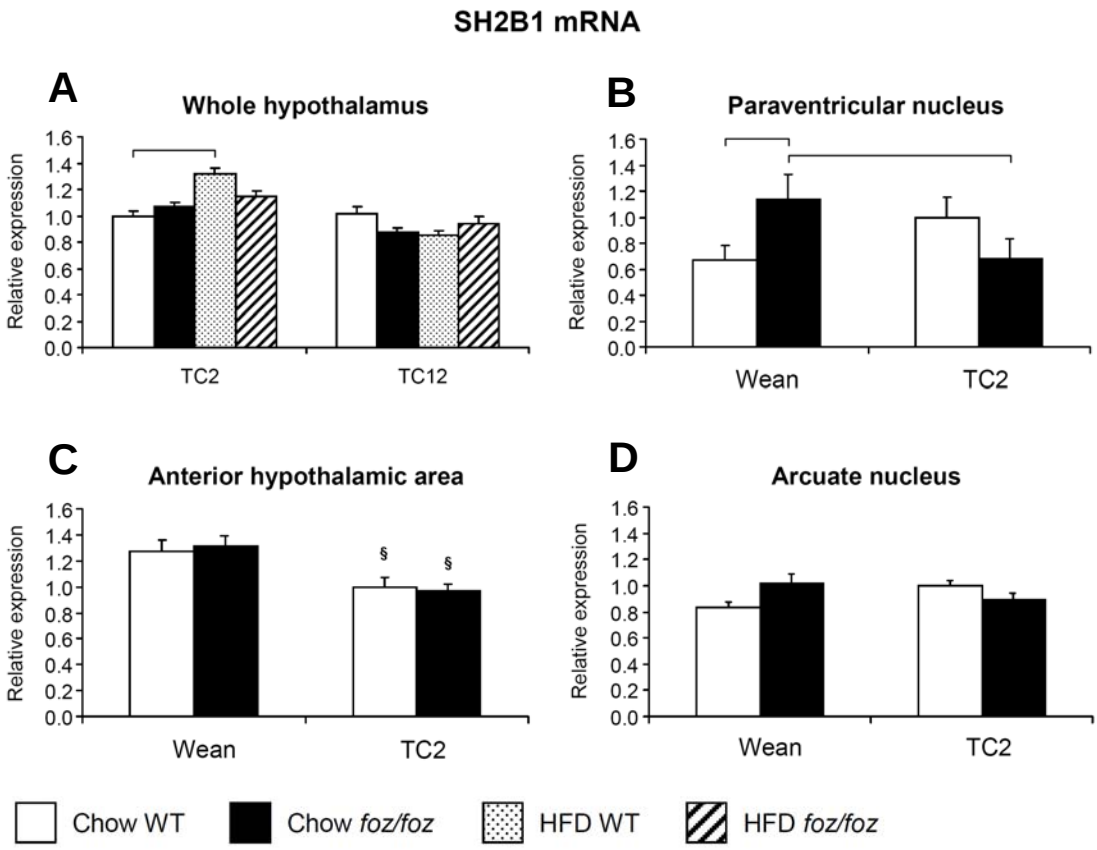

Figure 6.17. Hypothalamic SH2B1 mRNA levels in whole hypothalamus (A) and in hypothalamic nuclei (B-D) at weaning and during dietary regimes in *foz/foz* and WT mice

Dietary experiments and collection of samples are described in Figure 6.3. Total mRNA was extracted and SH2B1 mRNA levels were determined by semi-quantitative real time PCR (Chapter 2, section 2.6).

A: Whole hypothalamic SH2B1 mRNA levels were higher in high fat-fed WT mice at TC2 compared to chow-fed controls.

B: In the paraventricular nucleus, SH2B1 gene expression was higher in *foz/foz* mice compared to WT mice at weaning. At TC2, SH2B1 gene expression was lower in *foz/foz* mice compared to their genotype-matched littermates at weaning.

C: In the anterior hypothalamic area, SH2B1 mRNA levels were lower at TC2 in *foz/foz* and WT mice compared to weaning controls, but there were no difference between genotypes.

D: In the arcuate nucleus, there were no variations in SH2B1 mRNA levels.

Statistical bars show significance of post-hoc testing between indicated groups, $P < 0.05$. $^{\S}P < 0.05$, ANOVA results for effect of time. Experiments were repeated in duplicate.

6.4.11. Hypothalamic PTP1B expression at weaning, TC2 and TC12 in *foz/foz* and WT mice

Hypothalamic PTP1B mRNA levels

Whole hypothalamic PTP1B mRNA expression was similar between chow-fed *foz/foz* and WT mice at TC2. After 2-weeks of high fat-feeding PTP1B mRNA levels were increased in WT mice compared to chow-fed controls ($P < 0.05$; Figure 6.18A), whereas PTP1B mRNA expression remained stable in *foz/foz* mice at the same time. Thus, values between chow- and high fat-fed *foz/foz* mice were similar at TC2 (Figure 6.18A). After 12-weeks on diet, PTP1B mRNA levels between *foz/foz* and WT mice were similar, irrespective of diet (Figure 6.18A).

In the paraventricular nucleus, there were no differences in PTP1B transcript levels between genotypes or time (Figure 6.18B). Similarly, there were no variations in PTP1B anterior hypothalamic area mRNA levels between *foz/foz* and WT mice at weaning and TC2 (Figure 6.18C). In contrast, PTP1B transcript levels in the arcuate nucleus were lower at TC2 than at weaning in both *foz/foz* and WT mice ($P < 0.05$, Figure 6.18D).

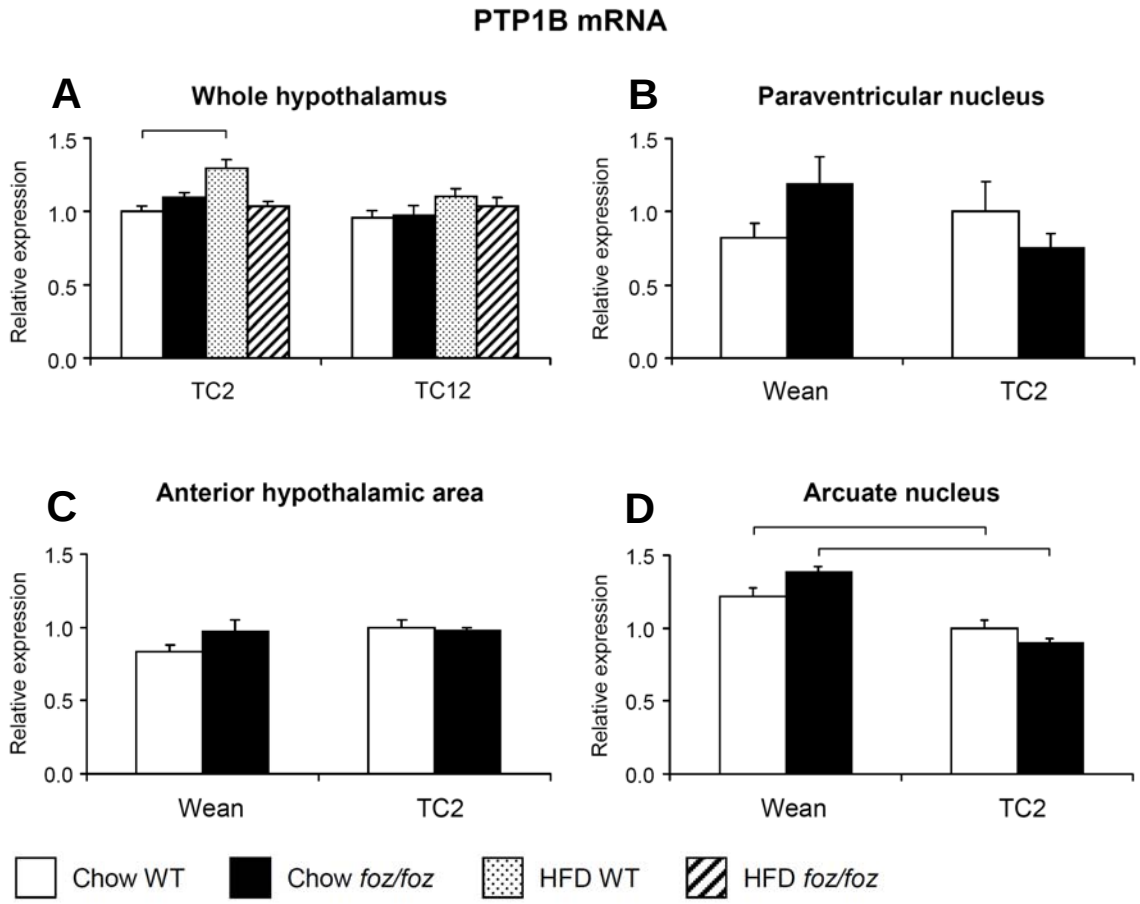

Figure 6.18. Hypothalamic PTP1B mRNA levels in whole hypothalamus (A) and in hypothalamic nuclei (B-D) at weaning and during dietary regimes in *foz/foz* and WT mice

Dietary experiments and collection of samples are described in Figure 6.3. Total mRNA was extracted and PTP1B mRNA levels were determined by semi-quantitative real time PCR (Chapter 2, section 2.6).

A: At TC2, hypothalamic PTP1B mRNA levels were higher in high fat-fed *foz/foz* mice, compared to chow-fed WT mice.

B: In the paraventricular nucleus, PTP1B gene expression was similar between *foz/foz* and WT mice, regardless of time.

C: In the anterior hypothalamic area, PTP1B mRNA expression was not affected by genotypes or time.

D: In the arcuate nucleus, PTP1B mRNA levels were lower in *foz/foz* and WT mice at TC2 compared to weanling mice, but there were no differences between genotypes.

Statistical bars show significance of post-hoc testing between indicated groups, $P < 0.05$. Experiments were repeated in duplicate.

Hypothalamic PTP1B protein levels

There were no differences in hypothalamic PTP1B protein expression in *foz/foz* and WT mice at weaning and TC2, irrespective of dietary regime. However, after 12-weeks on diet, hypothalamic PTP1B protein levels were significantly higher in *foz/foz* compared to WT mice, irrespective of diet ($^{\#}P < 0.01$; Figure 6.19). PTP1B protein levels remained stable in WT mice fed both diets.

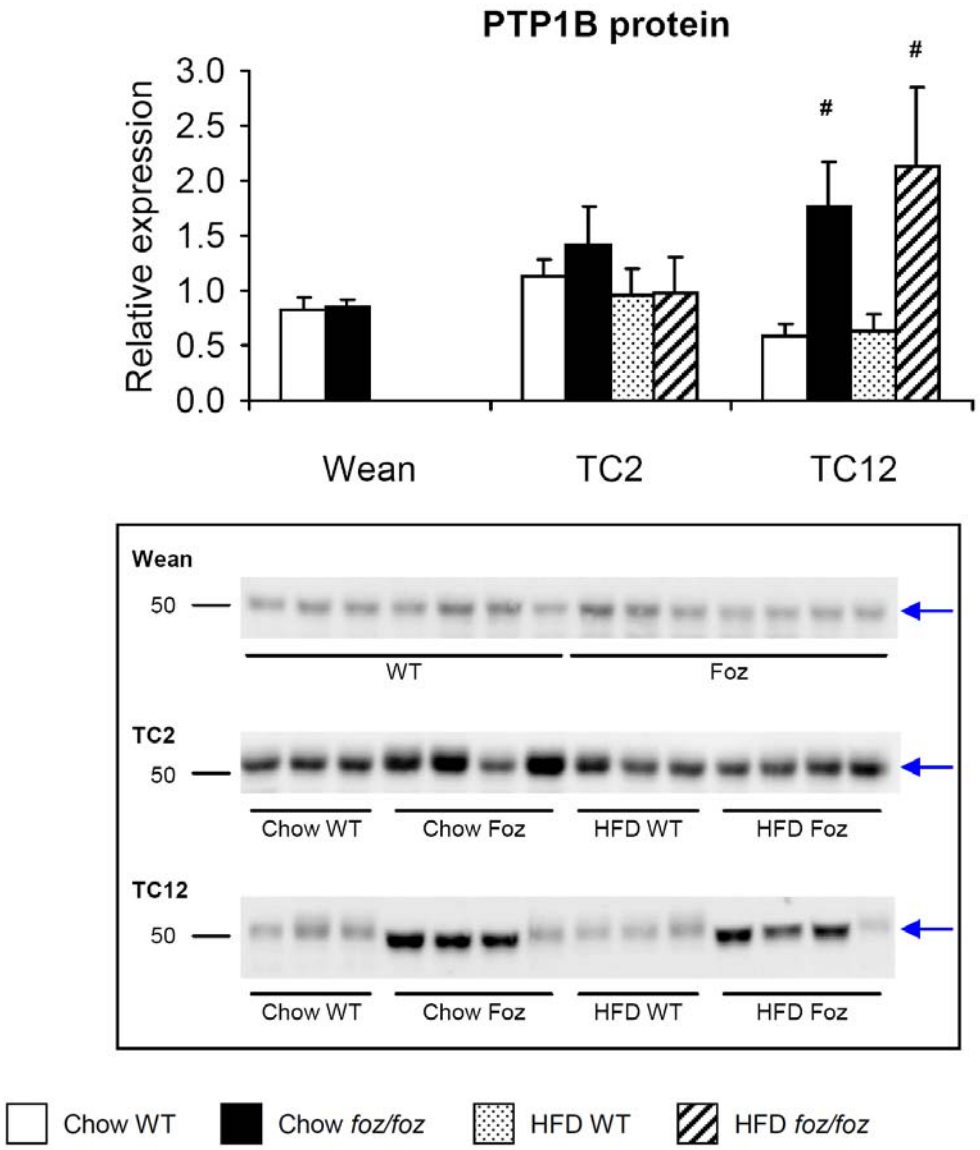

Figure 6.19. Hypothalamic PTP1B protein expression at different ages during dietary regimes in *foz/foz* and WT mice

There were no changes in PTP1B hypothalamic expression between *foz/foz* and WT mice at weaning and TC2. However, after 12-weeks on diet, PTP1B protein expression was higher in *foz/foz* mice compared to WT mice, regardless of the diet (n ≥ 5 mice per group).

On the above representative western blots, PTP1B migrates at ~50 kDa (arrows). Representative loading controls were performed for each experiment, but are not presented here for clarity reasons. Examples are presented in Chapter 2, Figure 2.7. Experiments were repeated in triplicate.

$^{\#}P < 0.01$, ANOVA results for effect of genotype.

6.5. Discussion

In the previous Chapter it was shown that *foz/foz* mice have high circulating leptin levels following weaning. However, these high circulating leptin levels are clearly unable to regulate *foz/foz* body weight appropriately, since the mice develop adiposity and obesity. Further, we showed that leptin responsiveness in *foz/foz* mice hypothalamus was altered, as the regulation of orexigenic and anorexigenic neuropeptide expression was not affected by high leptin levels. The conclusion was reached that *foz/foz* mice are leptin resistant. In the present Chapter, several key molecular mechanisms and signalling pathways involved in leptin resistance were studied and main results are summarised in Tables 6.1 and 6.2.

Table 6.1. Summary of changes in leptin, leptin receptor, signalling intermediates and leptin-regulated genes

Hypothalamic gene/protein expression		Effect of genotype (*foz/foz* vs. WT)	Effect of diet (HFD vs. Chow)		Effect of time	
			WT	*foz/foz*	WT	*foz/foz*
Ob-R	mRNA	↓ at TC2 in PVN	None	None	None	None
	Protein	None	None	None	-	-
Leprot	mRNA	None	None	None	None	None
Stat3	mRNA	↑ at Wean in PVN	None	None	None	↓ at TC2 in PVN and AH
	Protein	↑ at TC12	↑ at TC12	↑ at TC12	-	-
P-Stat3	Protein	↑ at TC2 (HFD)	None	↑ at TC2	-	-
SOCS3	mRNA	↑ at TC2 and TC12	↑ at TC2	↑ at TC2	↑ at TC2 in AH	↑ at TC2 in AH
PTEN	Protein	↑ at TC2 and TC12	None	None	-	-
P-PTEN	Protein	None	None	None	-	-
Akt	Protein	↑ at Wean	↑ at TC2 and TC12	None	-	-
P-Akt	Protein	↑ at Wean	↓ at TC2 and TC12	↓ at TC12	-	-
FoxO1	mRNA	↓ at TC2 (HFD) in whole hypothalamus ↑ at Wean and TC2 in PVN ↑ Wean in Arc	None	None	↓ at TC2 in AH	↓ at TC2 in AH
SHP2	mRNA	↑ Wean in PVN	↑ at TC2	↑ at TC2	↓ at TC2 in AH	↓ at TC2 in AH
	Protein	↑ at TC2 (HFD)	↓ at TC12	↓ at TC12	-	-
P-SHP2	Protein	↑ Wean	None	None	-	-
ERK	Protein	↑ Wean and TC12	None	None	-	-
P-ERK	Protein	↑ Wean and TC12	None	None	-	-

Table 6.2. Summary of changes in proteins that modulate Ob-R signalling

Hypothalamic gene/protein expression		Effect of genotype (*foz/foz* vs. WT)	Effect of diet (HFD vs. Chow)		Effect of time	
			WT	***foz/foz***	**WT**	***foz/foz***
SOCS3	Protein	↑ at TC2	↑ at TC2	↑ at TC2	-	-
SH2B1	mRNA	↑ Wean in PVN	↑ at TC2	None	↓ at TC2 in Arc	↓ at TC2 in Arc
PTP1B	mRNA	None	↑ at TC2	None	↓ at TC2 in Arc	↓ at TC2 in Arc
	Protein	↑ at TC12	None	None	-	-

The first hypothesis tested was that obesity in *foz/foz* mice is related to variations in hypothalamic Ob-R gene and protein expression. Thus, the first important result is that hypothalamic Ob-R mRNA and protein levels are not affected by high circulating leptin levels in *Alms1* mutant (*foz/foz*) mice (see Table 6.1 for summary). Previous studies have demonstrated that Ob-R gene expression can be responsive to feeding status or to genetic changes that favour obesity. Ob-R mRNA levels are increased in leptin deficient *ob/ob* mice, and following fasting in lean mice (Lin and Huang, 1997; Baskin *et al.*, 1998), while leptin administration in *ob/ob* mice decreases hypothalamic Ob-R mRNA levels (Baskin *et al.*, 1998). Taken together, these results indicate that leptin can modify Ob-R expression. However, the high circulating leptin levels observed in *foz/foz* mice did not affect hypothalamic Ob-R transcription or translation. Therefore, our results tend to indicate that leptin resistance in *foz/foz* mice is not related to Ob-R dysregulation. Attention was then focused on whether other molecules or signals are involved in the development of leptin resistance in these mice (discussed later).

In the present Chapter, we also studied the localisation of Ob-R in the hypothalamus. There were no changes in the general localisation (that is changes in hypothalamic nuclei expression) of Ob-R between *foz/foz* and WT mice. However, one cannot exclude the possibility that subcellular localisation of Ob-R occurs in *Alms1* mutant mice. Indeed, as explained in Chapter 4, Ob-R has been shown to be

expressed on olfactory cilia (Baly *et al.*, 2007). Furthermore, Seo *et al.* (2009) also showed that Bardet-Biedl syndrome proteins (BBS2, 4 and 6) are necessary for Ob-R signalling in the hypothalamus, and that BBS1 physically interacts with Ob-R. To confirm this hypothesis, immunocytofluorescent assays should be performed in order to determine Ob-R subcellular localisation in neurons from *foz/foz* and WT mice. The limitations of these experiments, which have been attempted in preliminary studies, were outlined in the Discussion of Chapter 4.

Couturier *et al.* showed in 2007 that Leprot negatively regulates Ob-R cell surface expression. However, studies on hypothalamic Leprot mRNA levels in *foz/foz* and WT mice showed no differences related to genotype or diet (Table 6.1). To date, very few studies have been performed on hypothalamic Leprot expression and its role in obesity and leptin resistance. Because there was no evidence of Leprot overexpression in *foz/foz* mice, it is concluded that this is unlikely to contribute to the leptin resistance phenotype in these obese mice.

In the present work, we also assessed the activation of Ob-R signalling pathways by measuring the expression of downstream messengers, Stat3 and P-Stat3. Hypothalamic Stat 3 gene and protein levels were measured in order to determine basal expression levels in the hypothalamus of *foz/foz* and WT mice. While no changes in whole hypothalamic Stat3 mRNA levels were observed, increases in its protein levels were detected at TC12 in chow and high fat-fed *foz/foz* mice as well as in high fat-fed WT mice (Table 6.1). This indicates that high circulating leptin levels correlate with increased expression of hypothalamic Stat3 at TC12 in *Alms1* mutant and control mice. The mechanisms of Stat3 regulation are not clear. Thus, a direct effect of high leptin levels on hypothalamic Stat3 expression has not been reported in the published literature. However, leptin-independent mechanisms could also be involved in the increase in Stat3 expression. Such mechanisms could involve increase in protein stability.

Hypothalamic P-Stat3 levels were then assessed by western blot and normalised to Stat3, as phosphorylation is the relevant transduction signal of Ob-R. In high fat-fed *foz/foz* mice at TC2, high P-Stat3 and P-Stat3 to Stat3 ratio was observed compared to their chow-fed *foz/foz* controls. Bearing in mind that these mice already exhibit elevated circulating leptin levels, these results are in accordance with previous work demonstrating that P-Stat3 increases following intravenous injection of leptin, whereas such an effect is not observed for Stat3 expression (McCowen *et al.*, 1998). The present results are interpreted as indicating that Ob-R signalling does increase at TC2 in high fat-fed *foz/foz* mice compared to high fat-fed WT and chow-fed *foz/foz* mice. On the other hand, by 12 weeks of dietary feeding, P-Stat3 levels were similar between genotypes despite much higher circulating leptin levels in *foz/foz* than WT mice. Despite this, the ratio P-Stat3 to Stat3 is lower in chow-fed *foz/foz* mice as well as in both high fat-fed *foz/foz* and WT mice at TC12 compared to chow-fed WT mice, mainly attributable to the increase in native Stat3 protein. Taken together, these results suggest that Ob-R activity is reduced at TC12 in *foz/foz* mice irrespective of diet, and in high fat-fed WT mice despite increased availability of the Ob-R signalling intermediate, Stat3. This leads us to conclude that hypothalamic leptin responsiveness is impaired in diet-induced obesity as well as in *Alms1* mutant mice. One caveat in drawing this conclusion should be mentioned: Ob-R is not the only receptor on hypothalamic cells that signals via Stat3. Thus, all the so-called IL-6-type cytokines (IL-6, IL-11, ciliary neurotrophic factor, etc) have been shown to activate Stat3 (Heinrich *et al.*, 1998).

In the present Chapter, studies were also focused on the interaction between leptin and the PI3K/PTEN/Akt/FoxO1 pathway. The main results comparing *foz/foz* versus WT mice are summarised in Figure 6.20.

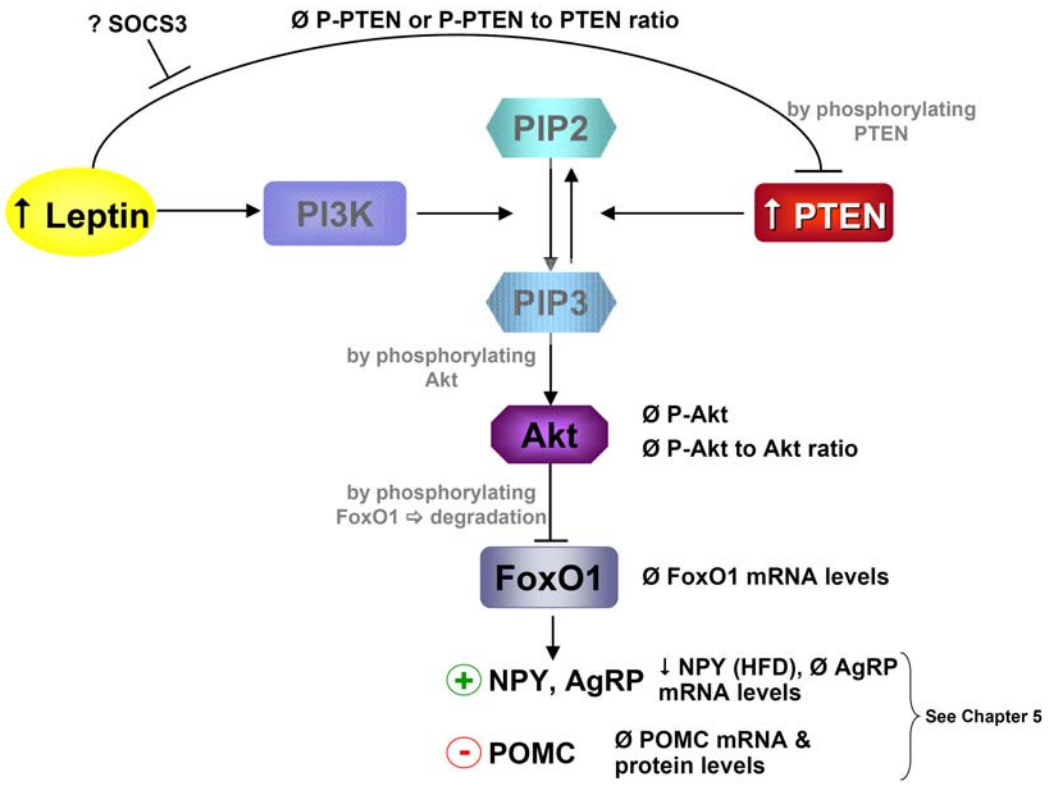

Figure 6.20. Diagram recapitulating the results (*foz/foz* vs. WT) from Chapter 6 on PI3K/PTEN/Akt/FoxO1 pathway, and proposed interactions between signalling peptides and transcriptional regulation

Ø: No significant differences in *foz/foz* vs. WT mice (regardless of time or diet)

Here we show that when the obese phenotype appears and develops (at TC2 and TC12), hypothalamic FoxO1 mRNA levels are not affected by the *Alms1* mutation, and nor are protein levels of its endogenous inhibitor, Akt (Table 6.1). Like Akt, P-Akt protein levels are unchanged between *foz/foz* and WT mice at TC2 and TC12. However, hypothalamic protein expression of PTEN, the PI3K/Akt pathway antagonist, is higher in *foz/foz* mice (at TC2 and TC12; Figure 6.20 and Table 6.1). Taken together, these results are consistent with the proposal that PTEN inhibits the PI3K/Akt pathway, preventing phosphorylation of Akt and leading to its inhibition. This should ultimately cause the maintenance/stability/non-degradation of the Akt downstream target, FoxO1. In turn this should lead to NPY and AgRP transcription, while inhibiting POMC transcription (Kim *et al.*, 2006; Kitamura *et al.*, 2006; Yang *et al.*, 2009), but this is not the case in *foz/foz* mice. As detailed, in the previous Chapter, NPY mRNA levels were only lower in high fat-fed *foz/foz* mice compared to WT diet-matched littermates, while AgRP mRNA and POMC mRNA and protein levels were similar between *foz/foz* and WT mice. One explanation could reside in the effect of leptin on PI3K/Akt/FoxO1 pathway. Specifically, leptin has been shown to interact with this pathway by stimulating Akt phosphorylation leading FoxO1 degradation (Niswender *et al.*, 2001; Niswender *et al.*, 2004; Xu *et al.*, 2005b). Here we show that, in *foz/foz* mice, Akt protein and FoxO1 mRNA levels, as well as its downstream targets are not affected by either leptin and/or PTEN overexpression (Table 6.1). Taken together, these data could indicate that, in *Alms1* mutant mice, PTEN and leptin may counterbalance each other's action on the PI3K/Akt/FoxO1 pathway.

The results from this study also show that hyperleptinaemic *foz/foz* mice do not express higher levels of P-PTEN than WT mice (Figure 6.20 and Table 6.1).

This is in opposition to data from *in vitro* experiments, which showed that leptin induces PTEN phosphorylation in hypothalamic cell lines, which in turn leads to an increase in PIP3 levels (Ning *et al.*, 2006). An explanation for this could be that leptin signalling is already inhibited by SOCS3 (which is increased; Table 6.2), and the normal effect of leptin is lost as a consequence of leptin resistance. This proposal is supported by results reported by Ning *et al.*, (2006), who showed that the phosphorylation of PTEN by leptin is mediated via Ob-R activation. However, none of these experiments have been performed *in vivo*. Therefore, one cannot rule out the possibilities that the phosphorylation of PTEN can be regulated differently *in vivo* than *in vitro*. Such mechanisms could involve molecule(s) that inhibit(s) the phosphorylation of PTEN, or induce its dephosphorylation.

Studies of hypothalamic SHP2 and P-SHP2 expression in *foz/foz* and WT mice showed a higher P-SHP2 to SHP2 ratio in *foz/foz* than WT mice at weaning, while at TC2 this ratio was lower in *foz/foz* compared to WT mice, regardless of diet. These differences had disappeared by TC12, but the P-SHP2 to SHP2 ratio was higher in both high fat-fed *foz/foz* and WT mice compared to chow-fed controls. There is very little information in the published literature on hypothalamic SHP2 and P-SHP2 expression in diet-induced obesity and genetic forms of obesity. Further, most reported studies have focused their attention on the role of SHP2 in Ob-R signal transduction by generating SHP2 mutants (Zhang *et al.*, 2004). The results of such studies show that SHP2 knock-out mice develop early-onset obesity. Although the P-SHP2 to SHP2 ratio is decreased in *foz/foz* mice, this finding was only present at TC12, indicating it is a late change and unlikely to be the major contributing factor to the obese phenotype. This conclusion is further supported by the relationship between SHP2 and activation of ERK. Here we show that P-ERK to ERK ratio is not

affected by genotype (or diet) at weaning and TC2, and that chow- or high fat-fed *foz/foz* mice exhibit a decrease in this ratio at TC12 compared to WT controls. It has previously been shown that in SHP2 knock-out mice, P-ERK is reduced (Zhang *et al.*, 2004). However, corresponding changes were not observed in *foz/foz* mice, therefore leading to the conclusion that the SHP2/ERK pathway is not involved in the development and maintenance of obesity in these animals. However, ERK signalling pathway has also been shown to be under the control of several other molecules in the brain, including gonadotropin releasing hormone (Dobkin-Bekman *et al.*, 2006) and corticotrophin-releasing hormone (Hauger *et al.*, 2009). Therefore the results observed in the current study may not all be attributable to leptin.

The emerging picture from the data showing no change in Ob-R expression, variable (and possibly opposed) changes in the principle Ob-R signalling pathways, indicate that hypothalamic leptin signalling is defective in *foz/foz* mice with the onset of occurring after weaning. To explore other possible modulators of leptin receptor signalling (see Figure 6.1), we studied SOCS3, SH2B1 and PTP1B hypothalamic expression in *foz/foz* mice, these results are summarised in Table 6.2.

Our finding that SOCS3 mRNA and protein levels are higher in *foz/foz* (fed both diets) and high fat-fed WT mice at TC2, compared to chow-fed WT mice, is consistent with an effect of high fat diet and genotype on SOCS3 hypothalamic expression (Tables 6.1 and 6.2). Keeping in mind that these mice exhibit high circulating leptin levels, these data are in accord with previous studies where it has been shown that leptin increases hypothalamic SOCS3 mRNA levels (Bjorbaek *et al.*, 1998; Peiser *et al.*, 2000). After 12-weeks on diet, SOCS3 mRNA levels stay elevated in *foz/foz* compared to WT mice (both diets). However, such differences were not observed in SOCS3 protein levels, which were similar between *foz/foz* and

WT mice. These results indicate, in *foz/foz* mice, that at TC12 high leptin levels are still able to induce SOCS3 transcription but its translation or protein stability seem to be impeded. Taken together, these data are consistent with a role for upregulation of SOCS3 as contributing to the central leptin resistance observed in *Alms1* mutant mice.

In the present Chapter, attention was also focused on the hypothalamic expression of another inhibitor of Ob-R signalling pathway, PTP1B. Although hypothalamic PTP1B mRNA levels were not affected by genotype, its protein expression was higher in *foz/foz* versus WT mice at TC12 (Table 6.2). This difference between transcript and protein levels could again be explained by a decrease in PTP1B degradation or an increase its stability. From 2002 onwards, studies on PTP1B genetic deletion have shown that the lack of PTP1B improves leptin sensitivity and reduces body adiposity in mice (Cheng *et al.*, 2002; Zabolotny *et al.*, 2002; Bence *et al.*, 2006). Furthermore, hypothalamic PTP1B expression has been shown to increase in leptin resistant animals (Morrison *et al.*, 2007; White *et al.*, 2009). All together, these results suggest that the overexpression of PTP1B contributes to leptin resistance and therefore the development of obesity in *foz/foz* mice.

In the present study, hypothalamic SH2B1 mRNA levels were not affected by genotype at TC2 or TC12. However, 2-weeks of high fat feeding increased SH2B1 transcript in WT mice, compared to their chow-fed controls (Table 6.2). Studies have previously shown that genetic deletion of SH2B1 results in hyperphagia and obesity. (Ren *et al.*, 2007; Morris *et al.*, 2010). Taken together, these results indicate that the obese phenotype observed in *foz/foz* mice is not

related to a deficiency in SH2B1 and that the *Alms1* mutation does not affect SH2B1 mRNA expression.

In summary, the present data provide clear evidence that leptin resistance occurs in *foz/foz* mice. This evidence includes not only the lack of a physiological response to high circulating leptin levels but also the inefficiency of leptin to modulate hypothalamic appetite-regulating neuropeptide gene expression (NPY, AgRP, POMC, etc). Furthermore, there seems to be a time-dependent pattern in the development of leptin resistance in *foz/foz* mice; for example, hypothalamic P-Stat3 expression correlates with leptin levels at TC2 but not TC12, when other pathways may have been turned on. Indeed, some other data derived from weaning pups is consistent with *increased sensitivity* to leptin at this stage of development in *foz/foz* mice (Table 6.1 and 6.2). Specifically, *foz/foz* mice exhibit greater Akt and ERK activation at this time. However, decreases in these Ob-R activated pathways occurs at late times when the major pathways involved in leptin resistance appear to be overexpressed. Two key inhibitors of the Ob-R signalling pathway, SOCS3 at TC2 and PTP1B at TC12 may be particularly important pathways. As demonstrated in the previous Chapters, *foz/foz* mice also present a deficiency in primary cilia after birth, which has been shown in other mouse models to lead to obesity. Therefore, it is possible that obesity in *Alms1* mutant mice could result from hypothalamic dysregulation of appetite (and physical activity) caused initially by the cilial defect, and compounded by the time course changes in SOCS3 and PTP1B on hypothalamic Ob-R signal transduction, or it could possibly be a combination of both factors. This will be discussed in the final Chapter.

CHAPTER 7

Chapter 7

General discussion

The aim of the research in this thesis was to explore the mechanisms that underlie the development of obesity and leptin resistance in *Alms1* mutant mice. Feeding *foz/foz* mice a high fat diet accelerates and worsens the obese phenotype, specifically accelerating onset of diabetes, hypercholesterolaemia and nonalcoholic steatohepatitis. Therefore, the experiments described in this thesis specifically focused on the role of the hypothalamus in the control of energy homeostasis, that is, the regulation of body weight via food intake and energy expenditure. The effects of genotype, development and diet were investigated by studies in *foz/foz* and WT mice fed chow or high fat diet from weaning to 18 weeks of age. Particular attention was given to the role of hypothalamic primary cilia and Alms1, as well as hypothalamic appetite-regulating neuropeptides, and leptin receptor signal transducers during these processes.

Each Chapter of this thesis includes a Discussion section, which has briefly outlined and discussed the presented results. In summary, the work described in this thesis demonstrates that *foz/foz* mice exhibit a deficiency in hypothalamic primary cilia that occurs after birth and which appears related to the lack of detectable Alms1 in hypothalamic primary cultures from *foz/foz* mice (Chapters 3 and 4). The present work also confirmed that *foz/foz* mice develop obesity associated with hyperleptinaemia, which indicates that these mice are leptin resistant (Chapter 5). Studies to characterise the mechanisms involved in leptin

resistance in these mice produced data that implicate hypothalamic overexpression of two negative regulators of the leptin receptor, SOCS3 and PTP1B (Chapter 6). In the current Chapter, the general significance of these results will be discussed, and important points that need further investigation will be addressed.

7.1. Is Alms1 involved in the stability and maintenance of primary cilia?

The assembly and disassembly of the primary cilium, its stability and maintenance coordinate complex mechanisms that involve a large number of molecules (centrosomal proteins, intraflagellar transport proteins, etc). We hypothesised that Alms1 is one such protein that could be particularly involved in cilia stability and maintenance. In Chapter 3, we show that the *Alms1* mutation is associated, most likely causally, in a decrease in the number of hypothalamic primary cilia between birth and 3 weeks of age. It would be of great interest to pinpoint the precise time when this decrease occurs. Therefore, future studies will examine more precisely the time when this drop/fall occurs. For example, a time course approach using mice every 3 days from birth to weaning should identify the time at which cilia loss occurs, and also identify if there is a sudden or gradual loss of cilia.

The centriolar localisation of Alms1 tends to suggest that it can be involved either as a centriolar docking site or as an intermediate protein in ciliary trafficking (Discussed in section 7.2). To assess the role of Alms1 in the stability of primary cilia and its maintenance, experiments will be conducted in *foz/foz* (expressing a shortened Alms1 protein) and WT mice primary cell culture, as well as WT mice cell

cultures treated with *Alms1* siRNA (in order to reduce Alms1 protein levels). By inducing a mechanical stress to the cell culture one would expect to be able to observe and measure cilial loss in cells with abnormal Alms1, if indeed Alms1 is important for cilia stabilisation. Several techniques have now been developed in order to specifically isolate primary cilia (Mitchell *et al.*, 2009). One of them consists of a mechanical shear (Mitchell *et al.*, 2004). Using this technique would allow the number of cilia that fall off in *foz/foz* and *Alms1* siRNA treated WT cell cultures compared to "normal" WT cell cultures to be measured. Furthermore, by collecting these cilia, proteomic studies would also be possible, enabling important information on the identity of ciliary proteins, including whether Ob-R and/or other elements of the leptin receptor scaffold/signalling apparatus is/are contained thereon.

7.2. Is obesity in *foz/foz* mice related to Alms1 function in intracellular trafficking and protein transport?

The potential role of truncated Alms1 and ciliary deficiency in the development of obesity and leptin resistance in *foz/foz* mice must be considered. In their review, "Can faulty antennae increase adiposity?", Sen Gupta and colleagues (2009), recapitulated all the latest findings that link disruption of ciliary protein function to obesity. This review concluded that the loss of ciliary protein function can lead to obesity, most likely via effects on leptin receptor signalling. It would therefore be of great interest to perform knock-in studies of Alms1 via adenovirus or retrovirus, in *foz/foz* mice, in order to restore the cellular function of Alms1. One would then assess whether the current phenotype observed in *foz/foz* mice can be

reversed, and, if so, whether this is due to a restoration of the number of primary cilia. If these experiments caused a reversal of obesity without increase in cilia number, then it could be concluded that Alms1 functions through a cilia-independent pathway to cause obesity. We believe the opposite is more likely.

Studies on primary cilia proteins are crucial in the understanding of related diseases, the so-called ciliopathies (Bisgrove and Yost, 2006; Pedersen *et al.*, 2008; Goetz and Anderson, 2010). In the past decade, research has been focused on the localisation and function of basal body and primary cilia proteins. However, complementary experiments are necessary to decipher the protein-protein interactions between Alms1 and other ciliary proteins, and its role in feeding behaviour. Our results are consistent with previous work that demonstrates Alms1 (murine)/ALMS1 (human) expression at the base of the primary cilium (Collin *et al.*, 2005; Hearn *et al.*, 2005). In order to characterise the cellular role of Alms1, immunocyto-, immunohisto-fluorescent studies have been conducted between Alms1 and proteins localised at the basal base of the primary cilium (Hearn *et al.*, 2005; Knorz *et al.*, 2010). It would be interesting to perform immunoprecipitation studies between Alms1 and these previously described proteins in order to clarify if there is any physical interaction between them. In addition, electron microscopy studies, which allow greater resolution of protein localisation within cellular structures, would enable a more detailed understanding of Alms1 localisation in normal neurons, as well as those from *foz/foz* mice.

7.3. What else could cause leptin resistance in *foz/foz* mice?

foz/foz mice are obese, hyperleptinaemic, and compared to WT mice have increased hypothalamic SOCS3 and PTP1B expression, which has been shown to result in leptin resistance (Banks *et al.*, 2000; Bjorbak *et al.*, 2000; Kaszubska *et al.*, 2002; Mori *et al.*, 2004; Bence *et al.*, 2006). Future experiments will test the hypothesis that these two molecules are by themselves responsible for the development of leptin resistance in *foz/foz* mice. Logically, the first set of experiments would involve pharmacological interventions in *foz/foz* mice. Thus, inhibition of PTP1B by trodusquemine and blockade of SOCS3 by a lentiviral vector-mediated RNA interference technique have been shown to substantially reduce body weight and adiposity in diet-induced obese rodents (both mice and rats; Lantz *et al.*, 2010; Liu *et al.*, 2011). These treatments could be used individually or in combination, where additional effects on the reduction body weights and body adiposity are expected.

A second set of experiments could utilise *foz/foz* mice with SOCS3 and/or PTP1B brain-specific (hypothalamic nucleus-specific or neuronal-specific) deletion (Cheng *et al.*, 2002; Zabolotny *et al.*, 2002; Howard *et al.*, 2004; Mori *et al.*, 2004; Bence *et al.*, 2006; Briancon *et al.*, 2010). For example, to generate *foz/foz* mice with PTP1B deletion in POMC neurons, *foz/foz* mice would have to be crossed with *Ptp1b*$^{loxP/loxP}$ POMC-Cre mice, obtained via the Cre/LoxP recombination system (Balthasar *et al.*, 2004; Bence *et al.*, 2006; Banno *et al.*, 2010). This approach would allow more discriminant localisation of the area (hypothalamic neuronal subpopulation) affected by leptin resistance. Ultimately, it would be anticipated that,

in both sets of experiments, obesity and leptin resistance would be prevented in *foz/foz* mice.

One cannot exclude that other mechanisms may be involved in leptin resistance in *foz/foz* mice. Thus, it is possible that leptin transport across the blood brain barrier is altered in these mice. In order to confirm or reject this hypothesis, cerebrospinal fluid could be collected intrathecally and central circulating leptin levels could be measured. To further confirm this hypothesis radio-labelled leptin could be injected intravenously followed by the same measurements. If a decrease in central compared to systemic leptin circulation is observed one can positively conclude that leptin transport through the blood brain barrier is deficient in *foz/foz* mice. The next experiment would then be to test whether leptin injected directly into the brain (intracerebroventricularly) stimulates normal leptin signal transduction, and also whether this manoeuvre prevents the development of obesity in *foz/foz* mice.

7.4. Other pathways involved in obesity

In the present thesis on the pathogenesis of obesity in *foz/foz* mice, research was focused specifically on leptin and its potential functional defect(s) which could lead to leptin resistance. In 2006, when Arsov and colleagues characterised the *foz/foz* model, they showed that *foz/foz* mice have elevated blood glucose levels, leading to insulin resistance (Arsov *et al.*, 2006a). This suggests that central insulin resistance may also be at play in these animals. Furthermore, insulin has been shown to negatively regulate the control of feeding behaviour and energy homeostasis (Baskin *et al.*, 1999b), while obesity has been linked with insulin

resistance (Kahn and Flier, 2000; Kahn *et al.*, 2006). Similarly to leptin, insulin is secreted in proportion to fat mass (Polonsky *et al.*, 1988), and enters the brain, where it interacts with its receptor in the hypothalamus (Unger *et al.*, 1989). In addition, central administration of insulin has been shown to reduce feeding and body weight (Benoit *et al.*, 2002). More interestingly, insulin has also been shown to interact with similar pathways to leptin in the hypothalamus, including PI3K/Akt and ERK (Carvalheira *et al.*, 2003; Niswender *et al.*, 2003; Xu *et al.*, 2005a). Taken together, these observations suggest that insulin could be another potential mediator of obesity in *foz/foz* mice, and could therefore be another subject of research.

To date, ghrelin is the only peripheral endogenous orexigenic peptide which has been characterised. Numerous studies in humans and rodents have shown that intracerebroventricular or peripheral injections of ghrelin causes a dose-dependent increase in food intake (Tschop *et al.*, 2000; Kamegai *et al.*, 2001; Wren *et al.*, 2001a; Wren *et al.*, 2001b), while its expression has been shown to be increased in obese states (Ariyasu *et al.*, 2001; DelParigi *et al.*, 2002; Haqq *et al.*, 2003). To further support the idea that obesity in *foz/foz* mice could be multifactorial, ghrelin levels could be measured peripherally and centrally in these mice, depending on the results, further physiological studies could be considered. Specifically, if ghrelin levels are increased, further investigation in this model would be warranted.

7.5. Is energy expenditure modified in *foz/foz* mice?

Three main factors contribute to the aetiology of obesity: genetics factors, diet, and physical activity. In *foz/foz* mice, obesity has been shown to be related to a genetic defect, while high fat-feeding accelerates the development of obesity-related metabolic complications such as type 2 diabetes, fatty liver disease, and coronary artery disease. To assess whether the development of obesity in *foz/foz* mice could also be related to a decrease in energy expenditure metabolic studies are currently being conducted. Preliminary data indicate that *foz/foz* mice not only consume substantially more food than WT mice, their physical activity is drastically reduced (~60%) compared to control mice (unpublished data C. Larter, G. Farrell, C. Bruce and M. Febbraio). It would be interesting to see if the *foz/foz* mice phenotype can be reversed by knocking in Alms1. Further, strategies to encourage normal physical activity in young *foz/foz* mice are now underway, with the intent to clarify whether this prevents hyperleptinaemia, obesity and its complications.

7.6. Concluding remarks

In conclusion, the mouse model of Alström syndrome described in this thesis recapitulates the human syndrome. Although monogenic causes of obesity are rare, understanding their mechanisms provide valuable information that can be applied to more common polygenetic and environmental causes of obesity. This mouse model provides a powerful research tool to study Alms1, basal bodies and the integrity and function of neuronal primary cilia. The study of this model will also assist in the

identification and understanding of the complex networks that regulate food consumption, energy homeostasis and the development of metabolic diseases. Understanding the precise function and mechanisms associated with these once-forgotten organelles could lead to a major breakthrough for the development of new therapeutic approaches to target obesity and its related metabolic disorders, type 2 diabetes, atherogenic dyslipidaemia, metabolic syndrome and severe forms of fatty liver disease and common cancers whose incidence increases with obesity.

APPENDIX 1

Appendix 1

Homogenising buffer

	Concentration	Volume in ml (for 50 ml)
Hepes	50 mM	2.5
NaCl	150 mM	3.75
$MgCl_2$	1.5 mM	0.075
EGTA	1 mM	0.25
Glycerol	10%	6.25
Triton X-100	0.1%	5
dH_2O		32.17

4x Reducing buffer

Glycerol	25 ml
SDS	2 g
1M Tris pH 6.8	6.3 ml
Bromophenol blue	10 mg
dH_2O	To make 45 ml

For working reducing buffer dilute at 2.5X and add 167 µl DTT for 1.5 ml of 2.5X reducing buffer.

10X TBS pH 7.4

Tris	121.14 g
NaCl	175.32 g
dH_2O	To make 2 l

25% Tween-20

Tween 20	12.5 ml
dH_20	To make 50 ml

1x TBST

10X TBS	100 ml
25% Tween 20	2 ml
dH_2O	To make 1 l

Buffers for western blots

Running buffer

Tris	9 g
Glycine	43 g
SDS	0.75 g
dH_20	To make 750 ml

Store at RT _ Ready to use

Transfer buffer

Tris	3 g
Glycine	14.4 g
Methanol	200 ml
dH_20	To make 1 l

Store in cold room _ Ready to use

High molecular weight transfer buffer

Tris	3 g
Glycine	14.4 g
Methanol	100 ml
10 % SDS	0.5 ml
dH_20	To make 1 l

Store in cold room _ Ready to use

Western blots gels

Resolving gel

(two sides)	**10%**	**7.5%**	**5%**
30% Acrylamide	4.4 ml	3.3 ml	2.2 ml
3 M Tris pH 8.8	3.3 ml	3.3 ml	3.3 ml
10% SDS	250 µl	250 µl	250 µl
dH2O	5.3 ml	6.4 ml	7.5 ml

Set with 100 µl (10%APS) and 10 µl TEMED

Stacking gel (4%)

(two sides)	
30% Acrylamide	1.04 ml
1 M Tris pH 8.8	2.0 ml
10% SDS	160 µl
dH2O	4.88 ml

Set with 100 µl (10% APS) and 10 µl TEMED

Cell culture media

Dissection medium

	Stock concentration	Final concentration	Volume
EBSS or HBSS divalent free			50 ml
Dnase I	100 µg/ml	1 µg/ml	500 ul

Adjust pH to 7.4 and filter sterile.

Enzyme solution

	Stock concentration	Final concentration	Volume
EBSS or HBSS divalent free			50 ml
Papain		20 u/ml	
Dnase I	100 µg/ml	1 µg/ml	500 ul

Adjust pH to 7.4 and filter sterile.

Culture medium

	Stock concentration	**Final concentration**	**Volume**
Neurobasal A			274.5 ml
B-27			6 ml
GlutaMAX	100 X (200 mM)	0.25 mM	375 µl
L-Glutamine	100 X (200 mM)	0.25 mM	375 µl
Insulin	25 mg/ml	25 µg/ml	300 µl
Transferrin	100 mg/ml	100 µg/ml	300 µl
EGF	20 µg/ml	0.01 µg/ml	150 µl
Fetal bovine serum	100 %	5 %	15 ml
Penicillin/streptomycin	100 X	1 X	3 ml

Adjust pH to 7.4 and filter sterile.

REFERENCES

References

Adage, T., Scheurink, A.J., de Boer, S.F., de Vries, K., Konsman, J.P., Kuipers, F., Adan, R.A., Baskin, D.G., Schwartz, M.W., and van Dijk, G. (2001). Hypothalamic, metabolic, and behavioral responses to pharmacological inhibition of CNS melanocortin signaling in rats. Journal of Neuroscience *21*, 3639-3645.

Ahima, R.S., and Hileman, S.M. (2000). Postnatal regulation of hypothalamic neuropeptide expression by leptin: implications for energy balance and body weight regulation. Regulatory Peptides *92*, 1-7.

Akirav, E.M., Chan, O., Inouye, K., Riddell, M.C., Matthews, S.G., and Vranic, M. (2004). Partial leptin restoration increases hypothalamic-pituitary-adrenal activity while diminishing weight loss and hyperphagia in streptozotocin diabetic rats. Metabolism: Clinical and Experimental *53*, 1558-1564.

Alaiwi, W.A.A., Lo, S.T., and Mauli, S. (2009). Primary cilia: Highly sophisticated biological sensors. Sensors *9*, 7003-7020.

Alstrom, C.H., Hallgren, B., Nilsson, L.B., and Asander, H. (1959). Retinal degeneration combined with obesity, diabetes mellitus and neurogenous deafness: a specific syndrome (not hitherto described) distinct from the Laurence-Moon-Bardet-Biedl syndrome: a clinical, endocrinological and genetic examination based on a large pedigree. Acta Psychiatrica et Neurologica Scandinavica, Supplementum *129*, 1-35.

Andersen, J.S., Wilkinson, C.J., Mayor, T., Mortensen, P., Nigg, E.A., and Mann, M. (2003). Proteomic characterization of the human centrosome by protein correlation profiling. Nature *426*, 570-574.

Ansley, S.J., Badano, J.L., Blacque, O.E., Hill, J., Hoskins, B.E., Leitch, C.C., Kim, J.C., Ross, A.J., Eichers, E.R., Teslovich, T.M., Mah, A.K., Johnsen, R.C.,

Cavender, J.C., Lewis, R.A., Leroux, M.R., Beales, P.L., and Katsanis, N. (2003). Basal body dysfunction is a likely cause of pleiotropic Bardet-Biedl syndrome. Nature *425*, 628-633.

Aoki, M., Jiang, H., and Vogt, P.K. (2004). Proteasomal degradation of the FoxO1 transcriptional regulator in cells transformed by the P3k and Akt oncoproteins. Proceedings of the National Academy of Sciences of the United States of America *101*, 13613-13617.

Arase, K., York, D.A., Shimizu, H., Shargill, N., and Bray, G.A. (1988). Effects of corticotropin-releasing factor on food intake and brown adipose tissue thermogenesis in rats. American Journal of Physiology *255*, E255-259.

Arase, K., Shargill, N.S., and Bray, G.A. (1989). Effects of corticotropin releasing factor on genetically obese (fatty) rats. Physiology and Behavior *45*, 565-570.

Ariyasu, H., Takaya, K., Tagami, T., Ogawa, Y., Hosoda, K., Akamizu, T., Suda, M., Koh, T., Natsui, K., Toyooka, S., Shirakami, G., Usui, T., Shimatsu, A., Doi, K., Hosoda, H., Kojima, M., Kangawa, K., and Nakao, K. (2001). Stomach is a major source of circulating ghrelin, and feeding state determines plasma ghrelin-like immunoreactivity levels in humans. Journal of Clinical Endocrinology and Metabolism *86*, 4753-4758.

Arora, S., and Anubhuti (2006). Role of neuropeptides in appetite regulation and obesity--a review. Neuropeptides *40*, 375-401.

Arsov, T., Larter, C.Z., Nolan, C.J., Petrovsky, N., Goodnow, C.C., Teoh, N.C., Yeh, M.M., and Farrell, G.C. (2006a). Adaptive failure to high-fat diet characterizes steatohepatitis in Alms1 mutant mice. Biochemical and Biophysical Research Communications *342*, 1152-1159.

Arsov, T., Silva, D.G., O'Bryan, M.K., Sainsbury, A., Lee, N.J., Kennedy, C., Manji, S.S., Nelms, K., Liu, C., Vinuesa, C.G., de Kretser, D.M., Goodnow, C.C., and Petrovsky, N. (2006b). Fat aussie--a new Alstrom syndrome mouse showing a

critical role for ALMS1 in obesity, diabetes, and spermatogenesis. Molecular Endocrinology *20*, 1610-1622.

Bagdade, J.D., Bierman, E.L., and Porte, D., Jr. (1967). The significance of basal insulin levels in the evaluation of the insulin response to glucose in diabetic and nondiabetic subjects. Journal of Clinical Investigation *46*, 1549-1557.

Bailleul, B., Akerblom, I., and Strosberg, A.D. (1997). The leptin receptor promoter controls expression of a second distinct protein. Nucleic Acids Research *25*, 2752-2758.

Balthasar, N., Coppari, R., McMinn, J., Liu, S.M., Lee, C.E., Tang, V., Kenny, C.D., McGovern, R.A., Chua, S.C., Jr., Elmquist, J.K., and Lowell, B.B. (2004). Leptin receptor signaling in POMC neurons is required for normal body weight homeostasis. Neuron *42*, 983-991.

Baly, C., Aioun, J., Badonnel, K., Lacroix, M.C., Durieux, D., Schlegel, C., Salesse, R., and Caillol, M. (2007). Leptin and its receptors are present in the rat olfactory mucosa and modulated by the nutritional status. Brain Research *1129*, 130-141.

Banks, A.S., Davis, S.M., Bates, S.H., and Myers, M.G., Jr. (2000). Activation of downstream signals by the long form of the leptin receptor. Journal of Biological Chemistry *275*, 14563-14572.

Banks, W.A., Kastin, A.J., Huang, W., Jaspan, J.B., and Maness, L.M. (1996). Leptin enters the brain by a saturable system independent of insulin. Peptides *17*, 305-311.

Banks, W.A., DiPalma, C.R., and Farrell, C.L. (1999). Impaired transport of leptin across the blood-brain barrier in obesity. Peptides *20*, 1341-1345.

Banno, R., Zimmer, D., De Jonghe, B.C., Atienza, M., Rak, K., Yang, W., and Bence, K.K. (2010). PTP1B and SHP2 in POMC neurons reciprocally regulate energy balance in mice. Journal of Clinical Investigation *120*, 720-734.

Baskin, D.G., Seeley, R.J., Kuijper, J.L., Lok, S., Weigle, D.S., Erickson, J.C., Palmiter, R.D., and Schwartz, M.W. (1998). Increased expression of mRNA for the long form of the leptin receptor in the hypothalamus is associated with leptin hypersensitivity and fasting. Diabetes *47*, 538-543.

Baskin, D.G., Breininger, J.F., and Schwartz, M.W. (1999a). Leptin receptor mRNA identifies a subpopulation of neuropeptide Y neurons activated by fasting in rat hypothalamus. Diabetes *48*, 828-833.

Baskin, D.G., Figlewicz Lattemann, D., Seeley, R.J., Woods, S.C., Porte Jr, D., and Schwartz, M.W. (1999b). Insulin and leptin: dual adiposity signals to the brain for the regulation of food intake and body weight. Brain Research *848*, 114-123.

Baskin, D.G., Schwartz, M.W., Seeley, R.J., Woods, S.C., Porte, D., Jr., Breininger, J.F., Jonak, Z., Schaefer, J., Krouse, M., Burghardt, C., Campfield, L.A., Burn, P., and Kochan, J.P. (1999c). Leptin receptor long-form splice-variant protein expression in neuron cell bodies of the brain and co-localization with neuropeptide Y mRNA in the arcuate nucleus. Journal of Histochemistry and Cytochemistry *47*, 353-362.

Baumann, H., Morella, K.K., White, D.W., Dembski, M., Bailon, P.S., Kim, H., Lai, C.F., and Tartaglia, L.A. (1996). The full-length leptin receptor has signaling capabilities of interleukin 6-type cytokine receptors. Proceedings of the National Academy of Sciences of the United States of America *93*, 8374-8378.

Baura, G.D., Foster, D.M., Porte, D., Jr., Kahn, S.E., Bergman, R.N., Cobelli, C., and Schwartz, M.W. (1993). Saturable transport of insulin from plasma into the central nervous system of dogs in vivo. A mechanism for regulated insulin delivery to the brain. Journal of Clinical Investigation *92*, 1824-1830.

Bence, K.K., Delibegovic, M., Xue, B., Gorgun, C.Z., Hotamisligil, G.S., Neel, B.G., and Kahn, B.B. (2006). Neuronal PTP1B regulates body weight, adiposity and leptin action. Nature Medicine *12*, 917-924.

Benoit, S.C., Air, E.L., Coolen, L.M., Strauss, R., Jackman, A., Clegg, D.J., Seeley, R.J., and Woods, S.C. (2002). The catabolic action of insulin in the brain is mediated by melanocortins. Journal of Neuroscience *22*, 9048-9052.

Berbari, N.F., Johnson, A.D., Lewis, J.S., Askwith, C.C., and Mykytyn, K. (2008a). Identification of ciliary localization sequences within the third intracellular loop of G protein-coupled receptors. Molecular Biology of the Cell *19*, 1540-1547.

Berbari, N.F., Lewis, J.S., Bishop, G.A., Askwith, C.C., and Mykytyn, K. (2008b). Bardet-Biedl syndrome proteins are required for the localization of G protein-coupled receptors to primary cilia. Proceedings of the National Academy of Sciences of the United States of America *105*, 4242-4246.

Bisgrove, B.W., and Yost, H.J. (2006). The roles of cilia in developmental disorders and disease. Development *133*, 4131-4143.

Bishop, G.A., Berbari, N.F., Lewis, J., and Mykytyn, K. (2007). Type III adenylyl cyclase localizes to primary cilia throughout the adult mouse brain. Journal of Comparative Neurology *505*, 562-571.

Bjorbaek, C., Uotani, S., da Silva, B., and Flier, J.S. (1997). Divergent signaling capacities of the long and short isoforms of the leptin receptor. Journal of Biological Chemistry *272*, 32686-32695.

Bjorbaek, C., Elmquist, J.K., Frantz, J.D., Shoelson, S.E., and Flier, J.S. (1998). Identification of SOCS-3 as a potential mediator of central leptin resistance. Molecular Cell *1*, 619-625.

Bjorbaek, C., El-Haschimi, K., Frantz, J.D., and Flier, J.S. (1999). The role of SOCS-3 in leptin signaling and leptin resistance. Journal of Biological Chemistry *274*, 30059-30065.

Bjorbaek, C., Buchholz, R.M., Davis, S.M., Bates, S.H., Pierroz, D.D., Gu, H., Neel, B.G., Myers, M.G., Jr., and Flier, J.S. (2001). Divergent roles of SHP-2 in ERK activation by leptin receptors. Journal of Biological Chemistry *276*, 4747-4755.

Bjorbak, C., Lavery, H.J., Bates, S.H., Olson, R.K., Davis, S.M., Flier, J.S., and Myers, M.G., Jr. (2000). SOCS3 mediates feedback inhibition of the leptin receptor via Tyr985. Journal of Biological Chemistry *275*, 40649-40657.

Blacque, O.E., and Leroux, M.R. (2006). Bardet-Biedl syndrome: an emerging pathomechanism of intracellular transport. Cellular and Molecular Life Sciences *63*, 2145-2161.

Borowsky, B., Durkin, M.M., Ogozalek, K., Marzabadi, M.R., DeLeon, J., Lagu, B., Heurich, R., Lichtblau, H., Shaposhnik, Z., Daniewska, I., Blackburn, T.P., Branchek, T.A., Gerald, C., Vaysse, P.J., and Forray, C. (2002). Antidepressant, anxiolytic and anorectic effects of a melanin-concentrating hormone-1 receptor antagonist. Nature Medicine *8*, 825-830.

Bradley, R.L., Kokkotou, E.G., Maratos-Flier, E., and Cheatham, B. (2000). Melanin-concentrating hormone regulates leptin synthesis and secretion in rat adipocytes. Diabetes *49*, 1073-1077.

Briancon, N., McNay, D.E., Maratos-Flier, E., and Flier, J.S. (2010). Combined neural inactivation of suppressor of cytokine signaling-3 and protein-tyrosine phosphatase-1B reveals additive, synergistic, and factor-specific roles in the regulation of body energy balance. Diabetes *59*, 3074-3084.

Cardenas-Rodriguez, M., and Badano, J.L. (2009). Ciliary biology: understanding the cellular and genetic basis of human ciliopathies. American Journal of Medical Genetics Part C, Seminars in Medical Genetics *151C*, 263-280.

Carpenter, L.R., Farruggella, T.J., Symes, A., Karow, M.L., Yancopoulos, G.D., and Stahl, N. (1998). Enhancing leptin response by preventing SH2-containing

phosphatase 2 interaction with Ob receptor. Proceedings of the National Academy of Sciences of the United States of America *95*, 6061-6066.

Carvalheira, J., Ribeiro, E., Araujo, E., Guimaraes, R., Telles, M., Torsoni, M., Gontijo, J., Velloso, L., and Saad, M. (2003). Selective impairment of insulin signalling in the hypothalamus of obese Zucker rats. Diabetologia *46*, 1629-1640.

Castaneda, T.R., Jurgens, H., Wiedmer, P., Pfluger, P., Diano, S., Horvath, T.L., Tang-Christensen, M., and Tschop, M.H. (2005). Obesity and the neuroendocrine control of energy homeostasis: the role of spontaneous locomotor activity. Journal of Nutrition *135*, 1314-1319.

Chaudhri, O.B., Salem, V., Murphy, K.G., and Bloom, S.R. (2008). Gastrointestinal satiety signals. Annual Review of Physiology *70*, 239-255.

Cheng, A., Uetani, N., Simoncic, P.D., Chaubey, V.P., Lee-Loy, A., McGlade, C.J., Kennedy, B.P., and Tremblay, M.L. (2002). Attenuation of leptin action and regulation of obesity by protein tyrosine phosphatase 1B. Developmental Cell *2*, 497-503.

Cheung, C.C., Clifton, D.K., and Steiner, R.A. (1997). Proopiomelanocortin neurons are direct targets for leptin in the hypothalamus. Endocrinology *138*, 4489-4492.

Ciofi, P., Garret, M., Lapirot, O., Lafon, P., Loyens, A., Prevot, V., and Levine, J.E. (2009). Brain-endocrine interactions: a microvascular route in the mediobasal hypothalamus. Endocrinology *150*, 5509-5519.

Clement, K., Vaisse, C., Lahlou, N., Cabrol, S., Pelloux, V., Cassuto, D., Gourmelen, M., Dina, C., Chambaz, J., Lacorte, J.M., Basdevant, A., Bougneres, P., Lebouc, Y., Froguel, P., and Guy-Grand, B. (1998). A mutation in the human leptin receptor gene causes obesity and pituitary dysfunction. Nature *392*, 398-401.

Cole, D.G., Chinn, S.W., Wedaman, K.P., Hall, K., Vuong, T., and Scholey, J.M. (1993). Novel heterotrimeric kinesin-related protein purified from sea urchin eggs. Nature *366*, 268-270.

Coleman, D.L., and Hummel, K.P. (1969). Effects of parabiosis of normal with genetically diabetic mice. American Journal of Physiology *217*, 1298-1304.

Coleman, D.L. (1973). Effects of parabiosis of obese with diabetes and normal mice. Diabetologia *9*, 294-298.

Coleman, D.L. (1978). Obese and diabetes: two mutant genes causing diabetes-obesity syndromes in mice. Diabetologia *14*, 141-148.

Collin, G.B., Marshall, J.D., Ikeda, A., So, W.V., Russell-Eggitt, I., Maffei, P., Beck, S., Boerkoel, C.F., Sicolo, N., Martin, M., Nishina, P.M., and Naggert, J.K. (2002). Mutations in ALMS1 cause obesity, type 2 diabetes and neurosensory degeneration in Alstrom syndrome. Nature Genetics *31*, 74-78.

Collin, G.B., Cyr, E., Bronson, R., Marshall, J.D., Gifford, E.J., Hicks, W., Murray, S.A., Zheng, Q.Y., Smith, R.S., Nishina, P.M., and Naggert, J.K. (2005). Alms1-disrupted mice recapitulate human Alstrom syndrome. Human Molecular Genetics *14*, 2323-2333.

Considine, R.V., Sinha, M.K., Heiman, M.L., Kriauciunas, A., Stephens, T.W., Nyce, M.R., Ohannesian, J.P., Marco, C.C., McKee, L.J., Bauer, T.L., and et al. (1996). Serum immunoreactive-leptin concentrations in normal-weight and obese humans. New England Journal of Medicine *334*, 292-295.

Couturier, C., Sarkis, C., Seron, K., Belouzard, S., Chen, P., Lenain, A., Corset, L., Dam, J., Vauthier, V., Dubart, A., Mallet, J., Froguel, P., Rouille, Y., and Jockers, R. (2007). Silencing of OB-RGRP in mouse hypothalamic arcuate nucleus increases leptin receptor signaling and prevents diet-induced obesity. Proceedings of the National Academy of Sciences of the United States of America *104*, 19476-19481.

Dahl, H.A. (1963). Fine structure of cilia in rat cerebral cortex. Zeitschrift fuer Zellforschung und Mikroskopische Anatomie *60*, 369-386.

Davenport, J.R., Watts, A.J., Roper, V.C., Croyle, M.J., van Groen, T., Wyss, J.M., Nagy, T.R., Kesterson, R.A., and Yoder, B.K. (2007). Disruption of intraflagellar transport in adult mice leads to obesity and slow-onset cystic kidney disease. Current Biology *17*, 1586-1594.

DelParigi, A., Tschop, M., Heiman, M.L., Salbe, A.D., Vozarova, B., Sell, S.M., Bunt, J.C., and Tataranni, P.A. (2002). High circulating ghrelin: a potential cause for hyperphagia and obesity in prader-willi syndrome. Journal of Clinical Endocrinology and Metabolism *87*, 5461-5464.

Dobkin-Bekman, M., Naidich, M., Pawson, A.J., Millar, R.P., Seger, R., and Naor, Z. (2006). Activation of mitogen-activated protein kinase (MAPK) by GnRH is cell-context dependent. Molecular and Cellular Endocrinology *252*, 184-190.

Doetsch, F., Caille, I., Lim, D.A., Garcia-Verdugo, J.M., and Alvarez-Buylla, A. (1999). Subventricular zone astrocytes are neural stem cells in the adult mammalian brain. Cell *97*, 703-716.

Dunn, S.L., Bjornholm, M., Bates, S.H., Chen, Z., Seifert, M., and Myers, M.G., Jr. (2005). Feedback inhibition of leptin receptor/Jak2 signaling via Tyr1138 of the leptin receptor and suppressor of cytokine signaling 3. Molecular Endocrinology *19*, 925-938.

Ebihara, K., Ogawa, Y., Katsuura, G., Numata, Y., Masuzaki, H., Satoh, N., Tamaki, M., Yoshioka, T., Hayase, M., Matsuoka, N., Aizawa-Abe, M., Yoshimasa, Y., and Nakao, K. (1999). Involvement of agouti-related protein, an endogenous antagonist of hypothalamic melanocortin receptor, in leptin action. Diabetes *48*, 2028-2033.

Edwards, J.A., Sethi, P.K., Scoma, A.J., Bannerman, R.M., and Frohman, L.A. (1976). A new familial syndrome characterized by pigmentary retinopathy,

hypogonadism, mental retardation, nerve deafness and glucose intolerance. American Journal of Medicine *60*, 23-32.

Elias, C.F., Aschkenasi, C., Lee, C., Kelly, J., Ahima, R.S., Bjorbaek, C., Flier, J.S., Saper, C.B., and Elmquist, J.K. (1999). Leptin differentially regulates NPY and POMC neurons projecting to the lateral hypothalamic area. Neuron *23*, 775-786.

Elmquist, J.K., Ahima, R.S., Elias, C.F., Flier, J.S., and Saper, C.B. (1998a). Leptin activates distinct projections from the dorsomedial and ventromedial hypothalamic nuclei. Proceedings of the National Academy of Sciences of the United States of America *95*, 741-746.

Elmquist, J.K., Bjorbaek, C., Ahima, R.S., Flier, J.S., and Saper, C.B. (1998b). Distributions of leptin receptor mRNA isoforms in the rat brain. Journal of Comparative Neurology *395*, 535-547.

Franklin, K.B.J., and Paxinos, G. (2008). The mouse brain in stereotaxic coordinates, 3rd edn (Amsterdam, Elsevier)

Gerdes, J.M., Davis, E.E., and Katsanis, N. (2009). The vertebrate primary cilium in development, homeostasis, and disease. Cell *137*, 32-45.

Ghilardi, N., and Skoda, R.C. (1997). The leptin receptor activates janus kinase 2 and signals for proliferation in a factor-dependent cell line. Molecular Endocrinology *11*, 393-399.

Gibson, W.T., Farooqi, I.S., Moreau, M., DePaoli, A.M., Lawrence, E., O'Rahilly, S., and Trussell, R.A. (2004). Congenital leptin deficiency due to homozygosity for the Delta133G mutation: report of another case and evaluation of response to four years of leptin therapy. Journal of Clinical Endocrinology and Metabolism *89*, 4821-4826.

Girard, D., and Petrovsky, N. (2011). Alstrom syndrome: insights into the pathogenesis of metabolic disorders. Nature Reviews Endocrinology *7*, 77-88.

Goetz, S.C., and Anderson, K.V. (2010). The primary cilium: a signalling centre during vertebrate development. Nature Reviews Genetics *11*, 331-344.

Goldstein, J.L., and Fialkow, P.J. (1973). The Alstrom syndrome. Report of three cases with further delineation of the clinical, pathophysiological, and genetic aspects of the disorder. Medicine *52*, 53-71.

Gong, L., Yao, F., Hockman, K., Heng, H.H., Morton, G.J., Takeda, K., Akira, S., Low, M.J., Rubinstein, M., and MacKenzie, R.G. (2008). Signal transducer and activator of transcription-3 is required in hypothalamic agouti-related protein/neuropeptide Y neurons for normal energy homeostasis. Endocrinology *149*, 3346-3354.

Gong, Y., Ishida-Takahashi, R., Villanueva, E.C., Fingar, D.C., Munzberg, H., and Myers, M.G., Jr. (2007). The long form of the leptin receptor regulates STAT5 and ribosomal protein S6 via alternate mechanisms. Journal of Biological Chemistry *282*, 31019-31027.

Graser, S., Stierhof, Y.D., Lavoie, S.B., Gassner, O.S., Lamla, S., Le Clech, M., and Nigg, E.A. (2007). Cep164, a novel centriole appendage protein required for primary cilium formation. Journal of Cell Biology *179*, 321-330.

Hahn, T.M., Breininger, J.F., Baskin, D.G., and Schwartz, M.W. (1998). Coexpression of Agrp and NPY in fasting-activated hypothalamic neurons. Nature Neuroscience *1*, 271-272.

Halaas, J.L., Gajiwala, K.S., Maffei, M., Cohen, S.L., Chait, B.T., Rabinowitz, D., Lallone, R.L., Burley, S.K., and Friedman, J.M. (1995). Weight-reducing effects of the plasma protein encoded by the obese gene. Science *269*, 543-546.

Hanaki, K., Becker, D.J., and Arslanian, S.A. (1999). Leptin before and after insulin therapy in children with new-onset type 1 diabetes. Journal of Clinical Endocrinology and Metabolism *84*, 1524-1526.

Handel, M., Schulz, S., Stanarius, A., Schreff, M., Erdtmann-Vourliotis, M., Schmidt, H., Wolf, G., and Hollt, V. (1999). Selective targeting of somatostatin receptor 3 to neuronal cilia. Neuroscience *89*, 909-926.

Hansen, M.J., Ball, M.J., and Morris, M.J. (2001). Enhanced inhibitory feeding response to alpha-melanocyte stimulating hormone in the diet-induced obese rat. Brain Research *892*, 130-137.

Haqq, A.M., Farooqi, I.S., O'Rahilly, S., Stadler, D.D., Rosenfeld, R.G., Pratt, K.L., LaFranchi, S.H., and Purnell, J.Q. (2003). Serum ghrelin levels are inversely correlated with body mass index, age, and insulin concentrations in normal children and are markedly increased in Prader-Willi syndrome. Journal of Clinical Endocrinology and Metabolism *88*, 174-178.

Harrold, J.A., Williams, G., and Widdowson, P.S. (1999). Changes in hypothalamic agouti-related protein (AGRP), but not alpha-MSH or pro-opiomelanocortin concentrations in dietary-obese and food-restricted rats. Biochemical and Biophysical Research Communications *258*, 574-577.

Haskell-Luevano, C., Chen, P., Li, C., Chang, K., Smith, M.S., Cameron, J.L., and Cone, R.D. (1999). Characterization of the neuroanatomical distribution of agouti-related protein immunoreactivity in the rhesus monkey and the rat. Endocrinology *140*, 1408-1415.

Haskell-Luevano, C., and Monck, E.K. (2001). Agouti-related protein functions as an inverse agonist at a constitutively active brain melanocortin-4 receptor. Regulatory Peptides *99*, 1-7.

Hauger, R.L., Risbrough, V., Oakley, R.H., Olivares-Reyes, J.A., and Dautzenberg, F.M. (2009). Role of CRF receptor signaling in stress vulnerability, anxiety, and depression. Annals of the New York Academy of Sciences *1179*, 120-143.

Hearn, T., Renforth, G.L., Spalluto, C., Hanley, N.A., Piper, K., Brickwood, S., White, C., Connolly, V., Taylor, J.F., Russell-Eggitt, I., Bonneau, D., Walker, M., and

Wilson, D.I. (2002). Mutation of ALMS1, a large gene with a tandem repeat encoding 47 amino acids, causes Alstrom syndrome. Nature Genetics *31*, 79-83.

Hearn, T., Spalluto, C., Phillips, V.J., Renforth, G.L., Copin, N., Hanley, N.A., and Wilson, D.I. (2005). Subcellular localization of ALMS1 supports involvement of centrosome and basal body dysfunction in the pathogenesis of obesity, insulin resistance, and type 2 diabetes. Diabetes *54*, 1581-1587.

Heinrich, P.C., Behrmann, I., Muller-Newen, G., Schaper, F., and Graeve, L. (1998). Interleukin-6-type cytokine signalling through the gp130/Jak/STAT pathway. Biochemical Journal *334 (Pt 2)*, 297-314.

Hildebrandt, F., Benzing, T., and Katsanis, N. (2011). Ciliopathies. New England Journal of Medicine *364*, 1533-1543.

Howard, J.K., Cave, B.J., Oksanen, L.J., Tzameli, I., Bjorbaek, C., and Flier, J.S. (2004). Enhanced leptin sensitivity and attenuation of diet-induced obesity in mice with haploinsufficiency of Socs3. Nature Medicine *10*, 734-738.

Huang, X.F., Han, M., South, T., and Storlien, L. (2003a). Altered levels of POMC, AgRP and MC4-R mRNA expression in the hypothalamus and other parts of the limbic system of mice prone or resistant to chronic high-energy diet-induced obesity. Brain Research *992*, 9-19.

Huang, X.F., Han, M., and Storlien, L.H. (2003b). The level of NPY receptor mRNA expression in diet-induced obese and resistant mice. Brain Research Molecular Brain Research *115*, 21-28.

Huda, M.S., Wilding, J.P., and Pinkney, J.H. (2006). Gut peptides and the regulation of appetite. Obesity Reviews *7*, 163-182.

Ingalls, A.M., Dickie, M.M., and Snell, G.D. (1950). Obese, a new mutation in the house mouse. Journal of Heredity *41*, 317-318.

Ishikawa, H., Kubo, A., and Tsukita, S. (2005). Odf2-deficient mother centrioles lack distal/subdistal appendages and the ability to generate primary cilia. Nature Cell Biology *7*, 517-524.

Jagger, D., Collin, G., Kelly, J., Towers, E., Nevill, G., Longo-Guess, C., Benson, J., Halsey, K., Dolan, D., Marshall, J., Naggert, J., and Forge, A. (2011). Alstrom Syndrome protein ALMS1 localizes to basal bodies of cochlear hair cells and regulates cilium-dependent planar cell polarity. Human Molecular Genetics *20*, 466-481.

Kahn, B.B., and Flier, J.S. (2000). Obesity and insulin resistance. Journal of Clinical Investigation *106*, 473-481.

Kahn, S.E., Hull, R.L., and Utzschneider, K.M. (2006). Mechanisms linking obesity to insulin resistance and type 2 diabetes. Nature *444*, 840-846.

Kamegai, J., Tamura, H., Shimizu, T., Ishii, S., Sugihara, H., and Wakabayashi, I. (2001). Chronic central infusion of ghrelin increases hypothalamic neuropeptide Y and Agouti-related protein mRNA levels and body weight in rats. Diabetes *50*, 2438-2443.

Kaszubska, W., Falls, H.D., Schaefer, V.G., Haasch, D., Frost, L., Hessler, P., Kroeger, P.E., White, D.W., Jirousek, M.R., and Trevillyan, J.M. (2002). Protein tyrosine phosphatase 1B negatively regulates leptin signaling in a hypothalamic cell line. Molecular and Cellular Endocrinology *195*, 109-118.

Kennedy, G.C. (1950). The hypothalamic control of food intake in rats. Proceedings of the Royal Society B: Biological Sciences *137*, 535-549.

Kim, M.S., Pak, Y.K., Jang, P.G., Namkoong, C., Choi, Y.S., Won, J.C., Kim, K.S., Kim, S.W., Kim, H.S., Park, J.Y., Kim, Y.B., and Lee, K.U. (2006). Role of hypothalamic Foxo1 in the regulation of food intake and energy homeostasis. Nature Neuroscience *9*, 901-906.

Kitamura, T., Feng, Y., Kitamura, Y.I., Chua, S.C., Jr., Xu, A.W., Barsh, G.S., Rossetti, L., and Accili, D. (2006). Forkhead protein FoxO1 mediates Agrp-dependent effects of leptin on food intake. Nature Medicine *12*, 534-540.

Klaman, L.D., Boss, O., Peroni, O.D., Kim, J.K., Martino, J.L., Zabolotny, J.M., Moghal, N., Lubkin, M., Kim, Y.B., Sharpe, A.H., Stricker-Krongrad, A., Shulman, G.I., Neel, B.G., and Kahn, B.B. (2000). Increased energy expenditure, decreased adiposity, and tissue-specific insulin sensitivity in protein-tyrosine phosphatase 1B-deficient mice. Molecular and Cellular Biology *20*, 5479-5489.

Knorz, V.J., Spalluto, C., Lessard, M., Purvis, T.L., Adigun, F.F., Collin, G.B., Hanley, N.A., Wilson, D.I., and Hearn, T. (2010). Centriolar association of ALMS1 and likely centrosomal functions of the ALMS motif-containing proteins C10orf90 and KIAA1731. Molecular Biology of the Cell *21*, 3617-3629.

Krisch, B., and Leonhardt, H. (1978). The functional and structural border of the neurohemal region of the median eminence. Cell and Tissue Research *192*, 327-339.

Kristensen, P., Judge, M.E., Thim, L., Ribel, U., Christjansen, K.N., Wulff, B.S., Clausen, J.T., Jensen, P.B., Madsen, O.D., Vrang, N., Larsen, P.J., and Hastrup, S. (1998). Hypothalamic CART is a new anorectic peptide regulated by leptin. Nature *393*, 72-76.

Lantz, K.A., Hart, S.G., Planey, S.L., Roitman, M.F., Ruiz-White, I.A., Wolfe, H.R., and McLane, M.P. (2010). Inhibition of PTP1B by trodusquemine (MSI-1436) causes fat-specific weight loss in diet-induced obese mice. Obesity (Silver Spring) *18*, 1516-1523.

Larter, C.Z., Yeh, M.M., Van Rooyen, D.M., Teoh, N.C., Brooling, J., Hou, J.Y., Williams, J., Clyne, M., Nolan, C.J., and Farrell, G.C. (2009). Roles of adipose restriction and metabolic factors in progression of steatosis to steatohepatitis in obese, diabetic mice. Journal of Gastroenterology and Hepatology *24*, 1658-1668.

Lee, G.H., Proenca, R., Montez, J.M., Carroll, K.M., Darvishzadeh, J.G., Lee, J.I., and Friedman, J.M. (1996). Abnormal splicing of the leptin receptor in diabetic mice. Nature *379*, 632-635.

Levine, A.S., Rogers, B., Kneip, J., Grace, M., and Morley, J.E. (1983). Effect of centrally administered corticotropin releasing factor (CRF) on multiple feeding paradigms. Neuropharmacology *22*, 337-339.

Li, C., and Friedman, J.M. (1999). Leptin receptor activation of SH2 domain containing protein tyrosine phosphatase 2 modulates Ob receptor signal transduction. Proceedings of the National Academy of Sciences of the United States of America *96*, 9677-9682.

Li, G., Vega, R., Nelms, K., Gekakis, N., Goodnow, C., McNamara, P., Wu, H., Hong, N.A., and Glynne, R. (2007a). A role for Alstrom syndrome protein, alms1, in kidney ciliogenesis and cellular quiescence. PLoS Genetics *3*, e8.

Li, M., Ren, D., Iseki, M., Takaki, S., and Rui, L. (2006). Differential role of SH2-B and APS in regulating energy and glucose homeostasis. Endocrinology *147*, 2163-2170.

Li, Z., Zhou, Y., Carter-Su, C., Myers, M.G., Jr., and Rui, L. (2007b). SH2B1 enhances leptin signaling by both Janus kinase 2 Tyr813 phosphorylation-dependent and -independent mechanisms. Molecular Endocrinology *21*, 2270-2281.

Lin, S., and Huang, X.F. (1997). Fasting increases leptin receptor mRNA expression in lean but not obese (ob/ob) mouse brain. Neuroreport *8*, 3625-3629.

Lin, S., Storlien, L.H., and Huang, X.F. (2000). Leptin receptor, NPY, POMC mRNA expression in the diet-induced obese mouse brain. Brain Research *875*, 89-95.

Liu, Z.J., Bian, J., Zhao, Y.L., Zhang, X., Zou, N., and Li, D. (2011). Lentiviral vector-mediated knockdown of SOCS3 in the hypothalamus protects against the development of diet-induced obesity in rats. Diabetes, Obesity and Metabolism.

Louvi, A., and Grove, E.A. (2011). Cilia in the CNS: the quiet organelle claims center stage. Neuron *69*, 1046-1060.

Ludwig, D.S., Mountjoy, K.G., Tatro, J.B., Gillette, J.A., Frederich, R.C., Flier, J.S., and Maratos-Flier, E. (1998). Melanin-concentrating hormone: a functional melanocortin antagonist in the hypothalamus. American Journal of Physiology *274*, E627-633.

Lund, I.K., Hansen, J.A., Andersen, H.S., Moller, N.P., and Billestrup, N. (2005). Mechanism of protein tyrosine phosphatase 1B-mediated inhibition of leptin signalling. Journal of Molecular Endocrinology *34*, 339-351.

Maehama, T., and Dixon, J.E. (1998). The tumor suppressor, PTEN/MMAC1, dephosphorylates the lipid second messenger, phosphatidylinositol 3,4,5-trisphosphate. Journal of Biological Chemistry *273*, 13375-13378.

Maehama, T., and Dixon, J.E. (1999). PTEN: a tumour suppressor that functions as a phospholipid phosphatase. Trends in Cell Biology *9*, 125-128.

Maffei, M., Halaas, J., Ravussin, E., Pratley, R.E., Lee, G.H., Zhang, Y., Fei, H., Kim, S., Lallone, R., Ranganathan, S., and et al. (1995). Leptin levels in human and rodent: measurement of plasma leptin and ob RNA in obese and weight-reduced subjects. Nature Medicine *1*, 1155-1161.

Marks, J.L., Porte, D., Jr., Stahl, W.L., and Baskin, D.G. (1990). Localization of insulin receptor mRNA in rat brain by in situ hybridization. Endocrinology *127*, 3234-3236.

Marshall, J.D., Ludman, M.D., Shea, S.E., Salisbury, S.R., Willi, S.M., LaRoche, R.G., and Nishina, P.M. (1997). Genealogy, natural history, and phenotype of Alstrom syndrome in a large Acadian kindred and three additional families. American Journal of Medical Genetics *73*, 150-161.

Marshall, J.D., Bronson, R.T., Collin, G.B., Nordstrom, A.D., Maffei, P., Paisey, R.B., Carey, C., Macdermott, S., Russell-Eggitt, I., Shea, S.E., Davis, J., Beck, S., Shatirishvili, G., Mihai, C.M., Hoeltzenbein, M., Pozzan, G.B., Hopkinson, I., Sicolo, N., Naggert, J.K., and Nishina, P.M. (2005). New Alstrom syndrome phenotypes based on the evaluation of 182 cases. Archives of Internal Medicine *165*, 675-683.

Matsuzaki, H., Daitoku, H., Hatta, M., Tanaka, K., and Fukamizu, A. (2003). Insulin-induced phosphorylation of FKHR (Foxo1) targets to proteasomal degradation. Proceedings of the National Academy of Sciences of the United States of America *100*, 11285-11290.

McCowen, K.C., Chow, J.C., and Smith, R.J. (1998). Leptin signaling in the hypothalamus of normal rats in vivo. Endocrinology *139*, 4442.

Mercer, J.G., Hoggard, N., Williams, L.M., Lawrence, C.B., Hannah, L.T., and Trayhurn, P. (1996). Localization of leptin receptor mRNA and the long form splice variant (Ob-Rb) in mouse hypothalamus and adjacent brain regions by in situ hybridization. FEBS Letters *387*, 113-116.

Mercer, J.G., Moar, K.M., Hoggard, N., Strosberg, A.D., Froguel, P., and Bailleul, B. (2000). B219/OB-R 5'-UTR and leptin receptor gene-related protein gene expression in mouse brain and placenta: tissue-specific leptin receptor promoter activity. Journal of Neuroendocrinology *12*, 649-655.

Michaud, J.L., Heon, E., Guilbert, F., Weill, J., Puech, B., Benson, L., Smallhorn, J.F., Shuman, C.T., Buncic, J.R., Levin, A.V., Weksberg, R., and Breviere, G.M. (1996). Natural history of Alstrom syndrome in early childhood: onset with dilated cardiomyopathy. Journal of Pediatrics *128*, 225-229.

Mirshamsi, S., Laidlaw, H.A., Ning, K., Anderson, E., Burgess, L.A., Gray, A., Sutherland, C., and Ashford, M.L. (2004). Leptin and insulin stimulation of signalling pathways in arcuate nucleus neurones: PI3K dependent actin reorganization and KATP channel activation. BMC Neuroscience *5*, 54.

Mitchell, K.A., Gallagher, B.C., Szabo, G., and Otero Ade, S. (2004). NDP kinase moves into developing primary cilia. Cell Motility and the Cytoskeleton *59*, 62-73.

Mitchell, K.A., Szabo, G., and Otero Ade, S. (2009). Methods for the isolation of sensory and primary cilia--an overview. Methods in Cell Biology *94*, 87-101.

Mizuno, T.M., Kleopoulos, S.P., Bergen, H.T., Roberts, J.L., Priest, C.A., and Mobbs, C.V. (1998). Hypothalamic pro-opiomelanocortin mRNA is reduced by fasting and [corrected] in ob/ob and db/db mice, but is stimulated by leptin. Diabetes *47*, 294-297.

Montague, C.T., Farooqi, I.S., Whitehead, J.P., Soos, M.A., Rau, H., Wareham, N.J., Sewter, C.P., Digby, J.E., Mohammed, S.N., Hurst, J.A., Cheetham, C.H., Earley, A.R., Barnett, A.H., Prins, J.B., and O'Rahilly, S. (1997). Congenital leptin deficiency is associated with severe early-onset obesity in humans. Nature *387*, 903-908.

Moore, S.J., Green, J.S., Fan, Y., Bhogal, A.K., Dicks, E., Fernandez, B.A., Stefanelli, M., Murphy, C., Cramer, B.C., Dean, J.C., Beales, P.L., Katsanis, N., Bassett, A.S., Davidson, W.S., and Parfrey, P.S. (2005). Clinical and genetic epidemiology of Bardet-Biedl syndrome in Newfoundland: a 22-year prospective, population-based, cohort study. American Journal of Medical Genetics Part A *132*, 352-360.

Mori, H., Hanada, R., Hanada, T., Aki, D., Mashima, R., Nishinakamura, H., Torisu, T., Chien, K.R., Yasukawa, H., and Yoshimura, A. (2004). Socs3 deficiency in the brain elevates leptin sensitivity and confers resistance to diet-induced obesity. Nature Medicine *10*, 739-743.

Morris, D.L., Cho, K.W., and Rui, L. (2010). Critical role of the Src homology 2 (SH2) domain of neuronal SH2B1 in the regulation of body weight and glucose homeostasis in mice. Endocrinology *151*, 3643-3651.

Morrison, C.D., White, C.L., Wang, Z., Lee, S.Y., Lawrence, D.S., Cefalu, W.T., Zhang, Z.Y., and Gettys, T.W. (2007). Increased hypothalamic protein tyrosine phosphatase 1B contributes to leptin resistance with age. Endocrinology *148*, 433-440.

Munzberg, H., Huo, L., Nillni, E.A., Hollenberg, A.N., and Bjorbaek, C. (2003). Role of signal transducer and activator of transcription 3 in regulation of hypothalamic proopiomelanocortin gene expression by leptin. Endocrinology *144*, 2121-2131.

Myers, M.P., Andersen, J.N., Cheng, A., Tremblay, M.L., Horvath, C.M., Parisien, J.P., Salmeen, A., Barford, D., and Tonks, N.K. (2001). TYK2 and JAK2 are substrates of protein-tyrosine phosphatase 1B. Journal of Biological Chemistry *276*, 47771-47774.

Nachury, M.V., Loktev, A.V., Zhang, Q., Westlake, C.J., Peranen, J., Merdes, A., Slusarski, D.C., Scheller, R.H., Bazan, J.F., Sheffield, V.C., and Jackson, P.K. (2007). A core complex of BBS proteins cooperates with the GTPase Rab8 to promote ciliary membrane biogenesis. Cell *129*, 1201-1213.

Nachury, M.V. (2008). Tandem affinity purification of the BBSome, a critical regulator of Rab8 in ciliogenesis. Methods in Enzymology *439*, 501-513.

Nakashima, K., Narazaki, M., and Taga, T. (1997). Leptin receptor (OB-R) oligomerizes with itself but not with its closely related cytokine signal transducer gp130. FEBS Letters *403*, 79-82.

Nakazato, M., Murakami, N., Date, Y., Kojima, M., Matsuo, H., Kangawa, K., and Matsukura, S. (2001). A role for ghrelin in the central regulation of feeding. Nature *409*, 194-198.

Nauli, S.M., Alenghat, F.J., Luo, Y., Williams, E., Vassilev, P., Li, X., Elia, A.E., Lu, W., Brown, E.M., Quinn, S.J., Ingber, D.E., and Zhou, J. (2003). Polycystins 1 and 2 mediate mechanosensation in the primary cilium of kidney cells. Nature Genetics *33*, 129-137.

Nijenhuis, W.A., Oosterom, J., and Adan, R.A. (2001). AgRP(83-132) acts as an inverse agonist on the human-melanocortin-4 receptor. Molecular Endocrinology *15*, 164-171.

Ning, K., Miller, L.C., Laidlaw, H.A., Burgess, L.A., Perera, N.M., Downes, C.P., Leslie, N.R., and Ashford, M.L. (2006). A novel leptin signalling pathway via PTEN inhibition in hypothalamic cell lines and pancreatic beta-cells. EMBO Journal *25*, 2377-2387.

Ning, K., Miller, L.C., Laidlaw, H.A., Watterson, K.R., Gallagher, J., Sutherland, C., and Ashford, M.L. (2009). Leptin-dependent phosphorylation of PTEN mediates actin restructuring and activation of ATP-sensitive K+ channels. Journal of Biological Chemistry *284*, 9331-9340.

Nishimura, D.Y., Fath, M., Mullins, R.F., Searby, C., Andrews, M., Davis, R., Andorf, J.L., Mykytyn, K., Swiderski, R.E., Yang, B., Carmi, R., Stone, E.M., and Sheffield, V.C. (2004). Bbs2-null mice have neurosensory deficits, a defect in social dominance, and retinopathy associated with mislocalization of rhodopsin. Proceedings of the National Academy of Sciences of the United States of America *101*, 16588-16593.

Niswender, K.D., Morton, G.J., Stearns, W.H., Rhodes, C.J., Myers, M.G., Jr., and Schwartz, M.W. (2001). Intracellular signalling. Key enzyme in leptin-induced anorexia. Nature *413*, 794-795.

Niswender, K.D., Morrison, C.D., Clegg, D.J., Olson, R., Baskin, D.G., Myers, M.G., Seeley, R.J., and Schwartz, M.W. (2003). Insulin activation of phosphatidylinositol 3-kinase in the hypothalamic arcuate nucleus. Diabetes *52*, 227.

Niswender, K.D., and Schwartz, M.W. (2003). Insulin and leptin revisited: adiposity signals with overlapping physiological and intracellular signaling capabilities. Frontiers in Neuroendocrinology *24*, 1-10.

Niswender, K.D., Baskin, D.G., and Schwartz, M.W. (2004). Insulin and its evolving partnership with leptin in the hypothalamic control of energy homeostasis. Trends Endocrinol Metab *15*, 362-369.

Nordman, S., Abulaiti, A., Hilding, A., Langberg, E.C., Humphreys, K., Ostenson, C.G., Efendic, S., and Gu, H.F. (2008). Genetic variation of the adenylyl cyclase 3 (AC3) locus and its influence on type 2 diabetes and obesity susceptibility in Swedish men. International Journal of Obesity *32*, 407-412.

Ogden, C.L., Yanovski, S.Z., Carroll, M.D., and Flegal, K.M. (2007). The epidemiology of obesity. Gastroenterology *132*, 2087-2102.

Ollmann, M.M., Wilson, B.D., Yang, Y.K., Kerns, J.A., Chen, Y., Gantz, I., and Barsh, G.S. (1997). Antagonism of central melanocortin receptors in vitro and in vivo by agouti-related protein. Science *278*, 135-138.

Olney, J.W. (1969). Brain lesions, obesity, and other disturbances in mice treated with monosodium glutamate. Science *164*, 719-721.

Olsen, B. (2005). Nearly all cells in vertebrates and many cells in invertebrates contain primary cilia. Matrix Biology *24*, 449-450.

Paez, J., and Sellers, W.R. (2003). PI3K/PTEN/AKT pathway. A critical mediator of oncogenic signaling. Cancer Treatment and Research *115*, 145-167.

Pan, J., Wang, Q., and Snell, W.J. (2005). Cilium-generated signaling and cilia-related disorders. Laboratory Investigation *85*, 452-463.

Pazour, G.J., Wilkerson, C.G., and Witman, G.B. (1998). A dynein light chain is essential for the retrograde particle movement of intraflagellar transport (IFT). Journal of Cell Biology *141*, 979-992.

Pazour, G.J., and Witman, G.B. (2003). The vertebrate primary cilium is a sensory organelle. Current Opinion in Cell Biology *15*, 105-110.

Pedersen, L.B., Veland, I.R., Schroder, J.M., and Christensen, S.T. (2008). Assembly of primary cilia. Developmental Dynamics *237*, 1993-2006.

Peiser, C., McGregor, G.P., and Lang, R.E. (2000). Leptin receptor expression and suppressor of cytokine signaling transcript levels in high-fat-fed rats. Life Sciences *67*, 2971-2981.

Pelleymounter, M.A., Cullen, M.J., Baker, M.B., Hecht, R., Winters, D., Boone, T., and Collins, F. (1995). Effects of the obese gene product on body weight regulation in ob/ob mice. Science *269*, 540-543.

Polonsky, K.S., Given, B.D., and Van Cauter, E. (1988). Twenty-four-hour profiles and pulsatile patterns of insulin secretion in normal and obese subjects. Journal of Clinical Investigation *81*, 442-448.

Purvis, T.L., Hearn, T., Spalluto, C., Knorz, V.J., Hanley, K.P., Sanchez-Elsner, T., Hanley, N.A., and Wilson, D.I. (2010). Transcriptional regulation of the Alstrom syndrome gene ALMS1 by members of the RFX family and Sp1. Gene *460*, 20-29.

Qu, D., Ludwig, D.S., Gammeltoft, S., Piper, M., Pelleymounter, M.A., Cullen, M.J., Mathes, W.F., Przypek, R., Kanarek, R., and Maratos-Flier, E. (1996). A role for melanin-concentrating hormone in the central regulation of feeding behaviour. Nature *380*, 243-247.

Rahmouni, K., Fath, M.A., Seo, S., Thedens, D.R., Berry, C.J., Weiss, R., Nishimura, D.Y., and Sheffield, V.C. (2008). Leptin resistance contributes to obesity and hypertension in mouse models of Bardet-Biedl syndrome. Journal of Clinical Investigation *118*, 1458-1467.

Rahmouni, K., Sigmund, C.D., Haynes, W.G., and Mark, A.L. (2009). Hypothalamic ERK mediates the anorectic and thermogenic sympathetic effects of leptin. Diabetes *58*, 536-542.

Ren, D., Li, M., Duan, C., and Rui, L. (2005). Identification of SH2-B as a key regulator of leptin sensitivity, energy balance, and body weight in mice. Cell Metabolism *2*, 95-104.

Ren, D., Zhou, Y., Morris, D., Li, M., Li, Z., and Rui, L. (2007). Neuronal SH2B1 is essential for controlling energy and glucose homeostasis. Journal of Clinical Investigation *117*, 397-406.

Robson, A.J., Rousseau, K., Loudon, A.S., and Ebling, F.J. (2002). Cocaine and amphetamine-regulated transcript mRNA regulation in the hypothalamus in lean and obese rodents. Journal of Neuroendocrinology *14*, 697-709.

Rosenbaum, J.L., and Witman, G.B. (2002). Intraflagellar transport. Nature Reviews Molecular Cell Biology *3*, 813-825.

Rossi, M., Kim, M.S., Morgan, D.G., Small, C.J., Edwards, C.M., Sunter, D., Abusnana, S., Goldstone, A.P., Russell, S.H., Stanley, S.A., Smith, D.M., Yagaloff, K., Ghatei, M.A., and Bloom, S.R. (1998). A C-terminal fragment of Agouti-related protein increases feeding and antagonizes the effect of alpha-melanocyte stimulating hormone in vivo. Endocrinology *139*, 4428-4431.

Rui, L., and Carter-Su, C. (1999). Identification of SH2-bbeta as a potent cytoplasmic activator of the tyrosine kinase Janus kinase 2. Proceedings of the National Academy of Sciences of the United States of America *96*, 7172-7177.

Sahu, A. (1998). Evidence suggesting that galanin (GAL), melanin-concentrating hormone (MCH), neurotensin (NT), proopiomelanocortin (POMC) and neuropeptide Y (NPY) are targets of leptin signaling in the hypothalamus. Endocrinology *139*, 795-798.

Saito, Y., Cheng, M., Leslie, F.M., and Civelli, O. (2001). Expression of the melanin-concentrating hormone (MCH) receptor mRNA in the rat brain. Journal of Comparative Neurology *435*, 26-40.

Sasmal, P.K., Sasmal, S., Rao, P.T., Venkatesham, B., Roshaiah, M., Abbineni, C., Khanna, I., Jadhav, V.P., Suresh, J., Talwar, R., Muzeeb, S., Receveur, J.M., Frimurer, T.M., Rist, O., Elster, L., and Hogberg, T. (2010). Discovery of novel, orally available benzimidazoles as melanin concentrating hormone receptor 1 (MCHR1) antagonists. Bioorganic and Medicinal Chemistry Letters *20*, 5443-5448.

Satoh, N., Ogawa, Y., Katsuura, G., Tsuji, T., Masuzaki, H., Hiraoka, J., Okazaki, T., Tamaki, M., Hayase, M., Yoshimasa, Y., Nishi, S., Hosoda, K., and Nakao, K. (1997). Pathophysiological significance of the obese gene product, leptin, in ventromedial hypothalamus (VMH)-lesioned rats: evidence for loss of its satiety effect in VMH-lesioned rats. Endocrinology *138*, 947-954.

Schwartz, M.W., Baskin, D.G., Bukowski, T.R., Kuijper, J.L., Foster, D., Lasser, G., Prunkard, D.E., Porte, D., Jr., Woods, S.C., Seeley, R.J., and Weigle, D.S. (1996a). Specificity of leptin action on elevated blood glucose levels and hypothalamic neuropeptide Y gene expression in ob/ob mice. Diabetes *45*, 531-535.

Schwartz, M.W., Peskind, E., Raskind, M., Boyko, E.J., and Porte, D., Jr. (1996b). Cerebrospinal fluid leptin levels: relationship to plasma levels and to adiposity in humans. Nature Medicine *2*, 589-593.

Schwartz, M.W., Seeley, R.J., Campfield, L.A., Burn, P., and Baskin, D.G. (1996c). Identification of targets of leptin action in rat hypothalamus. Journal of Clinical Investigation *98*, 1101-1106.

Schwartz, M.W., Seeley, R.J., Woods, S.C., Weigle, D.S., Campfield, L.A., Burn, P., and Baskin, D.G. (1997). Leptin increases hypothalamic pro-opiomelanocortin mRNA expression in the rostral arcuate nucleus. Diabetes *46*, 2119-2123.

Schweizer, S., and Hoyer-Fender, S. (2009). Mouse Odf2 localizes to centrosomes and basal bodies in adult tissues and to the photoreceptor primary cilium. Cell and Tissue Research *338*, 295-301.

Sen Gupta, P., Prodromou, N.V., and Chapple, J.P. (2009). Can faulty antennae increase adiposity? The link between cilia proteins and obesity. Journal of Endocrinology *203*, 327-336.

Seo, S., Guo, D.F., Bugge, K., Morgan, D.A., Rahmouni, K., and Sheffield, V.C. (2009). Requirement of Bardet-Biedl syndrome proteins for leptin receptor signaling. Human Molecular Genetics *18*, 1323-1331.

Shimada, M., Tritos, N.A., Lowell, B.B., Flier, J.S., and Maratos-Flier, E. (1998). Mice lacking melanin-concentrating hormone are hypophagic and lean. Nature *396*, 670-674.

Shutter, J.R., Graham, M., Kinsey, A.C., Scully, S., Luthy, R., and Stark, K.L. (1997). Hypothalamic expression of ART, a novel gene related to agouti, is up-regulated in obese and diabetic mutant mice. Genes and Development *11*, 593-602.

Signor, D., Wedaman, K.P., Orozco, J.T., Dwyer, N.D., Bargmann, C.I., Rose, L.S., and Scholey, J.M. (1999). Role of a class DHC1b dynein in retrograde transport of IFT motors and IFT raft particles along cilia, but not dendrites, in chemosensory neurons of living Caenorhabditis elegans. Journal of Cell Biology *147*, 519-530.

Sindelar, D.K., Havel, P.J., Seeley, R.J., Wilkinson, C.W., Woods, S.C., and Schwartz, M.W. (1999). Low plasma leptin levels contribute to diabetic hyperphagia in rats. Diabetes *48*, 1275-1280.

Singla, V., and Reiter, J.F. (2006). The primary cilium as the cell's antenna: signaling at a sensory organelle. Science *313*, 629-633.

Sipols, A.J., Baskin, D.G., and Schwartz, M.W. (1995). Effect of intracerebroventricular insulin infusion on diabetic hyperphagia and hypothalamic neuropeptide gene expression. Diabetes *44*, 147-151.

Sorokin, S. (1962). Centrioles and the formation of rudimentary cilia by fibroblasts and smooth muscle cells. Journal of Cell Biology *15*, 363-377.

Srinivasan, S., Lubrano-Berthelier, C., Govaerts, C., Picard, F., Santiago, P., Conklin, B.R., and Vaisse, C. (2004). Constitutive activity of the melanocortin-4 receptor is maintained by its N-terminal domain and plays a role in energy homeostasis in humans. Journal of Clinical Investigation *114*, 1158-1164.

Stepanyan, Z., Kocharyan, A., Pyrski, M., Hubschle, T., Watson, A.M., Schulz, S., and Meyerhof, W. (2003). Leptin-target neurones of the rat hypothalamus express somatostatin receptors. Journal of Neuroendocrinology *15*, 822-830.

Stepanyan, Z., Kocharyan, A., Behrens, M., Koebnick, C., Pyrski, M., and Meyerhof, W. (2007). Somatostatin, a negative-regulator of central leptin action in the rat hypothalamus. Journal of Neurochemistry *100*, 468-478.

Stephens, T.W., Basinski, M., Bristow, P.K., Bue-Valleskey, J.M., Burgett, S.G., Craft, L., Hale, J., Hoffmann, J., Hsiung, H.M., Kriauciunas, A., and et al. (1995). The role of neuropeptide Y in the antiobesity action of the obese gene product. Nature *377*, 530-532.

Stofkova, A., Skurlova, M., Kiss, A., Zelezna, B., Zorad, S., and Jurcovicova, J. (2009). Activation of hypothalamic NPY, AgRP, MC4R, AND IL-6 mRNA levels in young Lewis rats with early-life diet-induced obesity. Endocrine Regulations *43*, 99-106.

Takahashi, Y., Okimura, Y., Mizuno, I., Iida, K., Takahashi, T., Kaji, H., Abe, H., and Chihara, K. (1997). Leptin induces mitogen-activated protein kinase-dependent proliferation of C3H10T1/2 cells. Journal of Biological Chemistry *272*, 12897.

Tartaglia, L.A., Dembski, M., Weng, X., Deng, N., Culpepper, J., Devos, R., Richards, G.J., Campfield, L.A., Clark, F.T., Deeds, J., Muir, C., Sanker, S., Moriarty, A., Moore, K.J., Smutko, J.S., Mays, G.G., Wool, E.A., Monroe, C.A., and Tepper, R.I. (1995). Identification and expression cloning of a leptin receptor, OB-R. Cell *83*, 1263-1271.

Tartaglia, L.A. (1997). The leptin receptor. Journal of Biological Chemistry *272*, 6093-6096.

Tavares, F.X., Al-Barazanji, K.A., Bigham, E.C., Bishop, M.J., Britt, C.S., Carlton, D.L., Feldman, P.L., Goetz, A.S., Grizzle, M.K., Guo, Y.C., Handlon, A.L., Hertzog, D.L., Ignar, D.M., Lang, D.G., Ott, R.J., Peat, A.J., and Zhou, H.Q. (2006). Potent, selective, and orally efficacious antagonists of melanin-concentrating hormone receptor 1. Journal of Medicinal Chemistry *49*, 7095-7107.

Tobin, J.L., and Beales, P.L. (2007). Bardet-Biedl syndrome: beyond the cilium. Pediatric Nephrology *22*, 926-936.

Tschop, M., Smiley, D.L., and Heiman, M.L. (2000). Ghrelin induces adiposity in rodents. Nature *407*, 908-913.

Tucker, R.W., Pardee, A.B., and Fujiwara, K. (1979). Centriole ciliation is related to quiescence and DNA synthesis in 3T3 cells. Cell *17*, 527-535.

Tups, A. (2009). Physiological models of leptin resistance. Journal of Neuroendocrinology *21*, 961-971.

Unger, J., McNeill, T.H., Moxley, R.T., 3rd, White, M., Moss, A., and Livingston, J.N. (1989). Distribution of insulin receptor-like immunoreactivity in the rat forebrain. Neuroscience *31*, 143-157.

Villanueva, E.C., and Myers, M.G., Jr. (2008). Leptin receptor signaling and the regulation of mammalian physiology. International Journal of Obesity *32 Suppl 7*, S8-12.

Vrang, N., Larsen, P.J., Clausen, J.T., and Kristensen, P. (1999). Neurochemical characterization of hypothalamic cocaine- amphetamine-regulated transcript neurons. Journal of Neuroscience *19*, RC5.

Wang, C., Yang, N., Wu, S., Liu, L., Sun, X., and Nie, S. (2007). Difference of NPY and its receptor gene expressions between obesity and obesity-resistant rats in response to high-fat diet. Hormone and Metabolic Research *39*, 262-267.

Wang, M.Y., Zhou, Y.T., Newgard, C.B., and Unger, R.H. (1996). A novel leptin receptor isoform in rat. FEBS Letters *392*, 87-90.

Wang, Z., Li, V., Chan, G.C., Phan, T., Nudelman, A.S., Xia, Z., and Storm, D.R. (2009). Adult type 3 adenylyl cyclase-deficient mice are obese. PLoS One *4*, e6979.

Wheatley, D.N., Wang, A.M., and Strugnell, G.E. (1996). Expression of primary cilia in mammalian cells. Cell Biology International *20*, 73-81.

White, C.L., Whittington, A., Barnes, M.J., Wang, Z., Bray, G.A., and Morrison, C.D. (2009). HF diets increase hypothalamic PTP1B and induce leptin resistance through both leptin-dependent and -independent mechanisms. American Journal of Physiology Endocrinology and Metabolism *296*, E291-299.

Wilding, J.P., Gilbey, S.G., Bailey, C.J., Batt, R.A., Williams, G., Ghatei, M.A., and Bloom, S.R. (1993). Increased neuropeptide-Y messenger ribonucleic acid (mRNA) and decreased neurotensin mRNA in the hypothalamus of the obese (ob/ob) mouse. Endocrinology *132*, 1939-1944.

Williams, G., Steel, J.H., Cardoso, H., Ghatei, M.A., Lee, Y.C., Gill, J.S., Burrin, J.M., Polak, J.M., and Bloom, S.R. (1988). Increased hypothalamic neuropeptide Y concentrations in diabetic rat. Diabetes *37*, 763-772.

Williams, G., Gill, J.S., Lee, Y.C., Cardoso, H.M., Okpere, B.E., and Bloom, S.R. (1989). Increased neuropeptide Y concentrations in specific hypothalamic regions of streptozocin-induced diabetic rats. Diabetes *38*, 321-327.

Williams, G., Bing, C., Cai, X.J., Harrold, J.A., King, P.J., and Liu, X.H. (2001). The hypothalamus and the control of energy homeostasis: different circuits, different purposes. Physiology and Behavior *74*, 683-701.

Williams, G., Cai, X.J., Elliott, J.C., and Harrold, J.A. (2004). Anabolic neuropeptides. Physiology and Behavior *81*, 211-222.

Wren, A.M., Seal, L.J., Cohen, M.A., Brynes, A.E., Frost, G.S., Murphy, K.G., Dhillo, W.S., Ghatei, M.A., and Bloom, S.R. (2001a). Ghrelin enhances appetite and increases food intake in humans. Journal of Clinical Endocrinology and Metabolism *86*, 5992.

Wren, A.M., Small, C.J., Abbott, C.R., Dhillo, W.S., Seal, L.J., Cohen, M.A., Batterham, R.L., Taheri, S., Stanley, S.A., and Ghatei, M.A. (2001b). Ghrelin causes hyperphagia and obesity in rats. Diabetes *50*, 2540.

Xu, A.W., Kaelin, C.B., Takeda, K., Akira, S., Schwartz, M.W., and Barsh, G.S. (2005a). PI3K integrates the action of insulin and leptin on hypothalamic neurons. Journal of Clinical Investigation *115*, 951-958.

Xu, A.W., Kaelin, C.B., Takeda, K., Akira, S., Schwartz, M.W., and Barsh, G.S. (2005b). PI3K integrates the action of insulin and leptin on hypothalamic neurons. Journal of Clinical Investigation *115*, 951-958.

Xu, A.W., Ste-Marie, L., Kaelin, C.B., and Barsh, G.S. (2007). Inactivation of signal transducer and activator of transcription 3 in proopiomelanocortin (Pomc) neurons causes decreased pomc expression, mild obesity, and defects in compensatory refeeding. Endocrinology *148*, 72-80.

Yang, G., Lim, C.Y., Li, C., Xiao, X., Radda, G.K., Cao, X., and Han, W. (2009). FoxO1 inhibits leptin regulation of pro-opiomelanocortin promoter activity by blocking STAT3 interaction with specificity protein 1. Journal of Biological Chemistry *284*, 3719-3727.

Zabolotny, J.M., Bence-Hanulec, K.K., Stricker-Krongrad, A., Haj, F., Wang, Y., Minokoshi, Y., Kim, Y.B., Elmquist, J.K., Tartaglia, L.A., Kahn, B.B., and Neel, B.G. (2002). PTP1B regulates leptin signal transduction in vivo. Developmental Cell *2*, 489-495.

Zapala, M.A., Hovatta, I., Ellison, J.A., Wodicka, L., Del Rio, J.A., Tennant, R., Tynan, W., Broide, R.S., Helton, R., Stoveken, B.S., Winrow, C., Lockhart, D.J., Reilly, J.F., Young, W.G., Bloom, F.E., and Barlow, C. (2005). Adult mouse brain gene expression patterns bear an embryologic imprint. Proceedings of the National Academy of Sciences of the United States of America *102*, 10357-10362.

Zhang, E.E., Chapeau, E., Hagihara, K., and Feng, G.S. (2004). Neuronal Shp2 tyrosine phosphatase controls energy balance and metabolism. Proceedings of the National Academy of Sciences of the United States of America *101*, 16064-16069.